CORA Cork Open Research Archive
Cartlann Taighde Oscailte Chorcaí

Title	Investigation of catalyst effects in enantioselective copper- and rhodium-mediated transformations of α-diazocarbonyl compounds
Authors	Slattery, Catherine N.
Publication date	2012-04
Original Citation	Slattery, C. N. 2012. Investigation of catalyst effects in enantioselective copper- and rhodium-mediated transformations of α-diazocarbonyl compounds. PhD Thesis, University College Cork.
Type of publication	Doctoral thesis
Rights	© 2012, Catherine N. Slattery - http://creativecommons.org/licenses/by-nc-nd/3.0/
Download date	2026-11-16 10:14:42
Item downloaded from	https://hdl.handle.net/10468/619



UCC
University College Cork, Ireland
Coláiste na hOllscoile Corcaigh

Investigation of catalyst effects in enantioselective copper- and rhodium-mediated transformations of α-diazocarbonyl compounds



Catherine N. Slattery, B.Sc.

A thesis presented for the degree of

Doctor of Philosophy

to

THE NATIONAL UNIVERSITY OF IRELAND, CORK

Department of Chemistry

University College Cork

Supervisor: Prof. Anita R. Maguire

Head of Department: Prof. Michael Morris

April 2012

Acknowledgements

Firstly I would like to thank Prof. Anita Maguire for her supervision, support and encouragement during the course of this project and especially during the writing of this thesis. I am extremely grateful for all the opportunities she has afforded me. Thanks also to Dr. Dan McCarthy and Dr. Lorraine Bateman for NMR work conducted, to Dr. Florence McCarthy and Mick O'Shea for mass spectrometry services, to Barry O' Mahony and Helen Kelly for microanalysis, to Derry Kearney for glass-blowing services and to Dr. Simon Lawrence and Kevin Eccles for X-ray crystallography data, particularly during the last few weeks of this project. I am also very grateful to the technical staff at UCC for their help over the last three and a half years, in particular Chrissie O'Flaherty, Tina Kent, Noel Browne, Pat O'Connell, Dr. Matthias Jauch, Dr. Michael Cronin, Dr. Tom O'Mahony, Dr. Ken Devine and Dr. Noel O'Boyle. Special thanks to Dr. Nuala Maguire for her guidance and support with HPLC analysis and Debbie Curran for all her help. I would also like to express my gratitude to the Irish Research Council for Science Engineering and Technology (IRCSET) and Eli Lilly for funding my PhD studies.

Many thanks to all past and present members of the ARM research group who I have had the pleasure of working with, namely Carla, Chris, David, Denis, Graham, Kevin, Liam, Linda, Marie, Niamh, Naomi, Nico, Niki, Orla, Paul, Rebecca, Sarah, Seb, Shane, Stephen and in particular to my copper group buddies Aoife and Leslie-Ann and to Brian whose friendship made my time in Lab 2.34 so enjoyable. Special thanks are due to Francis for his tireless work in making Lab 2.34 such a easy place to work in and for never saying no when help was needed, and to Alan for his constant advice and guidance during my PhD work, for never laughing at a stupid question and for proof reading this thesis. Thanks also to Sinead for her friendship, advice, proof-reading, encouragement, motivational speeches and all the early tea breaks!

To John, I am grateful for an endless list of things which you have brought into my life, of which keeping me fed and sane during the last few months of this thesis deserve special mention. I could not have done this without you. Looking forward to a (hopefully) less stressful life together post-PhD!

Finally, thanks to my family; my brother Conor and sister Róisín for helping me enjoy life outside of college, to my Godmother Maureen for her generous support and guidance, and in particular to my parents Tom and Sheila for their constant love, support and encouragement over the course of my studies. To you both I dedicate this thesis, I will be forever grateful.

Abstract

This thesis describes the synthesis and reactivity of a series of α-diazocarbonyl compounds with particular emphasis on the use of copper-bis(oxazoline)-mediated enantioselective C–H insertion reactions leading to enantioenriched cyclopentanone derivatives. Through the use of additives, the enantioselectivity achieved with the copper catalysts for the first time reaches synthetically useful levels (up to 91% ee).

Chapter one provides a comprehensive overview of enantioselective C–H insertions with α-diazocarbonyl compounds from the literature. The majority of reports in this section involve rhodium-catalysed systems with limited reports to date of asymmetric C–H insertion reactions in the presence of copper catalysts.

Chapter two focuses on the synthesis and C–H insertion reactions of α-diazo-β-keto sulfones leading to α-sulfonyl cyclopentanones as the major product. Detailed investigation of the impact of substrate structure (both the sulfonyl substitutent and the substituent at the site of insertion), the copper source, ligand, counterion, additive and solvent was undertaken to provide an insight into the mechanistic basis for enantiocontrol in the synthetically powerful C–H insertion process and to enable optimisation of enantiocontrol and ligand design. Perhaps the most significant outcome of this work is the enhanced enantioselection achieved through use of additives, substantially improving the synthetic utility of the asymmetric C–H insertion process. In addition to the C–H insertion reaction, mechanistically interesting competing reaction pathways involving hydride transfer are observed.

Chapter three reports the extension of the catalyst-additive systems, developed for C–H insertions with α-diazo-β-keto sulfones in chapter two, to C–H insertion in analogous α-diazo-β-keto phosphonate and α-diazo-β-keto ester systems. While similar patterns were seen in terms of ligand effects, the enantiopurities achieved for these reactions were lower than those in the cyclisations with analogous α-diazo-β-keto sulfones. Extension of this methodology to cyclopropanation and oxium ylide formation/[2,3]-sigmatropic rearrangement was also explored.

Chapter four contains the full experimental details and spectral characterisation of all novel compounds synthesised in this project, while details of chiral stationary phase HPLC analysis and X-ray crystallography are included in the appendix.

To Mam and Dad

Contents

Chapter 1

Introduction.....1

Chapter 2

Intramolecular C–H insertion reactions of α-diazo-β-keto sulfones.....67

Chapter 3

Asymmetric intramolecular copper-bis(oxazoline)-catalysed α-diazocarbonyl transformations……...197

Chapter 4

Experimental.....252

Appendices

Chiral stationary phase HPLC and polarimetry data…….…….*i*

Single crystal analysis……..…….….*xxv*

PXRD analysis…….…..…….*xxviii*

List of abbreviations……..……..…..*xxix*

^{1}H NMR spectra……..……...*xxx*

Publications…….…….……...*xxxii*

Chapter 1

Introduction

Contents

1.1 Introduction 4
1.2 Copper catalysts 5
1.3 Rhodium(II) catalysts 7
1.3.1 Chiral rhodium(II) carboxylate catalysts 8
1.3.2 Chiral rhodium(II) carboxamidate catalysts 12
1.3.3 Chiral rhodium(II) phosphate catalysts 15
1.3.4 Chiral ortho-metalated rhodium(II) complexes 16
1.4 Other metal catalysts 16
1.5 Intramolecular carbocycle-producing C–H insertion reactions 18
1.6 Intramolecular heterocycle-producing C–H insertion reactions 25
1.6.1 Oxygen-containing heterocycle synthesis 25
1.6.1.1 Lactone synthesis 25
1.6.1.2 Chromanone synthesis 33
1.6.1.3 Dihydrobenzofuran synthesis 34
1.6.2 Nitrogen-containing heterocycle synthesis 38
1.6.2.1 Lactam synthesis 38
1.6.1 Sulfur-containing heterocycle synthesis 45
1.7 Intermolecular C–H insertion reactions 46
1.8 Concluding remarks 59
1.9 References 61

Note: this introduction is reproduced from:

"*Catalytic Asymmetric C–H insertion reactions of α-diazocarbonyl compounds*",

Catherine N. Slattery, Alan Ford, Anita R. Maguire,Tetrahedron, **2010**, *66*, 6681–6705.

Updates to this review article appear in red type.

1.1 Introduction

Catalytic C–H insertion reactions of α-diazocarbonyl compounds represent a very powerful transformation in organic chemistry, allowing activation of an unactivated C–H bond under very mild conditions, rendering this a very valuable synthetic process. Initial studies examining carbenoid insertions into C–H bonds employed catalytic copper complexes, however, few synthetically useful examples were reported during this early period of investigation. In 1981, Teyssié and co-workers reported the first example of successful insertion into a C–H bond in the presence of a rhodium(II) carboxylate catalyst.[1] This report proved to be a turning point in the field of carbenoid chemistry, providing proof of the synthetic utility of C–H insertion reactions for the formation of C–C bonds and leading subsequently to the development of numerous rhodium(II)-derived catalysts for application in the decomposition reactions of α-diazocarbonyl compounds.

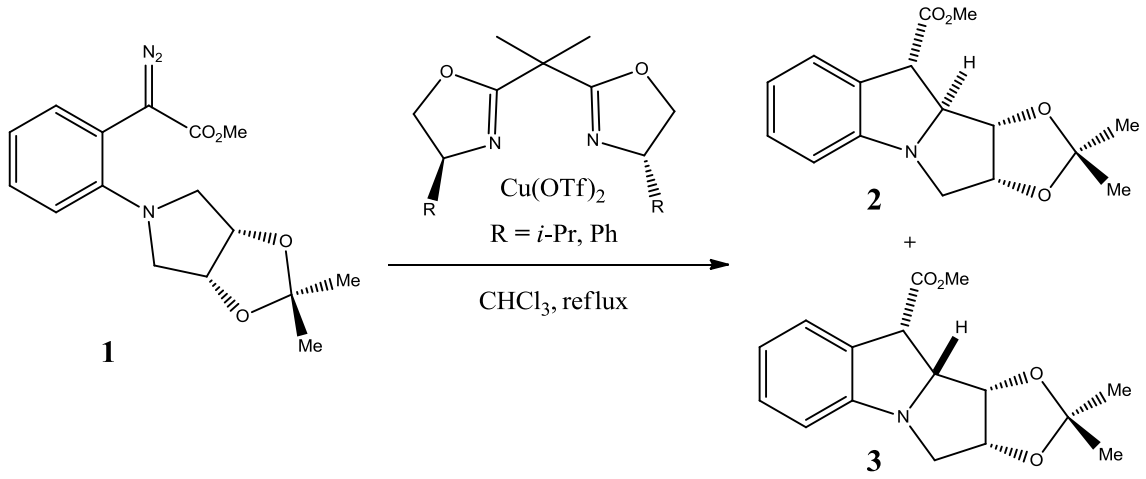
The potential for asymmetric induction in C–H insertion reactions was first realised in the early 1990s by researchers exploring the decomposition reactions of α-diazoketones[2] and α-diazo-β-keto esters.[3] The 20 years following this initial breakthrough have represented a period of vast growth and discovery in the area of enantioselective carbenoid C–H insertions. In excess of 60 chiral catalytic complexes have since been demonstrated to effect enantioinduction in intramolecular and intermolecular C–H insertion reactions. The large majority of these catalysts are rhodium(II)-based systems, however, recent reports have indicated the return of copper(I) complexes as viable catalyst choices for asymmetric carbenoid insertion into C–H bonds.[4] In addition, the possibility of broadening the range of available chiral catalysts for enantioselective C–H insertions beyond rhodium(II) and copper(I) complexes has recently been achieved with the development of iridium(III)-salen complexes capable of catalysing asymmetric intermolecular C–H insertion reactions.[5]

The importance of this area of organic chemistry is highlighted by the large number of published review articles detailing racemic[6-18] and asymmetric C–H insertion reactions.[8,9,13,14,17,19-25] The purpose of this review is to provide an overview of the development of asymmetric catalysts for C–H insertion reactions over the past two decades, focusing on the application of these catalysts in the decomposition of α-diazocarbonyl compounds. Given the rapid pace of development in the field of enantioselective C–H insertion chemistry, an up-to-date review of this type is warranted. While recent reviews[21,24,25] have dissected their content into intramolecular and intermolecular processes, this article is differentiated in extending this division to include classification of C–H insertion reactions according to product type. Thus, catalytic

methods for the asymmetric synthesis of carbocyclic compounds, oxygen-containing heterocycles, nitrogen-containing heterocycles and sulfur-containing heterocycles are readily identifiable. Due to the diversity of compounds resulting from intermolecular C–H insertion processes, classification of reactions by product type was not attempted in this section of the review.

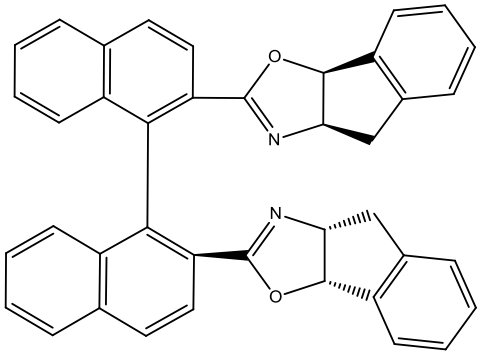
1.2 Copper catalysts

The majority of catalysts employed in early studies of diazo insertion reactions were copper-based systems,[6,26,27] showing varying levels of success in applied C–H insertion processes. Product yields were at best moderate and synthetic applications of these early copper catalysts were limited mainly to geometrically rigid diazo precursors.[6] The first enantioselective copper-catalysed C–H insertion reaction of α-diazocarbonyl compounds was reported in 1995 by Sulikowski and co-worker for the synthesis of 1,2-disubstituted mitosene.[28] Decomposition of aryldiazoacetate **1** in the presence of chiral copper-bis(oxazoline) catalysts was shown to provide the diastereomeric products **2** and **3** with moderate asymmetric induction (**Scheme 1.1**).

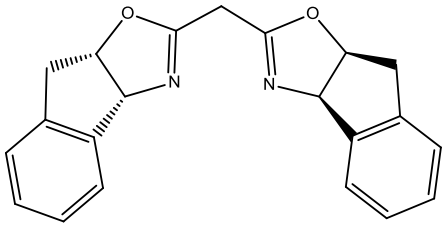


Scheme 1.1

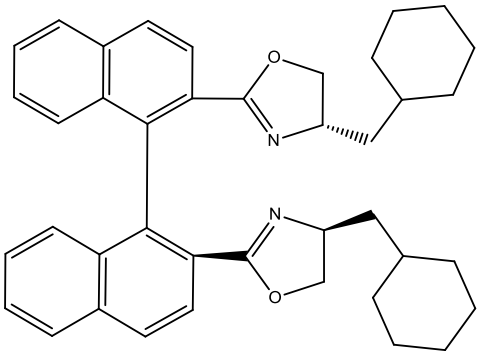
Bis(oxazoline) complexes have since been employed in several inter- and intramolecular C–H insertion reactions, with enantioinduction of up to 98% enantiomeric excess (ee) being achieved.[4,29-33] To date, in excess of 140 chiral bis(oxazoline) ligands have been synthesised,[34] finding applications in a wide range of asymmetric transformations.[34-36] The success of these catalysts may be attributed to the C_2-symmetry of the ligands which minimises the number of possible transition states for a given reaction,[37] and also the conformationally constrained metal chelate structure which places the donor nitrogens in close proximity to the chiral centres, resulting in a strong directing effect on the catalytic site. Selected examples of bis(oxazoline) ligands **4a**–**h** are displayed in **Figure 1.1**. Recently, the use of immobilised[32,38] and heterogeneous[39] copper-bis(oxazoline) catalysts has also been described for enantioselective intermolecular C–H insertion reactions with diazoacetate and ether substrates, however, the levels of enantioselectivity obtained for these transformations have been generally moderate.



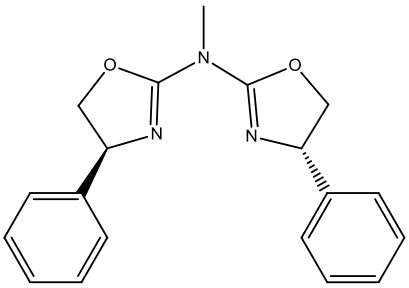
4a



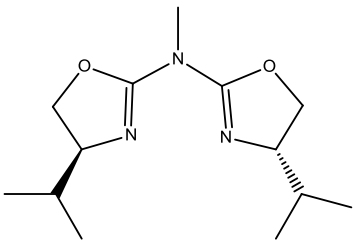
4b



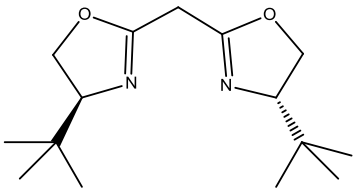
4c



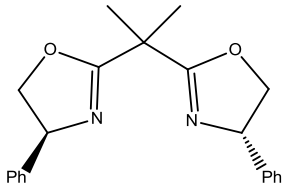
4d



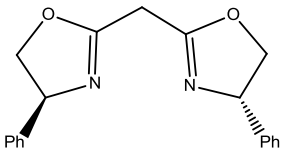
4e



4f



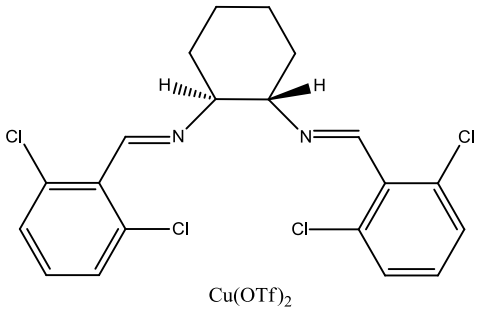
4g



4h

Figure 1.1

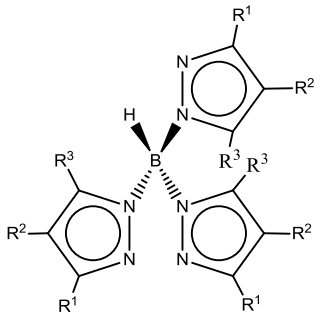
Additional copper catalysts employed in asymmetric C–H insertion processes include copper C_2-symmetric Schiff base complexes such as **5** (**Figure 1.2**), which have shown moderate success in the enantioselective synthesis of d-*threo*-methylphenidate.[40]



5

Figure 1.2

Amongst the most recent developments in the area of copper catalysis for C–H activation chemistry has been the introduction of copper-based catalysts possessing trispyrazolylborate (Tp^x) ligands **6a**–**c** (**Figure 1.3**).[41] Various complexes of general formula Tp^xCu have been shown to be efficient catalyts for carbene/diazoacetate insertion into C–H bonds of hydrocarbons.[41-45]



6a Tp^{Ms} : R^1 = Ms, $R^2 = R^3$ = H
6b Tp^{Br3}: $R^1 = R^2 = R^3$ = Br
6c Tp^{Cy} : R^1 = Cy, $R^2 = R^3$ = H

Figure 1.3

In general, superior results in terms of catalytic selectivity are observed for those systems in which the metal centre is bonded to a weakly electron-donating ligand, meaning electrophilicity at the metal centre is increased.[46] An asymmetric version of this transformation has yet to be described but may be achieved in the coming years.

1.3 Rhodium(II) catalysts

Rhodium(II) complexes have been widely established as the most effective and versatile catalysts for diazo decomposition.[6,7,10,12,15,47] Their popularity may be rationalised by the fact that rhodium(II)-catalysed carbene reactions proceed under much milder conditions than those employed for syntheses with copper(II) catalysts.[15] In

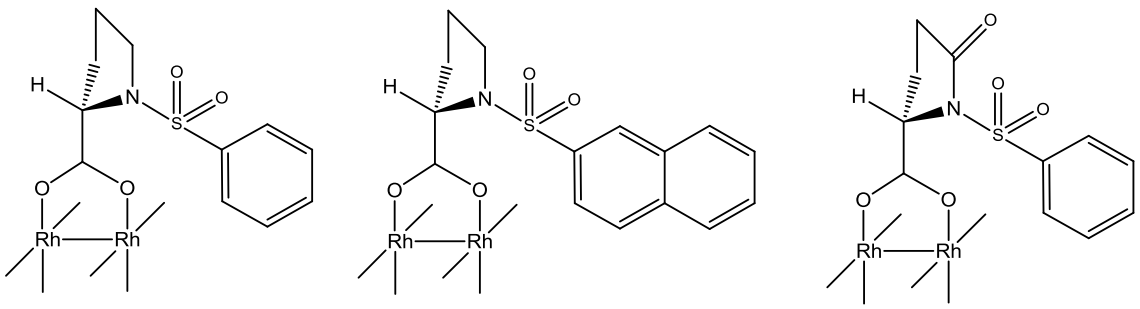
addition, a wide variety of rhodium(II) complexes are available, owing to the large number of bridging ligands that can be coordinated to the rhodium(II) skeleton.

A key property of rhodium(II) is its ability to form Rh–Rh bonds. This property allows for the formation of a dirhodium-bridged cage within a 'lantern' structure,[48-50] which is thought to be a critical feature in the success of Rh(II) complexes. It has been suggested that only one of the two rhodium centres functions as a binding site for the carbene generated from diazo decomposition. The second rhodium is believed to aid the reaction by behaving as an electron sink, thereby increasing the electrophilicity of the carbene and facilitating cleavage of the rhodium-carbene bond upon reaction completion.[51] Such a supporting role is not available to single metallic complexes such as copper-carbenoid species.

Rhodium catalysis for C–H insertion processes was first reported by Teyssié and co-workers in 1981.[1] Realisation of the potential of rhodium(II) complexes to induce diazo decomposition led to a significant focus on the development of related catalysts for application in diazo/carbenoid chemistry. Numerous achiral carboxylate and carboxamidate catalysts derived from the parent rhodium(II) tetraacetate [$Rh_2(OAc)_4$] have since been reported for carbenoid transformations.[52-55] Over the past two decades, the focus of study in the area of diazo chemistry has shifted to the development of chiral catalysts for asymmetric diazo decomposition reactions. A vast range of chiral rhodium(II) catalysts now exist encompassing rhodium(II) carboxylates, rhodium(II) carboxamidates, rhodium(II) phosphates, and rhodium(II) ortho-metalated complexes.

1.3.1 Chiral rhodium(II) carboxylate catalysts

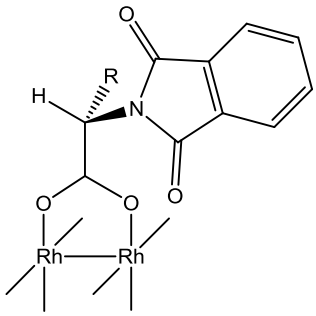
The first use of chiral rhodium(II) catalysts in C–C bond-forming reactions of α-diazocarbonyl compounds was reported by McKervey and co-workers in 1990.[2] Their novel rhodium(II) (*N*-benzenesulfonylprolinate) catalyst [$Rh_2(BSP)_4$] **7a**, (**Figure 1.4**) prepared by treatment of *N*-benzenesulfonyl-L-proline with $Na_4Rh_2(CO_3)_4$, was shown to be an effective catalyst in the intramolecular C–H insertion of an α-diazo-β-keto sulfone precursor (12% ee). Numerous related proline complexes, including **7b** and **7c**, have since been synthesised.[56]



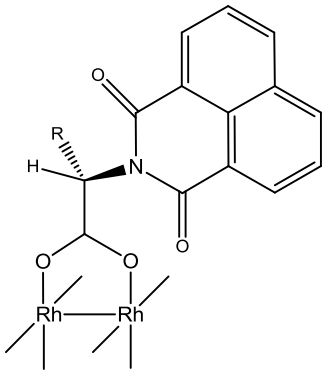
7a **7b** **7c**

Figure 1.4

In the same year, Hashimoto and Ikegami reported the use of phthalimide derivatives of amino acid-based chiral rhodium(II) carboxylates as catalysts for enantioselective intramolecular C–H insertion reactions of a series of α-diazo-β-keto esters.[3] These phthalimide catalysts (**8a** and **8d**) displayed considerable enantioselectivity (up to 46% ee) and several related complexes were later prepared to include *tert*-leucinate [Rh_2(*S*-PTTL)$_4$] **8e**, valine [Rh_2(*S*-PTV)$_4$] **8b**, phenylglycine [Rh_2(*S*-PTPG)$_4$] **8c** and triethylalanine [Rh_2(*S*-PTTEA)$_4$] **8f** derived catalysts (**Figure 1.5**), showing improvements in enantiocontrol in many cases due to the increased steric bulk of the alkyl group of the ligand.[57,58] The related catalysts Rh_2(*S*-NPV)$_4$ **9a** and Rh_2(*S*-NPTL)$_4$ **9b** (**Figure 1.5**) have also been developed by Chiu and co-workers, showing moderate enantioselectivity in the C–H insertion reactions of *meso* oxabicyclic compounds.[59]



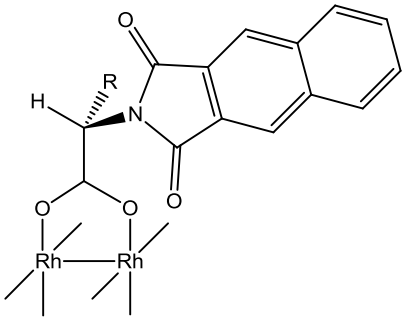
8a R = Me Rh_2(*S*-PTA)$_4$
8b R = *i*-Pr Rh_2(*S*-PTV)$_4$
8c R = Ph Rh_2(*S*-PTPG)$_4$
8d R = Bn Rh_2(*S*-PTPA)$_4$
8e R = *t*-Bu Rh_2(*S*-PTTL)$_4$
8f R = C(Et)$_3$ Rh_2(*S*-PTTEA)$_4$



9a R = *i*-Pr Rh_2(*S*-NPV)$_4$
9b R = *t*-Bu Rh_2(*S*-NPTL)$_4$

Figure 1.5

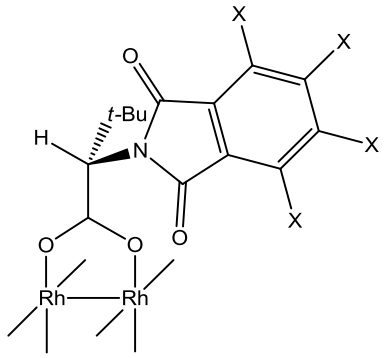
Subsequent work by Hashimoto and co-workers has included the development of a series of catalysts featuring an extended phthalimido wall (**Figure 1.6**), namely, Rh_2(*S*-BPTTL)$_4$ **10d**, Rh_2(*S*-BPTA)$_4$ **10a**, Rh_2(*S*-BPTPA)$_4$ **10c**, and Rh_2(*S*-BPTV)$_4$ **10b**, derived from *tert*-leucine, alanine, phenylalanine, and valine, respectively.[60] These highly structured complexes have displayed improved enantioselectivities for many C–H insertion reactions, compared to the original phthalimide catalysts.[61]



10a R = Me Rh_2(*S*-BPTA)$_4$
10b R = *i*-Pr Rh_2(*S*-BPTV)$_4$
10c R = Bn Rh_2(*S*-BPTPA)$_4$
10d R = *t*-Bu Rh_2(*S*-BPTTL)$_4$

Figure 1.6

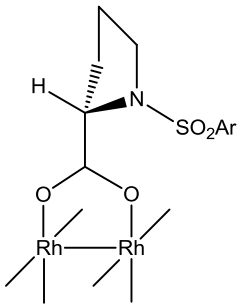
More recently, halogen-substituted phthaloyl catalysts (**Figure 1.7**) have been introduced.[62] These complexes are characterised by substitution of the phthalimido hydrogens of the parent rhodium(II) species by fluorine (**11a**) or chlorine (**11b**) atoms, resulting in improved reactivity and enantioselectivity owing to the electron-withdrawing effect of the halide substituents on the chiral ligands. Rh_2(*S*-TFPTTL)$_4$ **11a** has been particularly impressive, achieving an extremely high turnover number (up to 98,000) in the C–H insertion reactions of methyl 4-alkyl-2-diazo-4,4-diphenyl-3-oxo-propionates, with a catalyst loading of just 0.001 mol%.[62]



11a X = F Rh_2(*S*-TFPTTL)$_4$
11b X = Cl Rh_2(*S*-TCPTTL)$_4$

Figure 1.7

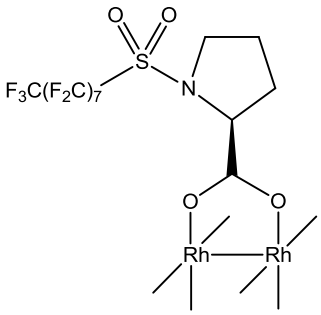
The catalogue of available proline-based chiral rhodium(II) carboxylates was extended by Davies, who reported the application of rhodium(II) (*S*)-*N*-(*tert*-butylbenzenesulfonyl) prolinate Rh_2(*S*-TBSP)$_4$ **12** and rhodium(II) (*S*)-*N*-(dodecylbenzenesulfonyl)prolinate Rh_2(*S*-DOSP)$_4$ **13** (**Figure 1.8**) for the enantioselective synthesis of vinylcyclopropanes[63] and 2-phenylcyclopropan-1-amino acids,[64] respectively. Despite showing moderate success for asymmetric C–H insertions with traditional diazoacetate substrates, Davies' rhodium(II) prolinate derivatives have become the catalysts of choice for intermolecular C–H insertion reactions with carbenoids substituted with an electron-donating and an electron-withdrawing group.



12 Ar = *p*-*t*-BuC_6H_4 Rh_2(*S*-TBSP)$_4$
13 Ar = *p*-($C_{12}H_{25}$)C_6H_4 Rh_2(*S*-DOSP)$_4$

Figure 1.8

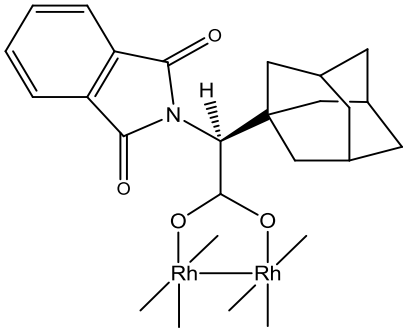
The bridged prolinate complexes, Rh_2(*S*-biDOSP)$_2$, Rh_2(*S*-biTBSP)$_2$ and Rh_2(*S*-biTISP)$_2$, have also been developed.[65] These rigid catalytic systems have shown success in C–H insertion reactions,[66-69] achieving high asymmetric induction in reactions employing non-hydrocarbon solvents, and in this respect are advantageous over Rh_2(*S*-DOSP)$_4$. Additional developments in the field of prolinate-based catalysis for carbenoid reactions have included the preparation of the fluorous complex, rhodium(II)-(*S*)-*N*-(*n*-perfluorooctylsulfonyl) prolinate [Rh_2(*S*-FOSP)$_4$] **14** (**Figure 1.9**), by Biffis and co-workers.[70] The perfluoroalkyl chains of this novel catalyst allow for its facile recovery from the reaction mixture by confining the catalyst in an isolated perfluorinated liquid or solid phase, making this an excellent recyclable asymmetric catalyst. Moderate enantioselectivity has been achieved for this catalyst in the asymmetric C–H bond activation of cyclohexane (61% ee).



14

Figure 1.9

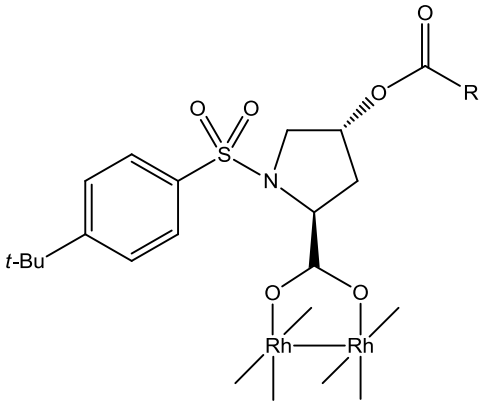
In 2006, Davies and co-workers reported the synthesis of a rhodium(II) tetracarboxylate catalyst derived from adamantylglycine Rh_2(*S*-PTAD)$_4$ **15** (**Figure 1.10**).[71] This adamantate complex has been proven an effective catalyst for carbenoid reactions, with high asymmetric induction being noted for both intermolecular (up to 92% ee) and intramolecular (up to 94% ee) C–H insertion reactions.[71] High enantioselectivity in the intermolecular C–H insertion of α-aryl-α-diazoketones with cyclohexadiene has also been achieved (89% ee).[72]



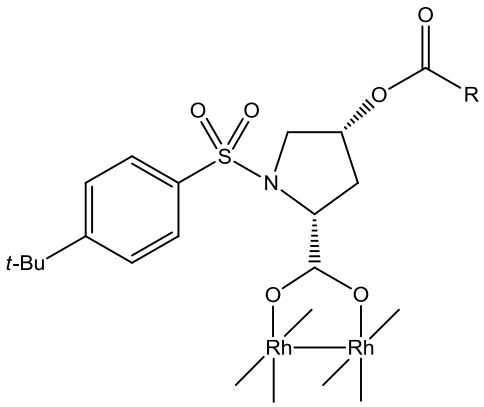
15

Figure 1.10

Recently, the preparation of three new chiral rhodium(II) catalysts **16**, **17** and **18** (**Figure 1.11**) with 4-hydroxyproline-derived ligands has been described.[73] In contrast to previous proline-based chiral rhodium(II) carboxylates, these hydroxyproline-derived complexes possess a hydrophobic side-chain at the 4-position of the pyrrolidine ring which aids solubility in organic solvents. They have been shown to give similar yields and enantioselectivities in C–H insertion and cyclopropanation reactions to the widely used $Rh_2(DOSP)_4$ and its analogues.



16 R = $C_{12}H_{25}$



17 R = $C_{12}H_{25}$
18 R = cyclohexyl

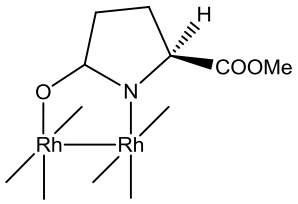
Figure 1.11

1.3.2 Chiral rhodium(II) carboxamidate catalysts

The first preparation of a rhodium(II) carboxamidate was described in 1982 by Dennis and co-workers, who isolated the rhodium(II) tetraacetamidate from a melt of trifluoroacetamide and rhodium(II) tetraacetate.[74] Several isomers of this carboxamidate complex are possible, however, the structure in which the two oxygens and two nitrogens are bound to each rhodium in a *cis* fashion was found to be dominant.[75] In general, decreased reactivity has been observed for catalytic reactions with α-diazocarbonyls in

the presence of carboxamidates, compared with the corresponding carboxylates, however, higher selectivites are possible making these complexes a popular catalytic choice for C–H insertion reactions.[76-78]

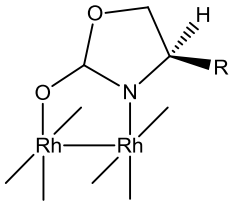
Doyle's chiral rhodium(II) carboxamidate complexes were first reported for enantioselective cyclopropanation reactions in 1990.[79] These catalysts have since been much exploited and remain today the primary catalysts for enantioselective C–H insertion reactions of electron-withdrawing group-substituted carbenoids derived from diazoacetamides and diazoesters.[6] The carboxamidate derivative $Rh_2(MEPY)_4$ **19** (**Figure 1.12**) was the first of Doyle's catalysts to be employed for asymmetric C–H insertions.[80] A high degree of enantiocontrol was achieved for this catalyst in the intramolecular C–H insertions of alkyl diazoacetates, thereby paving the way for the development of further carboxamidate derivatives.



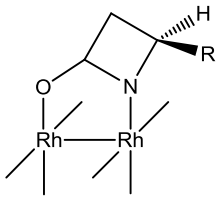
19

Figure 1.12

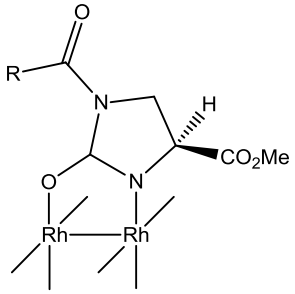
Numerous rhodium(II) carboxamidate catalysts developed by Doyle have since been employed for C–H insertion reactions including oxazolidinone **20a**–**c**,[29,81-86] azetidinone **21a**–**e**,[40,85,87] and imidazolidinone **22a**–**c**[29,83,85,88-92] complexes (**Figure 1.13**).



20a R = CO_2Me $Rh_2(4S\text{-MEOX})_4$
20b R = Bn $Rh_2(4R\text{-BNOX})_4$
20c R = Ph $Rh_2(4R\text{-PHOX})_4$



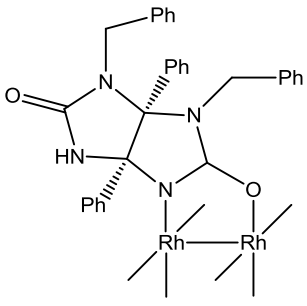
21a R = Me $Rh_2(4S\text{-MEAZ})_4$
21b R = *i*-Bu $Rh_2(4S\text{-IBAZ})_4$
21c R = Bn $Rh_2(4S\text{-BNAZ})_4$
21d R = *l*-menthyl $Rh_2(S,S\text{-MenthAZ})_4$
21e R = *d*-menthyl $Rh_2(S,R\text{-MenthAZ})_4$



22a R = Me $Rh_2(4S\text{-MACIM})_4$
22b R = c-$C_6H_{11}CH_2$ $Rh_2(4S\text{-MCHIM})_4$
22c R = $BnCH_2$ $Rh_2(4S\text{-MPPIM})_4$

Figure 1.13

The diastereomeric azetidinone complexes $Rh_2(S,S\text{-MenthAZ})_4$ **21d** and $Rh_2(S,R\text{-MenthAZ})_4$ **21e** have also been shown to be effective catalysts for the enantioselective intermolecular C–H insertion reactions of vinyldiazolactones.[87] Recently, 1,6-bis-(*N*-benzyl)-diphenylglycoluril (1,6-BPGlyc) **23** (**Figure 1.14**) has been reported as a ligand for dinuclear rhodium(II) complexes.[93] This glycouril derivative has been shown to be an effective catalyst for the cyclopropanation of styrene with diazoacetates, displaying reactivities and selectivities in the range of related rhodium(II) carboxamidates and may therefore represent a suitable catalytic choice for future asymmetric C–H insertion reactions.

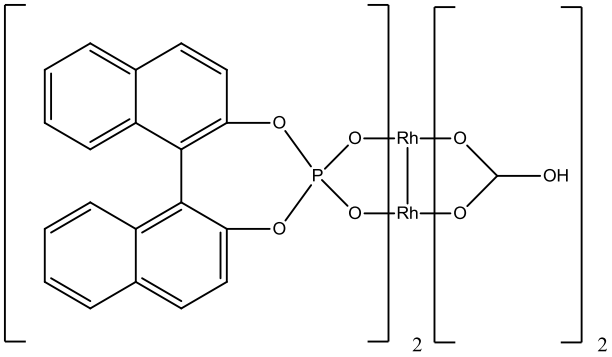


23

Figure 1.14

1.3.3 Chiral rhodium(II) phosphate catalysts

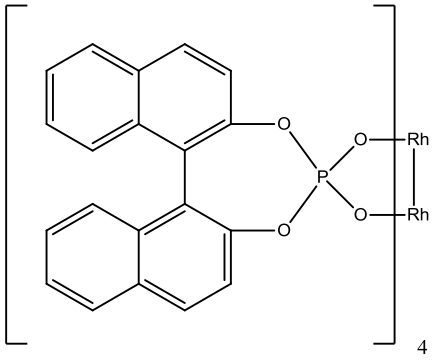
Chiral rhodium(II) binaphthylphosphate catalysts have been developed by both McKervey and Pirrung. McKervey's Rh_2(*S*-BNP)$_2$(HCO_3)$_2$ **24** (**Figure 1.15**) complex was first reported in 1992, and was shown to be an efficient catalyst for a range of diazocarbonyl decomposition reactions, including C–H insertions, with moderate-to-good levels of enantioselectivity being achieved.[94]



24

Figure 1.15

Pirrung's Rh_2(*R*-BNP)$_4$ complex **25** (**Figure 1.16**), reported in the same year, was also demonstrated to provide good asymmetric induction in the dipolar cycloaddition of diazo compounds to heterocyclic compounds.[95]



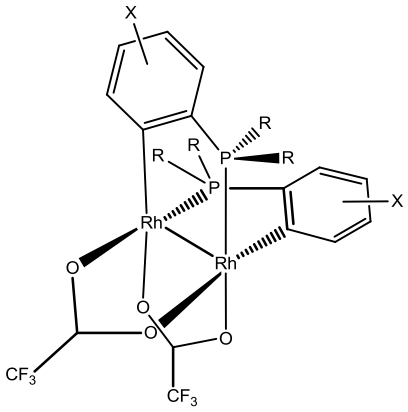
25

Figure 1.16

While some success in asymmetric C–H insertions has since been reported with these chiral rhodium(II) phosphate complexes,[59] their use to date in C–H activation chemistry remains minimal, with their primary application being found in enantioselective ylide formation reactions of α-diazocarbonyls.

1.3.4 Chiral ortho-metalated rhodium(II) complexes

The synthesis and X-ray characterisation of ortho-metalated rhodium(II) compounds of general formula $Rh_2(O_2CMe)[(Ph)_2P(C_6H_4)]_2 \cdot 2L$ was first described by Cotton in 1985.[96] These novel mixed-ligand bridging systems displayed characteristics not previously observed for rhodium(II) tetracarboxylates or tetraacetamides, including backbone chirality, possession of polarisable aromatic ligands, and the possibility of regulating electronic and steric properties of the catalyst by modification of both carboxylate and phosphine substituents. In 1999, Lahuerta and co-workers reported the synthesis of the first enantiomerically pure ortho-metalated rhodium(II) dimer,[97] paving the way for the development of a new series of chiral $Rh_2(OOCR)_2(PC)_2$ catalysts **26a**–**g** (PC = ortho-metalated phosphine) of which several now exist (**Figure 1.17**).



26a	R = Ph	X = H
26b	R = Me	X = H
26c	R = *p*-MeC_6H_4	X = *p*-Me
26d	R = *p*-FC_6H_4	X = *p*-F
26e	R = *m*-MeC_6H_4	X = *m*-Me
26f	R = 3,5-$Me_2C_6H_3$	X = 3,5-Me
26g	R = *p*-*t*-BuC_6H_4	X = *p*-*t*-Bu

Figure 1.17

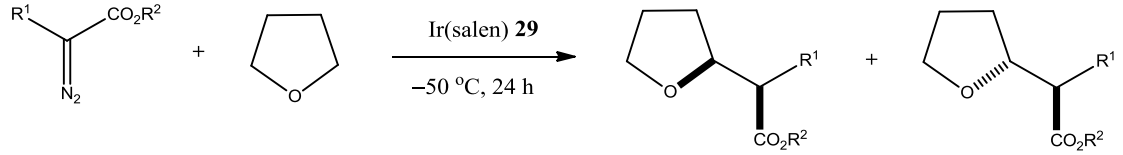
These complexes were subsequently shown to be effective catalysts for the asymmetric C–H insertion reactions of α-diazoketones,[98] producing cyclopentanone products with enantioselectivity as high as 74% ee, representing a significant improvement on previous attempts at enantiocontrol in the decomposition of α-diazoketones.[2] A new series of biscyclometalated Rh(II) compounds of general formula $Rh_2(OOCR)_2(PC)_2 \cdot N_2$ have recently been described.[99] These novel complexes possess different nitrogen donor ligands (N = NH_2Ph, py, 3-MeCO-py and 4-MeCO-py) axially coordinated to both rhodium atoms of the catalyst.

1.4 Other metal catalysts

The choice of catalyst for carbene transformation reactions may also comprise a variety of other transition-metal-based complexes including iron,[100] ruthenium,[101] osmium,[102] cobalt,[103] palladium,[104] platinum,[105] molybdenum,[106] iridium,[107] scandium,[108] silver[109] and gold.[110,111] Several of these catalytic systems have been successfully applied to C–H insertion processes,[100,106,108-110,112] mainly intermolecular reactions with ethyl diazoacetate, however, until recently none have been reported to induce enantioselectivity. A 2009 report by Katsuki and Suematsu[5] described the first example of iridium(III)-catalysed

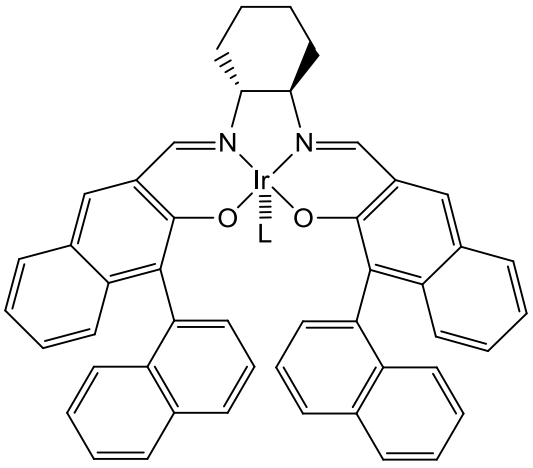
asymmetric carbenoid insertion (**Table 1.1**). This achievement was realised for the intermolecular C–H insertion of various α-substituted α-diazoacetates **27** into tetrahydrofuran **28** and 1,4-cyclohexadiene in the presence of a chiral iridium(III)-salen complex **29**, producing the corresponding α-aryl(tetrahydrofuran-2-yl)acetates **30** and **31** in moderate to high diastereoselectivity and high enantioselectivity (**Figure 1.18**). In addition to representing the first example of enantioselective iridium(III)-catalysed C–H insertion, this report was significant in demonstrating the ability of α-alkyl-α-diazoacetates to undergo efficient intermolecular C–H carbene insertion (**Table 1.1**, entry 4).

Table 1.1 *Enantioselective C–H insertion of α-substututed α-diazoacetates **27** into tetrahydrofuran.*



27 **28** **30** **31**

Entry	R^1	R^2	**30** : **31**	Yield (%) **30**	ee (%) **30**
1	Ph	Me	13 : 1	75	95
2	*p*-$MeOC_6H_4$	Me	>20 : 1	64	97
3	*m*-$MeOC_6H_4$	Me	9 : 1	75	97
4	Me	*t*-Bu	13 :1	70	90



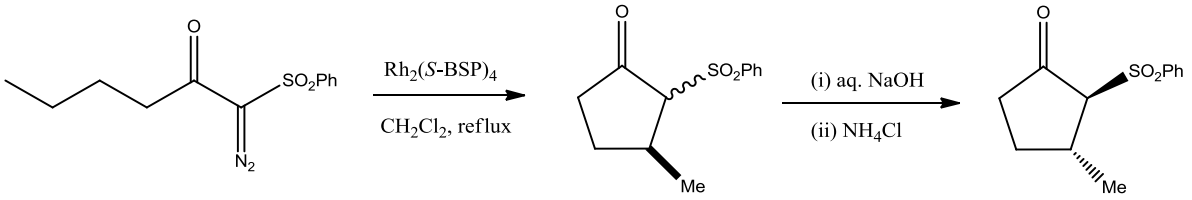
L = 4-MeC_6H_4

29

Figure 1.18

1.5 Intramolecular carbocycle-producing C–H insertion reactions

The first example of asymmetric induction for an intramolecular carbocycle-producing C–H insertion reaction was reported by McKervey and co-workers in 1990 for the Rh_2(*S*-BSP)$_4$-catalysed cyclisation of α-diazo-β-keto sulfone **32** (**Scheme 1.2**).[2] In this study, cyclopentanone **33** was obtained as a mixture of *cis* and *trans* isomers in >90% yield, with an enantioselectivity of 12% ee being recorded for the *trans* isomer.

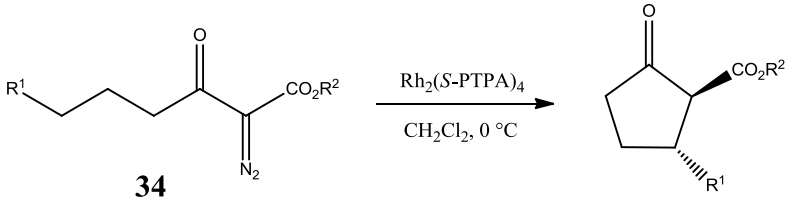


32 **33**

Scheme 1.2

The majority of studies exploring the C–H insertion route to five-membered-ring carbocyclic products have employed α-diazo-β-keto ester carbenoid precursors. Early work in this area was carried out by Ikegami and Hashimoto, who demonstrated the ability of *N*-phthaloyl amino acid catalysts to efficiently cyclise a range of α-diazo-β-keto esters (**Table 1.2**).[3,57,113]

Table 1.2 *Intramolecular C–H insertion reactions of α-diazo-β-keto esters **34**.*



34

Entry	R^1	R^2	Yield (%)	ee (%)[a]
1	Me	Me	76	24 (3*R*)
2	Ph	Me	96	46 (3*R*)
3	$CH=CH_2$	Me	44	38 (3*R*)
4	Ph	(+)-neomenthyl	78	53 (3*R*)
5[b]	Ph	(+)-neomenthyl	79	80 (3*S*)
6	Ph	CH*i*-Pr_2	86	76 (3*R*)
7	*p*-$MeOC_6H_4$	CH*i*-Pr_2	77	57 (3*R*)
8	*p*-BrC_6H_4	CH*i*-Pr_2	79	70 (3*R*)
9	*p*-$CF_3SO_3C_6H_4$	CH*i*-Pr_2	81	80 (3*R*)

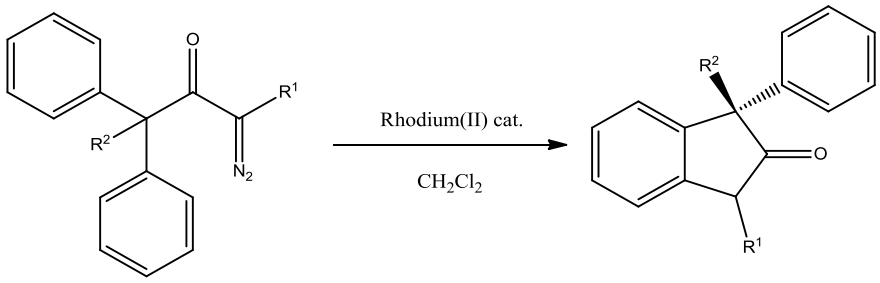
[a] Enantioselectivity determined following dealkoxycarbonylation. [b] Catalyst used was Rh_2(*R*-PTPA)$_4$.

Of the catalysts tested, Rh_2(*S*-PTPA)$_4$ was shown to be the catalyst of choice, providing enantioselectivities of up to 80% ee (**Table 1.2**, entry 9). The extent of asymmetric

induction achieved in the cyclisation of the α-diazo-β-keto esters was found to be heavily influenced by both the size of the alkoxy group of the ester moiety and the nature of the substituents adjacent to the target C–H bond. In general, increased steric bulk of the ester group was found to favour improved asymmetric induction, with change of ester moiety from methyl (**Table 1.2**, entry 2) to CH*i*-Pr_2 (**Table 1.2**, entry 6) inducing an increase from 46% ee to 76% ee. The presence of electron-withdrawing substituents (phenyl, vinyl) adjacent to the C–H insertion site was also proven to enhance asymmetric induction (**Table 1.2**, entries 2 and 3 *vs.* entry 1), owing to a decrease in electron density at the target site which reduced reactivity towards the electrophilic rhodium-carbene species, resulting in an increase in stereoselectivity. Highest enantioselectivies were achieved for substrates possessing electron-withdrawing group-substituted aryl rings adjacent to the insertion site (**Table 1.2**, entries 8 and 9), and for substrates containing the chiral ester substituent (+)-neomenthyl (**Table 1.2**, entries 4 and 5). The high level of enantiocontrol recorded in the latter case (**Table 1.2**, entry 5) was achieved through a process of double asymmetric induction for the matched pair of **34** and Rh_2(*R*-PTPA)$_4$. It is interesting to note in this study that benzylic C–H insertion occurred under the same conditions (CH_2Cl_2, 0 °C) and at the same rate (0.5 h) as the corresponding insertion into methylene sites, despite previous findings by Taber suggesting that benzylic and allylic C–H insertion is less favourable than aliphatic C–H insertion.[114]

Later work by Ikegami and Hashimoto included the examination of enantiotopically selective intramolecular aromatic C–H insertion reactions of α-diazoketones and α-diazo-β-keto esters (**Table 1.3**). [62,115,116]

Table 1.3 *Intramolecular aromatic C–H activation of α-diazoketones and α-diazo-β-keto esters.*



35 **36**

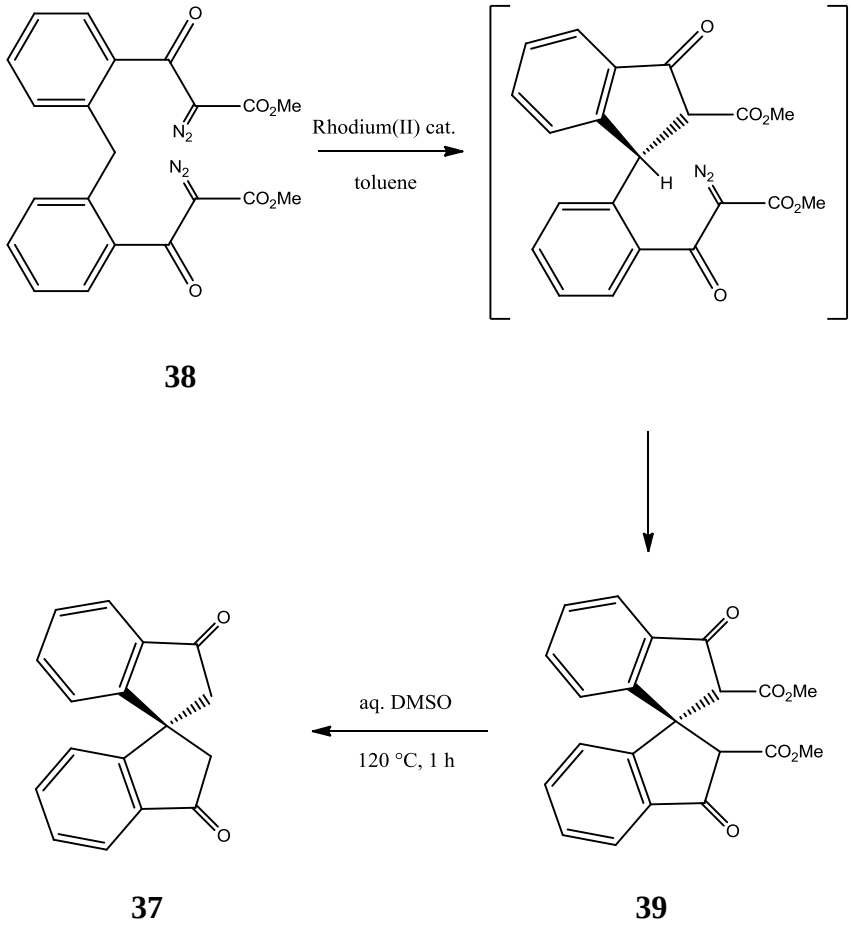
Entry	Rhodium(II) cat.	R^1	R^2	Temp (°C)	Yield (%) **36**	ee (%)[a] **36**
1	Rh_2(*S*-PTPA)$_4$	H	Me	–20	64	77
2	Rh_2(*S*-PTTL)$_4$	H	Me	–20	84	90
3	Rh_2(*S*-PTTL)$_4$	H	Et	–20	74	98
4	Rh_2(*S*-PTTL)$_4$	H	*n*-Pr	–10	75	88
5	Rh_2(*S*-PTTL)$_4$	CO_2Me	Me	0	89	92[a]
6	Rh_2(*S*-PTTL)$_4$	CO_2Me	Et	0	98	96[a]
7	Rh_2(*S*-TFPTTL)$_4$	CO_2Me	Me	–10	70	98[a]
8	Rh_2(*S*-TFPTTL)$_4$	CO_2Me	Et	0	94	97[a]

[a] Enantioselectivity determined following demethoxycarbonylation.

A high degree of differentiation between the enantiotopic benzene rings was achieved, producing (*S*)-1-alkyl-1-phenyl-2-indanones **36** in up to 98% ee. Dirhodium(II) [*N*-phthaloyl-(*S*)-*tert*-leucinate], Rh_2(*S*-PTTL)$_4$, was found to be the best-performing catalyst, providing excellent enantioinduction with a variety of R^1 and R^2 substituents (**Table 1.3**, entries 2–6).[62,115] The fluorine-substituted phthaloyl complex Rh_2(*S*-TFPTTL)$_4$ was also shown to be a successful catalytic choice for asymmetric intramolecular aromatic C–H insertion reactions of **35** (**Table 1.3**, entries 7 and 8), providing enantioselectivities comparable to Rh_2(*S*-PTTL)$_4$ with significantly shorter reaction times [2–20 min for Rh_2(*S*-TFPTTL)$_4$ *vs.* 1–2 h for Rh_2(*S*-PTTL)$_4$].[62]

The rhodium(II)-catalysed asymmetric synthesis of 1,1'-spirobi[indan-3,3'-dione] **37** *via* a double intramolecular C–H insertion process has also been reported (**Table 1.4**).[117] Of the rhodium(II) carboxylates tested, the best results were obtained for cyclisation with the bulky *tert*-butyl-substituted catalyst Rh_2(*S*-PTTL)$_4$, providing (*R*)-**37** in 78% yield and 80% ee (**Table 1.4**, entry 5). The use of Rh_2(*R*-PTTL)$_4$ also resulted in high enantioselectivity, producing (*S*)-**37** in 76% yield and 79% ee (**Table 1.4**, entry 6). The initial decomposition of **38** is thought to be responsible for the stereochemical outcome of the reaction *via* differentiation of the two enantiotopic hydrogens at the methylene insertion site. The subsequent C–H insertion at the methine C–H bond is believed to proceed with retention of configuration to generate **39**.

Table 1.4 *Asymmetric synthesis of 1,1'-spirobi[indan-3,3'-dione]* ***37****.*

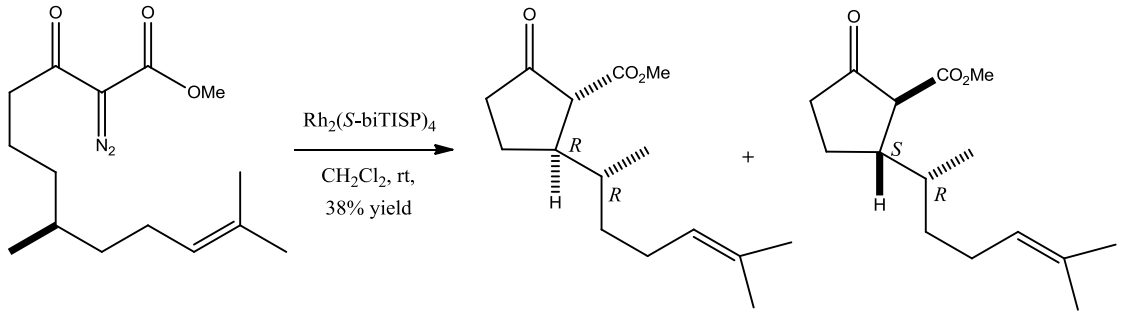


38

37 **39**

Entry	Rhodium(II) cat.	Temp.(°C)	Yield (%) **37**	ee (%) **37**
1	Rh_2(*S*-DOSP)$_4$	rt	48	8 (*R*)
2	Rh_2(*S*-PTPG)$_4$	0	67	21 (*R*)
3	Rh_2(*S*-PTPA)$_4$	0	71	25 (*R*)
4	Rh_2(*S*-PTTL)$_4$	0	83	68 (*R*)
5	Rh_2(*S*-PTTL)$_4$	–10	78	80 (*R*)
6	Rh_2(*R*-PTTL)$_4$	–10	76	79 (*S*)

The enantioselective synthesis of cyclic β-ketoester **40** was attempted by Taber and Malcolm in 2001.[118] For this purpose, several chiral rhodium(II) catalysts were examined, with Davies' bridged prolinate complex Rh_2(*S*-biTISP)$_4$ found to give the highest level of diastereocontrol (58% de) (**Scheme 1.3**). Interestingly, in contrast to previous observations by Hashimoto and co-workers, increased steric bulk at the ester moiety of **41** *via* change from the methyl (58% de) to dimethylpentyl (34% de) ester did not improve the level of stereocontrol achieved.[57]



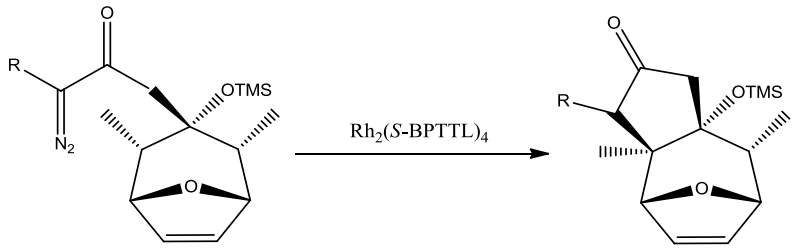
41 (*R*,*R*)-**40** (*S*,*R*)-**40**

79 : 21

Scheme 1.3

In 2004, Chiu and co-workers described the intramolecular C–H insertion of oxabicyclo[3.2.1]diazoketones **42** to produce oxatricyclic compounds **43**.[59] Eight different chiral rhodium(II) catalysts were tested for their ability to induce enantioselectivity in this desymmetrisation reaction, including two novel catalysts, Rh_2(*S*-NPTL)$_4$ and Rh_2(*S*-NPV)$_4$. The best results were achieved for the Rh_2(*S*-BPTTL)$_4$-catalysed reaction, showing moderate enantioselectivity for the cyclisation of **42** (**Table 1.5**). The use of copper-bis(oxazoline) complexes was later shown to be a viable catalytic choice for the desymmetrization of meso [3.2.1]oxabicyclic systems, with up to 50% ee achieved for the C–H insertion of a related cyclooctane diazoketone substrate in the presence of Cu(OTf)$_2$ and bis(oxazoline) **4h**.[119]

Table 1.5 *Intramolecular C–H insertions of meso oxabicyclo[3.2.1]diazoketones* ***42****.*



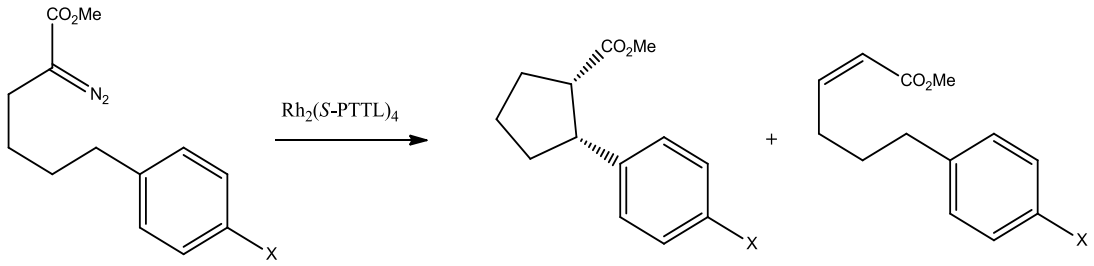
42 **43**

Entry	R	Solvent	Temp.	Yield (%) **43**	ee (%) **43**
1	H	CH_2Cl_2	rt	85	44
2	CO_2Et	$ClCH_2CH_2Cl$	reflux	73	30

The first highly enantio- and diastereoselective route to 1,2-disubstituted cyclopentanes *via* rhodium(II)-catalysed C–H insertion reactions of α-diazoesters was reported in 2005 (**Table 1.6**).[120] The Rh_2(*S*-PTTL)$_4$-catalysed cyclisation of **44** (X = H) in toluene at –78 °C was found to produce methyl *cis*-2-phenylcyclopentane-1-carboxylate **45** as the sole product in 95% ee, with no evidence of the corresponding *trans* isomer (**Table 1.6**, entry

2). The effect of temperature in this study was found to be of great importance, with an increase in reaction temperature corresponding to a decrease in enantioselectivity (**Table 1.6**, entry 1 *vs.* 2), as had previously been noted by Hashimoto and co-workers.[116] Solvent choice was also key, with the use of dichloromethane and ether as reaction solvent resulting in the formation of small quantities of α,β-unsaturated ester **46** *via* the competing 1,2-hydride shift pathway (**Table 1.6**, entry 2 *vs.* 3 and 4). High enantioselectivity and *cis* selectivity were also observed for insertions with electron-donating or -withdrawing groups on the *para* position of the benzene ring (**Table 1.6**, entries 5 and 6). Suprisingly, reduced asymmetric induction was observed for the Rh_2(*S*-BPTTL)$_4$-catalysed decomposition of **44** at –78 °C in toluene (67% ee), despite the increase in steric bulk of the catalyst. The use of immobilised polymer-supported Rh_2(*S*-PTTL)$_4$ was later investigated for this transformation.[121] The C–H insertion of **44** with the immobilised catalyst proceeded at –78 °C to provide *cis*-**45** as the sole product in 85% yield (**Table 1.6**, entry 7). Significantly, similar levels of enantioselectivity were recorded for the reaction of **44** in the presence of both polymer-supported and homogeneous Rh_2(*S*-PTTL)$_4$ (**Table 1.6**, entry 7 *vs.* 2).

Table 1.6 *Intramolecular C–H insertion reactions of α-diazo esters* ***44****.*



44 **45** **46**

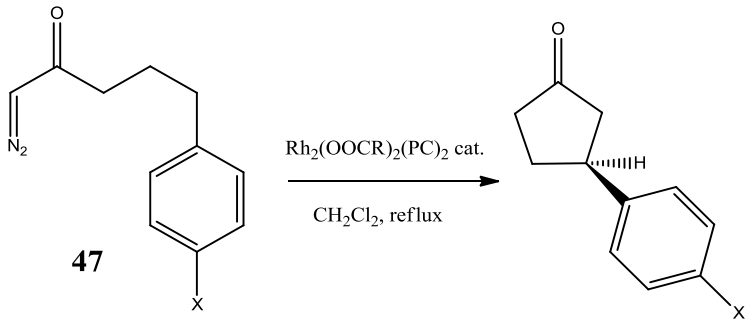
Entry	X	Solvent	Temp. (°C)	Yield (%)[a]	**45 : 46**	ee (%) **45**
1	H	toluene	0	80	82 : 18	81
2	H	toluene	–78	85	>99 : 0	95
3	H	CH_2Cl_2	–78	76	93 : 7	95
4	H	ether	–78	73	97 : 3	94
5	MeO	toluene	–78	85	>99 : 0	92
6	Cl	toluene	–78	81	>99 : 0	93
7[b]	H	toluene	–78	85	>99 : 0	94

[a] Combined yield of **45** and **46**, [b] Rh_2(*S*-PTTL)$_4$ immobilised on a polymer support was used as catalyst.

The enantioselective production of carbocyclic products *via* intramolecular C–H insertion reactions has been shown to successfully occur in the presence of rhodium(II) complexes derived from orthometalated arylphosphines, $Rh_2(O_2CMe)_2(PC)_2$. Moderate-to-good asymmetric induction was reported by Lahuerta and co-workers for the $Rh_2(O_2CCH_3)_2(PC)_2$-catalysed C–H insertion of α-diazoketone **47** (**Table 1.7**).[98] The electronic effects of the diazo substrates were of central importance in this study. Addition of an electron-withdrawing substituent (X = F, Cl) to the phenyl ring was shown to

correspond to an increase in enantioselectivity (**Table 1.7**, entry 1 *vs.* 2 and 4), while addition of an electron-donating group (X = OMe) provided no significant improvement in enantiocontrol (**Table 1.7**, entry 1 *vs.* 6). These results are in accordance with previous findings by Hashimoto and Ikegami.[113]

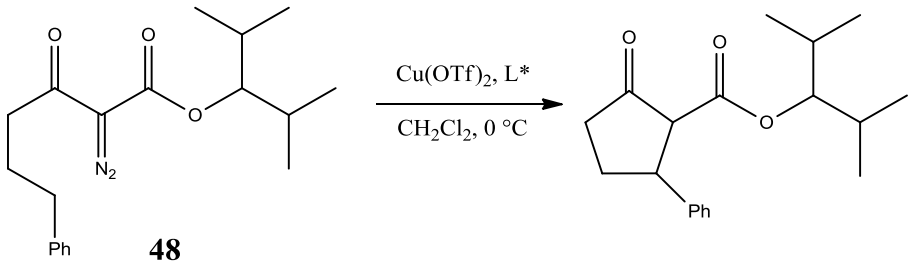
Table 1.7 *C–H insertion reactions of α-diazoketone **47** catalysed by ortho-metalated arylphosphine rhodium(II) complexes.*



Entry	X	Cat.	Yield (%)	ee (%)
1	H	**26a**	73	54 (*S*)
2	F	**26a**	68	60 (*S*)
3	F	**26g**	18	60 (*S*)
4	Cl	**26a**	87	65 (*S*)
5	Cl	**26e**	87	73 (*S*)
6	OMe	**26b**	95	56 (*R*)

The production of cyclopentanone products *via* C–H insertion reactions is also possible with copper catalysts. Moderate enantioselectivities were reported by Müller and co-workers for the intramolecular C–H insertion of α-diazo-β-keto ester **48** upon exposure to $Cu(OTf)_2$ in the presence of various chiral ligands (**Table 1.8**).[33,122]

Table 1.8 *Copper-catalysed C–H insertion reaction of α-diazo-β-keto ester **48**.*



Entry	Ligand (L*)	Yield (%)	ee (%)[a]
1	**4a**	17	51 (*S*)
2	**4b**	14	31 (*S*)
3	**4c**	35	60 (*R*)

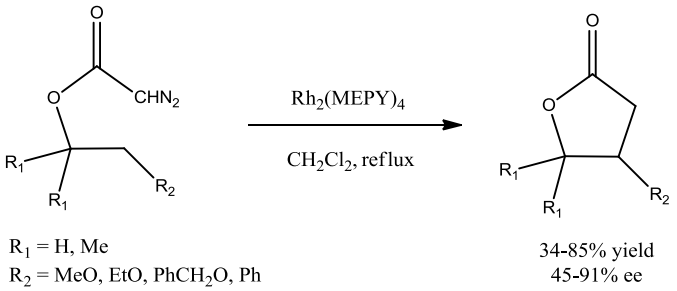
[a] Enantioselectivity determined following dealkoxycarbonylation.

1.6 Intramolecular heterocycle-producing C–H insertion reactions

1.6.1 Oxygen-containing heterocycle synthesis

1.6.1.1 Lactone synthesis

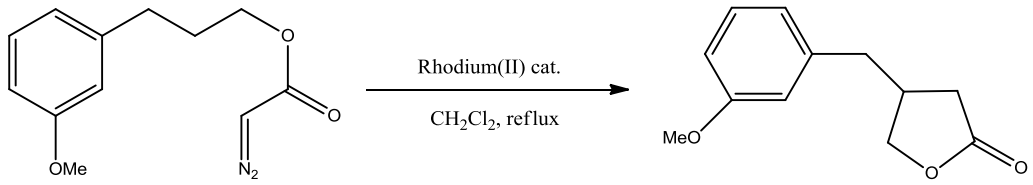
The asymmetric synthesis of oxygen-containing heterocycles, including lactones, chromanones and dihydrofurans, may be achieved *via* intramolecular C–H insertion reactions. Doyle's chiral rhodium(II) carboxamidates have proven themselves the catalysts of choice for the generation of lactone products, displaying high enantioselectivities for C–H insertion reactions with a variety of diazoacetates.[80,83,85,91,123,124] Early studies in this area demonstrated the effectiveness of Rh_2(*S*-MEPY)$_4$ and Rh_2(*R*-MEPY)$_4$ in providing an enantioselective route to trisubstituted γ-butyrolactones (**Scheme 1.4**).[80] In addition to producing high asymmetric induction, the chiral carboxamidate complexes were advantageous in suppressing competing intermolecular carbene dimer and azine formation with respect to rhodium(II) acetate-catalysed reactions, a phenomenon also observed in later reports.[84,125]



Scheme 1.4

A wide variety of Doyle's chiral carboxamidate catalysts have proven capable of effecting highly efficient intramolecular C–H activations. The imidazolidinone complex Rh_2(MPPIM)$_4$ has emerged as the superior catalytic choice in many cases, outperforming alternative rhodium(II) carboxamidates in terms of both yield and enantioselectivity (**Table 1.9**).[88,91,92,126] It has been suggested that the success of Rh_2(MPPIM)$_4$ may be attributed to its extended *N*-3 phenylpropanoyl chain which causes enhanced steric interactions between the catalyst ligands and the reacting carbene, thereby reducing the number of possible carbenoid orientations and resulting in increased enantioselectivity.[92,126]

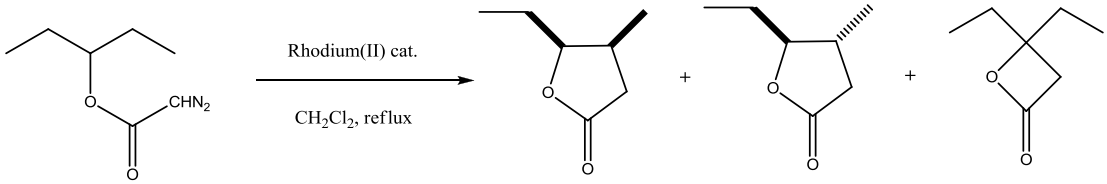
Table 1.9 *Intramolecular C–H insertion reactions of 3-(3-methoxyphenyl)propyl 2-diazoacetate in the presence of chiral carboxamidate complexes.*



Entry	Rhodium(II) cat.	Yield (%)	ee (%)
1	Rh_2(*R*-MPPIM)$_4$	63	93 (4*R*)
2	Rh_2(*S*-MACIM)$_4$	25	84 (4*S*)
3	Rh_2(*R*-MEPY)$_4$	66	68 (4*R*)

Excellent regio- and diastereocontrol may also be achieved for Rh_2(*S*-MPPIM)$_4$-catalysed C–H insertions. As shown in **Table 1.10**, diazo decomposition of 3-pentyl diazoacetate **49** results in three isomeric products (**50**, **51** and **52**). The oxazolidinone complex Rh_2(*S*-MEOX)$_4$ is seen to give the highest level of overall enantiocontrol, however, only Rh_2(*S*-MPPIM)$_4$ provides exceptional control in terms of regio-, diastereo- and enantioselectivity, producing lactone **50** as the major product in high ee.[88]

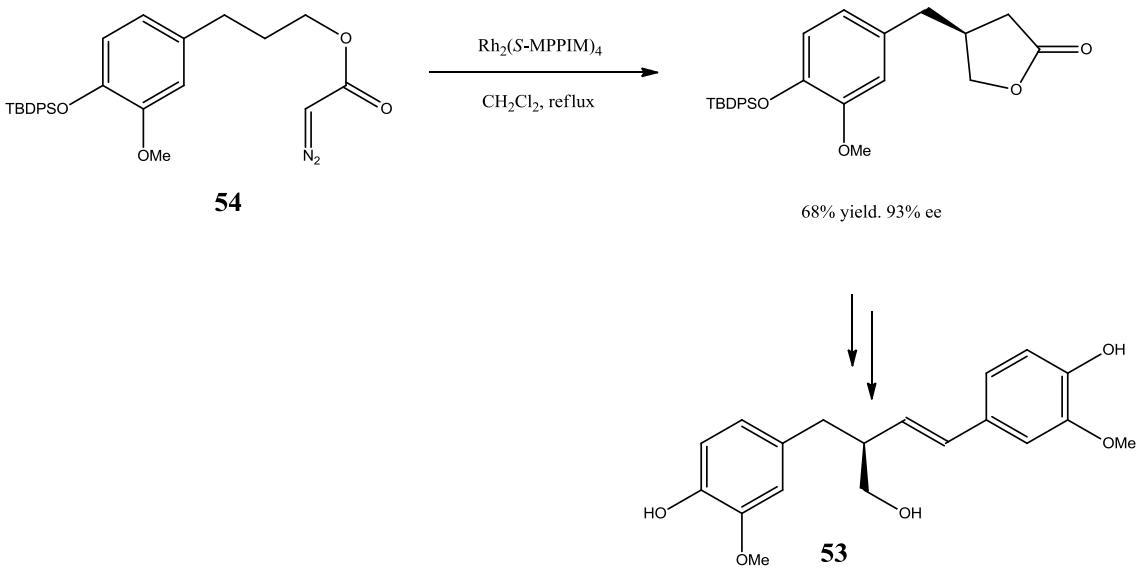
Table 1.10 *Intramolecular C–H insertion reactions of diazoacetate **49**.*



49 **50** **51** **52**

Entry	Rhodium(II) cat.	Yield (%)	Yield (relative %) **50** : **51** :**52**	ee (%) **50**	ee (%) **51**
1	Rh_2(*S*-MPPIM)$_4$	85	92 : 3 : 5	99	–
2	Rh_2(*S*-MACIM)$_4$	83	92 : 5 : 3	86	36
3	Rh_2(*S*-MEPY)$_4$	75	73 : 20 : 7	98	71
4	Rh_2(*S*-MEOX)$_4$	86	60 : 27 : 13	98	92

Rh_2(*S*-MPPIM)$_4$-catalysed C–H insertion reactions have been employed as key steps in syntheses of the natural lignan lactones, (–)- and (+)-enterolactone, (–)- and (+)-hinokinin, (–)-arctigenin, (+)-isodeoxy-podophyllotoxin, (+)-isolauricerisinol,[91] the necine base, (–)-turneforcidine,[127] and the platelet-aggregration inhibitor, (*S*)-(+)-imperanene **53**.[126] Synthesis of the latter was achieved with excellent enantioselectivity (93% ee) and without any evidence of competing β- or δ-lactone formation (**Scheme 1.5**).

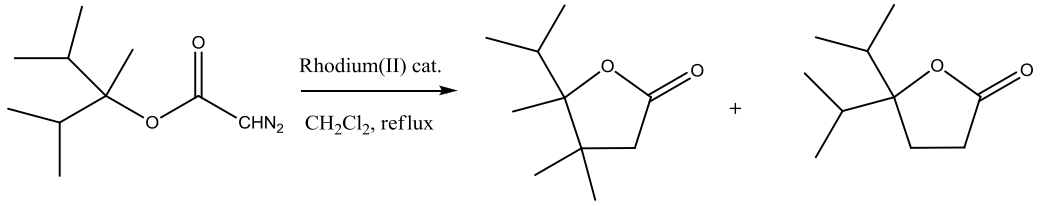


54

Scheme 1.5

In a 1995 report published by Doyle and co-workers, Rh_2(*S*-MACIM)$_4$ was shown to be the optimal catalyst for C–H insertion reactions of tertiary alkyl diazoacetates.[128] As seen in **Table 1.11**, decomposition of 2,3,4-trimethyl-3-pentyl diazoacetate **55** gave two γ-lactone products (**56** and **57**) resulting from insertion at methine and methyl sites, respectively.[128] For all catalysts tested, a strong preference for the tertiary insertion product **56** was observed, with Rh_2(*S*-MEPY)$_4$ giving the highest level of regiocontrol, but enantioselectivity in this case was low (61% ee). Despite previously showing success in the C–H insertion reactions of *N*-alkyl-*N*-(*tert*-butyldiazoacetamides),[86] no enantioinduction was recorded for the Rh_2(*S*-MEOX)$_4$-catalysed reaction. The use of Rh_2(*S*-MACIM)$_4$, however, resulted in good regio- and enantiocontrol, although failing to reach the levels of enantioselectivity commonly observed for insertion into methylene C–H bonds.[80,88,123,124] Similar results were obtained for the decomposition of tertiary 2-methyl-1-phenyl-propan-2-yl and *tert*-pentyl diazoacetates, with Rh_2(*S*-MACIM)$_4$ again inducing the highest levels of enantioselectivity.[128]

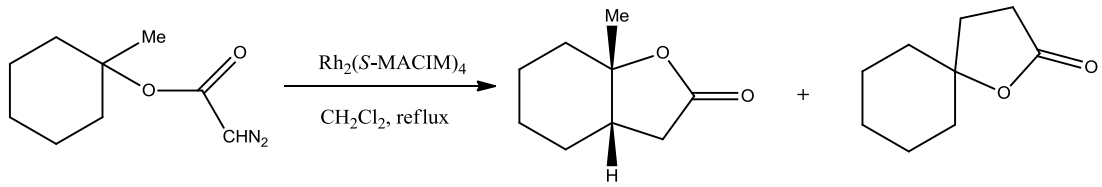
Table 1.11 *Rhodium(II)-catalysed insertion of 2,3,4-trimethyl-3-pentyl diazoacetate* ***55****.*



55 **56** **57**

Entry	Rhodium(II) cat.	Yield (%)	**56** : **57**	ee (%) **56**
1	Rh_2(*S*-MACIM)$_4$	73	83 : 17	85
2	Rh_2(*S*-MEPY)$_4$	66	93 : 7	61
3	Rh_2(*S*-MEOX)$_4$	70	70 : 30	0

The C–H activation of tertiary cycloalkyl diazoacetates is also possible;[125,128,129] Rh_2(*S*-MACIM)$_4$ was again found to the optimal catalytic choice for such a process, providing the *cis*-fused bicyclic lactone **58** in 61% yield and 90% ee (**Scheme 1.6**).[128] As with the previously described acyclic carbenoid reaction, insertion may occur at more than one site, resulting in both methylene (**58**) and methyl (**59**) insertion products. These results represent an improvement upon previous attempts by Müller and Polleux, who reported a 30% yield and 74% ee for **58** in the Rh_2(*S*-MEPY)$_4$-catalysed decomposition of **60** under similar conditions.[125]



90 : 10

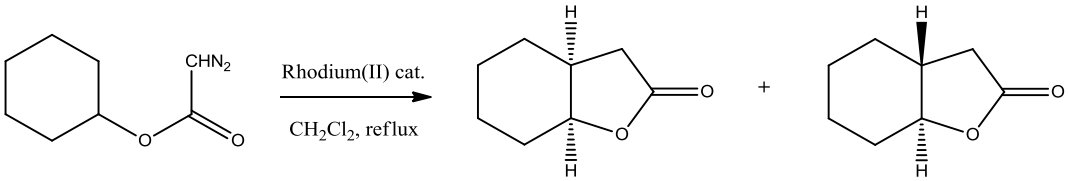
61% yield, 90% ee

60 **58** **59**

Scheme 1.6

Achievement of higher levels of asymmetric induction is possible for reactions with the related secondary cyclohexyl diazoacetate **61** in which the 1-methyl substituent is absent.[83,125] In this case, production of both *cis*- and *trans*-lactone products (**62** and **63**) was observed with greatest overall enantiocontrol being provided by Rh_2(*S*-MEPY)$_4$ and Rh_2(*S*-MEOX)$_4$, and greatest diastereocontrol being noted for decomposition in the presence of Rh_2(*S*-MACIM)$_4$ (**Table 1.12**). The reaction is believed to proceed *via* equatorial C–H bond insertion, with the *cis*- and *trans*-isomeric products resulting from equilibration between the two possible cyclohexyl chair conformations of the diazoacetate. Such a preference for equatorial C–H bond insertion over axial insertion has been widely observed in carbenoid reactions of cyclohexyl diazoacetates,[9,124,129,130] with only very few exceptions being noted to date.[124,131]

Table 1.12 *Intramolecular C–H insertion reactions of cyclohexyl diazoacetate **61**.*



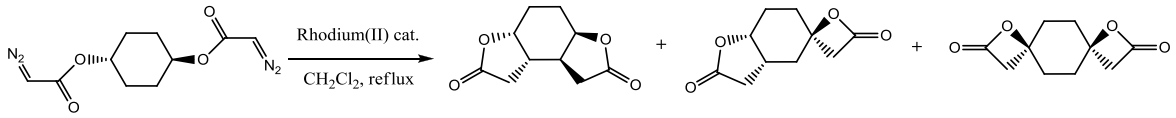
61 **62** **63**

Entry	Rhodium(II) cat.	Yield (%)	**62** : **63**	ee (%) **62**	ee (%) **63**
1[a]	Rh_2(*S*-MACIM)$_4$	70	99 : 1	97	65
2[a]	Rh_2(*R*-MEPY)$_4$	65	75 : 25	97	91
3[a]	Rh_2(*S*-MEOX)$_4$	50	55 : 45	96	95
4[b]	Rh_2(*S*-MEPY)$_4$	30	75 : 25	95	90

[a] Results reported by Doyle and co-workers.[83] [b] Results reported by Müller and Polleux.[125]

As previously discussed, the choice of catalytic system can often be a key decision in determining the regiochemical outcome of intramolecular C–H insertion reactions. This is clearly evident in the decomposition of the bis-diazoacetate of *trans*-1,4-cyclohexanediol **64**, which yields three insertion products (**Table 1.13**).[85] Use of the sterically complex imidazolidine catalysts, Rh_2(*S*-MPPIM)$_4$ and Rh_2(*S*-BSPIM)$_4$, in this reaction was seen to produce roughly equal amounts of the predicted bis-lactone **65** and the spirolactone **66**. In contrast, **66** was found to be the dominant product in reactions catalysed by Rh_2(*S*-MEPY)$_4$, Rh_2(*S*-IBAZ)$_4$ and Rh_2(*S*-MEOX)$_4$, which possess a more open catalytic framework by comparison with Rh_2(*S*-MPPIM)$_4$ and Rh_2(*S*-BSPIM)$_4$. The bis-spirolactone **67** was observed as a minor product only in the presence of Rh_2(*S*-MEPY)$_4$ and Rh_2(*S*-MEOX)$_4$. In all cases, two consecutive C–H insertion reactions were seen to occur. The first reaction induces the formation of an excess of one enantiomer over the other. Further enhancement of stereocontrol then occurs in the subsequent insertion reaction. This process of double stereodifferentiation results in extremely high levels of enantioselectivity, with all recorded chiral rhodium(II) carboxamidate-catalysed reactions resulting in ≥95% ee (**Table 1.13**). Amplification of asymmetric induction in this way has also been reported by Davies and co-workers for the intermolecular C–H activation of 2-substituted pyrrolidines[132] and dihydronaphthalenes.[133]

Table 1.13 *Bis-lactone vs. spirolactone formation in the decomposition of the bis-diazoacetate of* trans*-1,4-cyclohexanediol* ***64****.*

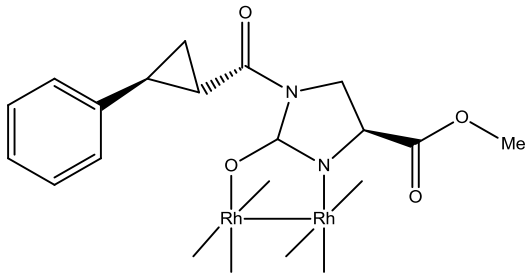


64 **65** **66** **67**

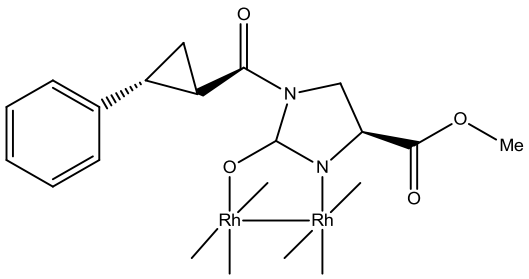
Entry	Rhodium(II) cat.	**65** : **66** : **67**	Yield (%)[a]	ee (%) **66**
1	Rh_2(*S*-MPPIM)$_4$	48 : 52 : 0	91	-
2	Rh_2(*S*,*S*-BSPIM)$_4$	48 : 52 : 0	90	99
3	Rh_2(*S*-MEPY)$_4$	11 : 80 : 9	58	95
4	Rh_2(*S*-IBAZ)$_4$	6 : 94 : 0	43	96
5	Rh_2(*S*-MEOX)$_4$	1 : 65 : 34	81	99

[a] Combined yield of **65**, **66** and **67**.

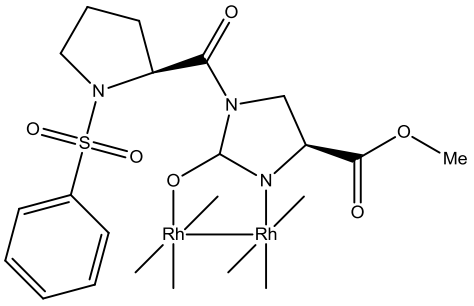
A different strategy towards achieving enhanced stereocontrol in C–H insertion reactions was adopted by Doyle and co-workers in 2005, who examined the application of catalysts possessing two stereogenic centres in the carbenoid reactions of cycloalkyl diazoacetates.[134] For this purpose, two diastereomeric rhodium(II) catalyst pairs were prepared by structural alteration of the *N*-acyl substituent of the methyl 2-oxo-imidazolidine-4*S*-carboxylate core structure (**Figure 1.19**).



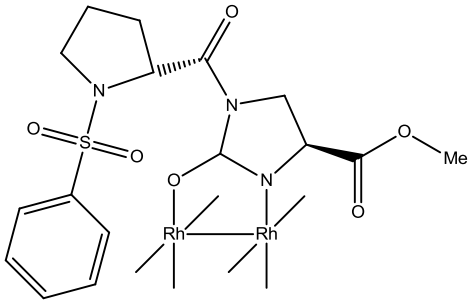
Rh_2(4*S*,2'*S*,3'*S*-MCPIM)$_4$-**68**



Rh_2(4*S*,2'*R*,3'*R*-MCPIM)$_4$-**69**



Rh_2(4*S*,2'*S*-BSPIM)$_4$-**70**

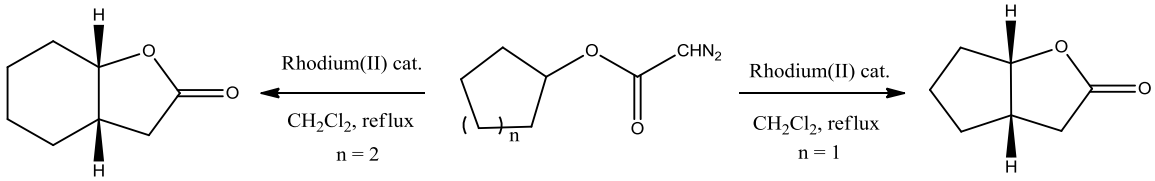


Rh_2(4*S*,2'*R*-BSPIM)$_4$-**71**

Figure 1.19

Employment of these novel rhodium(II) complexes in the decomposition of cyclopentyl- and cyclohexyl diazoacetate revealed the occurrence of a distinct "match/mismatch" phenomenon between the chiral ligand attachments (**Table 1.14**). In "matched" situations, where orientation of the ligand stereocentres was favourable, enantioselectivities for **72** and **73** were equivalent or improved with respect to that obtained with Rh_2(*S*-MPPIM)$_4$ (**Table 1.14**, entries 1 and 6 *vs.* 2, 4 and 7). In contrast, the "mismatched" case, defined by unfavourable catalyst orientations, resulted in a dramatic lowering of enantiocontrol (**Table 1.14**, entries 1 and 6 *vs.* 3, 5 and 8). "Matched/mismatched" effects were observed to the greatest effect with the *N*-benzenesulfonylprolinate-substituted catalysts **70** and **71**, with decreases in ee as large as 71% being recorded.

Table 1.14 *C–H insertion in the presence of rhodium(II) complexes possessing two stereogenic centres.*



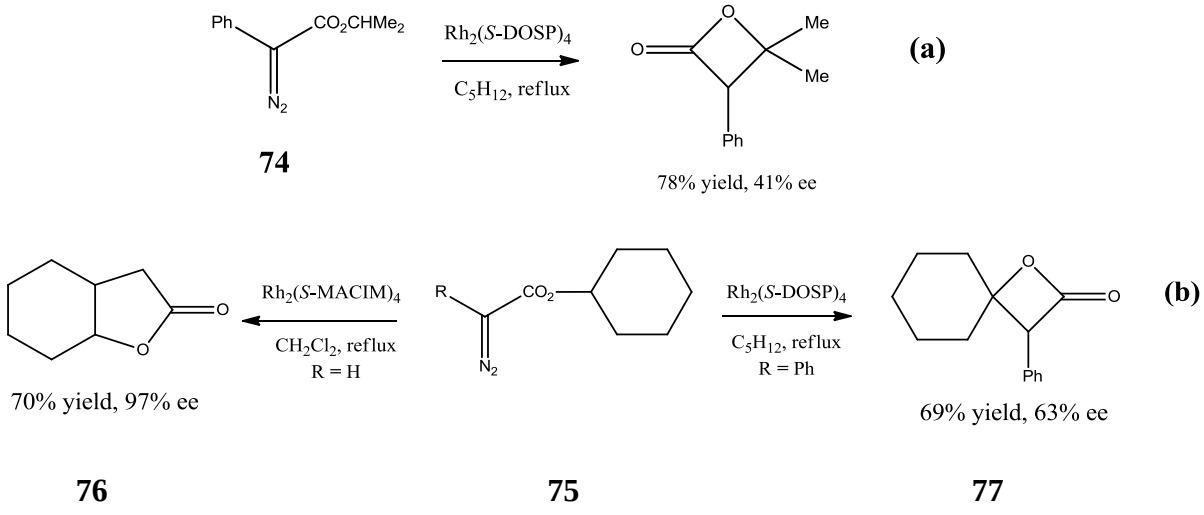
72 **73**

Entry	Rhodium(II) cat.	n	Yield (%) **72**/**73**	ee (%) **72**/**73**
1	Rh_2(*S*-MPPIM)$_4$	1	67	93
2	Rh_2(4*S*,2'*S*,3'*S*-MCPIM)$_4$ **68**	1	81	88
3	Rh_2(4*S*,2'*R*,3'*R*-MCPIM)$_4$ **69**	1	75	40
4	Rh_2(4*S*,2'*S*-BSPIM)$_4$ **70**	1	78	98
5	Rh_2(4*S*,2'*R*-BSPIM)$_4$ **71**	1	62	22
6	Rh_2(*S*-MPPIM)$_4$	2	71	92
7	Rh_2(4*S*,2'*S*-BSPIM)$_4$ **70**	2	88	>99[a]
8	Rh_2(4*S*,2'*R*-BSPIM)$_4$ **71**	2	89	74[a]

[a] Minor amounts of the *trans*-lactone also observed.

The propensity for five-membered ring formation in C–H insertion reactions has long been accepted.[6] However, as seen in the decomposition of **64**,[85] this preference is not absolute and the formation of four-membered ring products may also be observed. Such an occurrence has been noted in several intramolecular carbenoid reactions.[88,129,130,135] In 2001, Doyle and co-worker published a report of enantioselective β-lactone formation from phenyl diazoacetates.[135] Despite the introduction of considerable ring strain *via* its formation and the deactivating effect of the adjacent ester group, successful β-lactone formation was observed from *iso*-propyl and cyclohexyl diazoacetate precursors **74** and **75**, respectively [**Scheme 1.7**(a and b)]. In both instances, β-lactone formation was the dominant process over competing γ-lactone formation and moderate enantioselectivites were possible in the presence of Rh_2(*S*-DOSP)$_4$. The phenyl functionality at the α-diazo position of the isopropyl and cyclohexyl substrates is of critical importance in producing the targeted four-membered ring. Replacement of the phenyl group with hydrogen causes a shift in product formation towards the more sterically favourable γ-lactone, as observed

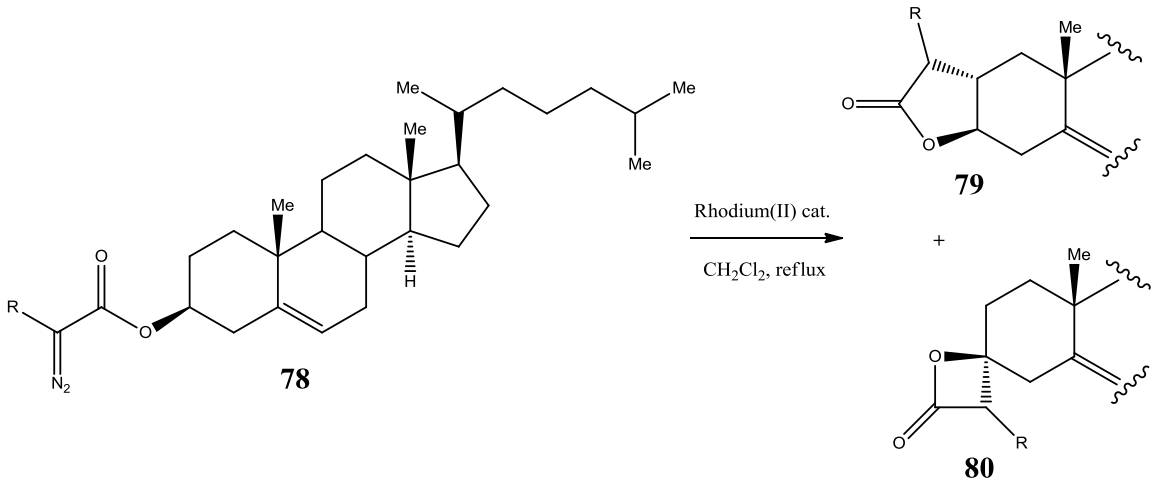
in the decomposition of cyclohexyl diazoacetate **75** (R = H), in which production of the γ-lactone **76** is dominant and formation of β-lactone **77** is negligible [**Scheme 1.7**(b)].[83]



Scheme 1.7

Competition between γ- and β-lactone formation was again observed for the C–H insertion reactions of 3-substituted steroidal diazoacetates **78** (**Table 1.15**).[130] Catalyst selection in this study was seen to have a significant effect on regioselectivity, with *R*-configured catalysts favouring formation of the γ-lactone product **79** (**Table 1.15**, entries 2 and 4) and *S*-configured catalysts favouring formation of the β-lactone product **80** (**Table 1.15**, entries 1 and 3). In all cases, insertion occurs *via* equatorial C–H bond insertion. Decomposition of **78** in the presence of chiral bis(oxazoline) copper(I) complexes was also shown to be a viable option, however, regioselectivities in this case were poor. As previously observed,[135] changing to the phenyl-substituted diazoacetate carbenoid precursor (R = Ph) resulted in exclusive β-lactone production (**Table 1.15**, entries 5 and 6).

Table 1.15 *β- vs. γ-lactone formation in the C–H insertion reactions of 3-substituted steroidal diazoacetates* ***78****.*

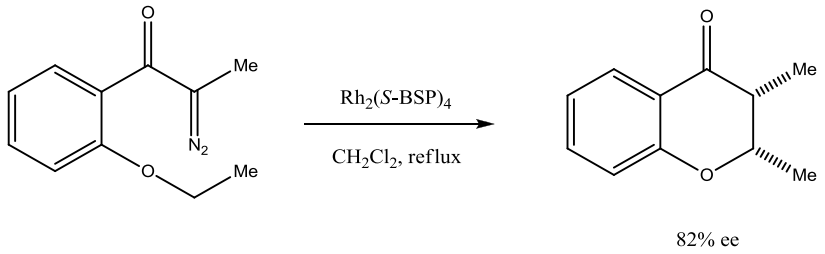


Entry	Rhodium(II) cat.	R	Yield (%)	**79** : **80**
1	Rh_2(*S*-MEPY)$_4$	H	74[a]	33 : 67
2	Rh_2(*R*-MEPY)$_4$	H	81[a]	94 : 6
3	Rh_2(*S*-MEOX)$_4$	H	80[a]	10 : 90
4	Rh_2(*R*-MEOX)$_4$	H	81[a]	89 : 11
5	Rh_2(*R*-MEAZ)$_4$	Ph	69	0 : 100
6[b]	Rh_2(*S*-DOSP)$_4$	Ph	58	0 : 100

[a] Combined yield of **79** and **80** following separation from the catalyst. [b] Reaction conducted in refluxing pentane.

1.6.1.2 Chromanone synthesis

The first application of C–H insertion chemistry for the enantioselective synthesis of six-membered oxygen heterocycles was published by McKervey and Ye in 1992.[136] In this study, the asymmetric production of various chromanones from α-diazoketone substrates in the presence of chiral rhodium(II) carboxylate catalysts was reported. Enantioselectivities obtained were in general moderate, with the best results being noted for the decomposition of **81** with the prolinate catalyst Rh_2(*S*-BSP)$_4$ providing primarily the *cis*-isomer of **82** in 82% ee (**Scheme 1.8**).

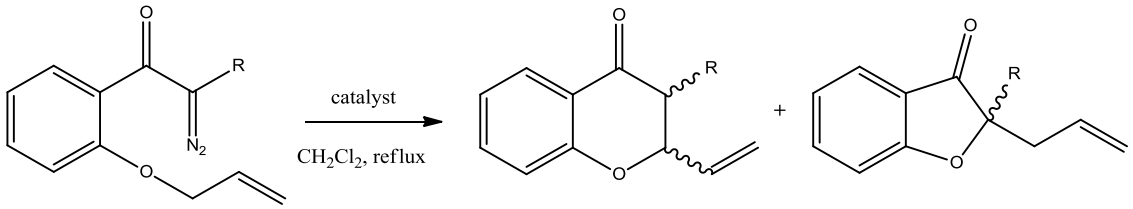


81 **82**

Scheme 1.8

The range of possible diazo precursors for carbenoid chromanone synthesis was later extended to include phenyl and vinyl derivatives of **81**.[56] Decomposition of **83** in the presence of a variety of different chiral rhodium(II) and copper(I) catalysts was shown to result in two isomeric products, arising from C–H insertion (**84**) and oxonium ylide-2,3-sigmatropic rearrangement pathways (**85**), respectively. Reaction with all tested carboxylate catalysts was seen to give predominantly the C–H insertion product **84** (**Table 1.16**, entries 1–4), while cyclisation under the influence of a chiral copper(I)-bis(oxazoline) complex provided solely benzofuranone **85** (**Table 1.16**, entries 5 and 6). Rh_2(*S*-BSP)$_4$ was again shown to induce the highest levels of asymmetric induction, producing *cis*-**84** in 60% ee. Improvement of this value to 79% ee was possible by a reduction of the reaction temperature to 0 °C.

Table 1.16 *C–H insertion vs. oxonium ylide-2,3-sigmatropic rearrangement in the decomposition of* ***83****.*



83 **84** **85**

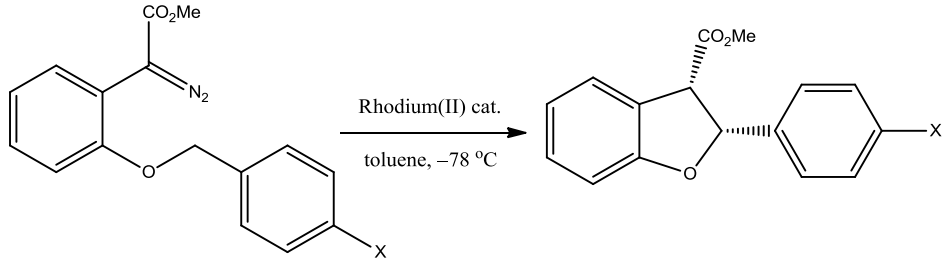
Entry	Catalyst	R	**84** : **85**	**84** *cis* : *trans*	% ee[a] **84**
1	Rh_2(*S*-BSP)$_4$	Me	97 : 3	93 : 7	60
2	Rh_2(*S*-BSP)$_4$	Ph	95 : 5	[b]	45
3	**7b**	Me	96 : 4	85 : 15	31
4	**7c**	Me	82 : 18	75 : 25	20
5	Cu/**4f**	Me	0 : 100	–	–
6	Cu/**4f**	Ph	0 : 100	–	–

[a] Enantioselectivity for *cis*-**84**. [b] Values not provided in original report.

1.6.1.3 Dihydrobenzofuran synthesis

Numerous research groups have undertaken investigations examining the synthesis of dihydrobenzofurans *via* aryl diazoacetate decomposition. In 2002, Hashimoto and co-workers reported the enantio- and diastereoselective synthesis of *cis*-2-aryl-3-methoxycarbonyl-2,3-dihydrobenzofurans *via* rhodium(II) carboxylate-catalysed C–H insertion reactions.[137] Choice of catalyst in this study was seen to be key, with only the phthaloyl catalysts Rh_2(*S*-PTTL)$_4$ and Rh_2(*S*-BPTTL)$_4$, both featuring a bulky *tert*-butyl substituent, providing exclusively the *cis*-isomer with good enantioselectivity (**Table 1.17**). This high level of asymmetric induction was found to be preserved for the decomposition of aryl diazoacetates possessing electron-withdrawing or -donating groups in the *para* position on the benzene ring (**Table 1.17**, entries 3–5).

Table 1.17 *Enantio- and diastereoselective synthesis of cis-2-aryl-3-methoxycarbonyl-2,3-dihydrobenzofurans* via *rhodium(II) carboxylate-catalysed C–H insertion reactions.*

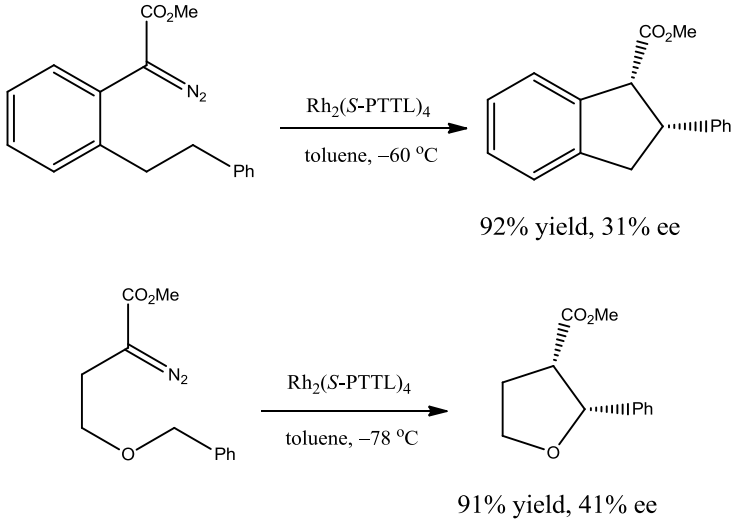


86 **87**

Entry	Rhodium(II) cat.	X	Yield (%)[a] **87**	ee (%) **87**
1	Rh_2(*S*-PTTL)$_4$	H	86	94
2	Rh_2(*S*-BPTTL)$_4$	H	70	91
3	Rh_2(*S*-PTTL)$_4$	Cl	79	94
4	Rh_2(*S*-PTTL)$_4$	Me	84	91
5	Rh_2(*S*-PTTL)$_4$	OMe	89	94

[a] Less than 1% of *trans* isomer observed.

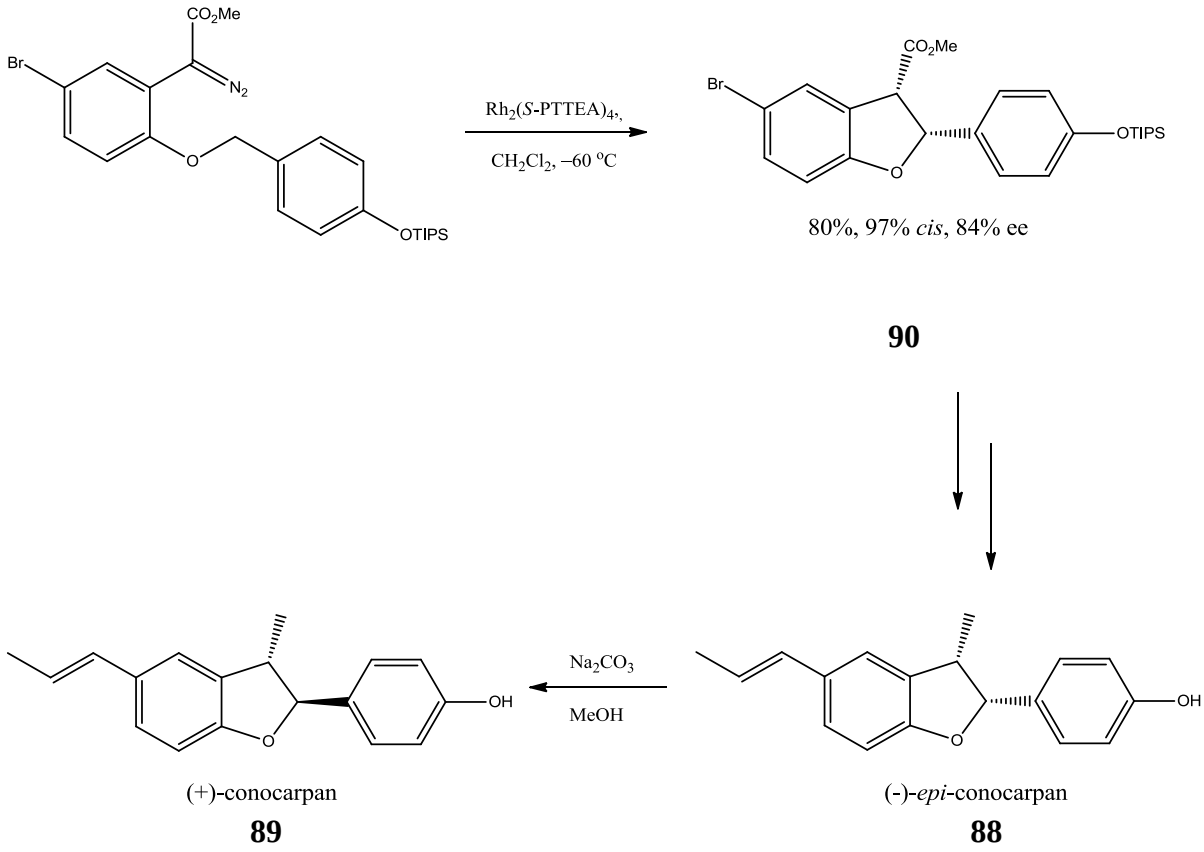
The presence of both the benzene ring of the aryl diazoacetate and the oxygen adjacent to the C–H insertion site is believed to be crucial in allowing highly enantioselective reactions to occur. As seen in **Scheme 1.9**, loss of either feature results in the destruction of enantiocontrol.[137] This result reinforces previous findings by McKervey, who noted very low asymmetric induction for the synthesis of *cis* disubstituted dihydrofurans from acyclic diazoacetate precursors.[138]



Scheme 1.9

The synthetic methodology, described above, has been successfully applied to the asymmetric synthesis of the neolignans, (–)-epi-conocarpan **88** and (+)-conocarpan **89**.[58] For this purpose, the newly developed rhodium(II) carboxylate complex Rh_2(*S*-PTTEA)$_4$ was found to be the most advantageous catalyst choice, providing the desired *cis* isomer

of **90** in 80% yield and 84% ee (**Scheme 1.10**). A similar synthetic strategy was adopted by Fukuyama and co-workers for the total syntheses of the macrocyclic spermine alkaloid, (–)-ephedradine,[139,140] and the pentacyclic indole alkaloid, (–)-serotobenine.[141] In contrast to the cyclisations carried out by Hashimoto and co-workers, exclusive formation of the thermodynamically favourable *trans* isomer of the dihydrobenzofuran products was reported for the production of both natural products. Such an outcome was achieved by an increase in steric bulk at the ester moiety of the aryl diazoacetate *via* attachment of a chiral auxiliary.

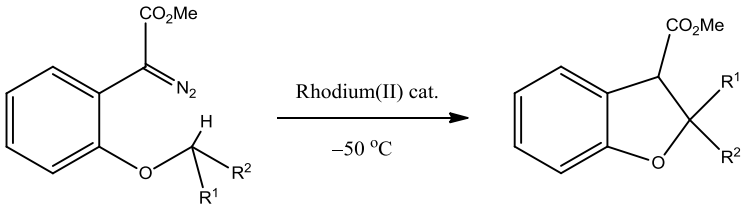


Scheme 1.10

Catalyst choice for the intramolecular C–H insertion formation of dihydrobenzofurans may be extended beyond Hashimoto's phthaloyl complexes to include proline-, adamantylglycine- and imidazolidinone-derived catalysts, namely Rh_2(*S*-DOSP)$_4$, Rh_2(*S*-PTAD)$_4$ and Rh_2(OAc)(DPTI)$_3$ (DPTI = diphenyltriflylimidazolidinone). Aryl diazoacetate decomposition in the presence of the latter complex has been shown to occur with moderate yield (51%) and excellent enantioselectivity (96% ee).[142] Insertion into methine, methylene and methyl sites is possible in the presence of Rh_2(*S*-DOSP)$_4$ or the related bridged complexes Rh_2(*S*-biTISP)$_4$ and Rh_2(*S*-biTBSP)$_4$ (**Table 1.18**).[143] Greatest enantiocontrol for primary C–H insertion reactions was observed with Rh_2(*S*-biTISP)$_4$ and Rh_2(*S*-biTBSP)$_4$ (**Table 1.18**, entries 1 and 2), while cyclisation with Rh_2(*S*-DOSP)$_4$ provided the highest levels of asymmetric induction for reaction at tertiary sites (**Table 1.18**, entries 6–8). All three catalysts proved proficient for C–H insertion into a

methylene group (**Table 1.18**, entries 3–5). That Rh_2(*S*-DOSP)$_4$ and the bridged catalysts Rh_2(*S*-biTISP)$_4$ and Rh_2(*S*-biTBSP)$_4$ provide the opposite sense of asymmetric induction has also been noted in both cyclopropanation[65,144] and intermolecular C–H insertion processes.[67,69]

Table 1.18 *Intramolecular C–H insertion of aryldiazoacetates into methine, methylene and methyl C–H bonds.*

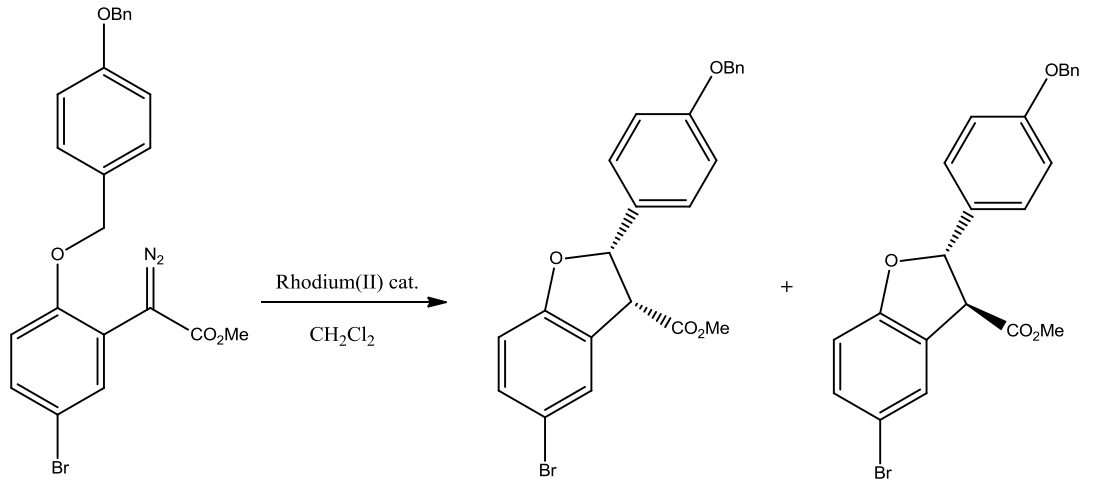


Entry	Rhodium(II) cat.	R^1	R^2	Solvent	Yield (%)	ee (%)
1	Rh_2(*S*-biTISP)$_4$	H	H	CH_2Cl_2	70	43 (–)
2	Rh_2(*S*-biTBSP)$_4$	H	H	CH_2Cl_2	70	68 (–)
3	Rh_2(*S*-DOSP)$_4$	H	Me	hexane	85[a]	60 (–)[d]
4	Rh_2(*S*-biTISP)$_4$	H	Me	CH_2Cl_2	50[b]	53 (+)[d]
5	Rh_2(*S*-biTBSP)$_4$	H	Me	CH_2Cl_2	70[c]	45 (+)[d]
6	Rh_2(*S*-DOSP)$_4$	Me	Me	hexane	98	94 (+)
7	Rh_2(*S*-biTISP)$_4$	Me	Me	CH_2Cl_2	48	60 (–)
8	Rh_2(*S*-biTBSP)$_4$	Me	Me	CH_2Cl_2	57	65 (–)

[a] Yield of *cis* and *trans* isomers, de (*cis*) = 60%. [b] Yield of *cis* and *trans* isomers, de (*cis*) = 70%. [c] Yield of *cis* and *trans* isomers, de (*cis*) = 75%. [d] % ee of *cis* isomer.

The ability of Davies' adamantate catalyst Rh_2(*S*-PTAD)$_4$ to successfully catalyse enantioselective intramolecular C–H insertions was first demonstrated for the synthesis of *cis*-2-aryl-3-methoxycarbonyl-2,3-dihydrobenzofurans,[71] in which the asymmetric induction obtained was seen to be in the range of previous results recorded by Hashimoto and co-workers for the same transformation.[137] In the same study, a vast improvement in stereochemical outcome was observed for employment of Rh_2(*S*-PTAD)$_4$ in a key step in the synthesis of the natural product, (–)-ephedradine A.[71] The synthetic route earlier adopted by Fukuyama and co-workers provided low levels of enantioselectivity (32% ee) and diastereoselectivity (20% de) in the presence of Rh_2(*S*-DOSP)$_4$. Reasonable stereocontrol [86% de (*trans*)] was obtained only when Rh_2(*S*-DOSP)$_4$ was used in conjunction with a lactamide-type chiral auxiliary.[139,145] In contrast, the Rh_2(*S*-PTAD)$_4$-catalysed decomposition of **91** provided predominantly the *cis* isomeric product **92** in 87% de and 79% ee in the absence of any chiral auxiliary. The desired *trans* isomer **93** could then be easily obtained by equilibration in the presence of sodium methoxide.

Table 1.19 *The key C–H insertion step in the synthesis of (–)-ephedradine A.*



91 **92** **93**

Entry	Rhodium(II) cat.	Temp. (°C)	Yield (%)	**92** : **93**	% ee **92**	% ee **93**
1[a]	Rh_2(*S*-DOSP)$_4$	23	72	2 : 3	–	32
2[b]	Rh_2(*S*-PTAD)$_4$	0	72	14 : 1	79	–

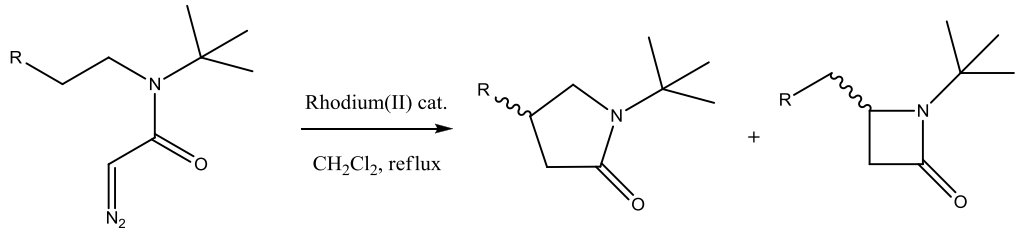
[a] Results reported by the Fukuyama group.[145] [b] Results reported by the Davies group.[71]

1.6.2 Nitrogen-containing heterocycle synthesis

1.6.2.1 Lactam synthesis

Early studies exploring the enantioselective synthesis of nitrogen-containing heterocycles were conducted by Doyle and co-workers, who examined the rhodium(II) carboxamidate catalysed C–H insertion reactions of *N*-alkyl-*N*-(*tert*-butyl)diazoacetamides.[86] As was observed with the corresponding lactone syntheses, production of both four- (β-lactam) and five- (γ-lactam) membered ring products may occur. Control of such regiochemical variation was shown to be possible by careful choice of *N*-alkyl substituent for the diazoamide precursor (**Table 1.20**). Thus, while a mixture of γ-**94** and β-**95** lactam products was observed for the C–H insertion reactions of *N*-(*tert*-butyl)-2-diazo-*N*-pentylacetamide and *N*-(*tert*-butyl)-2-diazo-*N*-(4-methylpentyl) acetamide (**Table 1.20**, entries 1–4), exclusive γ-lactam formation was recorded for decomposition of the ethoxy derivative of **96** (R = OEt), providing pyrrolidinone **94** in high yield and moderate enantioselectivity for cyclisation with both Rh_2(*S*-MEPY)$_4$ and Rh_2(*S*-MEOX)$_4$.

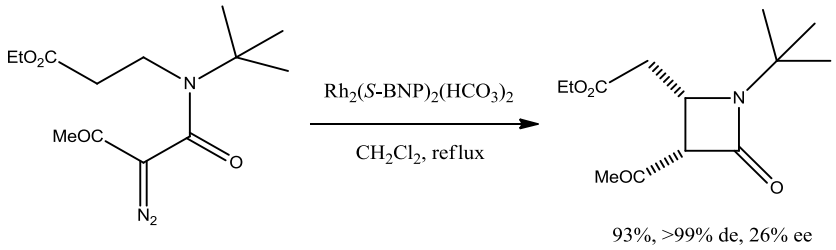
Table 1.20 *Rhodium(II) carboxamidate-catalysed C–H insertion reactions of* N-*alkyl*-N-*(*tert-*butyl)diazoacetamides.*



96 **94** **95**

Entry	Rhodium(II) cat.	R	Yield (%)	**94** : **95**	ee (%) **94**	ee (%) **95**
1	Rh_2(*S*-MEPY)$_4$	Et	74	88 : 12	63	73
2	Rh_2(*S*-MEOX)$_4$	Et	82	91 : 9	71	80
3	Rh_2(*S*-MEPY)$_4$	*i*-Pr	91	80 : 20	58	72
4	Rh_2(*S*-MEOX)$_4$	*i*-Pr	93	82 : 18	69	65
5	Rh_2(*S*-MEPY)$_4$	OEt	91	100 : 0	58	–
6	Rh_2(*S*-MEOX)$_4$	OEt	97	100 : 0	78	–

Although the formation of five-membered rings is typically favoured in C–H insertion reactions,[6] generation of β-lactam products is feasible, owing to the activating effect of the adjacent nitrogen atom at the insertion site.[146] In studies employing the achiral $Rh_2(OAc)_4$ catalyst, the *N*-*tert*-butyl group has proven superior to other possible substituents in inducing preferential β-lactam formation.[146] Such a trend is preserved for diazoacetamide decomposition in the presence of chiral rhodium(II) complexes. As seen in Scheme **1.11**, β-lactam **97** is the sole product from the Rh_2(*S*-BNP)$_2$(HCO$_3$)$_2$-catalysed C–H insertion reaction of the *N*-*tert*-butyl diazoacetamide **98**.[94]



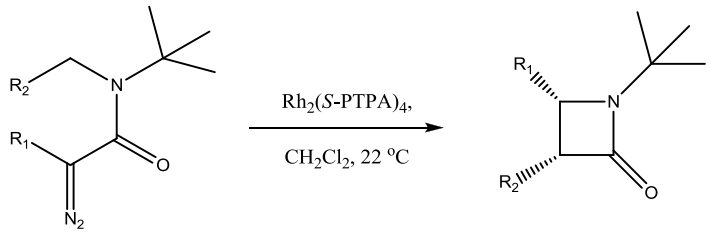
98 **97**

Scheme 1.11

A similar outcome was observed for the intramolecular C–H insertion reactions of *N*-alkyl-*N*-*tert*-butyl-α-methoxycarbonyl-α-diazoacetamides.[147] Cyclisation of **99** in the presence of the phthaloyl catalyst Rh_2(*S*-PTPA)$_4$ was seen to provide exclusively the *cis* isomer of azetidinone **100** (**Table 1.21**). Highest enantioselectivity was noted for the insertion of the *N*-benzyl-*N*-*tert*-butyl derivative of **99**, producing **100** in 94% yield and 74% ee (**Table 1.21**, entry 1). Interestingly, change of the substituent α to the diazo from

the methoxycarbonyl group to the acetyl group resulted in lower asymmetric induction and the formation of the *trans* isomer of **100** (**Table 1.21**, entry 4). This would seem to suggest that isomerisation of the initial *cis* product of **100** (R^1 = COMe) occurs to generate the observed *trans* stereoisomer. Isomerisation of this type had previously been encountered by Doyle and co-workers in a study of the C–H insertion reactions of *N*,*N*-disubstituted diazoacetoacetamides.[148]

Table 1.21 *Intramolecular C–H insertion reaction of* N-*alkyl*-N-*(*tert-*butyl)-α-methoxycarbonyl-α-diazoacetamides* ***99****.*



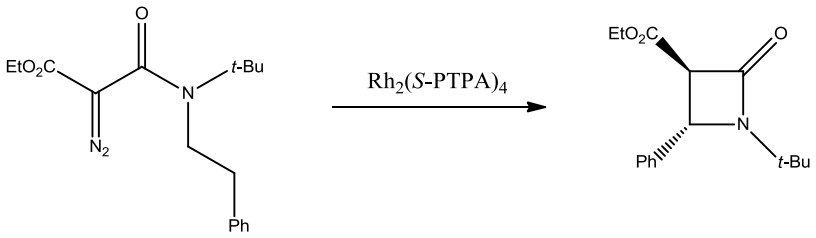
99 **100**

Entry	R^1	R^2	Yield (%) **100**	ee (%) **100**
1	CO_2Me	Ph	94	74 (3*R*, 4*R*)
2	CO_2Me	CH_2CO_2Me	98	56 (3*R*, 4*S*)
3[a]	CO_2Me	$CH_2CH_2CH_3$	97	60 (3*R*, 4*S*)
4	COMe	Ph	64[b]	50 (3*R*, 4*R*)

[a] Reaction was conducted at 16 °C. [b] *trans* Isomer of **100**.

Enantioselective intramolecular C–H insertion reactions of diazoacetamides using both supercriticial carbon dioxide (*sc*CO_2) and water as the reaction solvent have also been described (**Table 1.22**, entries 1 and 2).[149] A slight decrease in enantiocontrol was observed for the reactions in *sc*CO_2 and water compared to the corresponding process in dichloromethane (**Table 1.22**, entries 1 and 2 *vs.* entry 3), although notably the former two solvents are more environmentally friendly and permit facile catalyst recovery.

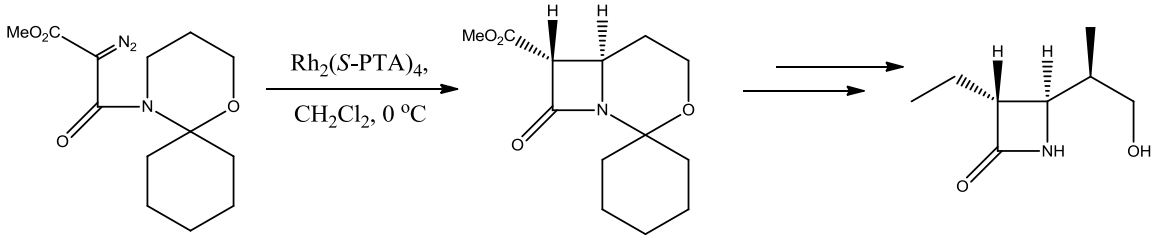
Table 1.22 *Asymmetric intramolecular C–H insertions of ethyl 3-[*tert-*butyl(phenethyl)amino]-2-diazo-3-oxopropanoate in* scCO_2 *and water.*



Entry	Solvent	Temp (°C)	Time (h)	Yield (%) **100**	ee (%) **100**
1	*sc*CO_2[a]	30	24	>97	52
2	H_2O	25	21	93	60
3	CH_2Cl_2	25	3.5	93	66

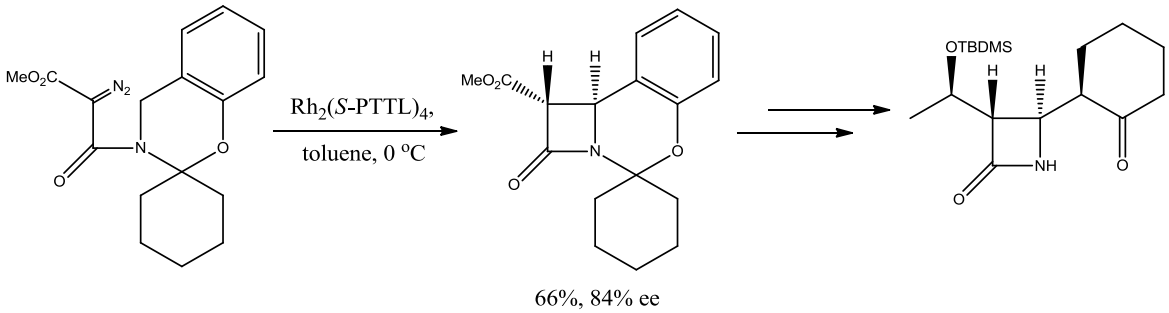
[a] pressure = 70 bar

While the ability of the *N*-*tert*-butyl group to induce preferential β-lactam formation in the above examples cannot be doubted, subsequent removal of this *tert*-butyl group may prove problematic. Such an obstacle was encountered by Hashimoto and co-workers in their attempts to produce a key azetidin-2-one for the synthesis of carbapenem antibiotics.[150] Resolution of this issue was possible by replacement of the troublesome *tert* butyl group with an *N*,*O*-acetal moiety. This strategy was found to maintain exclusive β-lactam formation, whilst also providing high levels of enantiocontrol in the presence of Rh_2(*S*-PTA)$_4$, thus allowing synthesis of the desired carbapenem **101** (**Scheme 1.12**). A similar approach was adopted for the generation of a key intermediate required for the synthesis of trinem antibiotics.[151] Interestingly, in this study, Rh_2(*S*-PTA)$_4$-catalysed decomposition of the *N*,*O*-cyclohexylidene acetal **102**, which differs from **103** by the incorporation of a benzene ring, provided predominantly the opposite enantiomer (–)-**104** than that expected from the cyclisation of **103**. Such a result was also observed for catalysis with Rh_2(*S*-PTPA)$_4$, Rh_2(*S*-PTPG)$_4$ and Rh_2(*S*-PTV)$_4$. Enantioselective production of the desired (+)-**104** was, however, found to be possible for reaction in the presence of Rh_2(*S*-PTTL)$_4$, thereby permitting synthesis of the trinem intermediate **105** (**Scheme 1.13**).



103 94%, 96% ee **101**

Scheme 1.12



66%, 84% ee

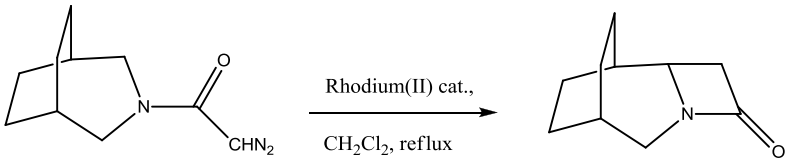
102 (+)-**104** **105**

Scheme 1.13

Preferential β-lactam formation may also be observed for the cyclisations of diazoacetylazacycloalkanes. The C–H insertion reaction of 3-diazoacetyl-3-azabicyclo[3.2.2]nonane **106** was shown to produce β-lactam **107** as the sole product in

high yield and high enantioselectivity (**Table 1.23**).[81] It is thought that the conformational rigidity imparted by the cyclic system of **106** is responsible for the observed exclusive β-lactam formation. Thus, reaction of the more flexible diazoamide **108** provides both β-(**109**) and γ-(**110**) lactam products (**Table 1.24**).

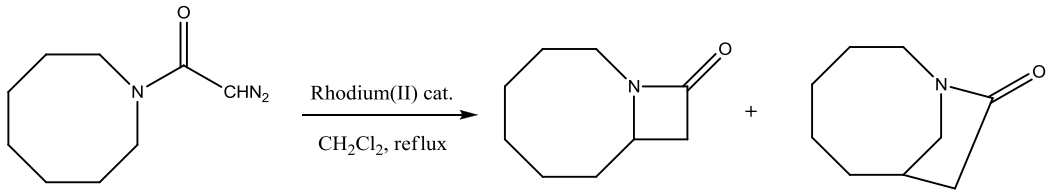
Table 1.23 *Preferential β-lactam formation in the C–H insertion reaction of 3-diazoacetyl-3-azabicyclo[3.2.2]nonane **106**.*



106 **107**

Entry	Rhodium(II) cat.	Yield (%) **107**	ee (%) **107**
1	Rh_2(*S*-MEOX)$_4$	81	93
2	Rh_2(*S*-MEPY)$_4$	70	96

Table 1.24 *β- vs. γ-lactam formation in the C–H insertion reaction of **108**.*



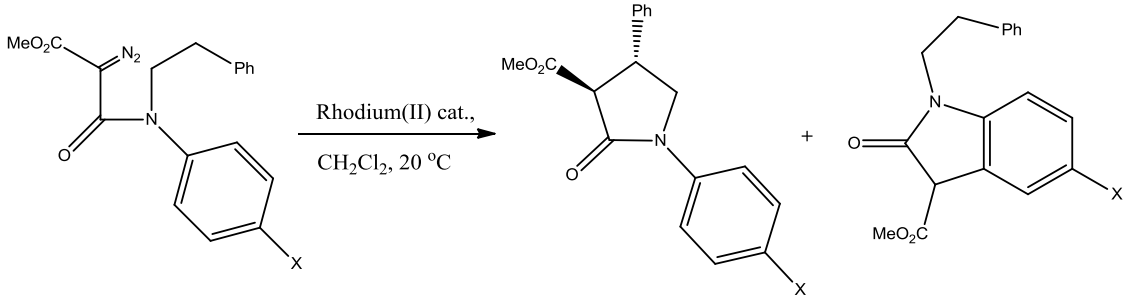
108 **109** **110**

Entry	Rhodium(II) cat.	Yield (%)	**109** : **110**	ee (%) **109**	ee (%) **110**
1	Rh_2(*S*-MEOX)$_4$	95	26 : 74	15	98
2	Rh_2(*S*-MEPY)$_4$	97	40 : 60	31	97

The first enantioselective catalytic synthesis of 4-aryl-substituted 2-pyrrolidinones was reported by Hashimoto and co-workers in 1998 (**Table 1.25**).[152] In this study, aromatic C–H insertion was found to be a competing reaction pathway in the decomposition of the α-methoxycarbonyl diazoacetamide **111** (X = OMe), producing an excess of 2(3*H*)-indolinone **112** over the desired aliphatic C–H insertion product *trans*-pyrrolidinone **113** for the Rh_2(*S*-PTPA)$_4$-catalysed reaction (**Table 1.25**, entry 1). It is believed that aromatic C–H insertion reactions proceed *via* a mechanism of electrophilic addition of the rhodium(II) carbenoid carbon to the aromatic ring followed by 1,2-hydride migration to give the aromatic insertion product.[76,153] Therefore, elimination of this competing process may be achieved by attachment of an electron-withdrawing substituent at the *para* position of the aromatic ring. This was indeed found to be true and exclusive production of **113** was observed for the C–H insertion reaction of **111** (X = NO_2) in the presence of

various rhodium(II) phthaloyl complexes (**Table 1.25**, entries 2–5). The success of this method was illustrated in the syntheses of the $GABA_A$ receptor agonist, (*R*)-(–)-baclofen,[152] and the phosphodiesterase type IV inhibitor, (*R*)-(–)-rolipram,[61] both of which feature enantioselective C–H insertion reactions of *N*-4-nitrophenyl-α-methoxycarbonyl-α-diazoacetamides as the key synthetic steps.

Table 1.25 *Enantioselective rhodium(II)-catalysed synthesis of 4-aryl-substituted 2-pyrrolidinones.*



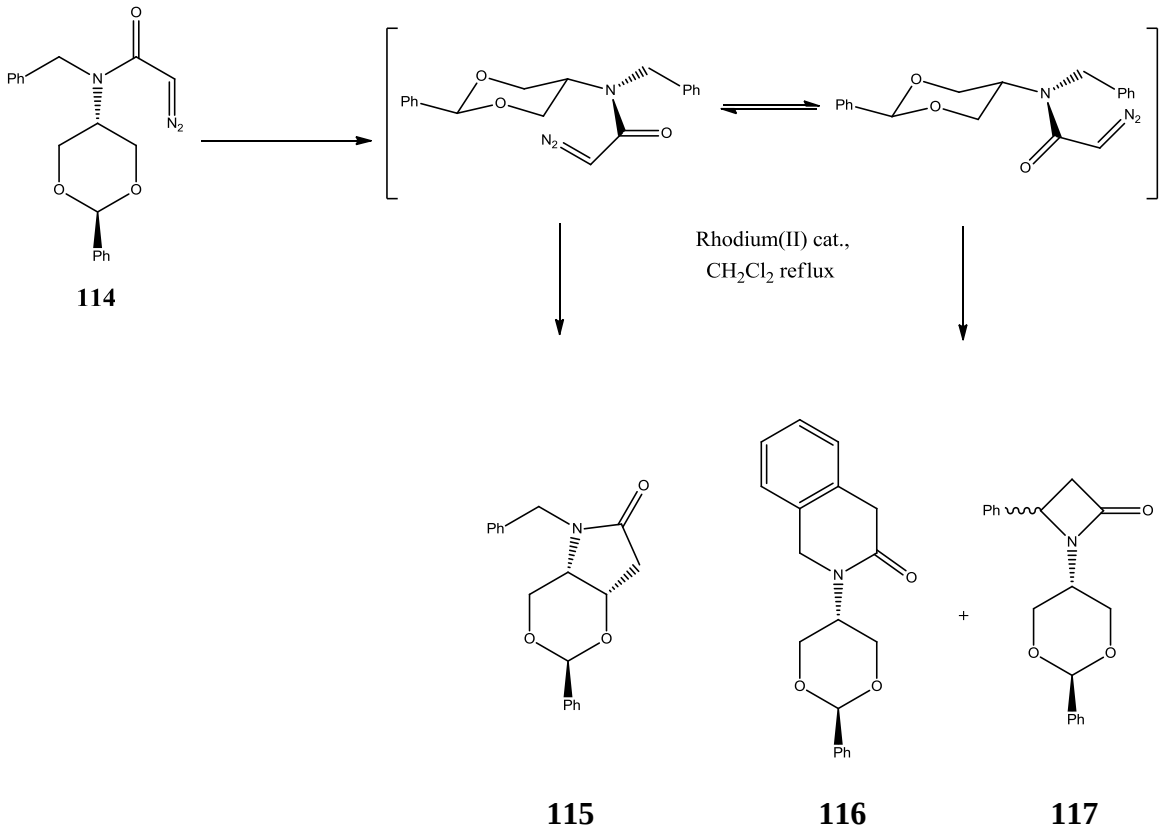
111 **113** **112**

Entry	Rhodium(II) cat.	X	Yield (%)	**113** : **112**	ee (%) **113**
1	Rh_2(*S*-PTPA)$_4$	OMe	73	5 : 68	[a]
2	Rh_2(*S*-PTPA)$_4$	NO_2	82	100 : 0	47
3	Rh_2(*S*-PTV)$_4$	NO_2	82	100 : 0	26
4	Rh_2(*S*-PTTL)$_4$	NO_2	80	100 : 0	74
5	Rh_2(*S*-PTA)$_4$	NO_2	83	100 : 0	47

[a] Value not provided in original report.

The elimination of competing reaction pathways may also be accomplished by careful choice of catalyst system.[131] As seen in **Table 1.26**, decomposition of diazoacetamide **114** may result in both C–H insertion product **115** and aromatic insertion product **116**, arising from two possible orientations of the carbenoid intermediate. Predominant γ-lactam production is achievable by reaction in the presence of Rh_2(*S*-MEPY)$_4$, providing **115** in good yield and high enantioselectivity. However, employment of the oxazolidinone, imidazolidinone and azetidinine catalysts, Rh_2(*S*-MEOX)$_4$, Rh_2(*S*-MPPIM)$_4$ and Rh_2(*S*-IBAZ)$_4$, respectively, was found to generate significant amounts of **116**, along with small quantities of the β-lactam product **117**.

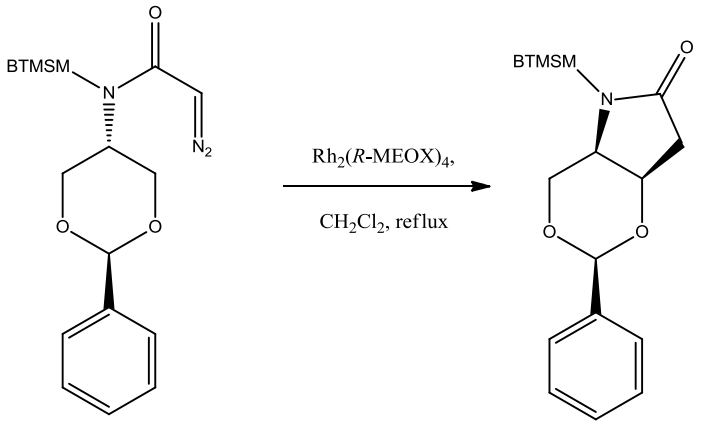
Table 1.26 *C–H insertion vs. aromatic cycloaddition in the rhodium(II)-catalysed decomposition of diazoacetamide **114**.*



114 **115** **116** **117**

Entry	Rhodium(II) cat.	**115** : **116**: **117**	Yield (%) **115**	ee (%) **115**
1	Rh_2(*S*-MEPY)$_4$	95 : 5 : 0	75	85
2	Rh_2(*S*-MEOX)$_4$	74 : 16 : 10	61	78
3	Rh_2(*S*-MPPIM)$_4$	53 : 18 : 29	48	37
4	Rh_2(*S*-IBAZ)$_4$	49 : 35 : 16	45	19

An enhancement in regio- and enantiocontrol is possible for the above process by exchange of the *N*-benzyl group for the more sterically demanding *N*-bis(trimethylsilyl)methyl (*N*-BTMSM) moiety.[154] This *N*-protecting group has previously been proven to deliver effective conformational control for the $Rh_2(OAc)_4$-catalysed intramolecular C–H insertion reactions of various diazoamides, permitting highly regioselective reactions to occur.[155,156] Despite possessing a tertiary C–H bond, the *N*-BTMSM group remains inert towards C–H insertion, due to probable shielding of the methine C–H bond by the two trimethylsilyl groups.[155] For the decomposition of **118** (**Scheme 1.14**), use of an *N*-BTMSM diazoamide not only provides exclusive access to the desired γ-lactam product **119**, but also allows for the subsequent facile removal of the *N*-silyl substituent, and is thus the optimum route for the production of 2-deoxylonolactam.[154]

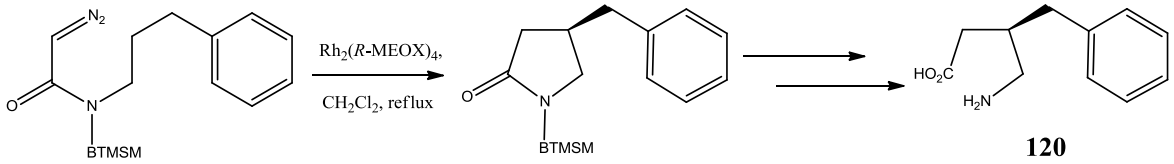


95% yield, 90% ee

118 **119**

Scheme 1.14

Such a strategy of *N*-BTMSM protection has been successfully adopted for the synthesis of the GABA analogue, (*R*)-β-benzyl-γ-aminobutyric acid **120** (**Scheme 1.15**).[157]



120

83% yield, 69% ee

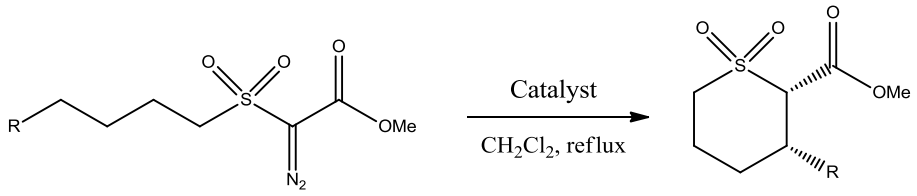
Scheme 1.15

1.6.1 Sulfur-containing heterocycle synthesis

Despite the wide interest in, and application of, sulfur-containing heterocycles in pharmaceutical chemistry,[158] the study of C–H insertion processes generating such compounds has remained a largely neglected area. Indeed, only a minimum of reports exist documenting the successful synthesis of sulfur heterocycles *via* carbenoid chemistry and, until recently, such reactions have been realised only in a racemic fashion.[159-162] In 2007, Novikov and co-workers reported the selective formation of six-membered cyclic sulfonates and sulfones by C–H insertion.[161] Such a finding was surprising given the large preference in diazo decomposition reactions for the formation of five-membered-ring products.[6] This outcome has been rationalised, however, by the difference in bond lengths and bond angles observed around the sulfur atom which are thought to mimic the geometry of the six-membered ring,[161,162] as was also observed for intramolecular C–H aminations.[163] The first, and only, report of the enantioselective production of sulfur heterocycles employing C–H insertion chemistry was published in 2010 by Maguire and co-workers for the C–H insertion reactions of α-diazosulfones (**Table 1.27**).[4] In addition

to providing a novel enantioselective reaction pathway to such compounds, this report was significant in achieving its goal with the use of copper catalysis. While copper catalysts have previously been employed in C–H insertion processes,[33,122] enantioselectivies achieved have been, in general, moderate with the highest asymmetric induction being noted for intermolecular C–H insertion in the presence of an immobilised copper(I)-bis(oxazoline) ligand (88% ee).[32] Thus, this publication represents the highest level of enantiocontrol achieved to date in a copper-mediated C–H insertion reaction. As seen in **Table 1.27**, enantioselectivites of up to 98% ee were realised for the decomposition of various substituted α-diazosulfones. The trend towards preferential six-membered-ring formation for carbenoid synthesis of sulfur heterocycles, as previously observed by Novikov and co-workers,[161,162] was seen to be preserved, with all thiopyran products forming in a highly enantioselective fashion (94–98% ee) and with *cis* selectivity.

Table 1.27 *Copper(I)-catalysed C–H insertion reactions of α-diazosulfones **121**.*



121 **122**

Entry	R	Cat.[a]	Yield (%) **122**	ee (%) **122**
1	Ph	Cu(I)Cl, NaBARF, **4g**	47	98
2	Ph	$Cu(MeCN)_4PF_6$, **4g**	19	94
3	*p*-Tol	Cu(I)Cl, NaBARF, **4g**	64	96
4	Bn	Cu(I)Cl, NaBARF, **4g**	42	96
5	Et	Cu(I)Cl, NaBARF, **4g**	68	97

[a] BARF = tetrakis[3,5-bis(trifluoromethyl)phenyl]borate.

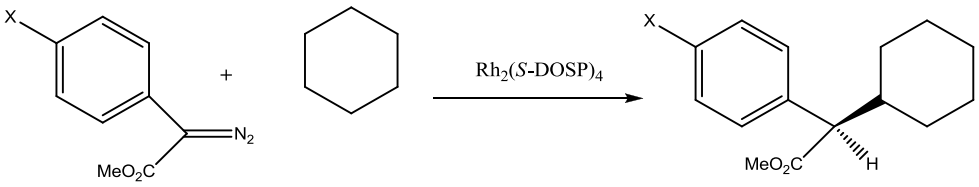
1.7 Intermolecular C–H insertion reactions

While the early 1990s represented a period of vast growth and research in the area of intramolecular carbenoid C–H insertion,[2,3,57,80,86] corresponding intermolecular C–H insertion processes at this time were not generally regarded as being synthetically efficient.[6,7] Such an opinion may be attributed to observed competing dimer formation[26,164] and the typically poor regioselectivities recorded.[26,165-168] Research published by Davies and co-workers in the late 1990s, however, served to provide a renewed interest in this previously neglected area, owing to the discovery that carbenoids substituted with one electron-donating group and one electron-withdrawing group (donor/acceptor-substituted carbenoids) are capable of undergoing highly chemo- and regioselective intermolecular C–H insertions.[169] The presence of a donor group in such species serves to stabilise the donor/acceptor carbenoid with respect to traditional

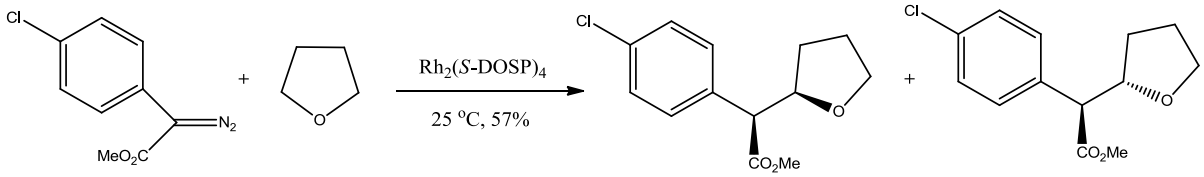
carbenoids derived from alkyl diazoacetates, with the result that insertion into the target C–H bond occurs in a more chemo- and regioselective manner.[170,171]

Highly enantioselective intermolecular C–H insertions can be achieved for donor/acceptor-substituted carbenoids when the reactions are catalysed by the chiral rhodium(II) tetraprolinate catalyst Rh_2(*S*-DOSP)$_4$. In 1997, Davies and co-workers reported the first asymmetric intermolecular C–H insertion reaction using metal carbenoid intermediates.[169] Decomposition of various aryl diazoacetates by Rh_2(*S*-DOSP)$_4$ in the presence of cyclohexane (**Table 1.28**) and tetrahydrofuran (**Scheme 1.16**) as solvents was shown to occur with high levels of enantioselectivity and in excellent yields.

Table 1.28 *Intermolecular C–H insertion reactions of cyclohexane and aryl diazoacetates.*



Entry	X	Temp. (°C)	Yield (%)	ee (%)
1	H	81	83	81
2	H	50	69	88
3	Cl	81	91	86
4	Cl	25	53	93
5	OMe	81	85	67



Scheme 1.16

A number of key trends were identified during this initial study which have been shown to parallel results obtained in subsequent investigations into intermolecular C–H insertion processes. Lower reaction temperatures were found to favour increased enantioselectivity.[68,172,173] Improvements in both yields and enantioselectivity were noted upon changing from an electron-donating (X = OMe) to an electron-withdrawing (X = Cl) aromatic substituent for aryl diazoacetate precursors,[71,172,174,175] as had previously been noted in intramolecular C–H insertion studies.[98,113] As seen in **Scheme 1.16**, insertion is favoured at positions α to oxygen,[66,176,177] with the same preference also holding true for

insertion adjacent to nitrogen,[67,69,132,173,178,179] and at benzylic[68,180] and allylic[20,181-183] sites. The use of hydrocarbon solvents (hexane, 2,2-dimethylbutane) for intermolecular C–H insertion processes has also been found to increase asymmetric induction, compared with the use of polar solvents,[68,182,184] a trend also observed for asymmetric cyclopropanation reactions.[64]

Control of regiochemistry is also possible for intermolecular C–H insertion reactions of donor/acceptor-substituted carbenoids in the presence of Rh_2(*S*-DOSP)$_4$.[8,17] In general, insertion into tertiary C–H bonds is preferred over competing secondary and primary insertion owing to the superior ability of tertiary sites to stabilise the electrophilic metal carbenoid.[6,7] However, steric factors may also contribute owing to the bulky nature of the rhodium carbenoid.[8,17] Thus, insertion into secondary C–H bonds is generally favoured for intermolecular diazo decomposition, as this represents the best balance between electronic and steric effects (**Figure 1.20**).[132,175,176,180]

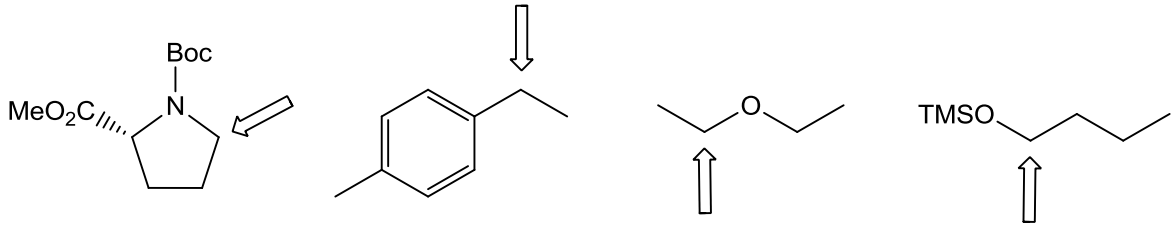
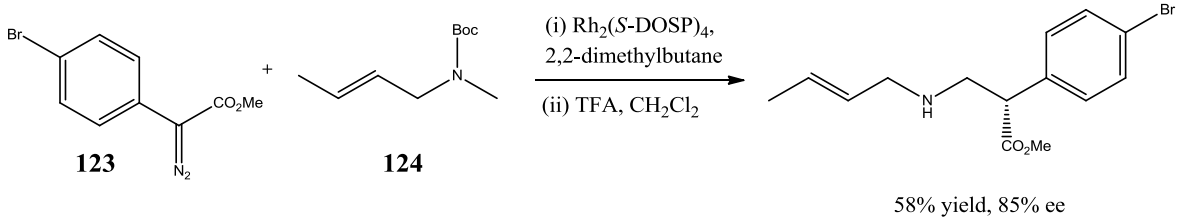


Figure 1.20

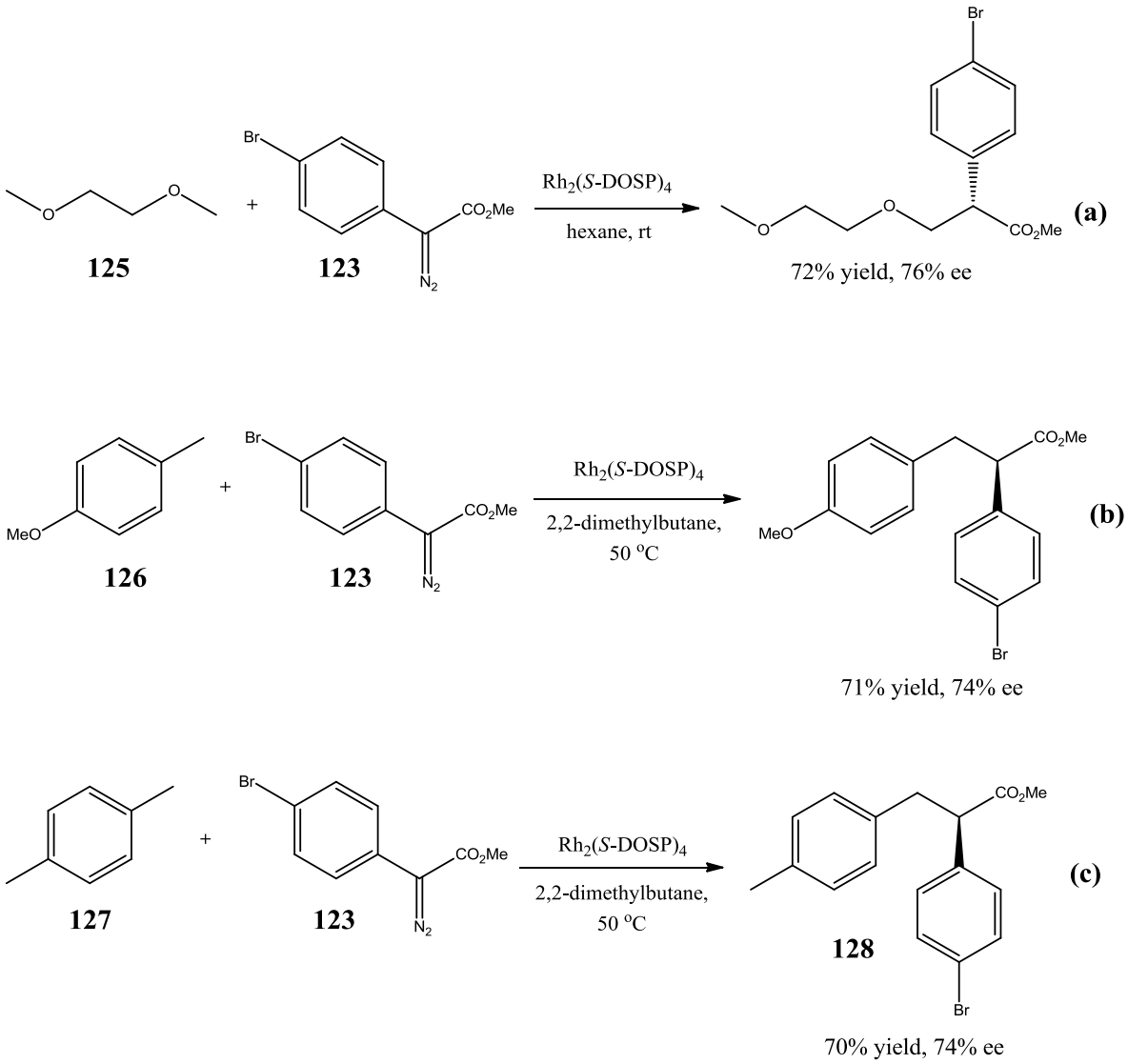
Nonetheless, selective C–H insertion at primary and tertiary C–H sites may be achieved. The first chemoselective C–H insertion into a methyl site was reported by Davies and co-worker in 2002 for the Rh_2(*S*-DOSP)$_4$-catalysed reaction of methyl *p*-bromophenyldiazoacetate **123** with Boc-protected *N*-methylcrotylamine **124** (**Scheme 1.17**).[179] It was suggested that regioselective insertion into the primary site occurs in preference to insertion at the more electronically favourable allylic site, due to the sterically demanding nature of the aryldiazoacetate rhodium carbenoid, which hinders its approach to the competing secondary site.[179]



Scheme 1.17

Thus, selective C–H insertion into methyl sites may be achieved when the target primary bond is sufficiently electronically activated and competing insertion sites in the remainder

of the molecule are sterically hindered or otherwise electronically deactivated. This was indeed found to be true and various examples of selective C–H insertions at methyl sites are now known (**Scheme 1.18**).[172,175]

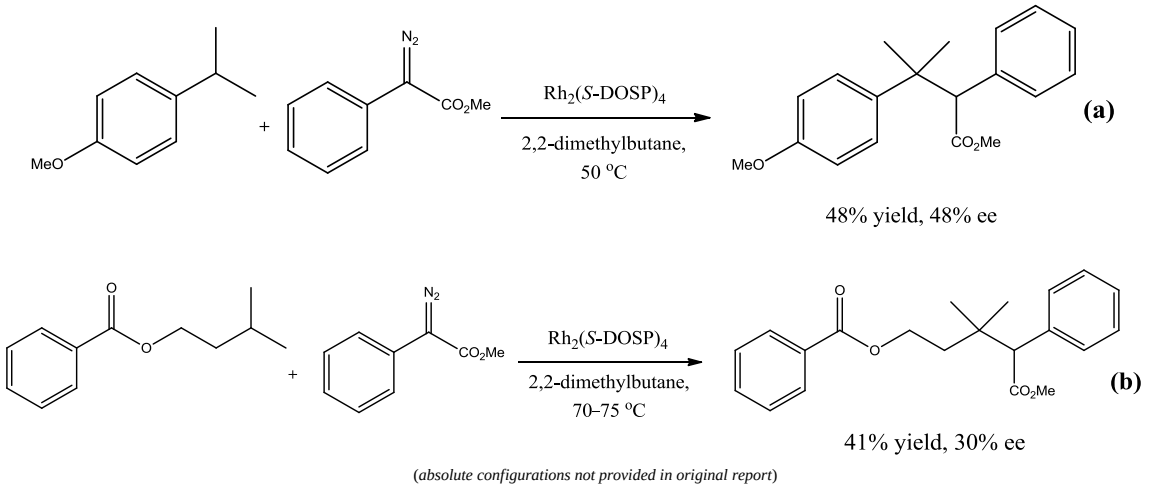


Scheme 1.18

Preferential C–H insertion is seen to occur at the primary C–H bond of 1,2-dimethoxyethane **125**, due to the deactivating effect of the β-oxygen on the competing secondary insertion site [**Scheme 1.18**(a)].[175] No C–H insertion is observed at the methyl group adjacent to oxygen in 1-methoxy-4-methylbenzene **126** [**Scheme 1.18**(b)], due to probable delocalisation of the electron lone pairs of oxygen into the benzene ring.[172] The *p*-methoxy group in this reaction serves the function of sterically protecting the ring from possible cyclopropanation as was observed for the reaction of methyl *p*-bromophenyldiazoacetate **123** and toluene. Steric protection of this kind may also be achieved with *p*-alkyl substituents, thus the reaction of **123** and *p*-xylene **127** generates the corresponding C–H activation product **128** in 70% yield and 74% ee [**Scheme**

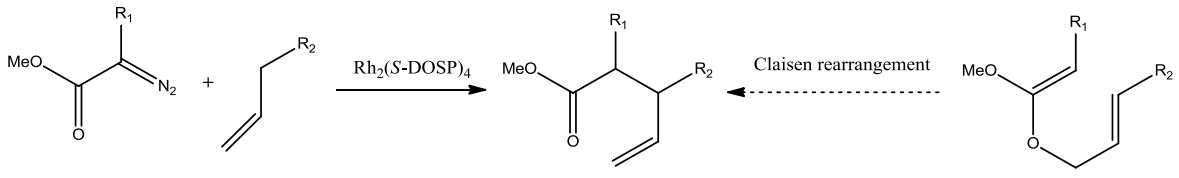
1.18(c)].[172] This strategy of selective methyl C–H insertion has been successfully applied to the total syntheses of the natural products (+)-imperanene,[172] (–)-α-conidendrin,[172] and to the synthesis of the enantiomers of the antidepressant, venlafaxine.[173]

Despite electronic preferences to the contrary,[6,7] regioselective intermolecular C–H insertion into tertiary bonds is a generally difficult process.[177,180,184] Until recently, reports of preferential insertion into tertiary C–H bonds were minimal.[71,184] However, research by Davies and co-workers published in 2009[185] has served to broaden the range of known substrates for which functionalisation of tertiary C–H bonds may be achieved (**Scheme 1.19**). Although the yields and enantioselectivities obtained for these reactions are moderate, they represent an encouraging platform on which to build future investigations.



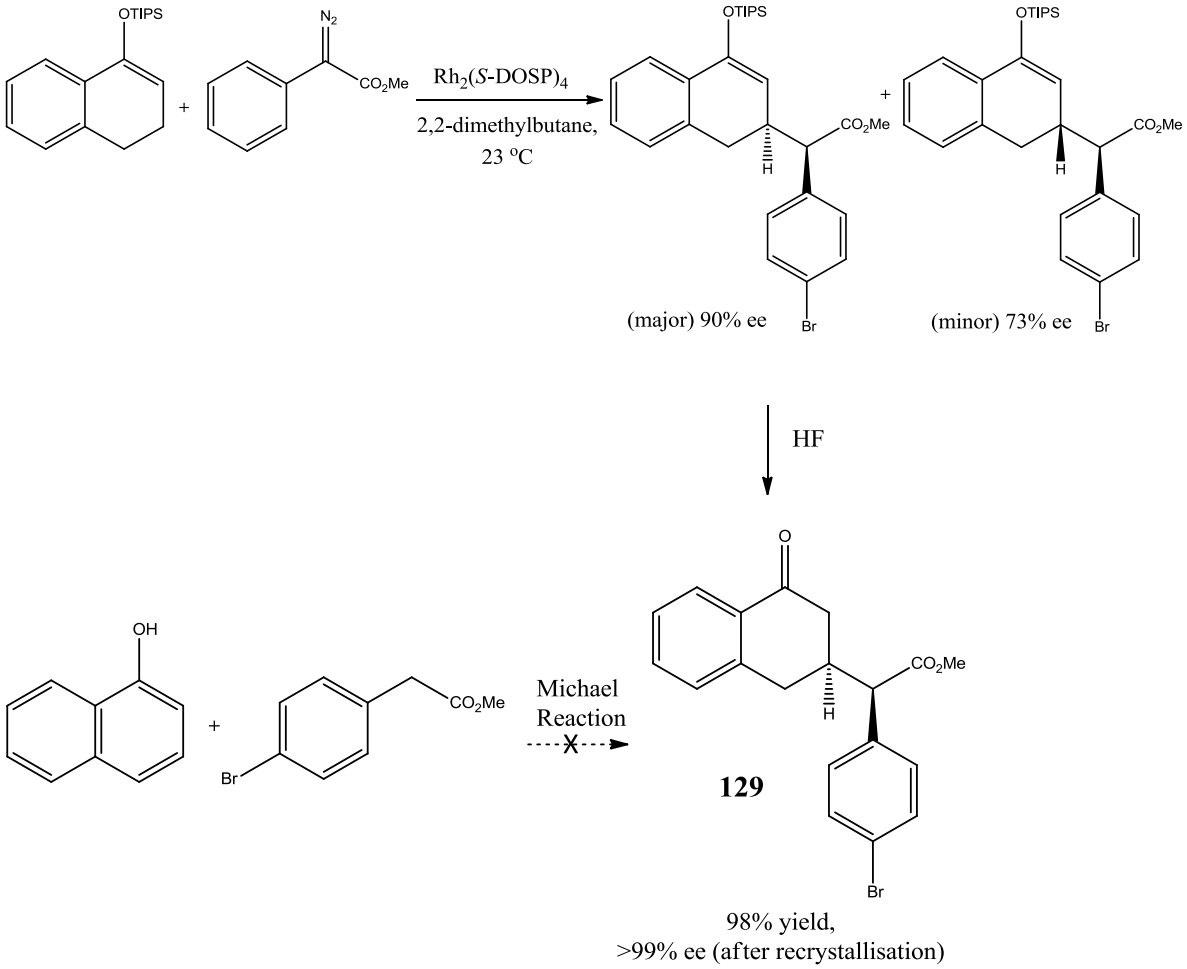
Scheme 1.19

Complementary reactions to several classic C–C bond-forming transformations, including the Claisen rearrangement,[182] the aldol reaction,[176,177,186] the Mannich reaction,[67,69] the Claisen condensation[66] and the Michael reaction,[181,183] may be achieved by intermolecular C–H insertion reactions in the presence of donor/acceptor-substituted carbenoids. The synthesis of γ,δ-unsaturated esters, products normally generated by an asymmetric Claisen rearrangement, is possible *via* allylic C–H activation of alkenes (**Scheme 1.20**).[182] Excellent regiocontrol was achieved in these reactions, with high enantioselectivities (up to 95% ee) and moderate diastereoselectivities (up to 88% de) also being recorded.



Scheme 1.20

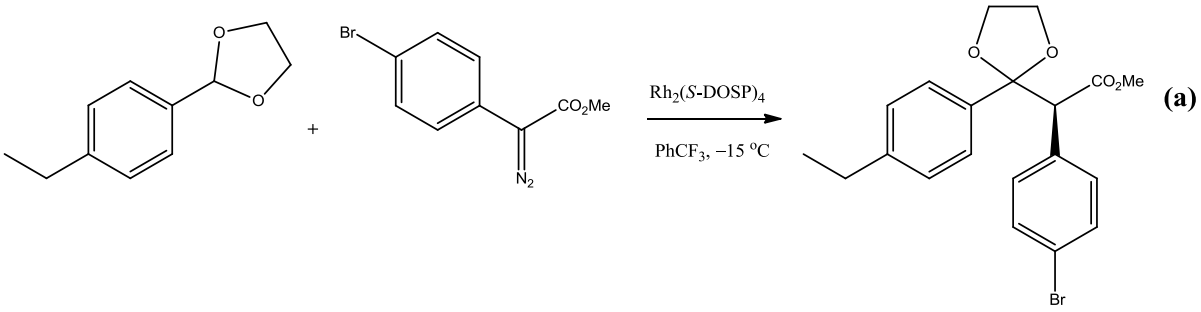
The Rh_2(*S*-DOSP)$_4$-catalysed decomposition of methyl aryldiazoacetates in the presence of silyl enol ethers may be used as an alternative route to typical Michael reaction products.[181] This surrogate reaction is particularly attractive, as it may be employed in the synthesis of compounds not possible with corresponding Michael reactions. Production of the 1,5-dicarbonyl **129** *via* the traditional Michael addition route would not be feasible as the necessary enone would be the keto tautomer of 1-naphthol. However, as seen in **Scheme 1.21**, **129** may be produced by an intermolecular C–H insertion reaction followed by desilylation with hydrogen fluoride.[181] The enantioselectivity for this reaction was later improved to 97.5% ee for the major diastereoisomer (≥ 98% de) by change to the TMS protecting group.[183]



Scheme 1.21

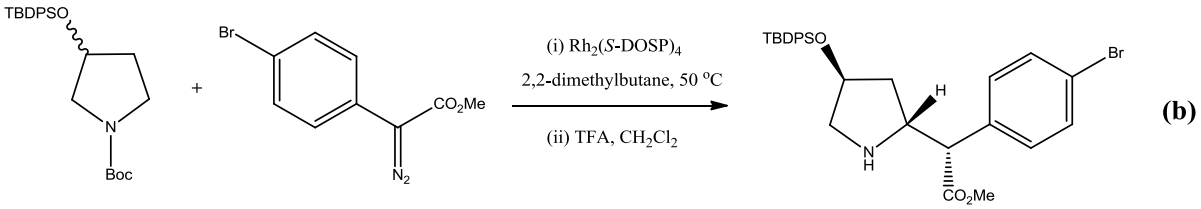
The development of surrogate reactions for the Claisen condensation,[66] the Mannich reaction[67,69] and the aldol reaction[176,177,186] has also been described, involving the asymmetric synthesis of β-keto esters, β-amino acid derivatives, and silyl-protected β-hydroxy esters, respectively. These novel reactions feature common C–H insertion at electronically favourable sites adjacent to oxygen or nitrogen, and have been achieved with excellent regiocontrol, and moderate-to-good diastereo- and enantiocontrol. An example of each surrogate reaction type is given in **Scheme 1.22**.[66,69,176]

Asymmetric Claisen Condensation Surrogate



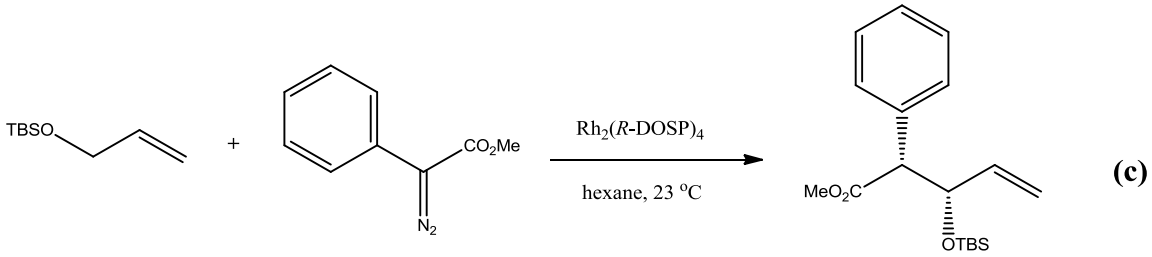
59% yield, 75% ee

Asymmetric Mannich Reaction Surrogate



64% yield, >94 % de, >99% ee

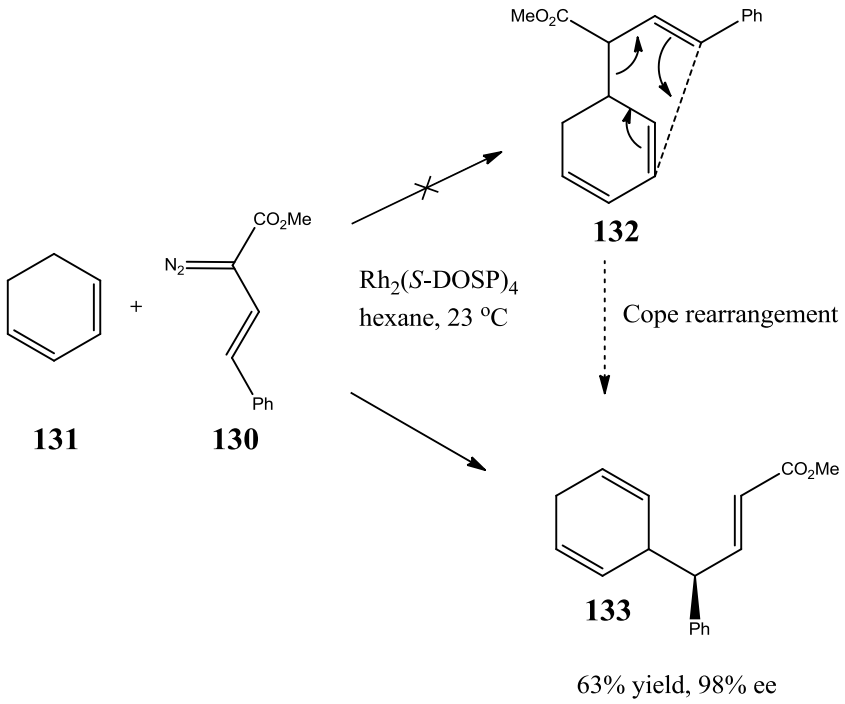
Asymmetric Aldol Reaction Surrogate



52% yield, >94% de, 92% ee

Scheme 1.22

A novel reaction pathway was discovered by Davies and co-workers in 1999, during the course of investigations into the asymmetric synthesis of 4,4-diarylbutanoates.[174] The reaction of vinyldiazoacetate **130** and 1,3-cyclohexadiene **131** did not result in the predicted C–H insertion product **132.** Rather, formation of the 1,4-cyclohexadiene **133** was observed in high yield (63%) and high enantioselectivity (98% ee). It was suggested that generation of **133** occurs *via* a combined C–H activation/Cope rearrangement pathway (**Scheme 1.23**).



Scheme 1.23

The direct C–H insertion product **132** was subsequently found to be the more thermodynamically stable product,[174,187] meaning that the reaction likely proceeds *via* a highly concerted, ordered transition state (**Figure 1.21**) as opposed to a two-step reaction.

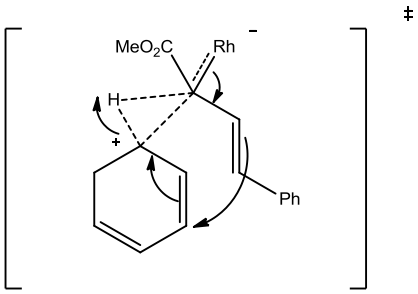
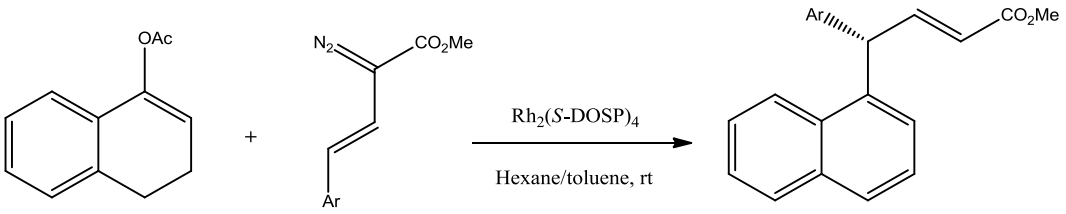


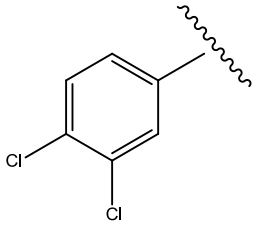
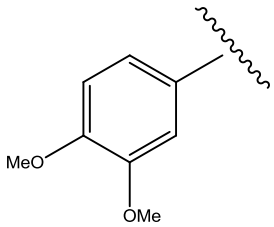
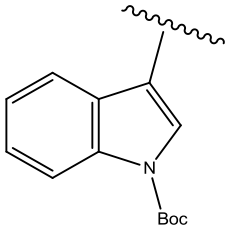
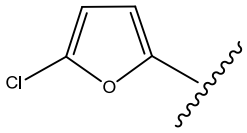
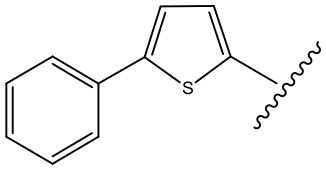
Figure 1.21

Highly enantioselective diazo decompositions have been observed for combined C–H activation/Cope rearrangements in the presence of Rh_2(*S*-DOSP)$_4$. 1,2-Dihydronaphthalenes in particular have proven themselves as excellent substrates for this type of chemistry, finding application in the synthesis of various naphthalene derivatives (**Table 1.29**),[188] Michael addition equivalent products,[183] and double C–H activation products.[133] Formation of **134** (**Table 1.29**) occurs *via* a combined C–H insertion/Cope rearrangement pathway, followed by elimination of acetic acid.

Table 1.29 *Combined C–H activation/Cope rearrangement reactions.*



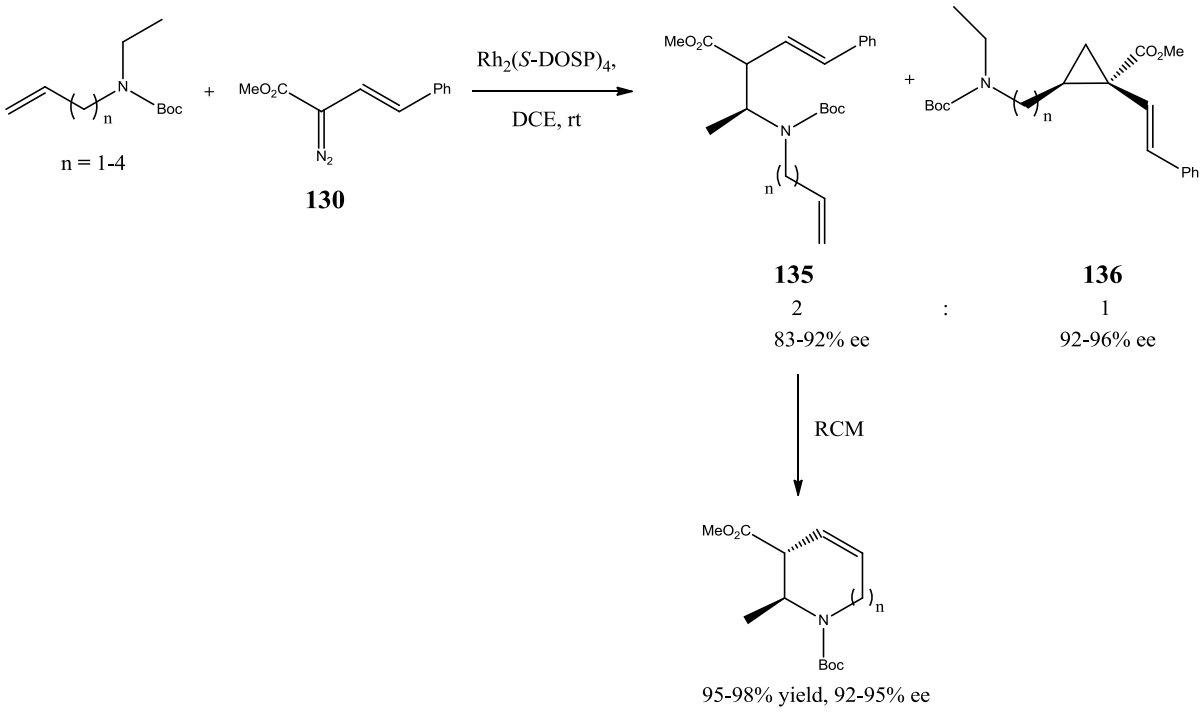
134

Entry	Ar	Yield (%) **135**	ee (%) **134**
1		79	>98
2		92	99.5
3		82	>98
4		45	99.6
5		66	99.3

This impressive chemical transformation has also been applied to a formal asymmetric synthesis of the antidepressant, (+)-sertraline,[174] to the synthesis of a series of selective monoamine reuptake inhibitors,[189] and to the synthesis of the diterpene natural products, (–)-colombiasin A,[190] (–)-elisapterosin B,[190] (+)-elisabethadione[191] and (+)-erogorgiaene,[192] all of which feature allylic C–H functionalisation by vinyldiazoacetates as the key step. In addition, the combined C–H functionalization/Cope rearrangement has recently been applied as a surrogate reaction to the vinylogous Mukaiyama aldol reaction,

producing a range of 1,2-disubstituted alkene products in high yield (67–89%) and with excellent enantioselectivity (93–99% ee).[193]

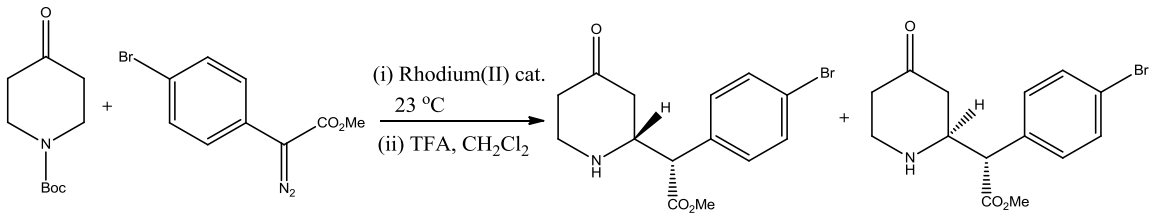
The vinyldiazoacetate **130** has recently been employed in the catalytic enantioselective synthesis of azacycloalkenes *via* an intermolecular rhodium carbenoid C–H insertion/ring-closing metathesis (RCM) sequence.[194] Interestingly, a mixture of C–H insertion (**135**) and cyclopropanation (**136**) products were observed for reaction of **130** and a series of Boc-protected alkenyl amines in an approximate 2 : 1 ratio (**Scheme 1.24**). This is in contrast to previous N–H insertion reactions of **130** where no cyclopropanation products were detected.[195] Synthesis of both the cyclopropane (**136**) and C–H insertion (**135**) products was achieved with high enantioselectivity. Enantioenriched six- to eight-membered nitrogen-containing heterocycles were subsequently prepared *via* ruthenium-catalysed ring-closing of the C–H insertion products.



Scheme 1.24

While Rh_2(*S*-DOSP)$_4$ is undoubtedly the catalyst of choice for intermolecular C–H insertions employing donor/acceptor-substituted carbenoids, in certain cases the reliability of this prolinate catalyst in achieving high levels of asymmetric induction has been seen to fail.[68,69,87] Alternative catalytic systems are, however, available which allow achievement of desired enantioselective intermolecular reactions. A vast improvement in both enantioselectivity and diastereoselectivity was recorded in the synthesis of *threo*-methylphenidate (Ritalin) upon change of catalyst from Rh_2(*S*-DOSP)$_4$ to Rh_2(*S*-biDOSP)$_2$.[67] A similar trend was observed for the reaction of *N*-Boc-piperidin-4-one **137** and **123**, in which change of catalyst from Rh_2(*S*-DOSP)$_4$ to Rh_2(*S*-biTISP)$_2$ resulted in increased asymmetric induction in the formation of **138** and **139** (**Table 1.30**).[69]

Table 1.30 *Rhodium(II) prolinate-catalysed C–H insertion reactions of* N-*Boc-piperidin-4-one* ***137****.*

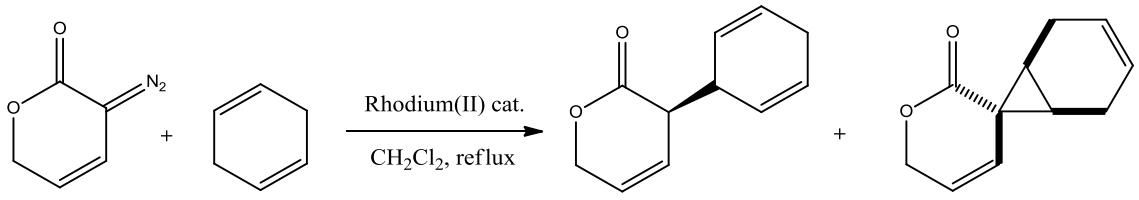


137 **123** **138** **139**

Entry	Rhodium(II) cat.	Yield (%)		ee (%)	
		138	**139**	**138**	**139**
1	Rh_2(*S*-DOSP)$_4$	31	20	83	53
2	Rh_2(*S*-biTISP)$_2$	46	23	88	76

Chiral rhodium(II) carboxamidate catalysts have been shown to outperform Rh_2(*S*-DOSP)$_4$ in terms of chemoselectivity and enantioinduction in the C–H insertion reactions of vinyldiazolactone **140** (**Table 1.31**).[87] This example is significant in that the rhodium(II) carboxamidate Rh_2(*S*-MEPY)$_4$ has previously been found to be unsuited to reactions with vinyldiazoacetates[196] and only a very limited number of published reports exist documenting successful chiral rhodium(II) carboxamidate-catalysed intermolecular C–H insertion.[40,197]

Table 1.31 *Intermolecular C–H insertion reactions of vinyldiazolactone* ***140*** *and 1,4-cyclohexadiene.*



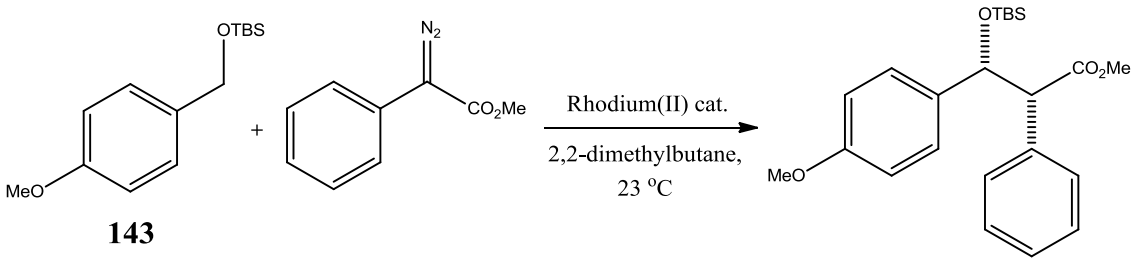
140 **141** **142**

Entry	Rhodium(II) cat.	**141**: **142**	Yield (%)**141**	ee (%)**142**
1	Rh_2(*S*-DOSP)$_4$	1 : 9	56	18
2	Rh_2(*S*-MEPY)$_4$	4 : 1	47	8
3	Rh_2(*S*-MEAZ)$_4$	9 : 1	43	60
4	Rh_2(*S*,*R*-MenthAZ)$_4$	9 : 1	50	80

Hashimoto's phthalimide catalyst Rh_2(*S*-PTTL)$_4$ was found to be the catalyst of choice ahead of Rh_2(*S*-DOSP)$_4$ for the asymmetric intermolecular C–H functionalisation of *para*-methoxybenzyl *tert*-butyldimethylsilyl ether **143** (**Table 1.32**).[68] This result was

again significant, given that Rh_2(*S*-PTTL)$_4$ had not previously been reported as an efficient catalyst for either intermolecular C–H insertion or cyclopropanation reactions.

Table 1.32 *Intermolecular C–H insertion reactions of* para-*methoxybenzyl* tert-*butyldimethylsilyl ether* ***143***.

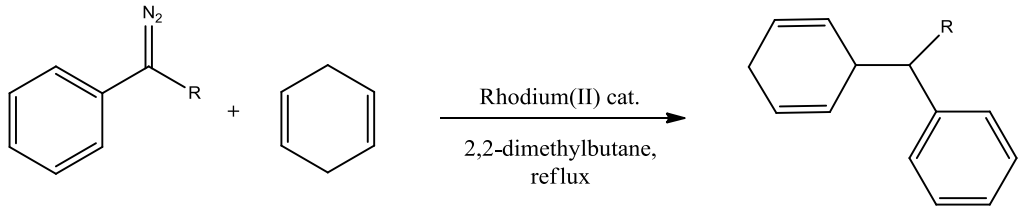


143

Entry	Rhodium(II) cat.	Yield (%)	de (%)	ee (%)
1	Rh_2(*R*-DOSP)$_4$	85	88	35 (2*R*, 3*R*)
2	Rh_2(*S*-PTTL)$_4$	64	91	97 (2*R*, 3*R*)

A range of additional chiral complexes have been shown to be efficient catalytic systems for intermolecular C–H insertion processes including a recyclable fluorous chiral rhodium(II) complex,[70] and copper-bis(oxazoline) complexes.[32] More recently, the adamantylglycine-derived chiral tetracarboxylate complex Rh_2(*S*-PTAD)$_4$ has been introduced as an additional catalytic choice for such transformations.[71] While Rh_2(*S*-DOSP)$_4$ has shown exceptional results for the majority of reactions of donor/acceptor carbenoids discussed above, it is not an effective catalytic option when the diazo acceptor group is changed from a methyl ester to another acceptor group.[184] In such cases, the adamantyl complex Rh_2(*S*-PTAD)$_4$ has been found to be an excellent substitute catalyst for Rh_2(*S*-DOSP)$_4$ (**Table 1.33**).[71,72]

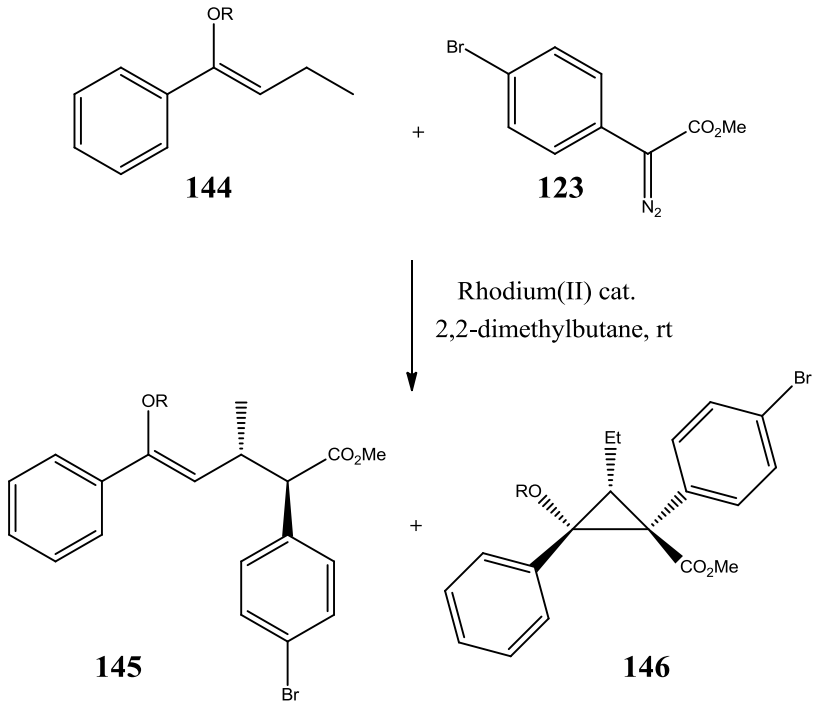
Table 1.33 *Intermolecular C–H insertion reactions of 1,4-cyclohexadiene.*



Entry	Rhodium(II) cat.	R	Yield (%)	ee (%)
1	Rh_2(*S*-DOSP)$_4$	$PO(OMe)_2$	62	41
2	Rh_2(*S*-PTAD)$_4$	$PO(OMe)_2$	83	92
3	Rh_2(*S*-PTAD)$_4$	COMe	90	80
4	Rh_2(*S*-PTAD)$_4$	COEt	84	71
5	Rh_2(*S*-PTAD)$_4$	CO*n*-Pr	81	80

Rh_2(*S*-PTAD)$_4$ may also be employed to promote C–H insertion over competing cyclopropanation in allylic substrates, as was observed in the intermolecular reactions of trisubstituted alkenes.[198] As seen in **Table 1.34**, intermolecular diazo decomposition of **144** in the presence of Rh_2(*S*-DOSP)$_4$ results in the formation of a 2 : 1 mixture of allylic C–H insertion (**145**) and cyclopropanation (**146**) products (**Table 1.34**, entry 1). In contrast, the Rh_2(*S*-PTAD)$_4$-catalysed reaction was seen to produce **145** as the sole product (**Table 1.34**, entry 2). The choice of siloxy group in this study was found to have a significant effect on the reaction outcome. Decreasing the size of the protecting group to TMS in the Rh_2(*S*-PTAD)$_4$-catalysed reaction was seen to correspond to a large decrease in preference for the C–H insertion product (**Table 1.34**, entry 3). The enantioselectivity obtained with Rh_2(*S*-PTAD)$_4$ (R = TBDPS) was good (86% ee) and could be improved to 93% ee without loss of yield upon lowering of the reaction temperature to 0 °C.

Table 1.34 *Rh_2(S-DOSP)$_4$- vs. Rh_2(S-PTAD)$_4$-catalysed C–H insertion reactions of* ***144****.*

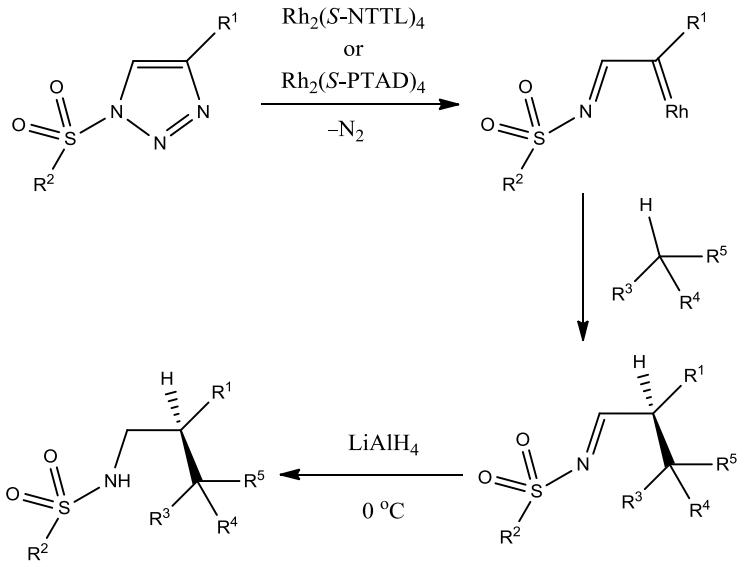


Entry	Rhodium(II) cat.	R	Yield (%)	**145** : **146**	ee (%)	
					145	**146**
1	Rh_2(*S*-DOSP)$_4$	TBDPS	87	2 : 1	65	78
2	Rh_2(*S*-PTAD)$_4$	TBDPS	89	>15 : 1	86[a]	–
3	Rh_2(*S*-PTAD)$_4$	TMS	63	1 : 1	83[a]	34

[a] Opposite enantiomer in excess.

While this review has focused on asymmetric C–H insertion reactions of α-diazocarbonyl compounds, very recently Fokin and co-workers have demonstrated that azavinyl carbenes derived from 1,2,3-triazoles can also be efficiently used for highly

enantioselective C–H functionalisation.[199] In this work transition metal carbenes were directly generated from readily available and stable 1-sulfonyl-1,2,3-triazoles in the presence of chiral rhodium(II) carboxylates and subsequently used for C–H insertions with a range of simple alkane substrates to access a variety of β-chiral sulfonamides in very good yields (63–98%) and high enantiomeric excess (86–97% ee). Application of 1-sulfonyl-1,2,3-triazoles, which can be viewed as synthetic equivalents of diazo compounds, has also been reported for asymmetric rhodium(II)-catalysed cyclopropanation reactions where similar high levels of enantiocontrol were observed.[200]



Scheme 1.25

1.8 Concluding remarks

The 20 intervening years between the first reports of asymmetric C–H insertion reactions to the present day have represented a period of rapid growth and learning in the field of enantioselective carbenoid C–H insertion chemistry. Large advances in both intramolecular and intermolecular C–H insertion reactions have been achieved, and the catalogue of possible substrates for both processes continues to grow. Since their initial introduction,[1] rhodium(II) compounds have remained the catalysts of choice for carbenoid insertions into C–H bonds. A wide variety of rhodium(II) catalysts are now known, encompassing carboxylate, carboxamidate, phosphate and ortho-metalated complexes. Rhodium(II) carboxylates and carboxamidates have proven themselves the most effective of these catalyst systems, finding applications across a range of intramolecular and intermolecular C–H insertion reactions.

In intramolecular carbocycle-producing C–H insertion reactions, Hashimoto's rhodium(II) phthalimide complexes have emerged as the primary catalytic choice,

effecting asymmetric cyclopentanone and cyclopentane synthesis in up to 80 and 95% ee, respectively.[113,120] Chiral copper-bis(oxazoline) and ortho-metalated rhodium(II) catalysts have also shown some success in this area,[33,98,122] however, enantioselectivities obtained with these complexes have been moderate.

Catalytic options for the synthesis of heterocyclic products *via* C–H insertion chemistry may include a range of rhodium(II) carboxylates and carboxamidates. Doyle's chiral rhodium(II) carboxamidates are reliable catalysts for highly enantioselective intramolecular lactone synthesis. The imidazolidinone catalyst Rh_2(*S*-MPPIM)$_4$ has proven particularly effective for the carbenoid decomposition reactions of primary and secondary alkyl diazoacetates,[88,91,92,126] while the related compound Rh_2(*S*-MACIM)$_4$ has found success in the C–H insertion reactions of tertiary alkyl diazoacetates.[83,128] For the generation of dihydrobenzofuran products, the choice of catalytic system may comprise both Hashimoto's phthalimide catalysts and Davies' prolinate- and adamantate-derived catalysts.[71,137,143] Asymmetric chromanone synthesis may be achieved in the presence of the carboxylate catalyst Rh_2(*S*-BSP)$_4$.[56,136] As was observed for the corresponding lactone syntheses, Doyle's chiral carboxamidate complexes are a viable catalytic option for the production of lactam products *via* intramolecular C–H insertion reactions. In particular, Rh_2(*S*-MEPY)$_4$ and Rh_2(*S*-MEOX)$_4$ have been exploited for this purpose in early studies examining the decomposition reactions of *N*-(*tert*-butyl)diazoacetamides[86] and cyclic diazoacetamides.[81] Very high regio- and enantioselectivities have also been obtained for β-lactam synthesis in the presence of Hashimoto's phthalimide catalysts for C–H insertion reactions with compounds featuring a bulky amide substituent. The only successful example of highly enantioselective thiopyran synthesis has been reported for C–H insertions catalysed by chiral copper-bis(oxazoline) complexes.[4]

Intermolecular C–H insertion chemistry has been dominated by catalytic processes employing Davies' rhodium(II) prolinate catalysts. Excellent enantioselectivities have been achieved for the reactions of donor/acceptor-substituted carbenoids in the presence of Rh_2(*S*-DOSP)$_4$, the bridged catalyst Rh_2(*S*-biDOSP)$_4$ and the adamantyl complex Rh_2(*S*-PTAD)$_4$.[20,71] Recently, iridium(III)-salen complexes have also been demonstrated as effective catalysts for the asymmetric intermolecular C–H insertion reactions of donor/acceptor-substituted carbenoids, and as the only catalytic choice to date for the intermolecular decompositions of α-alkyl-α-diazoacetates.[5]

While rhodium(II) complexes remain the dominant catalysts for application in enantioselective C–H insertion reactions, the possibility of extending this choice to include alternative metal catalysts is currently being realised. Nonetheless, the development of a catalyst system with general applicability across the spectrum of intramolecular and intermolecular C–H insertion reactions remains elusive, but may be achieved in future years as advances in catalytic techniques for carbenoid C–H insertions continue to grow.

1.9 References

1. Demonceau, A.; Noels, A. F.; Hubert, A. J.; Teyssié, P. *J. Chem. Soc., Chem. Commun.* **1981**, 688-689.
2. Kennedy, M.; McKervey, M. A.; Maguire, A. R.; Roos, G. H. P. *J. Chem. Soc., Chem. Commun.* **1990**, 361-362.
3. Hashimoto, S.-i.; Watanabe, N.; Ikegami, S. *Tetrahedron Lett.* **1990**, *31*, 5173-5174.
4. Flynn, C. J.; Elcoate, C. J.; Lawrence, S. E.; Maguire, A. R. *J. Am. Chem. Soc.* **2010**, *132*, 1184-1185.
5. Suematsu, H.; Katsuki, T. *J. Am. Chem. Soc.* **2009**, *131*, 14218-14219.
6. Doyle, M.; McKervey, M.; Ye, T. *Modern Catalytic Methods for Organic Synthesis with Diazo Compounds: From Cyclopropanes to Ylides*; Wiley: New York, **1998**.
7. Ye, T.; McKervey, M. A. *Chem. Rev.* **1994**, *94*, 1091-1160.
8. Davies, H. M. L.; Antoulinakis, E. G. *J. Organomet. Chem.* **2001**, *617-618*, 47-55.
9. Doyle, M. P.; Forbes, D. C. *Chem. Rev.* **1998**, *98*, 911-936.
10. Padwa, A.; Krumpe, K. E. *Tetrahedron* **1992**, *48*, 5385-5453.
11. Adams, J.; Spero, D. M. *Tetrahedron* **1991**, *47*, 1765-1808.
12. Doyle, M. P. *Chem. Rev.* **1986**, *86*, 919-939.
13. Davies, H. M. L. *J. Mol. Catal. A: Chem.* **2002**, *189*, 125-135.
14. Sulikowski, G. A.; Cha, K. L.; Sulikowski, M. M. *Tetrahedron: Asymmetry* **1998**, *9*, 3145-3169.
15. Padwa, A.; Austin, D. J. *Angew. Chem., Int. Ed.* **1994**, *33*, 1797-1815.
16. Taber, D. F.; Stiriba, S.-E. *Chem.-Eur. J.* **1998**, *4*, 990-992.
17. Davies, H. M. L. *Eur. J. Org. Chem.* **1999**, *1999*, 2459-2469.
18. Forbes, D. C.; McMills, M. C. *Curr. Org. Chem.* **2001**, *5*, 1091-1105.
19. Hansen, J.; Davies, H. M. L. *Coord. Chem. Rev.* **2008**, *252*, 545-555.
20. Davies, H. M. L.; Nikolai, J. *Org. Biomol. Chem.* **2005**, *3*, 4176-4187.
21. Davies, H. M. L.; Beckwith, R. E. J. *Chem. Rev.* **2003**, *103*, 2861-2904.
22. Pedro G. M. P, Carlos A. M. A. *Eur. J. Org. Chem.* **2004**, *2004*, 3773-3788.
23. Slattery, C. N.; Ford, A.; Maguire, A. R. *Tetrahedron* **2010**, *66*, 6681-6705.
24. Doyle, M. P.; Duffy, R.; Ratnikov, M.; Zhou, L. *Chem. Rev.* **2010**, *110*, 704-724.
25. Davies, H.; Dick, A.; Yu, J.-Q., Shi, Z., Eds.; Springer Berlin / Heidelberg: 2010; Vol. 292, p 303-345.
26. Scott, L. T.; DeCicco, G. J. *J. Am. Chem. Soc.* **1974**, *96*, 322-323.
27. Mass, G. *Top. Curr. Chem.* **1987**, *137*, 75-254.
28. Lim, H.-J.; Sulikowski, G. A. *J. Org. Chem.* **1995**, *60*, 2326-2327.
29. Doyle, M. P.; Kalinin, A. V. *Tetrahedron Lett.* **1996**, *37*, 1371-1374.
30. Wee, A. G. H. *J. Org. Chem.* **2001**, *66*, 8513-8517.
31. Doyle, M. P.; Hu, W. *J. Org. Chem.* **2000**, *65*, 8839-8847.
32. Fraile, J. M.; Garcia, J. I.; Mayoral, J. A.; Roldan, M. *Org. Lett.* **2007**, *9*, 731-733.
33. Müller, P.; Bolea, C. *Molecules* **2001**, *6*, 258-266.
34. Desimoni, G.; Faita, G.; Jorgensen, K. A. *Chem. Rev.* **2006**, *106*, 3561-3651.
35. Gant, T. G.; Noe, M. C.; Corey, E. J. *Tetrahedron Lett.* **1995**, *36*, 8745-8748.
36. Evans, D. A.; Woerpel, K. A.; Hinman, M. M.; Faul, M. M. *J. Am. Chem. Soc.* **1991**, *113*, 726-728.
37. Whitesell, J. K. *Chem. Rev.* **1989**, *89*, 1581-1590.
38. Fraile, J. M.; Lopez-Ram-de-Viu, P.; Mayoral, J. A.; Roldan, M.; Santafe-Valero, J. *Org. Biomol. Chem.* **2011**, *9*.

39. Fraile, J. M.; Mayoral, J. A.; Ravasio, N.; Roldán, M.; Sordelli, L.; Zaccheria, F. *J. Catal.* **2011**, *281*, 273-278.
40. Axten, J. M.; Ivy, R.; Krim, L.; Winkler, J. D. *J. Am. Chem. Soc.* **1999**, *121*, 6511-6512.
41. Diaz-Requejo, M. M.; Belderrain, T. R.; Nicasio, M. C.; Trofimenko, S.; Perez, P. J. *J. Am. Chem. Soc.* **2002**, *124*, 896-897.
42. Caballero, A.; Diaz-Requejo, M. M.; Belderrain, T. R.; Nicasio, M. C.; Trofimenko, S.; Perez, P. J. *Organometallics* **2003**, *22*, 4145-4150.
43. Díaz-Requejo, M. M.; Pérez, P. J. *J. Organomet. Chem.* **2005**, *690*, 5441-5450.
44. Diaz-Requejo, M. M.; Wehrmann, P.; Leatherman, M. D.; Trofimenko, S.; Mecking, S.; Brookhart, M.; Perez, P. J. *Macromolecules* **2005**, *38*, 4966-4969.
45. Rodríguez, P.; Álvarez, E.; Nicasio, M. C.; Pérez, P. J. *Organometallics* **2007**, *26*, 6661-6668.
46. Díaz-Requejo, M. M.; Pérez, P. J. *Chem. Rev.* **2008**, *108*, 3379-3394.
47. Davies, H. M. L. *Tetrahedron* **1993**, *49*, 5203-5223.
48. Ren, T. *Coord. Chem. Rev.* **1998**, *175*, 43-58.
49. Boyar, E. B.; Robinson, S. D. *Coord. Chem. Rev.* **1983**, *50*, 109-208.
50. Felthouse, T. R. *Progr. Inorg. Chem.* **1982**, *29*, 73-166.
51. Nakamura, E.; Yoshikai, N.; Yamanaka, M. *J. Am. Chem. Soc.* **2002**, *124*, 7181-7192.
52. Hashimoto, S.-i.; Watanabe, N.; Ikegami, S. *Tetrahedron Lett.* **1992**, *33*, 2709-2712.
53. Dennis, A. M.; Korp, J. D.; Bernal, I.; Howard, R. A.; Bear, J. L. *Inorg. Chem.* **1983**, *22*, 1522-1529.
54. Kadish, K. M.; Lancon, D.; Dennis, A. M.; Bear, J. L. *Inorg. Chem.* **1982**, *21*, 2987-2992.
55. Chavan, M. Y.; Zhu, T. P.; Lin, X. Q.; Ahsan, M. Q.; Bear, J. L.; Kadish, K. M. *Inorg. Chem.* **1984**, *23*, 4538-4545.
56. Ye, T.; Garcia, C. F.; McKervey, M. A. *J. Chem. Soc., Perkin Trans. 1* **1995**, 1373-1381.
57. Hashimoto, S.-i.; Watanabe, N.; Sato, T.; Shiro, M.; Ikegami, S. *Tetrahedron Lett.* **1993**, *34*, 5109-5112.
58. Natori, Y.; Tsutsui, H.; Sato, N.; Nakamura, S.; Nambu, H.; Shiro, M.; Hashimoto, S. *J. Org. Chem.* **2009**, *74*, 4418-4421.
59. Chiu, P.; Zhang, X.; Ko, R. Y. Y. *Tetrahedron Lett.* **2004**, *45*, 1531-1534.
60. Kitagaki, S.; Anada, M.; Kataoka, O.; Matsuno, K.; Umeda, C.; Watanabe, N.; Hashimoto, S.-i. *J. Am. Chem. Soc.* **1999**, *121*, 1417-1418.
61. Anada, M.; Mita, O.; Watanabe, H.; Kitagaki, S.; Hashimoto, S. *Synlett* **1999**, *1999*, 1775-1777.
62. Tsutsui, H.; Yamaguchi, Y.; Kitagaki, S.; Nakamura, S.; Anada, M.; Hashimoto, S. *Tetrahedron: Asymmetry* **2003**, *14*, 817-821.
63. Davies, H. M. L.; Hutcheson, D. K. *Tetrahedron Lett.* **1993**, *34*, 7243-7246.
64. Davies, H. M. L.; Bruzinski, P. R.; Lake, D. H.; Kong, N.; Fall, M. J. *J. Am. Chem. Soc.* **1996**, *118*, 6897-6907.
65. Davies, H. M. L.; Panaro, S. A. *Tetrahedron Lett.* **1999**, *40*, 5287-5290.
66. Davies, H. M. L.; Yang, J.; Nikolai, J. *J. Organomet. Chem.* **2005**, *690*, 6111-6124.
67. Davies, H. M. L.; Hansen, T.; Hopper, D. W.; Panaro, S. A. *J. Am. Chem. Soc.* **1999**, *121*, 6509-6510.
68. Davies, H. M. L.; Hedley, S. J.; Bohall, B. R. *J. Org. Chem.* **2005**, *70*, 10737-10742.
69. Davies, H. M. L.; Venkataramani, C.; Hansen, T.; Hopper, D. W. *J. Am. Chem. Soc.* **2003**, *125*, 6462-6468.

70. Biffis, A.; Braga, M.; Cadamuro, S.; Tubaro, C.; Basato, M. *Org. Lett.* **2005**, *7*, 1841-1844.
71. Reddy, R. P.; Lee, G. H.; Davies, H. M. L. *Org. Lett.* **2006**, *8*, 3437-3440.
72. Denton, J. R.; Davies, H. M. L. *Org. Lett.* **2009**, *11*, 787-790.
73. Bonge, H. T.; Kaboli, M.; Hansen, T. *Tetrahedron Lett.* **2010**, *51*, 5375-5377.
74. Dennis, A. M.; Howard, R. A.; Lancon, D.; Kadish, K. M.; Bear, J. L. *J. Chem. Soc., Chem. Commun.* **1982**, 399-401.
75. Ahsan, M. Q.; Bernal, I.; Bear, J. L. *Inorg. Chem.* **1986**, *25*, 260-265.
76. Padwa, A.; Austin, D. J.; Price, A. T.; Semones, M. A.; Doyle, M. P.; Protopopova, M. N.; Winchester, W. R.; Tran, A. *J. Am. Chem. Soc.* **1993**, *115*, 8669-8680.
77. Doyle, M. P.; Westrum, L. J.; Wolthuis, W. N. E.; See, M. M.; Boone, W. P.; Bagheri, V.; Pearson, M. M. *J. Am. Chem. Soc.* **1993**, *115*, 958-964.
78. Doyle, M. P.; Bagheri, V.; Wandless, T. J.; Harn, N. K.; Brinker, D. A.; Eagle, C. T.; Loh, K. L. *J. Am. Chem. Soc.* **1990**, *112*, 1906-1912.
79. Doyle, M. P.; Brandes, B. D.; Kazala, A. P.; Pieters, R. J.; Jarstfer, M. B.; Watkins, L. M.; Eagle, C. T. *Tetrahedron Lett.* **1990**, *31*, 6613-6616.
80. Doyle, M. P.; Van Oeveren, A.; Westrum, L. J.; Protopopova, M. N.; Clayton, T. W. *J. Am. Chem. Soc.* **1991**, *113*, 8982-8984.
81. Doyle, M. P.; Kalinin, A. V. *Synlett* **1995**, *1995*, 1075-1076.
82. Doyle, M. P.; Winchester, W. R.; Hoorn, J. A. A.; Lynch, V.; Simonsen, S. H.; Ghosh, R. *J. Am. Chem. Soc.* **1993**, *115*, 9968-9978.
83. Doyle, M. P.; Dyatkin, A. B.; Roos, G. H. P.; Canas, F.; Pierson, D. A.; van Basten, A.; Mueller, P.; Polleux, P. *J. Am. Chem. Soc.* **1994**, *116*, 4507-4508.
84. Doyle, M. P.; Dyatkin, A. B. *J. Org. Chem.* **1995**, *60*, 3035-3038.
85. Doyle, M. P.; Wang, Y.; Ghorbani, P.; Bappert, E. *Org. Lett.* **2005**, *7*, 5035-5038.
86. Doyle, M. P.; Protopopova, M. N.; Winchester, W. R.; Daniel, K. L. *Tetrahedron Lett.* **1992**, *33*, 7819-7822.
87. Bykowski, D.; Wu, K.-H.; Doyle, M. P. *J. Am. Chem. Soc.* **2006**, *128*, 16038-16039.
88. Doyle, M. P.; Zhou, Q.-L.; Dyatkin, A. B.; Ruppar, D. A. *Tetrahedron Lett.* **1995**, *36*, 7579-7582.
89. Doyle, M. P.; Timmons, D. J.; Arndt, M. M. R.; Duursma, A.; Colyer, J. T.; Brünner, H. *Russ. Chem. Bull., Int. Ed.* **2001**, *50*, 2156-2161.
90. Doyle, M. P.; Zhou, Q.-L.; Raab, C. E.; Roos, G. H. P.; Simonsen, S. H.; Lynch, V. *Inorg. Chem.* **1996**, *35*, 6064-6073.
91. Bode, J. W.; Doyle, M. P.; Protopopova, M. N.; Zhou, Q.-L. *J. Org. Chem.* **1996**, *61*, 9146-9155.
92. Doyle, M. P.; Protopopova, M. N.; Zhou, Q.-L.; Bode, J. W.; Simonsen, S. H.; Lynch, V. *J. Org. Chem.* **1995**, *60*, 6654-6655.
93. Nichols, J. M.; Liu, Y.; Zavalij, P.; Isaacs, L.; Doyle, M. P. *Inorg. Chim. Acta* **2008**, *361*, 3309-3314.
94. McCarthy, N.; McKervey, M. A.; Ye, T.; McCann, M.; Murphy, E.; Doyle, M. P. *Tetrahedron Lett.* **1992**, *33*, 5983-5986.
95. Pirrung, M. C.; Zhang, J. *Tetrahedron Lett.* **1992**, *33*, 5987-5990.
96. Chakravarty, A. R.; Cotton, F. A.; Tocher, D. A.; Tocher, J. H. *Organometallics* **1985**, *4*, 8-13.
97. Taber, D. F.; Malcolm, S. C.; Bieger, K.; Lahuerta, P.; Sanau, M.; Stiriba, S.-E.; Perez-Prieto, J.; Monge, M. A. *J. Am. Chem. Soc.* **1999**, *121*, 860-861.
98. Estevan, F.; Herbst, K.; Lahuerta, P.; Barberis, M.; Perez-Prieto, J. *Organometallics* **2001**, *20*, 950-957.

99. Esteban, J.; Estevan, F.; Sanaú, M. *Inorg. Chim. Acta* **2009**, *362*, 1179-1184.
100. Mbuvi, H. M.; Woo, L. K. *Organometallics* **2008**, *27*, 637-645.
101. Maas, G.; Werle, T.; Alt, M.; Mayer, D. *Tetrahedron* **1993**, *49*, 881-888.
102. Woo, L. K.; Smith, D. A. *Organometallics* **1992**, *11*, 2344-2346.
103. Nakamura, A.; Konishi, A.; Tatsuno, Y.; Otsuka, S. *J. Am. Chem. Soc.* **1978**, *100*, 3443-3448.
104. Tomilov, Y. V.; Kostitsyn, A. B.; Shulishov, E. V.; Nefedov, O. M. *Synthesis* **1990**, *1990*, 246-248.
105. Hanks, T. W.; Jennings, P. W. *J. Am. Chem. Soc.* **1987**, *109*, 5023-5025.
106. Jeyakumar, K.; Chand, D. K. *Synthesis* **2008**, *2008*, 1685-1687.
107. Kubo, T.; Sakaguchi, S.; Ishii, Y. *Chem. Commun.* **2000**, 625-626.
108. Moebius, D. C.; Kingsbury, J. S. *J. Am. Chem. Soc.* **2009**, *131*, 878-879.
109. Urbano, J.; Belderrain, T. R.; Nicasio, M. C.; Trofimenko, S.; Diaz-Requejo, M. M.; Perez, P. J. *Organometallics* **2005**, *24*, 1528-1532.
110. Fructos, M. R.; Belderrain, T. R.; de Frémont, P.; Scott, N. M.; Nolan, S. P.; Díaz-Requejo, M. M.; Pérez, P. J. *Angew. Chem., Int. Ed.* **2005**, *44*, 5284-5288.
111. Rivilla, I.; Gómez-Emeterio, B. P.; Fructos, M. R.; Díaz-Requejo, M. M.; Pérez, P. J. *Organometallics* **2011**, *30*, 2855-2860.
112. Dias, H. V. R.; Browning, R. G.; Richey, S. A.; Lovely, C. J. *Organometallics* **2004**, *23*, 1200-1202.
113. Hashimoto, S.-i.; Wantanabe, N.; Ikegami, S. *Synlett* **1994**, *1994*, 353-355.
114. Taber, D. F.; Ruckle, R. E. *J. Am. Chem. Soc.* **1986**, *108*, 7686-7693.
115. Watanabe, N.; Ogawa, T.; Ohtake, Y.; Ikegami, S.; Hashimoto, S.-i. *Synlett* **1996**, *1996*, 85-86.
116. Watanabe, N.; Ohtake, Y.; Hashimoto, S.-i.; Shiro, M.; Ikegami, S. *Tetrahedron Lett.* **1995**, *36*, 1491-1494.
117. Takahashi, T.; Tsutsui, H.; Tamura, M.; Kitagaki, S.; Nakajima, M.; Hashimoto, S. *Chem. Commun.* **2001**, 1604-1605.
118. Taber, D. F.; Malcolm, S. C. *J. Org. Chem.* **2001**, *66*, 944-953.
119. Zhang, X.; Li, Z.; Chu, J. C. K.; Chiu, P. *Tetrahedron Lett.* **2011**, *52*, 6763-6766.
120. Minami, K.; Saito, H.; Tsutsui, H.; Nambu, H.; Anada, M.; Hashimoto, S.-i. *Adv. Synth. Catal.* **2005**, *347*, 1483-1487.
121. Takeda, K.; Oohara, T.; Anada, M.; Nambu, H.; Hashimoto, S. *Angew. Chem., Int. Ed.* **2010**, *49*, 6979-6983.
122. Müller, P.; Boléa, C. *Helv. Chim. Acta* **2002**, *85*, 483-494.
123. Doyle, M. P.; Dyatkin, A. B.; Tedrow, J. S. *Tetrahedron Lett.* **1994**, *35*, 3853-3856.
124. Doyle, M. P.; Tedrow, J. S.; Dyatkin, A. B.; Spaans, C. J.; Ene, D. G. *J. Org. Chem.* **1999**, *64*, 8907-8915.
125. Müller, P.; Polleux, P. *Helv. Chim. Acta* **1994**, *77*, 645-654.
126. Doyle, M. P.; Hu, W.; Valenzuela, M. V. *J. Org. Chem.* **2002**, *67*, 2954-2959.
127. Wee, A. G. H. *Tetrahedron Lett.* **2000**, *41*, 9025-9029.
128. Doyle, M. P.; Zhou, Q.-L.; Raab, C. E.; Roos, G. H. P. *Tetrahedron Lett.* **1995**, *36*, 4745-4748.
129. Doyle, M. P.; Kalinin, A. V.; Ene, D. G. *J. Am. Chem. Soc.* **1996**, *118*, 8837-8846.
130. Doyle, M. P.; Davies, S. B.; May, E. J. *J. Org. Chem.* **2001**, *66*, 8112-8119.
131. Doyle, M. P.; Yan, M.; Phillips, I. M.; Timmons, D. J. *Adv. Synth. Catal.* **2002**, *344*, 91-95.
132. Davies, H. M. L.; Venkataramani, C. *Org. Lett.* **2001**, *3*, 1773-1775.
133. Davies, H. M. L.; Jin, Q. *Org. Lett.* **2005**, *7*, 2293-2296.

134. Doyle, M. P.; Morgan, J. P.; Fettinger, J. C.; Zavalij, P. Y.; Colyer, J. T.; Timmons, D. J.; Carducci, M. D. *J. Org. Chem.* **2005**, *70*, 5291-5301.
135. Doyle, M. P.; May, E. J. *Synlett* **2001**, *2001*, 967-969.
136. McKervey, M. A.; Ye, T. *J. Chem. Soc., Chem. Commun.* **1992**, 823-824.
137. Saito, H.; Oishi, H.; Kitagaki, S.; Nakamura, S.; Anada, M.; Hashimoto, S. *Org. Lett.* **2002**, *4*, 3887-3890.
138. Ye, T.; McKervey, M. A.; Brandes, B. D.; Doyle, M. P. *Tetrahedron Lett.* **1994**, *35*, 7269-7272.
139. Kurosawa, W.; Kan, T.; Fukuyama, T. *J. Am. Chem. Soc.* **2003**, *125*, 8112-8113.
140. Kurosawa, W.; Kobayashi, H.; Kan, T.; Fukuyama, T. In *Tetrahedron Chair Issue: Catalytic tools enabling total synthesis Symposia-in-Print 108* 2004; Vol. 60, p 9615-9628.
141. Koizumi, Y.; Kobayashi, H.; Wakimoto, T.; Furuta, T.; Fukuyama, T.; Kan, T. *J. Am. Chem. Soc.* **2008**, *130*, 16854-16855.
142. Lou, Y.; Horikawa, M.; Kloster, R. A.; Hawryluk, N. A.; Corey, E. J. *J. Am. Chem. Soc.* **2004**, *126*, 8916-8918.
143. Davies, H. M. L.; Grazini, M. V. A.; Aouad, E. *Org. Lett.* **2001**, *3*, 1475-1477.
144. Davies, H. M. L.; Kong, N. *Tetrahedron Lett.* **1997**, *38*, 4203-4206.
145. Kurosawa, W.; Kan, T.; Fukuyama, T. *Synlett* **2003**, *2003*, 1028-1031.
146. Doyle, M. P.; Oon, S.-M.; van der Heide, F. R.; Brown, C. B. *Bioorg. Med. Chem. Lett.* **1993**, *3*, 2409-2414.
147. Watanabe, N.; Anada, M.; Hashimoto, S.-i.; Ikegami, S. *Synlett* **1994**, *1994*, 1031-1034.
148. Doyle, M. P.; Taunton, J.; Pho, H. Q. *Tetrahedron Lett.* **1989**, *30*, 5397-5400.
149. Zakrzewska, M. E.; Cal, P. M. S. D.; Candeias, N. R.; Bogel-Łukasik, R.; Afonso, C. A. M.; Ponte, M. N.; Gois, P. M. P. *Green Chem. Lett. Rev.* **2011**, 1-30.
150. Anada, M.; Wantanabe, N. *Chem. Commun.* **1998**, 1517-1518.
151. Anada, M.; Hashimoto, S.-i. *Tetrahedron Lett.* **1998**, *39*, 9063-9066.
152. Anada, M.; Hashimoto, S.-i. *Tetrahedron Lett.* **1998**, *39*, 79-82.
153. Doyle, M. P.; Shanklin, M. S.; Pho, H. Q.; Mahapatro, S. N. *J. Org. Chem.* **1988**, *53*, 1017-1022.
154. Doyle, M. P.; Hu, W.; Wee, A. G. H.; Wang, Z.; Duncan, S. C. *Org. Lett.* **2003**, *5*, 407-410.
155. Wee, A. G. H.; Duncan, S. C. *J. Org. Chem.* **2005**, *70*, 8372-8380.
156. Wee, A. G. H.; Duncan, S. C. *Tetrahedron Lett.* **2002**, *43*, 6173-6176.
157. Wee, A. G. H.; Duncan, S. C.; Fan, G.-j. *Tetrahedron: Asymmetry* **2006**, *17*, 297-307.
158. Rezanka, T.; Sobotka, M.; Spizek, J.; Sigler, K. *Anti-Infective Agents Med. Chem.* **2006**, *5*, 187-224.
159. Hrytsak, M.; Etkin, N.; Durst, T. *Tetrahedron Lett.* **1986**, *27*, 5679-5682.
160. Babu, S. D.; Hrytsak, M. D.; Durst, T. *Can. J. Chem.* **1989**, *67*, 1071-1076.
161. John, J. P.; Novikov, A. V. *Org. Lett.* **2007**, *9*, 61-63.
162. Jungong, C. S.; John, J. P.; Novikov, A. V. *Tetrahedron Lett.* **2009**, *50*, 1954-1957.
163. Espino, C. G.; Wehn, P. M.; Chow, J.; Du Bois, J. *J. Am. Chem. Soc.* **2001**, *123*, 6935-6936.
164. Wulfman, D. S.; Peace, B. W.; McDaniel, R. S. *Tetrahedron* **1976**, *32*, 1251-1255.
165. Adams, J.; Poupart, M.-A.; Grenier, L.; Schaller, C.; Ouimet, N.; Frenette, R. *Tetrahedron Lett.* **1989**, *30*, 1749-1752.
166. Callot, H. J.; Metz, F. *Tetrahedron Lett.* **1982**, *23*, 4321-4324.

167. Demonceau, A.; Noels, A. F.; Costa, J.-L.; Hubert, A. J. *J. Mol. Catal.* **1990**, *58*, 21-26.
168. Demonceau, A.; Noels, A. F.; Teyssie, P.; Hubert, A. J. *J. Mol. Catal.* **1988**, *49*, 13-17.
169. Davies, H. M. L.; Hansen, T. *J. Am. Chem. Soc.* **1997**, *119*, 9075-9076.
170. Davies, H. M. L.; Panaro, S. A. *Tetrahedron* **2000**, *56*, 4871-4880.
171. Hansen, J.; Autschbach, J.; Davies, H. M. L. *J. Org. Chem.* **2009**, *74*, 6555-6563.
172. Davies, H. M. L.; Jin, Q. *Tetrahedron: Asymmetry* **2003**, *14*, 941-949.
173. Davies, H. M. L.; Ni, A. *Chem. Commun.* **2006**, 3110-3112.
174. Davies, H. M. L.; Stafford, D. G.; Hansen, T. *Org. Lett.* **1999**, *1*, 233-236.
175. Davies, H. M. L.; Yang, J. *Adv. Synth. Catal.* **2003**, *345*, 1133-1138.
176. Davies, H. M. L.; Beckwith, R. E. J.; Antoulinakis, E. G.; Jin, Q. *J. Org. Chem.* **2003**, *68*, 6126-6132.
177. Davies, H. M. L.; Antoulinakis, E. G. *Org. Lett.* **2000**, *2*, 4153-4156.
178. Davies, H. M. L.; Jin, Q. *Org. Lett.* **2004**, *6*, 1769-1772.
179. Davies, H. M. L.; Venkataramani, C. *Angew. Chem., Int. Ed.* **2002**, *41*, 2197-2199.
180. Davies, H. M. L.; Jin, Q.; Ren, P.; Kovalevsky, A. Y. *J. Org. Chem.* **2002**, *67*, 4165-4169.
181. Davies, H. M. L.; Ren, P. *J. Am. Chem. Soc.* **2001**, *123*, 2070-2071.
182. Davies, H. M. L.; Ren, P.; Jin, Q. *Org. Lett.* **2001**, *3*, 3587-3590.
183. Davies, H. M. L.; Jin, Q. *J. Am. Chem. Soc.* **2004**, *126*, 10862-10863.
184. Davies, H. M. L.; Hansen, T.; Churchill, M. R. *J. Am. Chem. Soc.* **2000**, *122*, 3063-3070.
185. Nadeau, E.; Li, Z.; Morton, D.; Davies, H. M. L. *Synlett* **2009**, *2009*, 151-154.
186. Davies, H. M. L.; Antoulinakis, E. G.; Hansen, T. *Org. Lett.* **1999**, *1*, 383-386.
187. Davies, H. M. L.; Stafford, D. G.; Hansen, T.; Churchill, M. R.; Keil, K. M. *Tetrahedron Lett.* **2000**, *41*, 2035-2038.
188. Davies, H. M. L.; Yang, J.; Manning, J. R. *Tetrahedron: Asymmetry* **2006**, *17*, 665-673.
189. Manning, J. R.; Sexton, T.; Childers, S. R.; Davies, H. M. L. *Bioorg. Med. Chem. Lett.* **2009**, *19*, 58-61.
190. Davies, H. M. L.; Dai, X.; Long, M. S. *J. Am. Chem. Soc.* **2006**, *128*, 2485-2490.
191. Davies, H. M. L.; Dai, X. *Tetrahedron* **2006**, *62*, 10477-10484.
192. Davies, H. M. L.; Walji, A. M. *Angew. Chem., Int. Ed.* **2005**, *44*, 1733-1735.
193. Lian, Y.; Davies, H. M. L. *J. Am. Chem. Soc.* **2011**, *133*, 11940-11943.
194. McMills, M. C.; Humes, R. J.; Pavlyuk, O. M. *Tetrahedron Lett.* **2012**, *53*, 849-851.
195. Pavlyuk, O.; Teller, H.; McMills, M. C. *Tetrahedron Lett.* **2009**, *50*, 2716-2718.
196. Davies, H. M. L.; Huby, N. J. S.; Cantrell, W. R.; Olive, J. L. *J. Am. Chem. Soc.* **1993**, *115*, 9468-9479.
197. Müller, P.; Tohill, S. *Tetrahedron* **2000**, *56*, 1725-1731.
198. Ventura, D. L.; Li, Z.; Coleman, M. G.; Davies, H. M. L. *Tetrahedron* **2009**, *65*, 3052-3061.
199. Chuprakov, S.; Malik, J. A.; Zibinsky, M.; Fokin, V. V. *J. Am. Chem. Soc.* **2011**, *133*, 10352-10355.
200. Chuprakov, S.; Kwok, S. W.; Zhang, L.; Lercher, L.; Fokin, V. V. *J. Am. Chem. Soc.* **2009**, *131*, 18034-18035.

Chapter 2

Intramolecular C–H insertion reactions of α-diazo-β-keto sulfones

Contents

2.1 Introduction 70
2.1.1 Project background 70
2.1.2 Project objectives 74
2.2 Synthesis of β-keto sulfones 75
2.2.1 Alcohol synthesis 77
2.2.2 Iodide synthesis 78
2.2.3 Malonate synthesis 79
2.2.4 Carboxylic acid synthesis 81
2.2.5 Ester synthesis 82
2.2.6 β-Keto sulfone synthesis 85
2.3 Synthesis of α-diazo-β-keto sulfones 86
2.4 Synthesis of racemic 2-phenylsulfonyl cyclopentanones 90
2.5 Enantioselective rhodium-catalysed C–H insertion reactions of α-diazo-β-keto sulfones 97
2.6 Enantioselective copper-catalysed C–H insertion reactions of α-diazo-β-keto sulfones 103
2.6.1 C–H insertion reactions with copper-bis(oxazoline) catalysts 104
2.6.2 Investigation of additive effects 114
2.6.2.1 C–H insertions in the presence of NaBARF 114
2.6.2.2 C–H insertions in the presence of a range of additive species 124
2.6.3 Investigation of reaction conditions 131
2.6.3.1 Investigation of solvent effects 131
2.6.3.2 Investigation of catalyst complexation time 133
2.7 Examination of α-diazo-β-keto sulfone substrate modification 134
2.7.1 Investigation of modifications to the sulfone substituent 135
2.7.2 Investigation of modifications to the phenyl ring adjacent to the C–H insertion site 142
2.7.3 Investigation of diastereocontrol 152
2.8 Synthesis of bis(oxazoline) ligands and investigation of effects on enantiocontrol 161
2.8.1 Synthesis of bis(oxazoline) ligands 165
2.8.2 C–H insertion reactions with modified bis(oxazoline) ligands 172
2.9 Transition state studies of enantioselective copper-catalysed C–H insertion reactions of α-diazo-β-keto sulfones 177
2.10 Conclusions 187
2.11 References 190

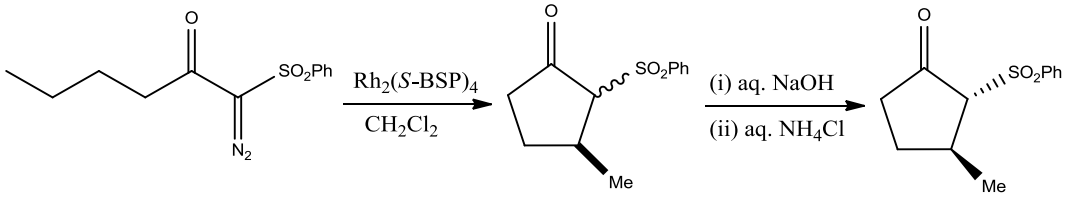
2.1 Introduction

Access to enantiopure forms of compounds destined for use as pharmaceuticals is of critical importance from a regulatory and safety viewpoint. In 2006 it was estimated that chiral compounds comprised more than half of drugs approved worldwide,[1] including many of the world's top-selling drugs. Indeed, in 2007, five of the six top-selling drugs worldwide were sold as single enantiomers: Lipitor®, Plavix®, Nexium®, Diovan® and Advair®.[2] While resolution has been traditionally used for accessing enantiopure materials, alternative approaches through enantioselective synthesis exist, namely; synthesis with chiral pool substrates, employment of chiral auxiliaries as temporary tethers and asymmetric catalysis. The latter process involves the application of enantiopure catalysts to transform prochiral and racemic substrates into enantiomerically enriched products. Asymmetric catalysis offers advantages over alternative methods in terms of chiral economy *i.e.* trace amounts of enantiopure catalyst can produce large quantities of enantiopure product, low cost and high efficiency. As a result, asymmetric catalysis is now an established field which is widely used both in research and industrial laboratories.

Highly regioselective carbenoid C–H insertion reactions of α-diazocarbonyl compounds catalysed by rhodium(II) catalysts lead to very efficient cyclopentanone formation, with activation of the unactivated C–H bond occurring under very mild conditions rendering this a very valuable synthetic process. The cyclopentane subunit is found in many important bioactive compounds *e.g.* prostaglandins. To date a number of research groups have explored the development of asymmetric catalysts for C–H insertion reactions, however, the identification of a generally applicable catalyst system delivering consistently high enantioselectivity remains elusive.

2.1.1 Project background

The work described in this research project was prompted by pioneering investigations of the asymmetric synthesis of 2-sulfonylcyclopentanones undertaken by McKervey, Maguire and co-workers in the late 1980's.[3,4] The Rh_2(*S*-BSP)$_4$-catalysed decomposition of α-diazo-β-keto sulfone **1** (**Scheme 2.1**), described in this early work, represented the first reported example of asymmetric induction in C–H insertion chemistry.[3] In this previous study, cyclopentanone **2** was obtained as a mixture of *cis* and *trans* isomers in >90% yield, with 12% ee being recorded for the *trans* isomer following base-mediated equilibration.

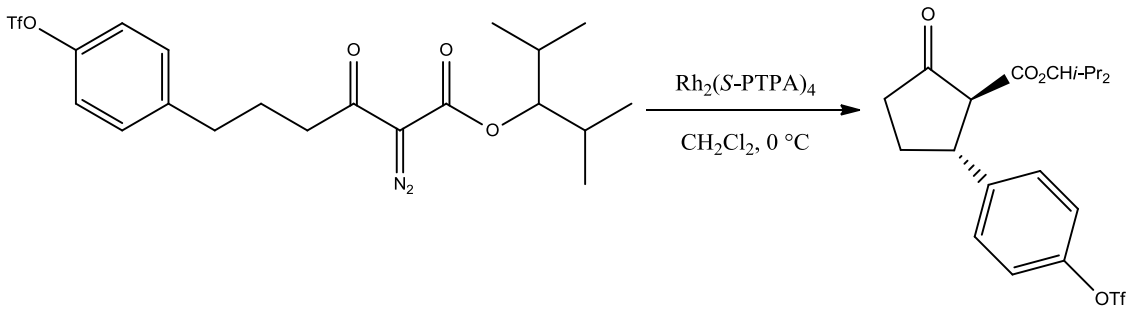


>90% yield *12% ee*

1 **2**

Scheme 2.1

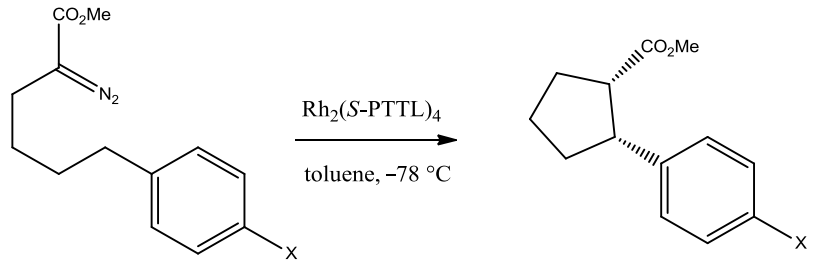
Work in the area of intramolecular carbocycle-producing C–H insertion has since focused mainly on cyclisation with α-diazo-β-keto ester carbenoid precursors. The highest enantioselectivity achieved to date for the production of cyclopentanone products has been recorded at 80% ee by Hashimoto and co-workers (**Scheme 2.2**, see also **Table 1.2**).[5] Although, notably, in this previous report high levels of asymmetric induction were achieved only for substrates possessing aryl substituents at the C–H insertion site and bulky alkoxy ester groups.



84% yield, 80% ee

Scheme 2.2

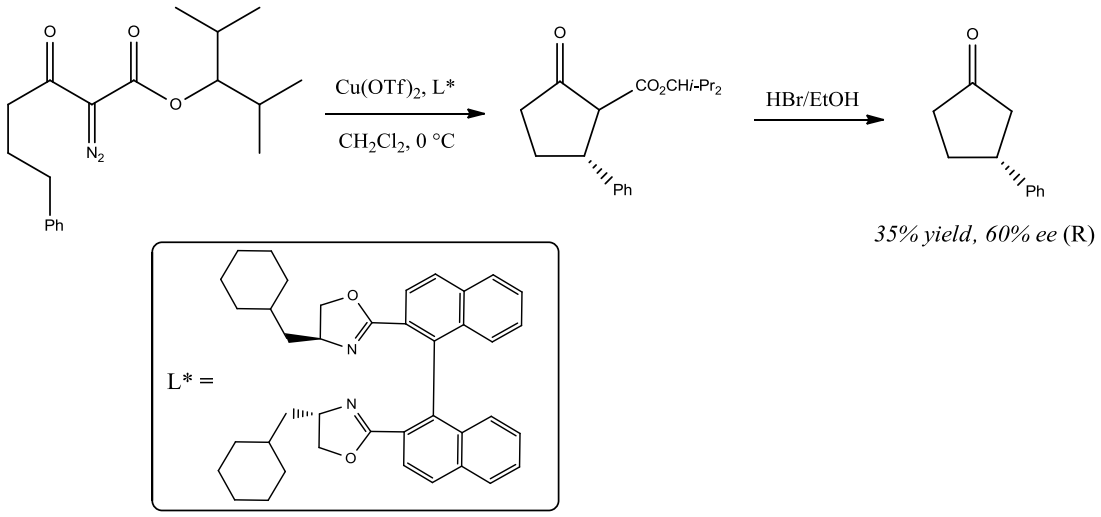
High levels of enantioselectivity (up to 95% ee) were also obtained by Hashimoto and co-workers for the synthesis of 1,2-disubstituted cyclopentanes *via* rhodium(II)-catalysed C–H insertion of a range of α-diazoester substrates (**Scheme 2.3**, see also **Table 1.6**).[6]



X = H, OMe, Cl *92-95% ee*

Scheme 2.3

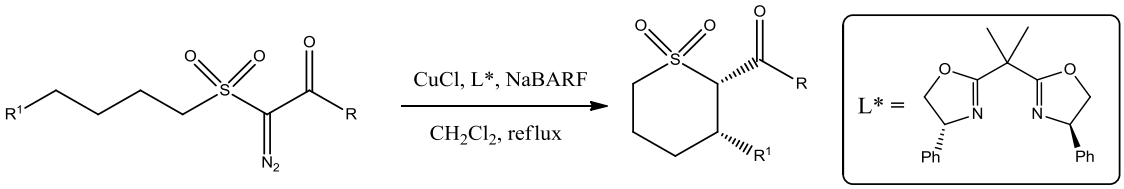
While the use of copper catalysts dominated early investigations of C–H insertion reactions,[7] recent examples of enantioselective C–H insertions employing catalytic copper complexes are sparse. Limited reports exist, however, the level of enantiocontrol achieved has been generally moderate, up to a maximum of 60% ee for intramolecular C–H insertion[8] (**Scheme 2.4**, see also **Table 1.8**) and 88% ee for the intermolecular reaction[9].



Scheme 2.4

Recently, Maguire and Flynn have demonstrated that copper-bis(oxazoline) complexes are highly effective catalysts for C–H insertion reactions of α-diazosulfones.[10,11] In this previous work, thiopyran products were prepared in up to 98% ee, representing the highest level of enantioselectivity reported to date for copper-catalysed C–H insertion (**Table 2.1**, entries 1–9). The substrate scope for the copper-bis(oxazoline) methodology was shown to be wide ranging, with all-but-one of the α-diazosulfones examined (**Table 2.1**, entry 8) leading to enantioenriched thiopyrans in excess of 90% ee. Formation of six-membered cyclic sulfones in the C–H insertions examined was unexpected given that C–H insertion reactions usually display a strong preference for five-membered ring formation.

Table 2.1 *Asymmetric copper-catalysed C–H insertion to provide thiopyrans*[a]

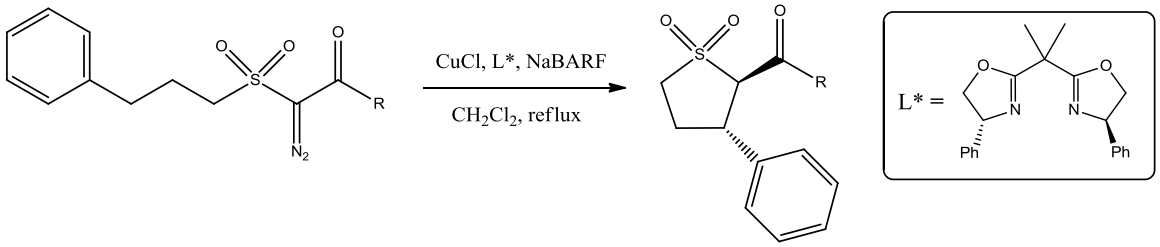


Entry	R	R^1	Time (h)	Yield (%)[b]	ee (%)[c]
1	OMe	Ph	5	47	98
2	OMe	4-tolyl	5	64	96
3	OMe	4-anisyl	22	56	91
4	OMe	4-nitrophenyl	2.5	–	–
5	OMe	benzyl	7	42	96
6	OMe	ethyl	16	68	97
7	OBn	octyl	22	66	90
8	Me	Ph	22	30	85
9	Ph	Ph	6	49	97

[a] General procedure: 5 mol% CuCl, 6 mol% L*, 6 mol% NaBARF and diazo (200 mg) in DCM (10 mL) at reflux.
[b] Yield of *cis*-thiopyran after column chromatography.
[c] Determined by chiral stationary phase HPLC.

Interestingly, C–H insertions with substrates featuring a reduction of the alkyl chain length, where six-membered ring formation is not possible (**Table 2.2**),[10,11] resulted in decreased levels of asymmetric induction compared to the synthesis of thiopyrans (**Table 2.1**). This result suggests that the key features affecting the degree of enantioselection in the transition states leading to five- or six-membered ring formation differ significantly, presumably due to conformational and/or steric effects.

Table 2.2 *Asymmetric copper-catalysed C–H insertion to provide sulfolanes*[a]



Entry	R	Time (h)	Yield (%)[b]	ee (%)[c]
1	OEt	5	57	60
2	Me	3	40	40

[a] General procedure: 5 mol% CuCl, 6 mol% L*, 6 mol% NaBARF and diazo (200 mg) in DCM (10 mL) at reflux.
[b] Yield of *cis*-thiopyran after column chromatography.
[c] Determined by chiral stationary phase HPLC.

2.1.2 Project objectives

Despite the results described above, asymmetric catalysis in intramolecular C–H insertion processes producing carbocyclic products remains a relatively underexplored area in recent literature by comparison with related intramolecular heterocycle producing and intermolecular C–H insertion processes. In addition, reports examining the insertion reactions of carbenoids possessing sulfonyl substituents are minimal. Therefore further exploration of intramolecular α-diazosulfonyl insertions is warranted. While earlier results in this area by Flynn[11] demonstrated excellent enantiocontrol leading to enantioenriched thiopyrans, and to a lesser extent sulfolanes, extension of this work to the more synthetically powerful and challenging cyclopentanone series was identified as a key priority.

The specific aims of this project may be summarised as follows:

- To synthesise a range of α-diazo-β-keto sulfone substrates (**Figure 2.1**) to enable investigation of steric and electronic effects on the outcome of C–H insertions.

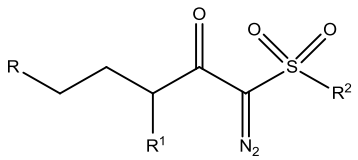
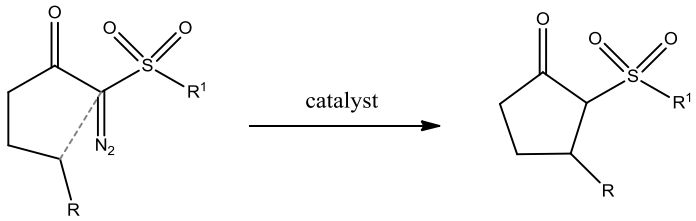


Figure 2.1

- To investigate the C–H insertion reactions of the α-diazo-β-keto sulfone substrates using achiral and chiral rhodium and copper catalysts (**Scheme 2.5**); to characterise the cyclopentanone products obtained and identify competing side-reactions.



Scheme 2.5

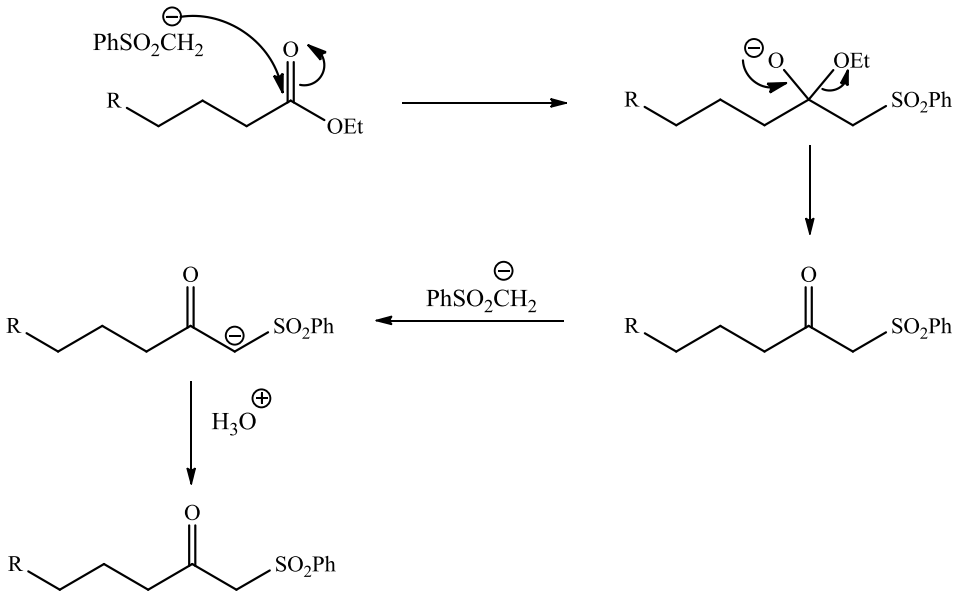
- To examine the influence of steric and electronic effects of various ligands for enantiopure rhodium and copper catalysts on the stereochemical outcome of the C–H insertion reactions.

- To probe the influence of temperature, solvent, catalyst preparation, additive and counterion effects and substrate modification on the C–H insertion processes.

- Based on the observed trends, to explore the development of novel asymmetric catalysts for C–H insertions with the objective of designing a catalyst system with general substrate scope.

2.2 Synthesis of β-keto sulfones

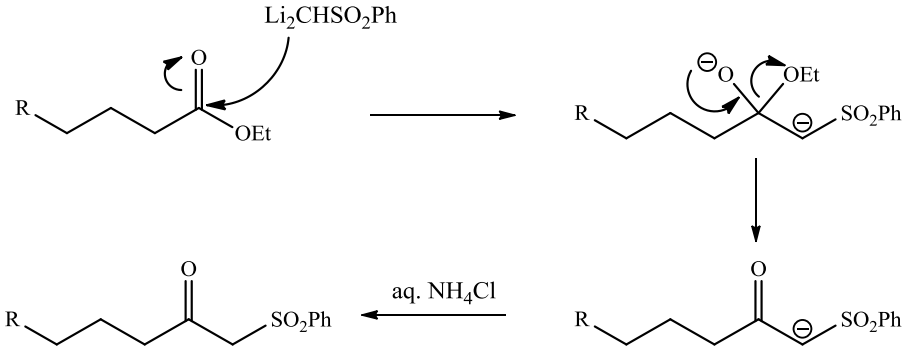
As diazo transfer to β-keto sulfones provides a well established route to analogous α-diazo-β-keto sulfones required for this study,[7,12] the first synthethic challenge was to develop a versatile synthetic strategy providing access to a range of β-keto sulfone substrates. The preparation of β-keto sulfone products may be achieved by a variety of synthetic methods. Among these methods is the 1965 procedure described by Corey and Chaykovsky[13] involving the sodium hydride induced deprotonation of methyl phenyl sulfone, readily prepared by oxidation of thioanisole with hydrogen peroxide,[14] followed by nucleophilic attack of the resulting methyl phenyl sulfonyl anion at the carbonyl group of a series of esters. Subsequent displacement of the ester ethoxy group provides the targeted β-keto sulfone derivatives (**Scheme 2.6**). The β-keto sulfones produced are considerably more acidic (pK_a ~ 10)[15] than the methyl phenyl sulfone starting material (pK_a ~ 29)[16] and undergo easy deprotonation by unreacted methyl phenyl sulfonyl anion. Thus, two equivalents of the methyl phenyl sulfonyl anion are required to achieve reaction completion. Following acidification, the desired β-keto sulfones are isolated, along with approximately one equivalent of methyl phenyl sulfone which was removed chromatographically.



Scheme 2.6

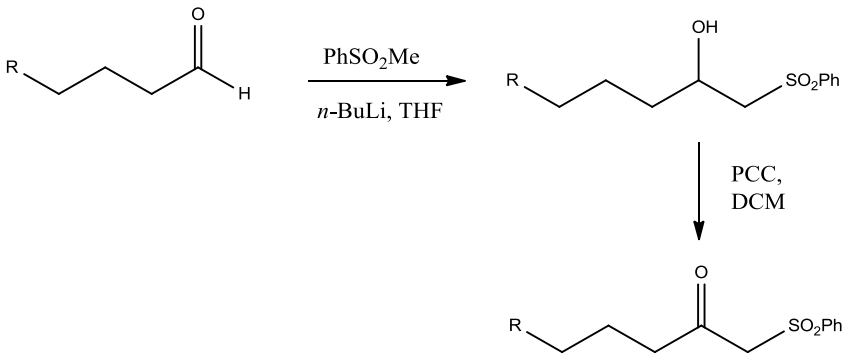
An alternative procedure[17-19] employing *n*-butyllithium was adopted in this project for the synthesis of our targeted β-keto sulfones. For this purpose, *n*-butyllithium (2 equivalents) was added to a solution of methyl phenyl sulfone in tetrahydrofuran (THF) at 0 °C. The

resulting solution was stirred for 1.5 h at 0 °C then a solution of ethyl ester in THF was added to the reaction mixture. Use of two equivalents of *n*-butyllithium in this reaction serves to generate the dilithio derivative of methyl phenyl sulfone. Attack of the dilithio species at the ester carbonyl group results in direct generation of the deprotonated β-keto sulfone, which, upon protonation with aqueous ammonium chloride, provides the desired β-keto sulfone products (**Scheme 2.7**). Although comparable yields are obtained for both the Corey and Chaykovsky and the alternative *n*-butyllithium-mediated method,[20,21] the latter procedure is advantageous in that only one equivalent of methyl phenyl sulfone is required, in contrast to the two equivalents necessary for the sodium hydride reaction. Accordingly, chromatographic purification is simplified due to the lower quantities of methyl phenyl sulfone remaining in the mixture upon reaction completion.



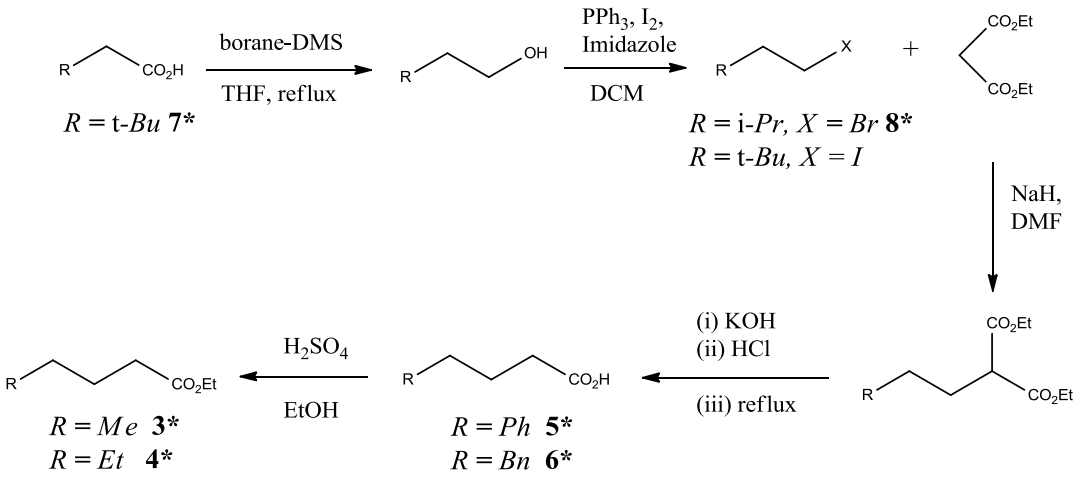
Scheme 2.7

An additional procedure (**Scheme 2.8**) has also previously been used to good effect in this research group, providing access to a range of β-keto sulfones in good yields, albeit with an additional synthetic step required.[21] This approach involves the addition of one equivalent of *n*-butyllithium to methyl phenyl sulfone. The resulting anion reacts with the aldehyde substrate to produce, after acidic work-up, the β-hydroxy sulfone intermediates. Oxidation of the β-hydroxy sulfones with pyridinium chlorochromate (PCC) yields the desired β-keto sulfone products.



Scheme 2.8

The synthetic strategy for β-keto sulfone synthesis adopted in this project required access to a range of ester starting materials. The esters ethyl pentanoate **3** and ethyl hexanoate **4** were commercially available, allowing synthesis of the corresponding β-keto sulfone products to be readily achieved. 4-Phenylbutanoic acid **5** and 5-phenylpentanoic acid **6** could also be purchased and converted to their ester counterparts *via* acid-catalysed esterification. However, the carboxylic acids or related compounds required for preparation of β-keto sulfone derivatives bearing *iso*-propyl and *tert*-butyl groups at the R position were not accessible commercially and, therefore, a synthetic plan (**Scheme 2.9**) was devised to allow synthesis of the required starting materials. The approach chosen for this purpose employs commercially available 3,3-dimethylbutanoic acid **7** and isopentylbromide **8**.

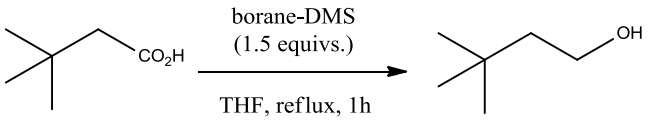


* = commercially available

Scheme 2.9

2.2.1 Alcohol synthesis

Synthesis of the β-keto sulfone derivative bearing a γ-*tert*-butyl substituent began from commercially available 3,3-dimethylbutanoic acid **7** (**Scheme 2.10**). The acid starting material was reduced with borane-dimethylsulfide (DMS) to provide the desired alcohol product **9** as a light yellow oil in quantitative yield. The reaction was initially conducted at room temperature following literature procedures,[22] however, a higher temperature was required to achieve reaction completion. Spectroscopic characteristics of alcohol **9** were consistent with those previously described for this compound.[23] This reaction was readily conducted on a multi-gram scale, providing sufficient material for subsequent synthetic steps.



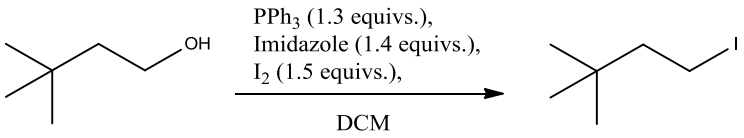
99% yield

7 **9**

Scheme 2.10

2.2.2 Iodide synthesis

3,3-Dimethylbutan-1-ol **9** was converted to the corresponding iodide **10** by treatment with triphenylphosphine, imidazole and iodine in dichloromethane (DCM) at 0 °C following literature procedures (**Scheme 2.11**).[24] The isolated product was very volatile and precautions were therefore taken to minimise product loss during work-up procedures *e.g.* rotary evaporation concentration of the crude product mixture was conducted in an ice-cold water bath and the product was stored in a sealed container in the freezer. Despite these attempts, some loss of product was observed to occur resulting in a moderate 66% overall yield following purification by trap-to-trap distillation. Once again, product synthesis was readily achieved on a multi-gram scale.



66% yield

9 **10**

Scheme 2.11

Interestingly, distinctive peak signals were observed in the ^{1}H NMR spectrum of 1-iodo-3,3-dimethylbutane **10** for the C(1)H_2 and C(2)H_2 protons. These signals were previously reported as triplets in the only literature reference[25] for iodide **10**, however, as shown in **Figure 2.2**, the peak pattern observed was much more complex, with an AA'XX' splitting pattern instead observed. Very similar peak patterns were also seen for the methylene signal adjacent to the *tert*-butyl group for the subsequent malonate (**Section 2.2.3**), carboxylic acid (**Section 2.2.4**), ester (**Section 2.2.5**), β-keto sulfone (**Section 2.2.6**) and α-diazo-β-keto sulfones (**Section 2.3**) derivatives of **10**.

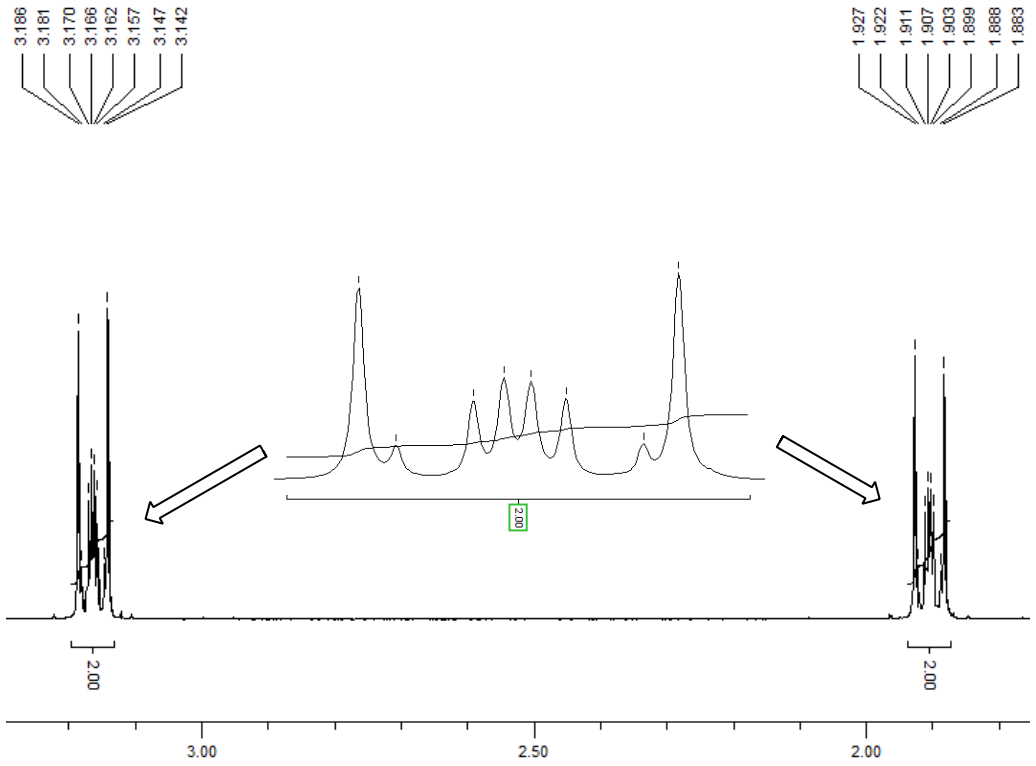
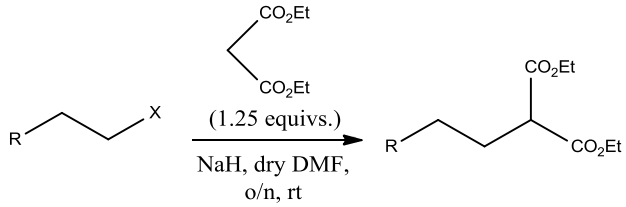


Figure 2.2 *δ_H (300 MHz, $CDCl_3$)*

2.2.3 Malonate synthesis

The next synthetic step involved the preparation of diethyl 2-isopentylmalonate **11** and diethyl 2-(3,3-dimethylbutyl)malonate **12**, from isopentyl bromide **8**, which was commercially available, and 1-iodo-3,3-dimethylbutane **10**, respectively (**Table 2.3**, entries 1–4). Malonate synthesis was achieved by reaction of sodium hydride, diethyl malonate and the appropriate alkyl halide in dimethylformamide (DMF). Following literature procedures (*method a*),[26] the reaction mixture was stirred at room temperature until complete by TLC analysis, triturated with ether, washed with acid and purified by column chromatography to provide the desired malonate products. Yields obtained using this procedure were moderate for the *iso*-propyl derivative **11** (**Table 2.3**, entry 1) and poor for the *tert*-butyl compound **12** (**Table 2.3**, entry 3). Although this outcome was predicted as the literature reference[26] also reported a poor overall yield of 33%, attempts were made to increase product yields in repeat experiments. Gentle heating of the reaction mixture to 60 °C for 1 h (*method c*) resulted in an additional 26% product yield for the synthesis of diethyl 2-(3,3-dimethylbutyl)malonate **12** (**Table 2.3**, entry 4). Extraction of an ether solution of the crude reaction mixture with 10% aqueous sodium hydroxide (*method b*) was also found to be a successful strategy for increasing product yields (**Table 2.3**, entry 2). This procedure works to remove excess diethyl malonate following several washes with the basic solution, with the result that purification by column chromatography was no longer required.

Table 2.3 *Synthesis of diethyl malonates*



Entry	Halide	Malonate	X	R	Yield (%)
1[a]	**8**[b]	**11**[c]	Br	*i*-Pr	55
2[d]	**8**[b]	**11**	Br	*i*-Pr	70
3[a]	**10**	**12**[e]	I	*t*-Bu	35
4[f]	**10**	**12**	I	*t*-Bu	61

[a] Reaction conducted using method a (**Section 4.2.3**)
[b] Halide was commercially available.
[c] Compound previously synthesised and characterised.[27]
[d] Reaction conducted using method b (**Section 4.2.3**).
[e] Novel compound; full characterisation conducted (see **Section 4.2.3** for details).
[f] Reaction conducted using method c (**Section 4.2.3**).

An interesting CH_2CH_3 spin system was observed in the ^1H NMR spectra of the synthesised *iso*-propyl **11** and *tert*-butyl **12** diethyl malonate derivatives. A normal ethoxy A_2X_3 system was expected according to literature precedent for **11** and related diethyl malonate compounds,[26-29] however, a far more elaborate spin system was instead observed (**Figure 2.3**). In place of the expected A_2X_3 system, the CH_2CH_3 spin system of the two ethoxy groups was actually an ABX_3 system owing to the diastereotopic nature of the methylene protons. Thus, a symmetrical multiplet was observed for the $CO_2CH_2CH_3$ methylene protons in place of the predicted quartet signal. Literature research revealed the description of a similar spin-spin coupling pattern for the diethyl malonate compound diethyl 4-iodo-3-phenylnaphthalene-2,2(1*H*)-dicarboxylate.[30] In this report, YuXin and co-workers described the observation of a fourteen line symmetrical multiplet for the $CO_2CH_2CH_3$ methylene signals (**Figure 2.4**), which were chemically non-equivalent owing to the effect of the aromatic ring current and restricted rotation.

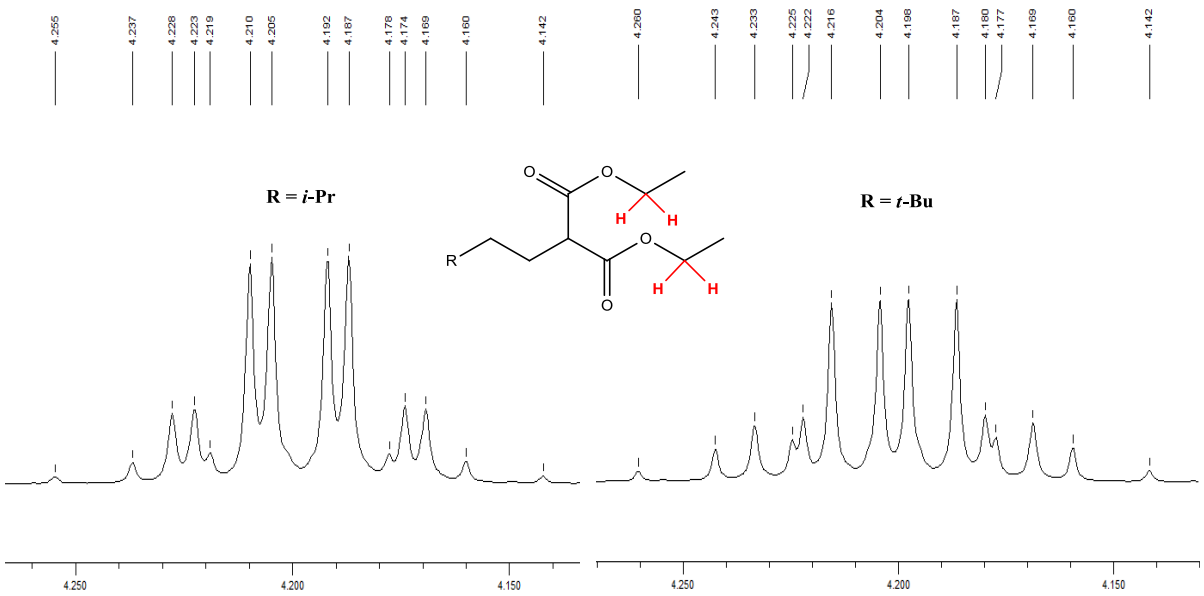


Figure 2.3 δ_H *(400 MHz, $CDCl_3$)*

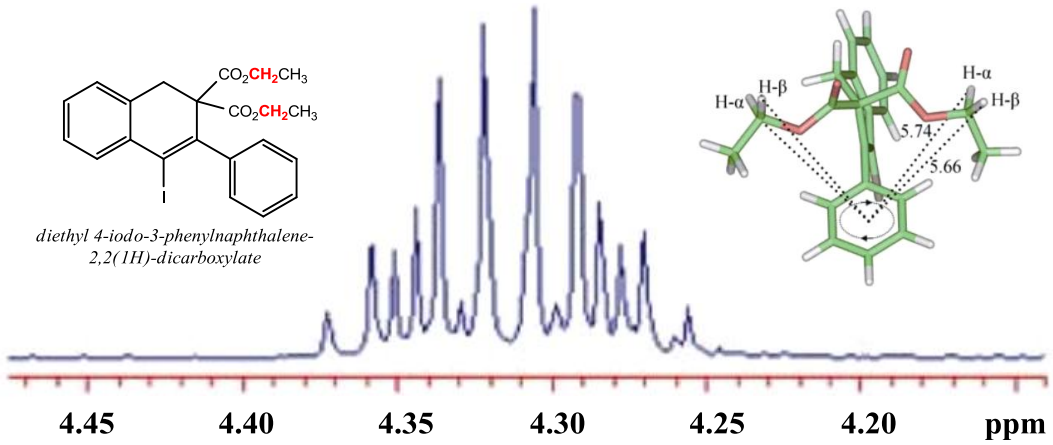


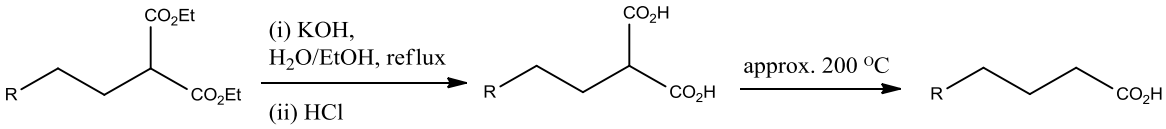
Figure 2.4

2.2.4 Carboxylic acid synthesis

Transformation of the malonates **11** and **12** to the corresponding carboxylic acid derivatives was achieved by treatment with potassium hydroxide in 50% aqueous ethanol. The mixture was heated under reflux until saponification was complete to provide, following acidification with aqueous hydrochloric acid, the intermediates 2-isopentylmalonic acid **13** and 2-(3,3-dimethylbutyl)malonic acid **14**, respectively (**Table 2.4**, entries 1 and 2). Decarboxylation of the intermediate malonic acids, *via* heating neat under a reflux condenser in an oil bath at high temperature, gave the desired carboxylic acids products **15** (**Table 2.4**, entry 1) and **16** (**Table 2.4**, entry 2) in high yield. A minor amount (~5%) of ethyl 5-methylhexanoate **17** and ethyl 5,5-dimethylhexanoate **18** were

also observed in the ^{1}H NMR spectra of the final product mixtures for the synthesis of 5-methylhexanoic acid **15** and 5,5-dimethylhexanoic acid **16**, respectively. Removal of these esters by column chromatography was conducted on initial samples for characterisation purposes, however, in general the carboxylic acid products were carried through to the next stage of synthesis without further purification. This procedure allowed for ready access to carboxylic acids **15** and **16** on a multi-gram scale.

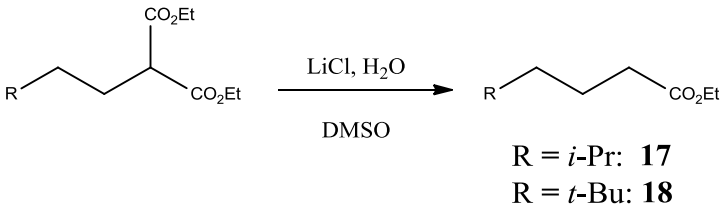
Table 2.4 *Synthesis of carboxylic acids*



Entry	Malonate	R	Malonic acid	Yield (%)[a]	Carboxylic acid	Yield (%)[b]
1	**11**	*i*-Pr	**13**	95	**15**[c]	96
2	**12**	*t*-Bu	**14**	86	**16**[c]	82

[a] Yield of malonic acid.
[b] Yield of carboxylic acid following column chromatography.
[c] Novel compound; full characterisation conducted (see **Section 4.2.5** for details).

Elimination of the saponification and decarboxylation steps described above may be possible in future syntheses of the *iso*-propyl **17** and *tert*-butyl **18** ester derivatives by employment of the Krapcho dealkoxycarbonylation methodology (**Scheme 2.12**).[31] This alternative method, involving a formal loss of CO_2R and protonation of the intermediate carbanion, would allow for direct synthesis of the desired ester products from the diethyl malonate substrates, thereby, reducing the steps required to reach the target compounds **17** and **18**. The Krapcho reaction has been successfully used for the dealkoxylcarbonylation of a wide variety of dimethyl and diethyl malonate compounds in the literature.[32]



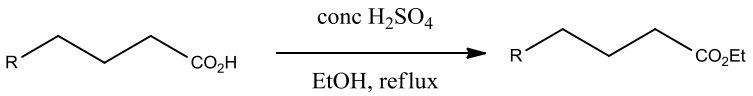
Scheme 2.12

2.2.5 Ester synthesis

5-Methylhexanoic acid **15**, 4-phenylbutanoic acid **5** and 5-phenylpentanoic acid **6** were converted to their ester derivatives *via* acid-catalysed esterification in refluxing ethanol (**Table 2.5**, entries 1–3). Yields obtained were moderate to good ranging from 69% for synthesis of ethyl-5-methylhexanoate **17** (**Table 2.5**, entry 1) to 96% for preparation of

ethyl 5-phenylpentanoate **19** (**Table 2.5**, entry 3). The esters were characterised by strong carbonyl absorptions in the IR spectra at ν_{max} 1733–1738 cm^{-1}, and in the ^{1}H NMR spectra by a 2H quartet at δ_H 4.12 representing the methylene protons of the ethoxy group. The products obtained (**17**, **19** and **20**) from the Fischer esterification reactions were sufficiently clean to use without further purification. Ester syntheses using this method were readily completed on a large scale.

Table 2.5 *Synthesis of ethyl esters*



Entry	Carboxylic acid	Ester	R	Yield (%)
1	**15**	**17**[a]	*i*-Pr	69
2	**5**[b]	**20**[c]	Ph	88
3	**6**[b]	**19**[c]	Bn	96

[a] Compound previously synthesised and characterised.[33]
[b] Carboxylic acid was commercially available.
[c] Compound previously synthesised and characterised.[20,21]

Attempted synthesis of the novel ester ethyl 5,5-dimethylhexanoate **18** *via* the acid-catalysed Fischer esterification route proved problematic. The ^{1}H and ^{13}C NMR spectra of the reaction mixture following an 18 h reflux of 5,5-dimethylhexanoic acid **16** and concentrated sulfuric acid in ethanol showed a mixture of product **18** and unknown signals; δ_H(400 MHz) 1.38 (t, *J* 7.2), 1.41 (t, *J* 7.2), 4.00 (q, *J* 7.2), 4.32 (q, *J* 7.2) 10.58 (bs), 10.66 (s) [**Figure 2.5**, (a)]; δ_C(75.5 MHz) 14.7 (CH_2), 16.0 (CH_2), 60.8 (CH_3), 67.02 (CH_3). The reaction mixture was subsequently re-dissolved in ethanol and refluxed again with sulfuric acid for a further 12 h. The ^{1}H NMR spectrum recorded after this additional reaction time revealed an increase in formation of the unknown byproduct, with only a minor amount of the desired ester **18** present [**Figure 2.5**, (b)], suggesting that product degradation was occurring. The IR spectrum of the isolated byproduct showed signals at ν_{max} 3470 (broad), 1642 and 1221 cm^{-1}.

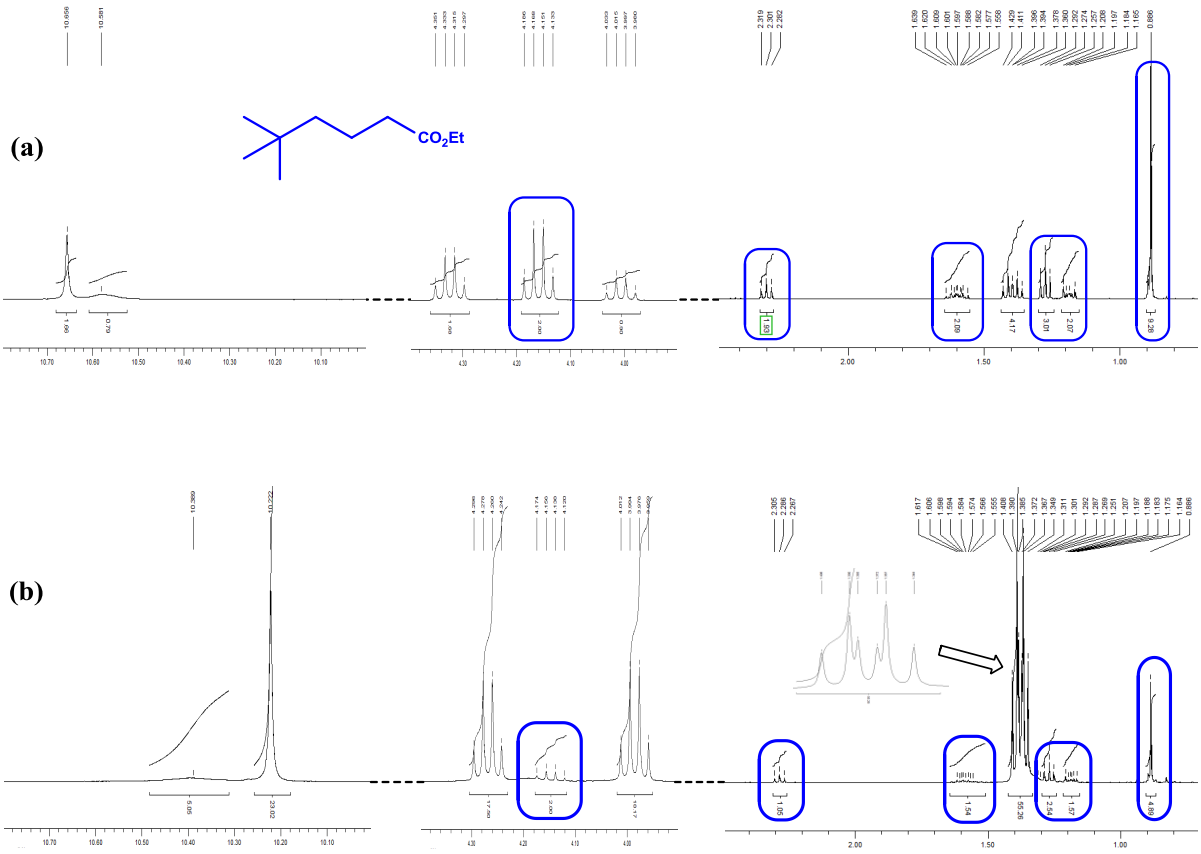
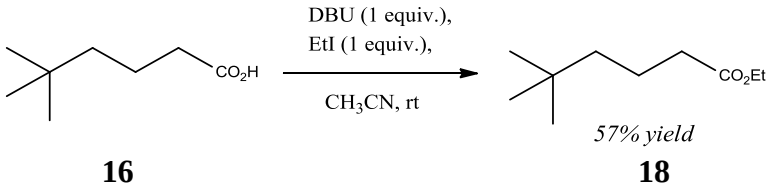


Figure 2.5 δ_H *(400 MHz, $CDCl_3$)*

An alternative, milder esterification procedure[34,35] was, therefore, chosen to access the desired *tert*-butyl-substituted ester **18**. For this purpose, 5,5-dimethylhexanoic acid **16** was reacted with diazabicycloundecene (DBU) and ethyl iodide in acetonitrile at room temperature, to provide the ester **18** as a sweet-smelling, colourless oil in moderate yield (**Scheme 2.13**).



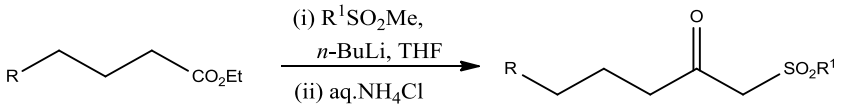
16 **18**

Scheme 2.13

2.2.6 β-Keto sulfone synthesis

With the required ester substrates now in hand, the preparation of the targeted β-keto sulfone products was next conducted employing the *n*-butyllithium-mediated procedure previously discussed (**Scheme 2.7**). For this purpose, methyl phenyl sulfone **21** and dimethyl sulfone were used for the synthesis of the phenylsulfone and methylsulfone compounds, respectively. Yields obtained for the synthesis of the β-keto sulfones **23**–**30** were moderate to good (**Table 2.6**, entries 1–8). The moderate yields recorded may be attributed to loss of product during chromatographic purification procedures as, in general, the initial crude yields obtained were high. In all cases, this protocol allowed for ready access to multigram quantities of the desired β-keto sulfone products.

Table 2.6 *Synthesis of β-keto sulfones*



Entry	Ester	Sulfone	R	R^1	Yield (%)[a]
1	**3**[b]	**23**[c]	Me	Ph	92
2	**4**[b]	**24**[c]	Et	Ph	65
3	**17**	**25**[d]	*i*-Pr	Ph	50
4	**18**	**26**[d]	*t*-Bu	Ph	72
5	**20**	**27**[c]	Ph	Ph	41
6	**19**	**28**[c]	Bn	Ph	76
7	**22**[a]	**29**[c]	Me	Me	56
8	**20**	**30**[d]	Ph	Me	42

[a] Yield following column chromatography.
[b] Ester was commercially available.
[c] Compound previously synthesised and characterised.[20,21]
[d] Novel compound; full characterisation conducted (see **Section 4.2.7** for details).

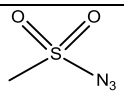
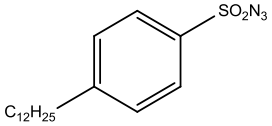
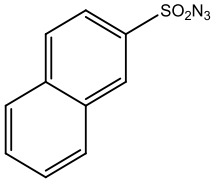
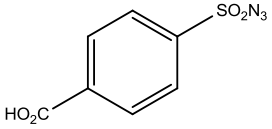
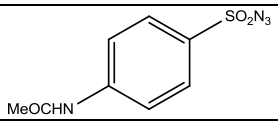
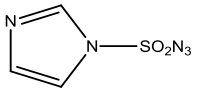
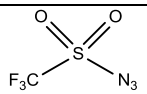
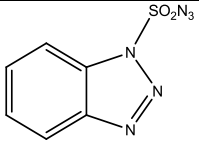
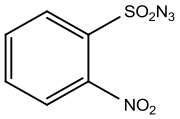
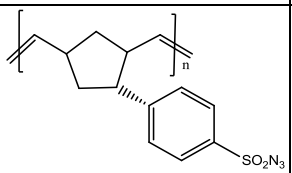
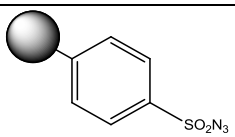
Successful product synthesis was indicated by the observation of carbonyl and sulfonyl absorptions in the IR spectra of the β-keto sulfones at ν_{max} 1709–1721 cm^{-1} and ν_{max} 1144–1160 (symmetric stretch), 1311–1322 (asymmetric stretch) cm^{-1}, respectively, and by the appearance of a characteristic singlet at δ_H 4.11–4.15 for the phenylsulfones **23**–**28** and δ_H 3.97–4.02 for the methylsulfones **29** and **30** in their ^{1}H NMR spectra, assigned to the C(1)H_2 methylene protons. Spectral characteristics of **23, 24, 27, 28** and **29** were consistent with those reported by Kelleher[20] and O'Keeffe.[21] The β-keto sulfones **25**, **26** and **30** are novel and were fully characterised during this work (see **Section 4.2.7** for details).

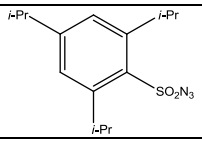
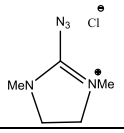
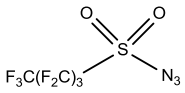
2.3 Synthesis of α-diazo-β-keto sulfones

The application of α-diazocarbonyl compounds has been widely observed in organic chemistry. These versatile reagents may undergo a large variety of synthetic transformations including X–H insertion, cyclopropanation, ylide formation and Wolff rearrangement.[7] Diazo transfer reactions, developed by Regitz,[12] are generally regarded as one of the principal method for the synthesis of α-diazocarbonyl compounds. Such reactions involve the transfer of a diazo moiety from a donor to an active methylene compound. For this purpose, a base of adequate strength to deprotonate the acidic α-methylene substrate is required *e.g.* potassium carbonate, triethylamine, sodium hydroxide, along with a suitable diazo transfer reagent. To ensure the protons at the α-methylene position are sufficiently acidic to allow an efficient reaction to occur, they must be flanked by two electron-withdrawing groups. This method is therefore suitable for the synthesis of the diazo derivatives of β-keto sulfones, β-diketones, β-keto phosphonates and β-keto esters.[36]

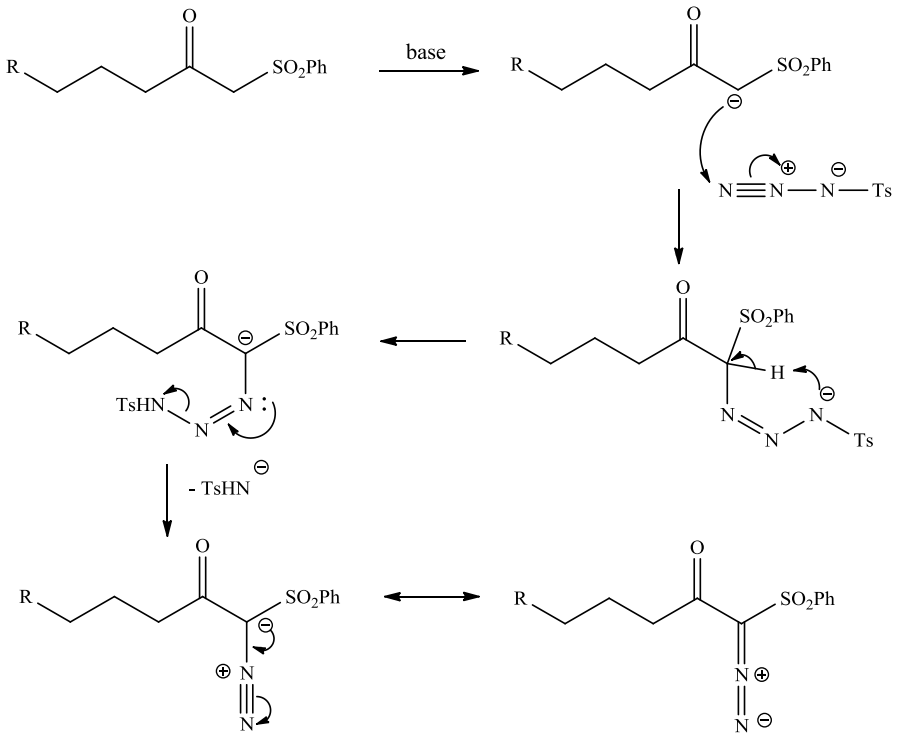
During this research, diazo transfer reactions were carried out primarily with the use of *p*-toluenesulfonyl (tosyl) azide **31** as the donor and potassium carbonate as the base. *p*-Tosyl azide **31** has proven a popular diazo transfer reagent owing to the ease of preparation and general high efficiency of this compound.[37] However, it is a hazardous reagent, possessing a high impact sensitivity and low initiation temperature and is, therefore, potentially explosive.[38] In addition, difficulties have been experienced in the chromatographic separation of diazo products from excess **31** and the byproduct *p*-toluenesulfonylamide.[39] The search for alternatives to *p*-tosyl azide **31** is, therefore, a high priority in organic chemistry with the aim of identifying an azide substrate which is safer, easier to handle and permits convenient and efficient purification of diazo products. A wide variety of diazo transfer reagents are now known which have been extensively reviewed in the literature (**Table 2.7**).[36,38,40,41]

Table 2.7 *Advantages and disadvantages of various diazo transfer reagents*

Diazo transfer reagent	Structure	Advantages	Disadvantages	Ref.
Methanesulfonyl azide		- removal of azide and byproduct amide possible by base extraction	- poor reaction yields - extremely high impact sensitivity and heat of decomposition	42
p-Dodecylbenzene sulfonyl azide		- relatively safe reagent (low impact sensitivity and heat of decomposition) - byproduct sulfonamide is non-crystalline, therefore, diazo products may be purified by recrystallisation	- *p*-dodecylsulfonyl chloride not readily available	40
Naphthalenesulfonyl azide		- easier to handle and safer than *p*-tosyl azide (low impact sensitivity) - byproduct sulfonamide is crystalline and poorly soluble, therefore, easily separable from liquid diazo products	- starting materials for synthesis of azide are expensive	43
p-Carboxylbenzene sulfonyl azide		- safer reagent than *p*-tosyl azide (high initiation temperature, low impact sensitivity) - water soluble - easy separation from amide byproduct	- requires two moles of base per one mole of substrate - not suitable for base-sensitive compounds - slower reaction times due to electron-withdrawing effect of the CO_2H group	44
p-Acetamidobenzene sulfonyl azide		- improved safety, yields and ease of manipulation *vs. p*-tosyl azide - relatively simple product purification	- slower reaction times due to electron-withdrawing effect of the NHCOMe group	45,46
Imidazole-1-sulfonyl azide		- easily prepared, long shelf-life - handled conveniently as its hydrochloride salt - can be prepared on a large scale from inexpensive materials	- violent decomposition occurs above 150 °C	47
Trifluoromethane sulfonyl azide		- useful for diazo transfer to primary amines	- poor shelf life - must be used *in situ* as a solution because explosive nature	48
Benzotriazol-1-yl-sulfonyl azide		- crystalline solid; easy to purify - long shelf life at rt - high solubility in many organic and aqueous solvents - allows convenient and efficient synthsis of wide range of azides and diazo compounds	- acid sensitive	49
o-Nitrobenzene sulfonyl azide		- more energetic reagent than *p*-tosyl azide; capable of increased transfer of the azido group - soluble in most organic solvents	- highly unstable	
Oligomeric benzenesulfonyl azide		- efficient diazo transfer with range of methylene compounds - insoluble sulfonamide byproduct can be removed by single filtration through a silica gel SPE cartridge - high-load capacity - useful for the preparation of highly unstable diazocarbonyls	- insoluble in heptane, ethyl acetate, methanol, acetonitrile and benzene - poor long-term stability	50
Polystyrene-supported bezenesulfonyl azide		- rapid isolation of diazo product with no aqueous workup and in most cases no need for purification - improved yields and shorter reaction times *vs. p*-CBSA and other reagents - thermally stable and not friction sensitive	- expensive	51

2,4,6-Triisopropyl benzenesulfonyl azide		- useful for diazo transfer to methylene groups activated by one carbonyl group in linear and hindered cyclic systems	- sensitive to strong oxidising agents	52
2-Azido-1,3-dimethylimidazolium chloride		- byproduct 2-imidazolidinone easily removed by water wash - diazo transfer requires mild reaction conditions	- small substrate scope described to date	53
Nonafluorobutane sulfonyl azide		- shelf-stable - cost-effective - safer reagent than trifluoromethane sulfonyl azide - diazo products readily isolated in pure form after simple aqueous extractive work-up	- decomposition temperature of 120 °C	54,55

p-Tosyl azide **31** was prepared in good yield (77%) using sodium azide and recrystallised *p*-tosyl chloride in acetone at 0 °C according to the procedure described by Curphey.[37] It was used without further purification in the synthesis of various α-diazo-β-keto sulfones. The mechanism of diazo transfer is illustrated in **Scheme 2.14**.

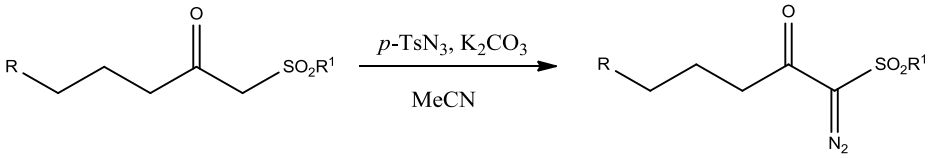


Scheme 2.14

The procedure adopted for α-diazo-β-keto sulfone synthesis in this project was based on that first described by Koskinen in 1990.[56] Accordingly, a solution of *p*-tosyl azide **31** in acetonitrile was added dropwise to a mixture of potassium carbonate and β-keto sulfone in acetonitrile at 0 °C. Reaction progress was monitored by TLC and/or IR analysis and diazo transfer was generally complete within 5 h of stirring at room temperature. The reported advantage of this method was that the work-up consisted simply of the addition

of a non-polar organic co-solvent (mixture of hexane and ether) to the crude reaction mixture, followed by filtration to remove the inorganic salt and sulfonamide byproduct. In practice, however, it was observed that small quantities of the *p*-tosyl amide remained after filtration, meaning further purification by column chromatography was necessary. The *p*-tosyl amide byproduct was observed in the ^{1}H NMR spectrum of the crude product mixture as a singlet at δ_H 2.43, representing the methyl protons of the toluene substituent, and also in the aromatic region at δ_H 7.32 (d, *J* 8.1) and δ_H 7.82 (d, *J* 8.3). Yields of the pure α-diazo-β-keto sulfone products obtained are shown in **Table 2.8**. Removal of the sulfonamide byproduct and any remaining *p*-tosyl azide **31** *via* column chromatography was often a difficult task due to close elution of these compounds with the desired diazo products. Thus, several rounds of chromatography were often required to isolate the α-diazo-β-keto sulfones in their pure form, which contributed to some loss of product. Diazo synthesis on a relatively large scale (typically 4–6 g) was possible using this method. Despite the synthetic ease of this procedure, larger scale syntheses were not attempted due to safety concerns regarding the use of *p*-tosyl azide.[38,40]

Table 2.8 *Synthesis of α-diazo-β-keto sulfones*



Entry	Sulfone	Diazo	R	R^1	Yield (%)[a]
1	**23**	**1**[b]	Me	Ph	88
2	**24**	**32**[b]	Et	Ph	60
3	**25**	**33**[c]	*i*-Pr	Ph	67
4	**26**	**34**[c]	*t*-Bu	Ph	78
5	**27**	**35**[b]	Ph	Ph	77
6	**28**	**36**[b]	Bn	Ph	87
7	**29**	**37**[b]	Me	Me	86
8	**30**	**38**[c]	Ph	Me	76

[a] Yield following column chromatography.
[b] Compound previously synthesised and characterised.[20,21]
[c] Novel compound; full characterisation conducted (see **Section 4.2.8** for details).

The aromatic α-diazo-β-keto sulfones **35**, **36** and **38** were isolated as yellow solids, while the alkyl derivatives **1**, **32**, **33**, **34** and **37** were obtained as oils which solidified upon storage at low temperatures. The diazo products were very stable compounds and were readily stored in the freezer for prolonged periods without degradation. The IR spectra of the isolated diazo products were characterised by a carbonyl stretch at ν_{max} 1656–1670 cm^{-1}, representing a significant shift from the carbonyl stretch (ν_{max} 1717–1721 cm^{-1}) in the spectra of the corresponding β-keto sulfones. Characteristic absorptions were also observed in the IR spectra at ν_{max} 2112–2117 cm^{-1} and ν_{max} 1144–1158 (symmetric stretch), 1330–1340 (asymmetric stretch) cm^{-1} representing the diazo and sulfonyl groups, respectively. Confirmation of reaction completion was possible by observation of the disappearance of the singlet at δ_H 3.97–4.15 in the ^{1}H NMR spectra of the crude

reaction mixtures, proving that the two C(1)H_2 protons of the β-keto sulfones **23**–**30** were replaced by the diazo functionality. Spectral characteristics of **1**, **32**, **35**, **36** and **37** were consistent with those reported by Kelleher[20] and O'Keeffe.[21] The α-diazo-β-keto sulfones **33**, **34** and **38** are novel and were fully characterised during this work (see **Section 4.2.8** for details).

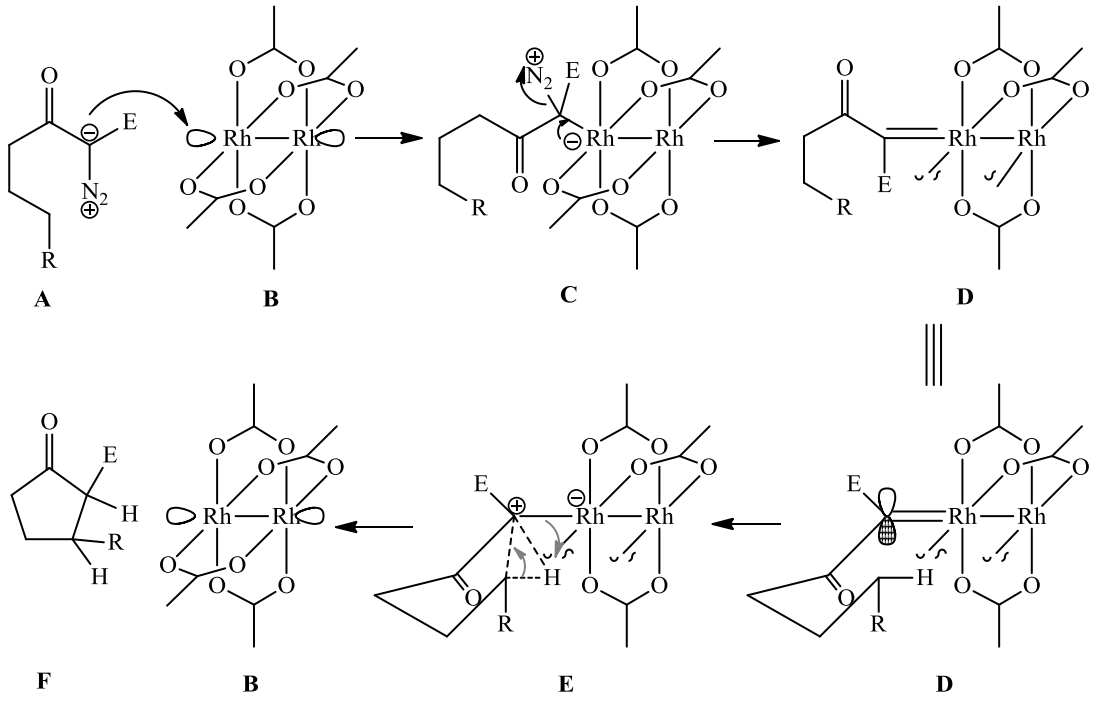
2.4 Synthesis of racemic 2-phenylsulfonyl cyclopentanones

Intramolecular rhodium(II)-catalysed C–H insertion reactions of α-diazocarbonyl compounds lead to very efficient cyclopentanone formation, offering excellent regioselectivity in the remote functionalisation of an unactivated C–H bond.[7,57-60] This methodology was originally developed by Taber,[61-64] who explored the decomposition of α-diazo-β-keto esters, and was later extended by Monteiro[65] to include the carbenoid reactions of α-diazo-β-keto sulfones. The potential for asymmetric induction in C–H insertion processes was first demonstrated by McKervey and co-workers in 1990 (**Scheme 2.1**).[3] Since this time enantioselective rhodium-catalysed C–H insertion has attracted enormous attention, with excellent enantiocontrol achieved in many cases using a range of chiral carboxylate and carboxamidate catalysts.[57]

A number of general trends have been identified for intramolecular carbenoid C–H insertions which can be used to predict the reactivity and selectivity of these reactions. The formation of five-membered rings is preferred over other possible ring sizes, due mainly to entropic considerations.[66] However, this preference is not absolute and additional ring sizes may be observed for insertion into allylic and benzylic bonds and insertion adjacent to electron-donating heteroatoms.[67-69] If the formation of more than one five-membered ring can occur, reactivity generally follows the order 3°>2°>>1°,[61,70,71] however, exceptions may again exist and product outcome is usually dictated by a balance of steric and electronic effects.[70,72,73] In terms of stereoselectivity, *trans*-cyclopentanone products are generally produced and insertion into equatorial C–H bonds is usually preferred over axial C–H insertion.

The mechanism of transition metal catalysed C–H insertion of α-diazocarbonyl compounds has been the subject of considerable speculation,[7,59,61,70,71,74-77] but it is generally agreed that insertion occurs *via* an electrophilic metal carbene. Complexation of the electron rich α-carbon of the diazoketone **A** with the vacant apical coordination site of the rhodium(II) carboxylate **B** gives **C** (**Scheme 2.15**). Expulsion of nitrogen generates the intermediate rhodium carbenoid **D**. Extrusion of nitrogen is believed to be the rate-determining step for C–H insertion processes.[59] It has been proposed that the regioselectivity of the C–H insertion reaction is due to the formation of a highly ordered transition state with the hydrogen to be transferred oriented towards the carbene centre. Doyle[70] suggested a model where overlap of the electrophilic *p*-orbital of the carbene carbon with the σ-orbital of the reacting C–H bond by way of a 3-centre-2-electron transition state **E** initiates a process in which C–C and C–H bond formation with the

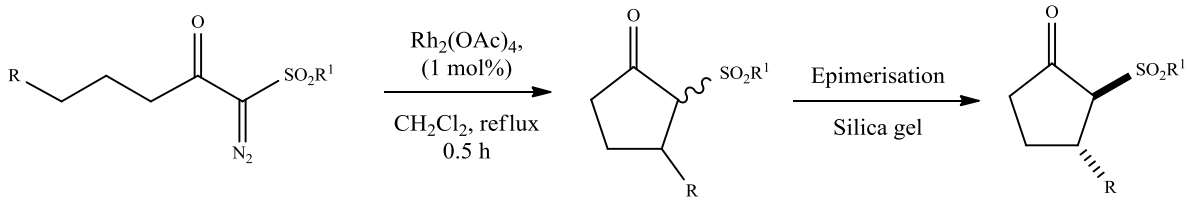
carbenoid carbon proceeds as the metal dissociates providing cyclopentanone **F**. This mechanistic proposal was later reinforced by density functional theory (DFT) studies undertaken by Nakamura and co-workers.[78] It is interesting to note that although only one of the two rhodium atoms functions as a binding site for the carbene, the other rhodium atom behaves as a ligand to the carbene-bound rhodium to enhance the electrophilicity of the bound carbene and facilitate cleavage of the rhodium-carbon bond.[77] Thus, neither of the two rhodium atoms interacts directly with the C–H bond undergoing insertion. Rhodium(II)-catalysed C–H insertion occurs with retention of configuration at the carbon undergoing insertion.[79]



Scheme 2.15

In this project, racemic samples of all targeted cyclopentanone products were first prepared *via* rhodium(II) acetate-catalysed intramolecular C–H insertion of the corresponding α-diazo-β-keto sulfones **1**, **32**–**38** in refluxing dichloromethane (**Table 2.9**, entries 1–8). These cyclisations involve insertion into a methylene site adjacent to a variety of alkyl and aryl groups. The well known propensity for five-membered ring formation in intramolecular C–H insertion processes was seen to be maintained in these reactions, with cyclopentanones **2**, **39**–**45** being the major product in all cases examined. Despite previous observations by Taber suggesting that insertion into benzylic sites is disfavoured when competing C–H insertion sites exist,[61] efficient insertion at the benzylic methylene site of **35** was recorded.

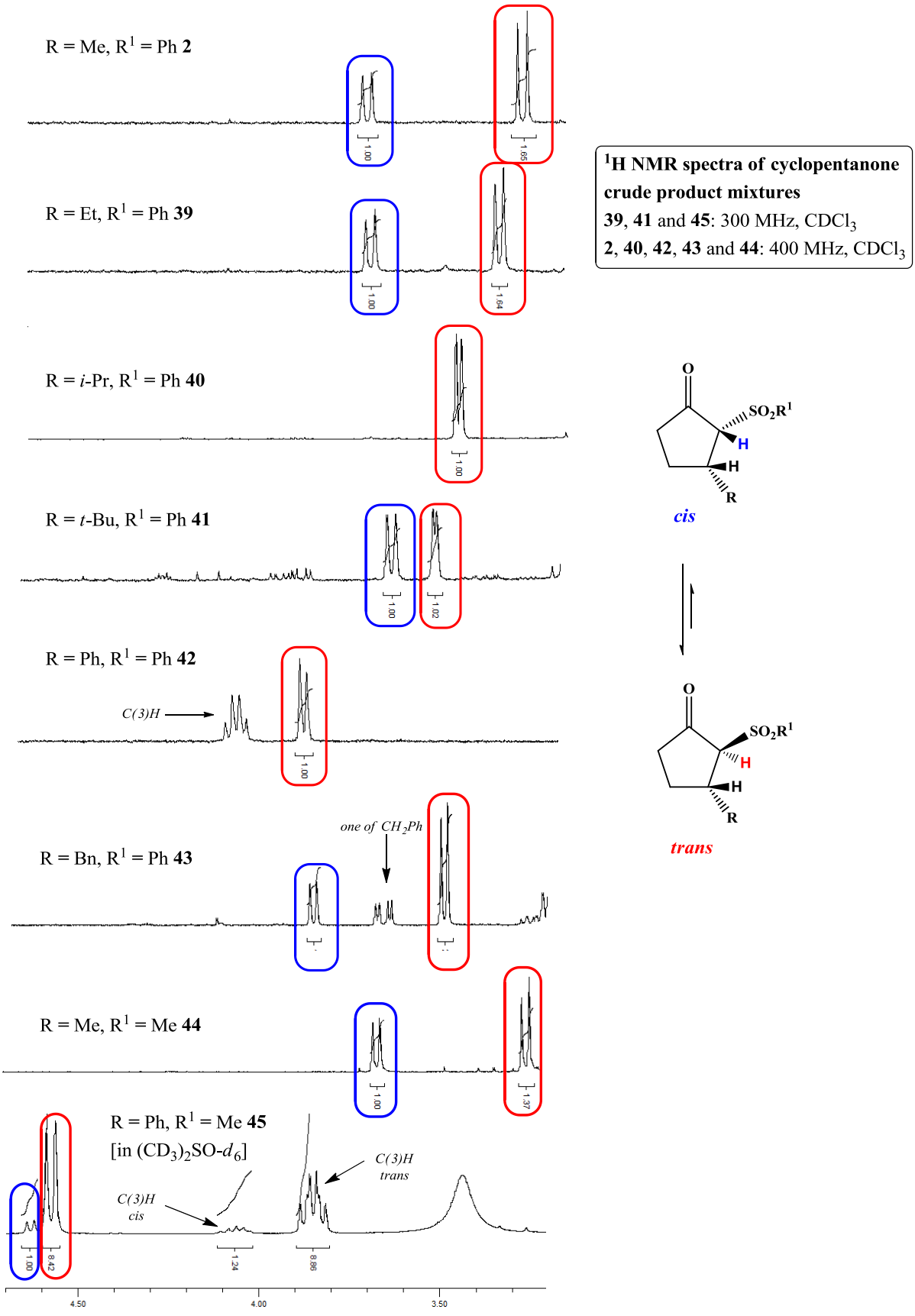
Table 2.9 *Rhodium(II) acetate-catalysed C–H insertion reactions*[a]



Entry	Diazo	Product	R	R^1	*cis* : *trans*[b]	C–H : O–H[c]	Yield (%)[d]
1	**1**	**2**[e]	Me	Ph	1 : 1.7	1 : 0.03	76
2	**32**	**39**[e]	Et	Ph	1 : 1.6	1 : 0.02	84
3	**33**	**40**[f]	*i*-Pr	Ph	0 : 1.0	1 : 0.12	98
4	**34**	**41**[f]	*t*-Bu	Ph	1 : 1.0[g]	1 : 0.22	30
5	**35**	**42**[e]	Ph	Ph	0 : 1.0	1 : 0.01	99
6	**36**	**43**[e]	Bn	Ph	1 : 2.4	1 : 0.25	76
7	**37**	**44**[e]	Me	Me	1 : 1.4	1 : 0.03	95
8	**38**	**45**[h]	Ph	Me	1 : 8.4	1 : 0.04	90

[a] Reactions conducted using the general procedure for rhodium-catalysed C–H insertion reactions (**Section 4.2.9**).
[b] Ratio of *cis*- : *trans*-cyclopentanone as determined by integration of the *cis* and *trans* signals for the C(2)*H* proton in the ^{1}H NMR spectra of the crude reaction mixtures.
[c] Ratio of C–H insertion : O–H insertion based on integration of the C(2)H doublet of the cyclopentanone product and the δ_H 5.14–5.16 singlet of the O–H insertion product (see **Figure 2.9** for general structure) in the ^{1}H NMR spectra of the crude reaction mixtures, respectively.
[d] Yields obtained following column chromatography.
[e] Compound previously prepared (*via* C–H insertion) and characterised.[20,21]
[f] Compound previously prepared (*via* nucleophilic addition of RMgCl to 2-phenylsufonylcyclopent-2-en-1-one) and characterised.[80]
[g] Tentatively assigned.
[h] Novel compound; full characterisation conducted (see **Section 4.2.9** for details).

Reactions were monitored by TLC and IR analysis, where reaction completion was indicated by the disappearance of peaks at ν_{max} 2112–2117 cm^{-1} (CN_2) and ν_{max} 1656–1670 cm^{-1} (C=O) characteristic of the α-diazo-β-keto sulfones and by the appearance of the cyclopentanone carbonyl absorption at ν_{max} 1743–1750 cm^{-1}. The rhodium(II)-catalysed C–H insertion reactions examined (**Table 2.9**) were complete within 0.5 h, irrespective of the nature of the R and R^1 substituents. Two new stereogenic centres are produced in the above C–H insertion process, resulting in four possible stereoisomeric products (two *cis* and two *trans* enantiomers). The *cis* and *trans* diastereomers were easily distinguished by examination of the ^{1}H NMR spectra of the crude reaction mixtures (**Figure 2.6**). Reactions of the methylsulfonyl derivates **37** and **38** proceeded in essentially the same manner as the corresponding phenyl sulfones **1** and **35**.



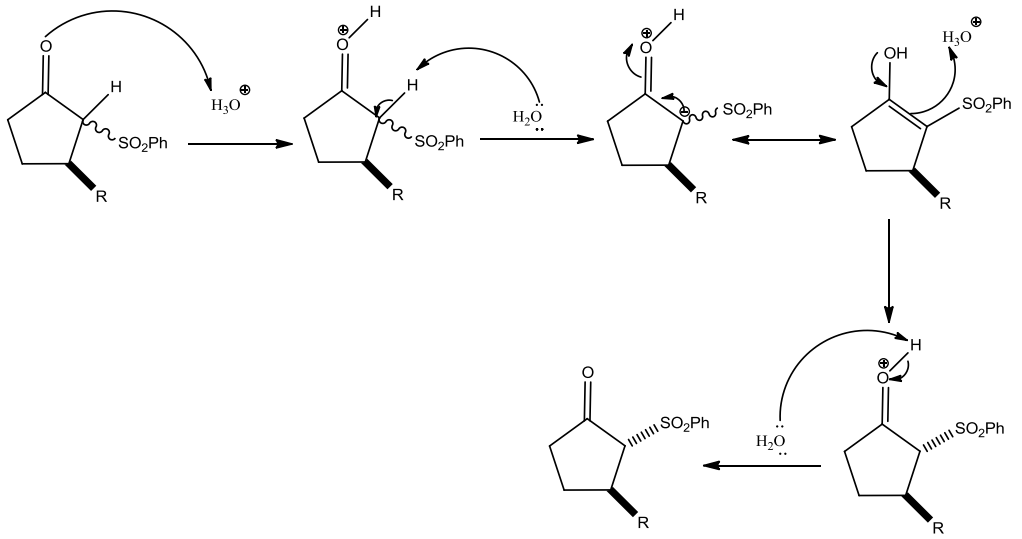
^{1}H NMR spectra of cyclopentanone crude product mixtures
39, **41** and **45**: 300 MHz, $CDCl_3$
2, **40**, **42**, **43** and **44**: 400 MHz, $CDCl_3$

Figure 2.6

Determination of *cis* : *trans* ratios was achieved by calculation of the relative integration of the *cis* and *trans* signals for the C(2)*H* proton adjacent to the sulfonyl substituent (**Figure 2.6**). For the synthesis of cyclopentanones **2**, **39**, **43**, **44** and **45**, predominant formation of the thermodynamically more stable *trans* isomer was seen to occur. Exclusive *trans* cyclopentanone formation was noted for the synthesis of **40** and **42**, possessing *iso*-propyl and phenyl groups at the C(3) position, respectively. Interestingly, a 1 : 1 mixture of *cis* : *trans* isomers was observed for C–H insertion of α-diazo-β-keto sulfone **34**. This isomeric ratio is surprising given that exclusive *trans*-cyclopentanone formation was noted for cyclisation of the less sterically hindered *iso*-propyl-substituted derivative **33**, therefore, this assignment is tentatively made. The ^{1}H NMR spectrum for cyclopentanone **45** (R = Ph, R^1 = Me) was recorded in deuterated DMSO, as poor resolution of signals for the *cis* and *trans* C(2)*H* protons was observed in deuterated chloroform.

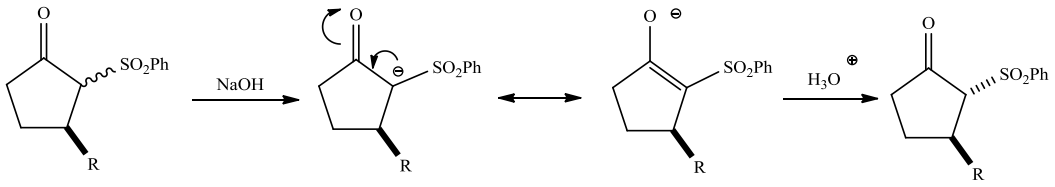
Procedures previously adopted by Kelleher[20] and O'Keeffe[21] involved two 0.5 mol% additions of rhodium(II) acetate to the reaction mixture over a 48 h reaction period (*method a*, see **Section 4.2.9** for experimental details). Such an approach was trialed in this research for the C–H insertion reaction of α-diazo-β-keto sulfone **1** and was found to produce the desired cyclopentanone **2** as an initial 1 : 1.9 mixture of *cis* : *trans* products and solely *trans*-**2** in 57% yield after column chromatography. As seen in **Table 2.9**, entry 1, rhodium(II) acetate-catalysed decomposition of **1** involving a single addition of 1 mol% of the catalyst and a reaction time of 0.5 h, was found to provide *trans*-**2** in higher yield (76%) and similar initial *cis* : *trans* ratio (1 : 1.7) compared with the longer 48 h reaction. Thus, as the older procedure offered no apparent advantage in terms of yield or reaction efficiency its use was not explored in subsequent C–H insertion reactions. It is believed that longer reaction times are required when the sample of diazo is not fully pure, leading to catalyst deactivation. In this work, diazo substrates were isolated in excellent purity and underwent C–H insertion very efficiently in all cases.

While the crude product mixture may contain a combination of *cis* and *trans* isomers, equilibration to form exclusively the more thermodynamically stable *trans* product is readily achieved owing to the acidity of the α-phenylsulfonyl proton (**Scheme 2.16**). Hence, following column chromatography on silica gel, *trans*-cyclopentanones were exclusively obtained.



Scheme 2.16

Alternatively, base mediated epimerisation may be employed to simplify the product mixture.[20,21] Washing a dichloromethane solution of the crude cyclopentanone with aqueous sodium hydroxide solution (0.15 M) results in deprotonation at C(2) (pK_a~10)[4] generating a planar enolate (**Scheme 2.17**). Reprotonation with dilute aqueous acid gives exclusively the thermodynamically favoured *trans* product. As treatment of the cyclopentanone with base can lead to competing ring opening *via* a retro-Claisen-type process,[81,82] rapid reprotonation with ammonium chloride solution is required. While this method provided the desired *trans*-cyclopentanone product **2** exclusively when trialed for the reaction of 1-diazo-1-phenylsulfonylhexan-2-one **1**, a significantly lower yield (34%) was obtained compared with epimerisation by chromatography. Thus, purification of all subsequent C–H insertion reactions was achieved *via* chromatographic separation.



Scheme 2.17

Following chromatographic purification, each of the cyclopentanone products was isolated as a white solid. High yields were generally recorded (**Table 2.9**, entries 1–3 and 5–8), however, a low yield of just 30% was obtained for synthesis of the *tert*-butyl-substituted cyclopentanone **41** (**Table 2.9**, entry 4). The ^{1}H NMR spectrum of the crude product mixture for this reaction was more complex than observed for synthesis of the other cyclopentanones (R = Me, Et, *i*-Pr, Ph, Bn), indicating the occurrence of competing reaction processes. The decreased chemoselectivity towards C–H insertion observed for reaction of **34** is presumably related to the bulky nature of the *tert*-butyl substituent which hinders C–H insertion at the adjacent reaction site. An unknown byproduct was isolated

in ~20% yield following column chromatography displaying a distinctive doublet at δ_H 6.05 (*J* 2.7), along with various multiplet signals in the regions δ_H 0.80–1.30, 2.25–3.20 and 7.19–7.93. A minor amount of competing O–H insertion into adventitious water was observed to occur for each of the rhodium(II) acetate-catalysed C–H insertion reactions examined. The O–H insertion byproducts (see **Figure 2.9** for general structures) were characterised by the appearance of a 1H singlet at δ_H 5.14–5.17 in the ^{1}H NMR spectra, in line with literature reports for similar hydroxy compounds,[83,84] and two distinctive doublet of triplets signals in the region of δ_H 2.74–3.05, representing the two diastereotopic protons adjacent to the carbonyl group. Confirmation of byproduct assignment was achieved by high resolution mass spectrometry (HRMS) analysis of 1-hydroxy-5-phenyl-1-(phenylsulfonyl)pentan-2-one **46** (R = Ph) (see **Section 4.2.9** for details). The O–H insertion byproduct 1-hydroxy-6-methyl-1-(phenylsulfonyl)heptan-2-one (R = *i*-Pr) **47** was also isolated and characterised in this project (see **Section 4.2.9** for details). The presence of the remaining O–H insertion byproducts (R = Me, Et, *t*-Bu and Bn), although not isolated in analytically pure form, was assigned by observation of the characteristic singlet signal at δ_H 5.14–5.17 in the ^{1}H NMR spectra of the crude reaction mixtures.

Spectral characteristics for the isolated cyclopentanones were in agreement with previously reported data.[20,21,80] Characteristic carbonyl and sulfonyl absorptions were observed in the IR spectra at ν_{max} 1743–1750 cm^{-1} and ν_{max} 1140–1153 (symmetric stretch), 1302–1308 (asymmetric stretch) cm^{-1}, respectively. In the ^{1}H NMR spectra, the proton geminal to the sulfone appeared as a doublet, due to coupling with the C(3) proton, in the region of δ_H 3.20–3.55 for the C(3)-alkyl cyclopentanones **2**, **39**, **40**, **41**, **43** and **44**, but slightly downfield at δ_H 3.76–3.91 in the spectra of **42** and **45** due to the deshielding effect of the phenyl group. Coupling constants of *J* 6.9–8.7 Hz for the cyclopentanones **2**, **39**, **42**, **43**, **44** and **45** were consistent with a *trans* arrangement of the C(2) and C(3) protons. The coupling constants observed for the *iso*-propyl- and *tert*-butyl-substituted cyclopentanones **40** and **41**, *J* = 5.2 and 3.6, respectively, were considerably lower than observed for the other cyclopentanones, in agreement with previous assignments of *trans* stereochemistry for these compounds.[80] The observed difference in coupling pattern for **40** and **41** reflects alterations of the conformational properties of the cyclopentanones due to the presence of the bulky 3-alkyl substituents. Such alterations also result in the appearance of fine splitting in the C(2)*H* signal of **41** (R = *t*-Bu) due to W-coupling, presumably to one of the C(5)H_2 protons. W-Coupling was also noted to a lesser extent for the C(2)*H* signal of **40** (R = *i*-Pr). The signal for the cyclopentanone proton at C(3) was observed as a multiplet in the region of δ_H 2.82–3.24 for the alkyl-substituted products **2**, **39**, **41**, **43** and **44**, and as an apparent quintet (*J* ~6.6) for the *iso*-propyl compound **40**. As before, the corresponding signal for phenyl-substituted cyclopentanones **42** and **45** was found further downfield as a multiplet at δ_H 4.05–4.19. The non-equivalent benzylic protons of **43** gave rise to two doublets of doublets at δ_H 2.78 and 3.06, due to coupling with one another and with the C(3) proton.

The geminal protons at C(4) and C(5) of **2**, **39**–**45** are diastereotopic, accounting for the observed differences in chemical shifts and splitting patterns of these protons. For example, the C(3) methylene protons of the α-diazo-β-keto sulfones **1**, **32**–**38** appeared as a triplet in the region of δ_H 2.52–2.62, however, upon cyclisation to the cyclopentanones the corresponding signal for the C(5) methylene protons was observed as a multiplet at δ_H 2.18–2.70. The chemical shifts of the C(4) protons were seen to vary depending on whether they were on the α- or β-face of the cyclopentanone. The upfield signals typically appeared in the region of δ_H 1.39–2.18, while the downfield signals were generally observed in the region of δ_H 2.10–2.70, often overlapping the signals of the C(5) protons.

The *trans* isomeric products were assigned the relative stereochemistry (2*R**, 3*S**) for the 3-methyl- and ethyl-substituted cyclopentanones **2**, **39** and **44**, while the 3-*iso*-propyl-, *tert*-butyl-, phenyl- and benzyl-substituted derivatives **40**, **41**, **42**, **43** and **45**, which possess the same relative stereochemistry as the major alkyl substituted product but differ in assignment due to the change in priority of the substituents at C(3), were assigned as (2*R**, 3*R**). Single crystal analysis of the 2-methylsulfonyl-3-phenylcyclopentanone **45** was conducted to confirm the relative stereochemistry assigned to this novel cyclopentanone product (**Figure 2.7**).

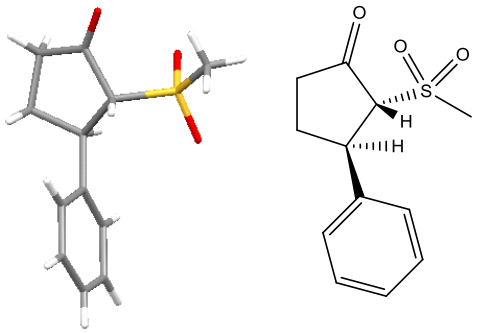
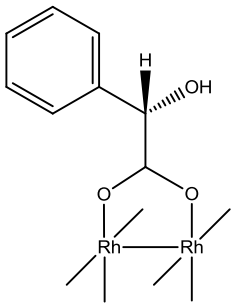


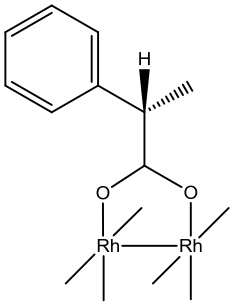
Figure 2.7

2.5 Enantioselective rhodium-catalysed C–H insertion reactions of α-diazo-β-keto sulfones

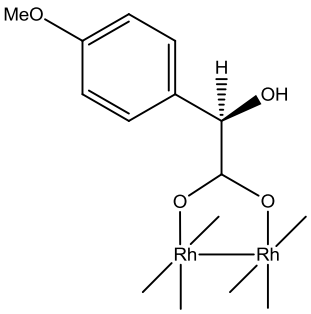
Having ascertained the spectral characteristics and relative stereochemistry of the racemic cyclopentanones **2**, **39**–**45**, the enantioselective formation of these insertion products was next envisioned. For this purpose, a variety of chiral rhodium(II) catalysts (**Figure 2.8**) were employed to investigate their influence on the stereochemical outcome of cyclopentanone formation. All chiral rhodium(II) catalysts used in this project were prepared in University College Cork by Dr. Alan Ford. Synthesis of the catalysts Rh_2(*S*-Mand)$_4$, Rh_2(*S*-Phpa)$_4$.2H_2O, Rh_2(*S*-O-*i*-PrMand)$_4$ and Rh_2(*S*-O-MeMand)$_4$ has previously been reported in the literature.[85] Rh_2(*R*-*p*-MeOMand)$_4$ and Rh_2(*R*-*p*-ClMand)$_4$ are novel catalytic structures.



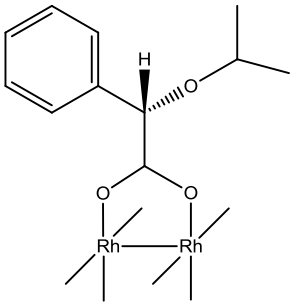
Rh_2(*S*-Mand)$_4$



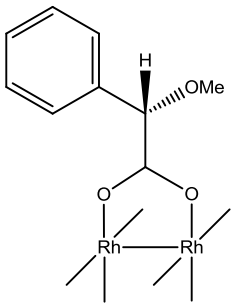
Rh_2(*S*-Phpa)$_4$.2$H_2$0



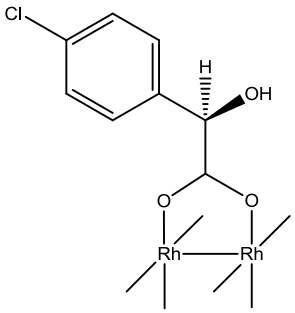
Rh_2(*R*-*p*-MeOMand)$_4$



Rh_2(*S*-O-*i*-PrMand)$_4$



Rh_2(*S*-O-MeMand)$_4$



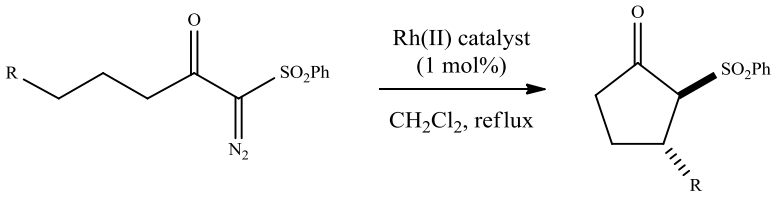
Rh_2(*R*-*p*-ClMand)$_4$

Figure 2.8

As for the racemic syntheses, reactions were conducted in refluxing dichloromethane in the presence of 1 mol% of the rhodium(II) catalyst (**Table 2.10**). All chiral catalytic reactions were complete within 0.5 h, as indicated by TLC or IR analysis, with the exception of Rh_2(*S*-O-*i*-PrMand)$_4$-catalysed insertions, whose reaction times were seen to vary from 45–72 h (**Table 2.10**, entries 4, 5, 11, 12 and 18). A mixture of *cis* and *trans* isomers was once again noted in the ^{1}H NMR spectra of the crude reaction mixtures for the C–H insertion reactions of **1**, **32** and **36**. The observed *cis* : *trans* ratio was seen to vary for the different catalytic reactions, ranging from exclusive *trans* cyclopentanone formation to preferential *cis* cyclopentanone formation.

Enantiopurity of the synthesised cyclopentanones was determined by chiral stationary phase high performance liquid chromatography (HPLC) performed on a Chiralpak® ASH, Chiralpak® OJ-H or Chiralcel® OD-H column. Details of the column conditions and mobile phases employed are included in appendix I. The absolute stereochemistry of the products was assigned by comparison of recorded optical rotation measurements to previously reported values. No optical rotation values were available for the *tert*-butyl-substituted cyclopentanone **41** and the novel cyclopentanone **45**, therefore, single crystal analysis was performed for these compounds to determine absolute stereochemistry (see **Section 2.6** for enantioselective synthesis of **41** and **45**). The isolated single crystal was then analysed by chiral HPLC to allow assignment of the enantiomeric peaks in the HPLC trace.

Table 2.10 *Chiral rhodium(II)-catalysed C–H insertions of α-diazo-β-keto sulfones*[a]



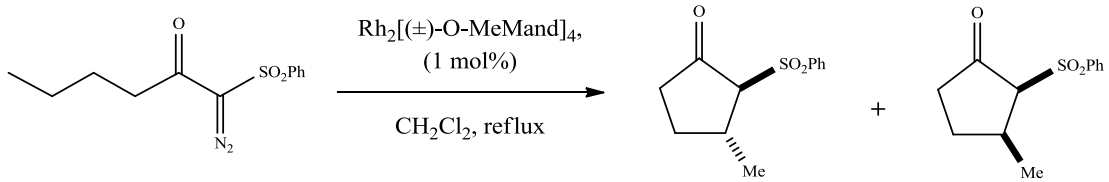
Entry	Diazo	Product	R	Catalyst	Time (h)	*cis* : *trans*[b]	C–H : O–H[c]	Yield (%)[d]	ee (%)[e,f]
1	**1**	**2**	Me	Rh_2(*S*-Mand)$_4$	0.5	1 : 0.8	1 : 0.00	80	20 (2*R*, 3*S*)
2	**1**	**2**	Me	Rh_2(*S*-Phpa)$_4$.2H$_2$0	0.5	1 : 4.6	1 : 0.04	71	~0
3	**1**	**2**	Me	Rh_2(*S*-O-MeMand)$_4$	0.5	1 : 0.5	1 : 0.00	87	20 (2*R*, 3*S*)
4	**1**	**2**	Me	Rh_2(*S*-O-*i*-PrMand)$_4$	72	0 : 1.0	1 : 0.00	76	~0
5[g]	**1**	**2**	Me	Rh_2(*S*-O-*i*-PrMand)$_4$	3.5	0 : 1.0	1 : 0.00	61	~0
6	**1**	**2**	Me	Rh_2(*R*-*p*-MeOMand)$_4$	0.5	1 : 0.9	1 : 0.00	89	25 (2S, 3*R*)
7	**1**	**2**	Me	Rh_2(*R*-*p*-ClMand)$_4$	0.5	1 : 0.6	1 : 0.00	94	17 (2*S*, 3*R*)
8	**32**	**39**	Et	Rh_2(*S*-Mand)$_4$	0.5	1 : 0.9	1 : 0.08	92	9 (2*R*, 3*S*)
9	**32**	**39**	Et	Rh_2(*S*-O-MeMand)$_4$	0.5	1 : 5.7	1 : 0.02	77	~0
10	**32**	**39**	Et	Rh_2(*S*-Phpa)$_4$.2H$_2$0	0.5	1 : 2.6	1 : 0.07	81	~0
11	**32**	**39**	Et	Rh_2(*S*-O-*i*-PrMand)$_4$	45	0 : 1.0	1 : 0.00	88	~0
12[g]	**32**	**39**	Et	Rh_2(*S*-O-*i*-PrMand)$_4$	5.5	0 : 1.0	1 : 0.02[h]	47	~0
13	**32**	**39**	Et	Rh_2(*R*-*p*-MeOMand)$_4$	0.5	1 : 0.8	1 : 0.01	91	8 (2S, 3*R*)
14	**32**	**39**	Et	Rh_2(*R*-*p*-ClMand)$_4$	0.5	1 : 1.1	1 : 0.00	91	9 (2*S*, 3*R*)
15	**35**	**42**	Ph	Rh_2(*S*-Mand)$_4$	0.5	0 : 1.0	1 : 0.04[i]	87	~0
16	**35**	**42**	Ph	Rh_2(*S*-O-MeMand)$_4$	0.5	0 : 1.0	1 : 0.02	80	~0
17	**35**	**42**	Ph	Rh_2(*S*-Phpa)$_4$.2H$_2$0	0.5	0 : 1.0	1 : 0.08	91	23 (2*S*, 3*S*)
18	**35**	**42**	Ph	Rh_2(*S*-O-*i*-PrMand)$_4$	48	0 : 1.0	1 : 0.00	72	~0
19	**35**	**42**	Ph	Rh_2(*R*-*p*-MeOMand)$_4$	0.5	0 : 1.0	1 : 0.02[i]	57	~0
20	**35**	**42**	Ph	Rh_2(*R*-*p*-ClMand)$_4$	0.5	0 : 1.0	1 : 0.00[h]	91	9 (2*R*, 3*R*)
21	**36**	**43**	Bn	Rh_2(*S*-Mand)$_4$	0.5	1 : 2.0	1 : 0.02	73	~0
22	**36**	**43**	Bn	Rh_2(*S*-O-MeMand)$_4$	0.5	1 : 25.0	1 : 0.06	75	10 (2*S*, 3*S*)
23	**36**	**43**	Bn	Rh_2(*S*-Phpa)$_4$.2H$_2$0	0.5	0 : 1.0	1 : 0.16[h]	51	~0
24	**36**	**43**	Bn	Rh_2(*R*-*p*-MeOMand)$_4$	0.5	0 : 1.0	1 : 0.07	67	8 (2*R*, 3*R*)
25	**36**	**43**	Bn	Rh_2(*R*-*p*-ClMand)$_4$	0.5	1 : 14.3	1 : 0.05	71	7 (2*R*, 3*R*)

[a] Reactions conducted using the general procedure for rhodium-catalysed C–H insertion reactions (**Section 4.2.9**).
[b] As determined by integration of the *cis* and *trans* signals for the C(2)*H* proton in the ^{1}H NMR spectrum of the crude reaction mixtures.
[c] Ratio of C–H insertion : O–H insertion based on integration of the C(2)H doublet of the cyclopentanone product and the δ_H 5.14–5.17 singlet of the O–H insertion product (see **Figure 2.9** for general structure), respectively, in the ^{1}H NMR spectra of the crude reaction mixtures.
[d] Yield of *trans*-cyclopentanone following column chromatography.
[e] Enantiopurity of *trans*-cyclopentanone determined by chiral stationary phase HPLC (see appendix I for details).
[f] Stereochemical assignments made by comparison with previously reported rotation and HPLC data (see Appendix I).[20]
[g] Reaction conducted in refluxing toluene.
[h] ^{1}H NMR of crude reaction mixture was complex.
[i] Minor amount (≤5%) of hydride abstraction byproduct **48** observed in the ^{1}H NMR spectra of the crude reaction mixture.

Note: throughout this thesis enantiopurity was recorded as ~0% ee when the figure estimated from chiral HPLC analysis was less than 5%.

Yields recorded for the C–H insertion reactions of the α-diazo-β-keto sulfones **1**, **32**, **35** and **36** in refluxing dichloromethane were generally high, ranging from 51% (**Table 2.10**, entry 23) to 94% (**Table 2.10**, entry 7). Large variations were noted for the *cis* : *trans* product ratios observed in the ^{1}H NMR spectra of the crude reaction mixtures. Exclusive *trans* cyclopentanone formation was recorded for all chiral rhodium(II)-catalysed reactions of 1-diazo-1-phenylsulfonylpentan-2-one **35**. In contrast, a mixture of *cis* and *trans* isomeric products was observed for the majority of cyclisations of **1**, **32** and **36**. In such cases, production of thermodynamically favourable *trans*-cyclopentanones was generally seen to dominate, however, for certain reactions preferential *cis*-cyclopentanone formation was observed (**Table 2.10**, entries 1, 3, 6–8 and 13). Although no clear trend relating to the observed *cis* : *trans* ratio was evident, it is thought that reaction time may influence the isomeric balance of the C–H insertion products. Thus, for all Rh_2(S-O-*i*-PrMand)$_4$-catalysed reactions, which required 45–72 h to reach completion, no *cis*-cyclopentanone production was recorded. In addition, the amount of *trans*-**2** relative to *cis*-**2** was seen to increase for the Rh_2[(±)-O-MeMand]$_4$-catalysed decomposition of **1** upon an additional hour of refluxing in dichloromethane (**Table 2.11**).

Table 2.11 *Relationship between reaction time & cis : trans ratio for the cyclisation of **1***



1 *cis*-**2** *trans*-**2**

Entry	Time (h)	*cis*-2 : *trans*-2[a]
1	1	1 : 1.3
2	2	1 : 2.3

[a] As determined by integration of the *cis* and *trans* signals for the C(2)*H* proton in the ^{1}H NMR spectrum of the crude reaction mixture.

Decreased reaction times for Rh_2(*S*-O-*i*-PrMand)$_4$-catalysed cyclopentanone synthesis were achieved by change of reaction solvent from dichloromethane to the higher boiling point solvent toluene, resulting in a reduction in reaction times to 3.5 h (from 72 h) and 5.5 h (from 45 h) for the synthesis of **2** and **39**, respectively, while still maintaining exclusive *trans*-cyclopentanone formation (**Table 2.10**, entries 5 and 12 *vs.* entries 4 and 11). Unfortunately, a decrease in reaction yield was also found to be associated with this change of solvent and for this reason, the use of toluene as a reaction solvent was not pursued in further rhodium(II)-catalysed C–H insertion reactions.

While C–H insertion reactions exhibit a well-documented preference for five-membered ring formation, competing processes such as O–H insertion, dimerisation, diazo reduction and hydride abstraction may also occur (**Figure 2.9**).[7] Minor amounts of O–H insertion and hydride abstraction byproducts were observed in the ^{1}H NMR spectra of the crude

reaction mixtures for some of the chiral rhodium(II)-catalysed C–H insertions of α-diazo-β-keto sulfones **1**, **32**, **35** and **36** (**Table 2.10**). The hydride abstraction byproduct **48**, which was observed only for reactions of the phenyl-substituted α-diazo-β-keto sulfone **35** (**Table 2.10**, entries 15 and 19), was characterised by distinctive signals in the ^{1}H NMR spectrum at δ_H 6.22 [dt, *J* 7.0/16.0, C(4)*H*] and δ_H 6.51 [d, *J* 15.6, C(5)*H*], in line with previous reports for similar sulfone compounds.[11] In general, however, the crude reaction mixtures isolated for the rhodium-catalysed reactions were relatively clean by ^{1}H NMR analysis.

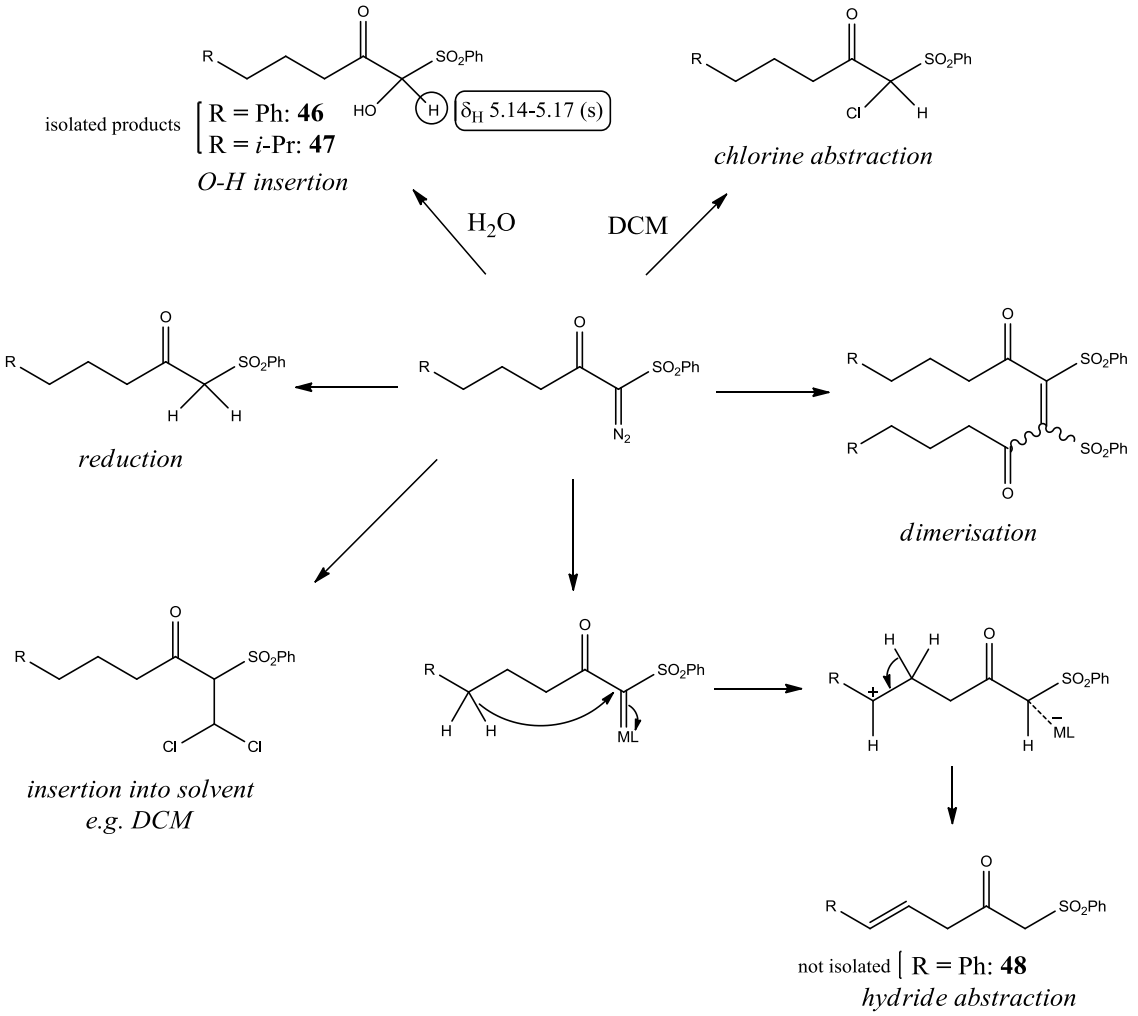
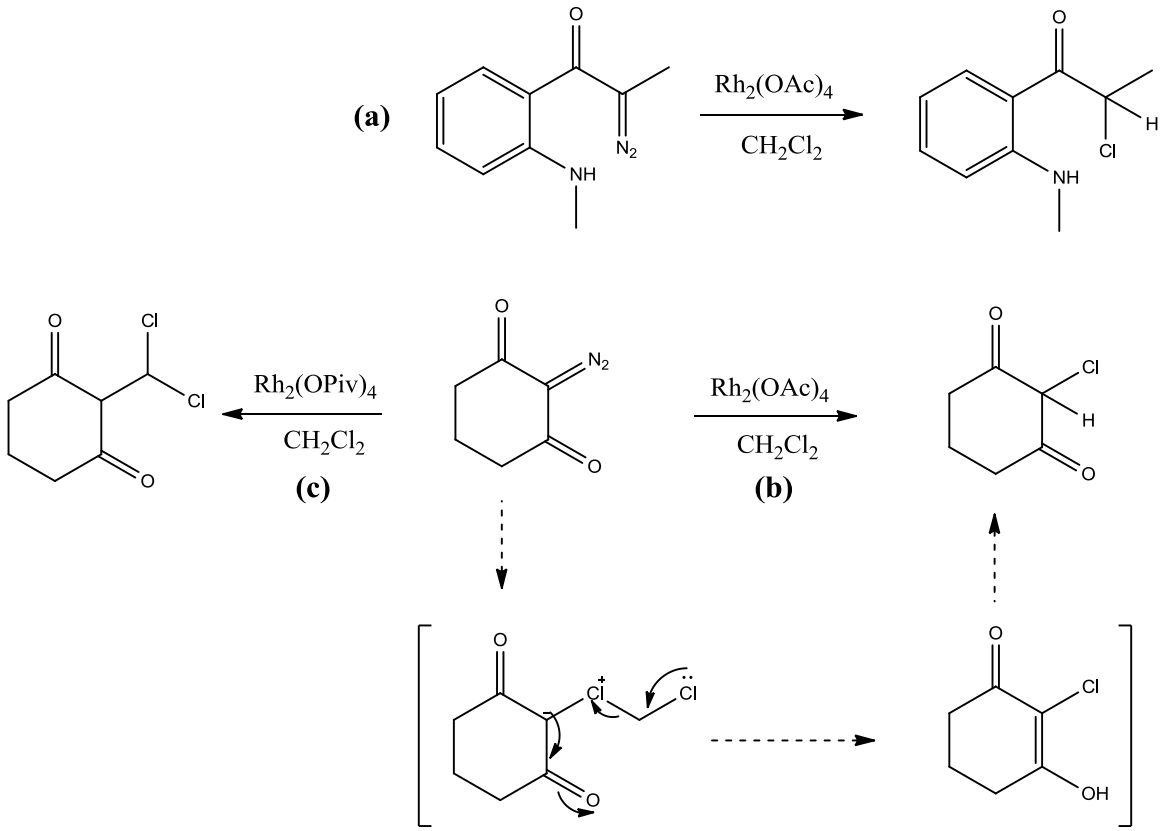


Figure 2.9

Abstraction of chlorine from dichloromethane to form an α-chloro-β-keto sulfone compound may also compete with desired C–H insertion. This side-reaction has previously been described by Mountjoy[86] and Pirrung[87] for rhodium-catalysed decomposition of α-diazo ketones [**Scheme 2.18**, (a) and (b), respectively]. A mechanism involving formation of a chloronium ylide was proposed by Pirrung to explain the synthesis of the observed chlorinated product [**Scheme 2.18**, (a)].[87] In the same study, Pirrung also reported the formation of a product arising from C–H insertion into dichloromethane in the presence of rhodium(II) pivalate [**Scheme 2.18**, (c)].



Scheme 2.18

Generation of both chlorine products is possible for the α-diazo-β-keto sulfone reactions under investigation in this project, however, no analytically pure sample to confirm their presence was obtained in any of the experiments conducted. Reports of similar compounds in the literature indicate that the chlorine abstraction and dichloromethane insertion products would display characteristic singlet and doublet signals, respectively, in the region of δ_H 4.4–6.1 (**Figure 2.10**).[88-90] Various baseline peaks were typically observed in this region in the crude reaction mixtures obtained for rhodium- and copper-catalysed reactions of our α-diazo-β-keto sulfones, therefore, quantification of the chlorinated byproducts was not attempted.

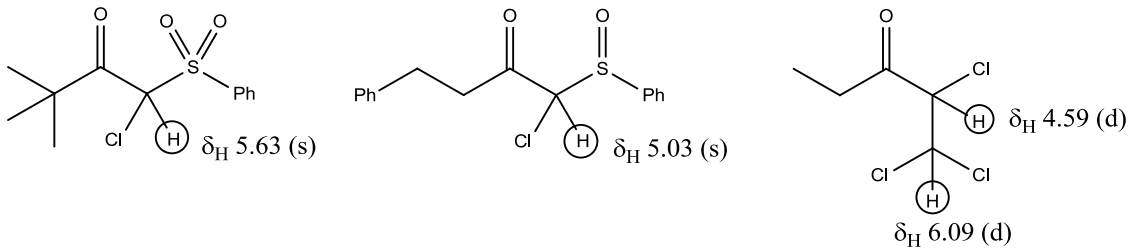


Figure 2.10

Byproducts formed in this project were generally removed during chromatographic purification, providing analytically pure samples for subsequent chiral HPLC analysis. Various precautions were taken to minimise the occurrence of these unwanted side

reactions, including the use of dichloromethane distilled from phosphorous pentoxide followed by distillation with calcium hydride, drying of reagents before use, the flushing the reaction vessel with nitrogen prior to reaction commencement and the slow, dilute addition of the α-diazo-β-keto sulfones to the rhodium(II) catalyst solution. In some instances, the isolated product samples were not fully clean, however, the presence of minor amounts of byproduct(s) did not interfere with the determination of enantiomeric excess by chiral HPLC analysis.

The extent of asymmetric induction achieved in the C–H insertion reactions of **1**, **32**, **35** and **36** was generally poor, ranging from ~0% ee (**Table 2.10**, entries 2, 4, 5, 9–12, 15, 16, 18, 19, 21 and 23) to 25% ee (**Table 2.10**, entry 6). Variations in enantioselectivities, albeit with low ee's in all cases, were noted for cyclisation of the different diazo precursors (R = Me, Et, Ph, Bn). Decomposition of the methyl derivative **1** was found to be the most consistent for permitting enantioselective syntheses, with four of the six chiral catalytic complexes trialed resulting in some extent of asymmetric induction (**Table 2.10**, entries 1, 3, 6 and 7). This ratio was seen to decrease for the remaining diazo compounds, with only three catalytic choices proving successful for the C–H insertion reactions of **32** (**Table 2.10**, entries 8, 13 and 14) and **36** (**Table 2.10**, entries 22, 24 and 25) and only two chiral rhodium(II) complexes providing enantiocontrol in the cyclisation of **35** (**Table 2.10**, entries 17 and 20). The latter finding is surprising given that the presence of a phenyl group adjacent to the C–H insertion site has previously been found to enhance asymmetric induction owing to the electron-withdrawing abilities of this group.[91,92]

No one chiral rhodium(II) catalyst employed in this study was found to provide consistent enantiocontrol across the range of diazo compounds tested, *e.g.* Rh_2(*R*-*p*-MeOMand)$_4$-catalysed insertion of **1** (**Table 2.10**, entry 6) resulted in the synthesis of cyclopentanone **2** in 25% ee, however, cyclisation of **32**, **36** and **35** under the same conditions generated **39** and **43** in just 8% ee (**Table 2.10**, entries 13 and 24) and **42** in ~0% ee (**Table 2.10**, entry 19), respectively. Despite longer reaction times, the *iso*-propylmandelate catalyst Rh_2(*S*-O-*i*-PrMand)$_4$ failed to provide any asymmetric induction in the syntheses of **2**, **39** and **42** (**Table 2.10**, entries 4, 5, 11, 12 and 18). As expected, catalysts derived from the *S*- and *R*-series of mandelate derivatives were seen to provide cyclopentanone products with the opposite sense of enantioinduction.

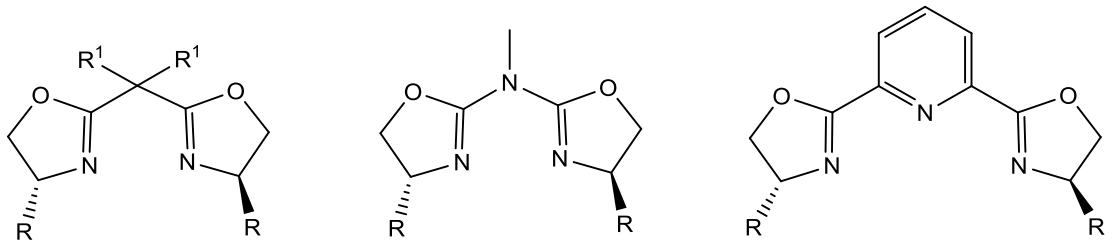
2.6 Enantioselective copper-catalysed C–H insertion reactions of α-diazo-β-keto sulfones

It was clearly evident from the results presented in **Section 2.5** that the use of mandelate-derived chiral rhodium(II) catalysts was not a viable option for achieving highly enantioselective cyclopentanone synthesis *via* C–H insertion. Thus, an alternative method was sought for fulfilling this goal. Recent work in this research group has lead to the emergence of chiral copper bis(oxazoline) complexes as an attractive catalytic choice

for asymmetric carbenoid transformations.[10,93,94] The application of asymmetric copper catalysts in C–H insertion reactions has not been widely exploited in recent times. Limited reports exist, however, the level of enantiocontrol achieved has been generally moderate, up to a maximum of 60% ee for intramolecular[8] and 88% ee for the intermolecular reaction[9]. Indeed, Davies has suggested that copper catalysts tend to be highly electrophilic and so typically generate carbenoids that are too reactive to undergo selective C–H activation reactions.[59] Thus, the investigation of copper catalysis for our desired asymmetric cyclopentanone synthesis was an appealing choice owing both to the potential for highly enantioselective syntheses and the possibility of achieving this goal by application of relatively underexploited catalytic complexes.

2.6.1 C–H insertion reactions with copper-bis(oxazoline) catalysts

Chiral bis(oxazoline) complexes are among the most successful, versatile and commonly used class of ligands in asymmetric catalysis due to their ready accessibility from inexpensive amino alcohols, modular nature, ability to coordinate a large number of metals and applicability in a wide range of metal-catalysed transformations including aziridination reactions, cyclopropanations, Diels-Alder reactions, hydrosilylations and 1,3-dipolar cycloaddition reactions.[95,96] Notably, examples in the literature of C–H insertion reactions employing bis(oxazoline) ligands are minimal (see **Section 1.2** for details).[8,9,97] Three different families of oxazoline-derived chiral ligands may be identified (**Figure 2.11**), namely; bis(oxazolines) themselves (BOX), aza-bis(oxazolines) (azaBOX) and pyridine-bis(oxazolines) (PyBOX).



BOX *azaBOX* *PyBOX*

Figure 2.11

When a chiral bis(oxazoline) ligand is mixed with an inorganic salt in an organic solvent, a chiral BOX-metal complex (**Figure 2.12**) is formed which behaves as a very efficient asymmetric catalyst. Complexes with a metal : ligand ratio of 1 : 1 are generally considered as the decisive intermediates for asymmetric catalysis.[98] Two metal sites are thus occupied by the ligand, leaving typically up to four sites available for interaction with substrates, solvent molecules or counteranions, the latter arising from the metal salt employed for complexation. The actual species present in solution depends on many subtle factors and can have a very significant influence on the stereochemical outcome of a given reaction.

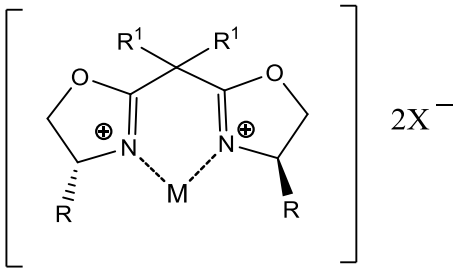


Figure 2.12

A number of the features of the chiral bis(oxazoline)-derived catalysts are noteworthy. The chiral BOX complexes display a C_2-axis (**Figure 2.13**)[98] which minimises the number of possible transition states in a particular reaction due to the equivalency of structures upon rotation by 180°. The enantiocontrolling stereocentre of the catalysts resides on the carbon atom adjacent to the coordinating nitrogen and is, therefore, in close proximity to the metal active site, permitting a direct influence on the stereochemical outcome of the reaction.[96] Several strategies have been developed for the immobilisation of oxazoline-based ligands offering advantages in terms of ease of separation and handling and recyclability over corresponding homogeneous systems.[99,100]

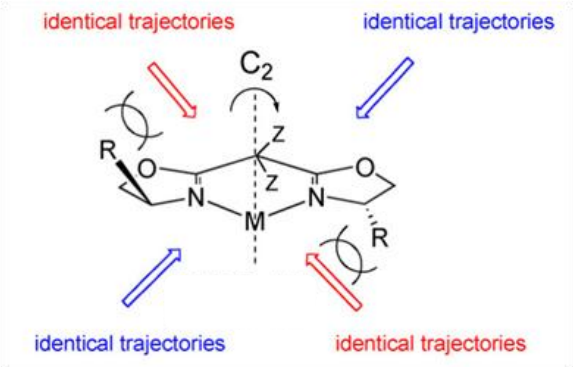
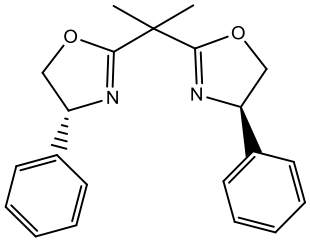
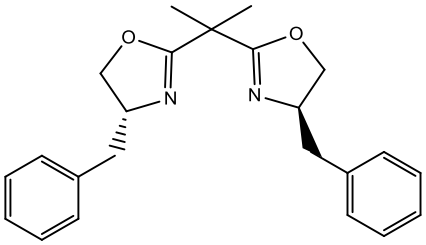


Figure 2.13 *ref.*[98]

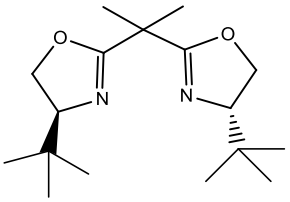
Five commercially available bis(oxazoline) ligands (**Figure 2.14**) were initially examined in this project for their potential to induce enantioselectivity in the C–H insertion reactions of α-diazo-β-keto phenylsulfones **1**, **32**, **33**, **35** and **36**. Four different copper sources, namely, CuCl, $CuCl_2$, $Cu(OTf)_2$ and $Cu(MeCN)_4PF_6$, were also investigated. In contrast to previous rhodium-catalysed insertions (**Section 2.5**), copper-catalysed reactions in this project involved pre-generation of the catalytic complex [copper/bis(oxazoline)] for 1.5 h in refluxing solvent prior to dropwise addition of the diazo substrate. This procedure is in line with literature reports for X–H insertion reactions employing copper-bis(oxazoline) catalysts.[101,102] Results obtained for these early experiments are presented in **Table 2.12**. Exclusive *trans*-cyclopentanone formation was recorded in each of the copper-catalysed reactions conducted, however, in some cases, minor amounts of byproduct(s) were also observed.



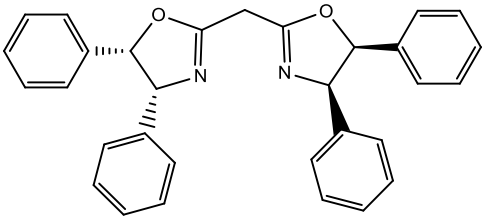
2,2'-*i*-propylidenebis-(4*R*)-Ph
(4*R*)-Ph **49**



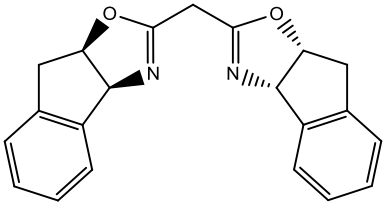
2,2'-*i*-propylidenebis-(4*R*)-Bn
(4*R*)-Bn **50**



2,2'-*i*-propylidenebis-(4*S*)-*t*-Bu
(4*S*)-*t*-Bu **51**



2,2'-methylenebis-(4*R*,5*S*)-Ph
(4*R*,5*S*)-diPh **52**



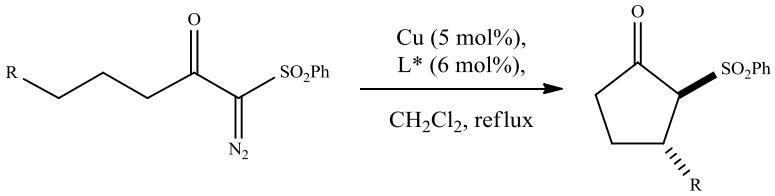
2,2'-methylenebis-(3*S*,8*R*)-dihydroindeno
(3*S*,8*R*)-Ind **53**

Note: shorthand ligand names used for convenience

Figure 2.14

Large variations in reaction times were recorded for the copper-bis(oxazoline)-catalysed C–H insertions, ranging from 1.5 h (**Table 2.12**, entry 7) to 42 h (**Table 2.12**, entry 17). The reactions were thus considerably longer than the corresponding rhodium-catalysed insertions, which were typically complete within 0.5 h. In general, shorter reaction times were noted for cyclisations in the presence of $Cu(OTf)_2$ and $Cu(MeCN)_4PF_6$ *vs.* the corresponding CuCl- and $CuCl_2$-catalysed reactions, although exceptions to this trend were observed (**Table 2.12**, entry 21 *vs.* 22).

Table 2.12 *Copper-bis(oxazoline)-catalysed C–H insertion reactions*[a]



Entry	Diazo	Product	R	Cu	L*	Time (h)	C–H : Red : O–H[b]	Yield (%)[c]	ee (%)[d,e]
1	**1**	**2**	Me	CuCl	(4*R*)-Ph **49**	22	1 : 0.52 : 0.14[f]	72[g]	~0
2	**1**	**2**	Me	$Cu(MeCN)_4PF_6$	(4*R*)-Ph **49**	20	1 : 0.09 : 0.00[f]	84	17 (2*S*,3*R*)
3	**1**	**2**	Me	CuCl	(4*R*)-Bn **50**	40	1 : 0.41 : 0.08[f]	71[g]	~0
4	**32**	**39**	Et	CuCl	(4*R*)-Ph **49**	24	1 : 0.70 : 0.15	42[g]	~0
5	**32**	**39**	Et	$Cu(MeCN)_4PF_6$	(4*R*)-Ph **49**	20	1 : 0.11 : 0.00	53[g]	29 (2*S*,3*R*)
6	**33**	**40**	*i*-Pr	CuCl	(4*R*)-Ph **49**	21	1 : 1.00 : 0.31[h]	68[g]	~0
7	**33**	**40**	*i*-Pr	$Cu(MeCN)_4PF_6$	(4*R*)-Ph **49**	1.5	1 : 0.46 : 0.00[h]	39[g]	33 (2*S*,3*S*)
8	**33**	**40**	*i*-Pr	CuCl	(4*R*,5*S*)-Ph **52**	21	1 : 2.50 : 0.40[h]	54[g]	~0
9	**35**	**42**	Ph	CuCl	(4*R*)-Ph **49**	26	1 : –[i] : 0.30	42[g]	~0
10	**35**	**42**	Ph	$CuCl_2$	(4*R*)-Ph **49**	30	1 : –[i] : 0.61	48[g]	~0
11	**35**	**42**	Ph	$Cu(MeCN)_4PF_6$	(4*R*)-Ph **49**	3	1 : –[i] : 0.00[h]	90	52 (2*S*,3*S*)
12	**35**	**42**	Ph	$Cu(OTf)_2$	(4*R*)-Ph **49**	5	1 : –[i] : 0.00[h]	90[g]	46 (2*S*,3*S*)
13	**35**	**42**	Ph	CuCl	(4*R*)-Bn **50**	24	1 : –[i] : 0.19[h]	40[g]	8 (2*S*,3*S*)
14	**35**	**42**	Ph	$CuCl_2$	(4*R*)-Bn **50**	21	1 : –[i] : 0.46	57	9 (2*S*,3*S*)
15	**35**	**42**	Ph	$Cu(MeCN)_4PF_6$	(4*R*)-Bn **50**	2	1 : –[i] : 0.10	83	71 (2*S*,3*S*)
16	**35**	**42**	Ph	$Cu(OTf)_2$	(4*R*)-Bn **50**	2	1 : –[i] : 0.00	79	76 (2*S*,3*S*)
17	**35**	**42**	Ph	CuCl	(4*R*,5*S*)-diPh **52**	42	1 : –[i] : 0.27	47	33 (2*S*,3*S*)
18	**35**	**42**	Ph	$CuCl_2$	(3*S*,8*R*)-Ind **53**	21	1 : –[i] : 0.18	62	14 (2*R*,3*R*)
19	**35**	**42**	Ph	$Cu(MeCN)_4PF_6$	(3*S*,8*R*)-Ind **53**	4	1 : –[i] : 0.05[j]	56	60 (2*R*,3*R*)
20	**35**	**42**	Ph	$Cu(OTf)_2$	(3*S*,8*R*)-Ind **53**	4	1 : –[i] : 0.18	66	57 (2*R*,3*R*)
21	**36**	**43**	Bn	CuCl	(4*R*)-Ph **49**	24	1 : 1.89 : 0.45[h]	42[g]	5 (2*S*,3*S*)
22	**36**	**43**	Bn	$Cu(MeCN)_4PF_6$	(4*R*)-Ph **49**	27	1 : –[k] : 0.00	47[g]	14 (2*S*,3*S*)

[a] Reactions conducted using the general procedure for copper-catalysed C–H insertion reactions (see **Section 4.2.9** for details).

[b] Ratio of C–H insertion : diazo reduction (Red) : O–H insertion based on integration of the C(2)H doublet of the cyclopentanone product, the $C(1)H_2$ singlet of the β-keto sulfone and the δ_H 5.14–5.17 singlet of the O–H insertion product (see **Figure 2.9** for general structure), respectively, in the ^{1}H NMR spectra of the crude reaction mixtures.

[c] Yield of *trans*-cyclopentanone after column chromatography.

[d] Enantiopurity of *trans*-cyclopentanone determined by chiral stationary phase HPLC (see appendix I for details).

[e] Stereochemical assignments were made by comparison with previously reported rotation and HPLC data (see Appendix I for details).[80,103]

[f] Unknown singlet observed at δ_H 6.04 in the ^{1}H NMR spectrum of the crude reaction mixture.

[g] Isolated product not fully clean.

[h] ^{1}H NMR spectra of crude reaction mixture was complex.

[I] Ratio of β-keto sulfone **27** (R = Ph) not determined due to overlap with the C(3)H signal of cyclopentanone **42**, but **27** is presumed to be present in low levels.

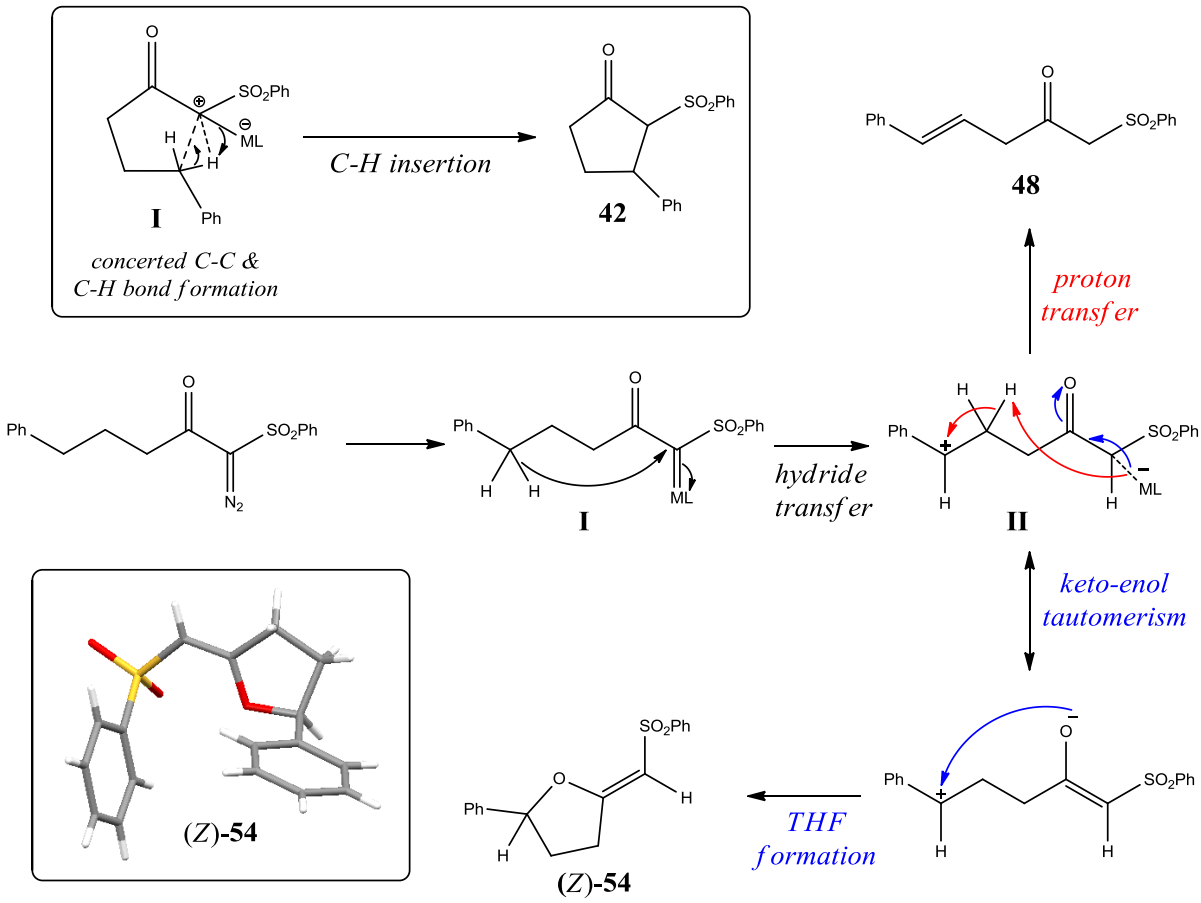
[j] Approximately 3% hydride abstraction byproduct **48** observed in the ^{1}H NMR spectrum of the crude reaction mixture.

[k] Value not determined due to overlap with solvent peak.

Yields obtained for the copper-catalysed reactions were moderate to good, ranging from 39% for cyclisation of the *iso*-propyl-substituted diazo **33** in the presence of $Cu(MeCN)_4PF_6$ and (4*R*)-Ph **49** (**Table 2.12**, entry 7) to 90% for the $Cu(OTf)_2$- and $Cu(MeCN)_4PF_6$-catalysed insertions of **35** employing the same bis(oxazoline) ligand (**Table 2.12**, entries 11 and 12). Loss of yield in certain cases may be attributed to the formation of byproducts, which were observed in the ^{1}H NMR spectra of the crude reaction mixtures. Chromatographic purification was generally sufficient in removing these side products, however, in certain instances traces of byproduct(s) were still observed in the ^{1}H NMR spectra following column chromatography. O–H insertion and β-keto sulfone formation (see **Figure 2.9** for byproduct structures), arising from intermolecular insertion into water and diazo reduction, respectively, were found to be the main competing processes in the copper-bis(oxazoline)-catalysed reactions described in **Table 2.12**. Interestingly, byproduct formation was found to be far more prevalent for reactions employing CuCl and $CuCl_2$, compared to reactions with $Cu(OTf)_2$ and $Cu(MeCN)_4PF_6$, suggesting that C–H insertion in the presence of the latter two copper sources is a more favourable process.

Interestingly, a number of different competing reaction pathways were observed for decomposition of 1-diazo-1-phenylsulfonyl-5-phenylpentan-2-one **35** (R = Ph). In addition to the previously described processes of O–H insertion and diazo reduction, competition between C–H insertion and hydride transfer was also found to occur (**Scheme 2.19**). Hydride transfer to the carbenoid carbon was not observed for reactions with the other diazosulfones (R = Me, Et, *i*-Pr, *t*-Bu, Bn), presumably because the carbocationic intermediate **II** is sufficiently stable to form when it is benzylic but not with the other diazo substrates. The benzylic carbocation **II** may subsequently undergo proton transfer to provide the alkene product **48**, as has been described in the literature for similar diazo substrates.[11,84,104] An alternative reaction pathway was also observed in this project which had not previously been reported. This pathway involves intramolecular attack of the anionic oxygen atom at the electron-deficient benzylic carbocation resulting in the formation of 2-phenyl-5-[(phenylsulfonyl)methylene] tetrahydrofuran **54**. Notably, the formation of **54** was not found to occur for rhodium-catalysed reactions of **35**.

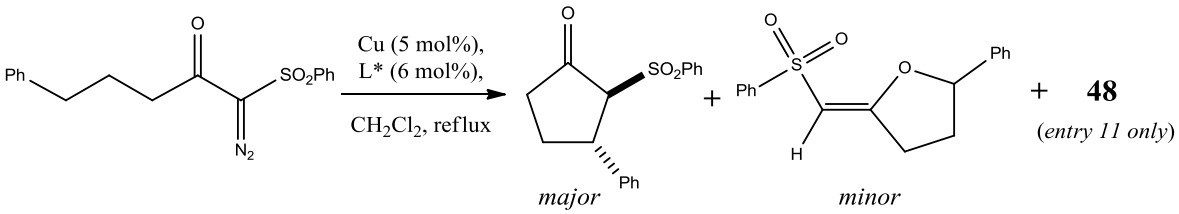
The formation of the two products (**54** and **48**) derived from hydrogen abstraction in competition with the C–H insertion pathway provides interesting mechanistic insight into the nature of the C–H insertion process. Thus, in intermediate **I** concerted C–C and C–H bond formation with concomitant cleavage of the γ-C–H bond leads to insertion product **42**, while transfer of hydride from the γ-carbon to the carbene centre competes through asynchronous bond formation and breaking in the same transition state, but only when the γ-C–H bond is benzylic. Earlier work by Flynn and Maguire observed similar patterns in the reactions of α-diazo-β-oxo sulfones.[11]



Scheme 2.19

The tetrahydrofuran side product **54** was observed in varying amounts (up to 30% relative to cyclopentanone formation) in the ^{1}H NMR spectra of the crude reaction mixtures for the reactions of **35** (**Table 2.13**, entries 1–12). No clear pattern could be discerned relating side product formation to the catalyst employed. Isolation of **54** was possible *via* chromatographic purification of the crude reaction mixture, with the tetrahydrofuran compound eluting as the most polar fraction. 2-Phenyl-5-[(phenylsulfonyl)methylene] tetrahydrofuran **54** was isolated as the *Z*-isomer exclusively following column chromatography, as confirmed by X-ray crystallography (**Scheme 2.19**). A 50 : 50 mixture of enantiomers was observed upon chiral HPLC analysis of **54** (see appendix I for HPLC trace), indicating that no asymmetric induction occurred for the formation of the chiral centre at C(2). This outcome reflects the likely involvement of a free carbene in the formation of the THF ring of **54** rather than a copper catalyst-mediated process.

Table 2.13 *Cyclopentanone versus tetrahydrofuran formation*[a]



35 **42** **54**

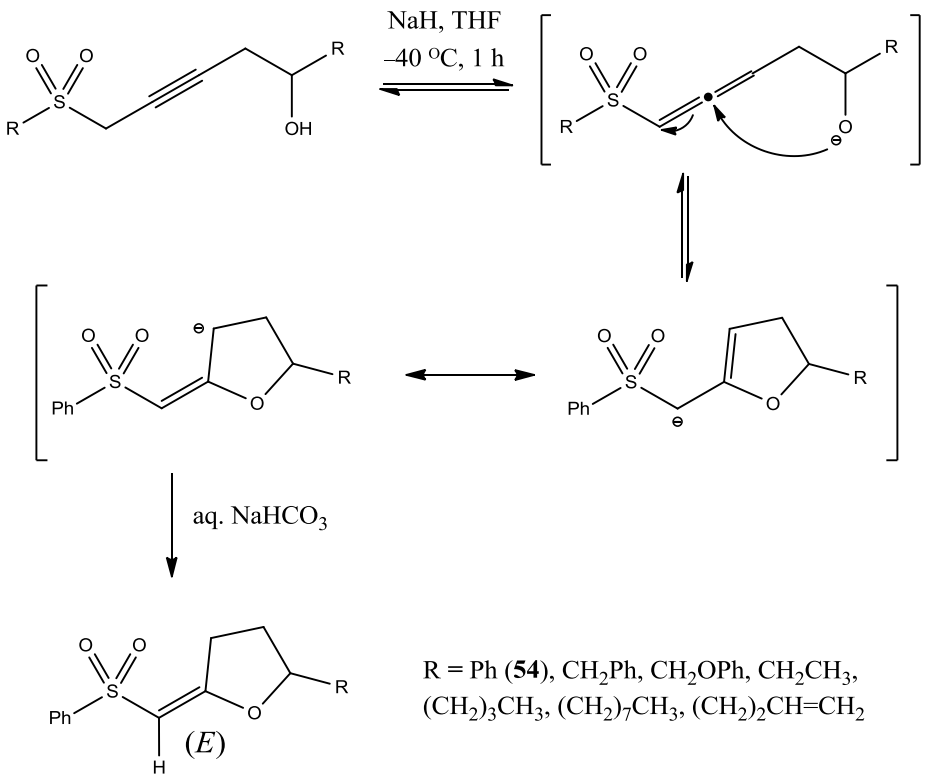
Entry	Cu	L*	**42** : **54**[b]
1	CuCl	(4*R*)-Ph **49**	1 : 0.15
2	$CuCl_2$	(4*R*)-Ph **49**	1 : 0.00
3	$Cu(MeCN)_4PF_6$	(4*R*)-Ph **49**	1 : 0.02
4	$Cu(OTf)_2$	(4*R*)-Ph **49**	1 : 0.30
5	CuCl	(4*R*)-Bn **50**	1 : 0.16
6	$CuCl_2$	(4*R*)-Bn **50**	1 : 0.12
7	$Cu(MeCN)_4PF_6$	(4*R*)-Bn **50**	1 : 0.00
8	$Cu(OTf)_2$	(4*R*)-Bn **50**	1 : 0.19
9	CuCl	(4*R*,5*S*)-Ph **52**	1 : 0.19
10	$CuCl_2$	(3*S*,8*R*)-Ind **53**	1 : 0.15
11	$Cu(MeCN)_4PF_6$	(3*S*,8*R*)-Ind **53**	1 : 0.20[c]
12	$Cu(OTf)_2$	(3*S*,8*R*)-Ind **53**	1 : 0.22

[a] Reactions conducted using the general procedure for copper-catalysed C–H insertion reactions (see Section **4.2.9** for details).

[b] Ratios based on integration of the C(2)H doublet of **42** and the δ_H 5.62 singlet of **54** in the ^{1}H NMR spectra of the crude reaction mixture.

[c] Approximately 3% hydride abstraction byproduct **48** observed in the ^{1}H NMR spectrum of the crude reaction mixture.

Literature research revealed the description of a number of related tetrahydrofuran products, including 2-phenyl-5-[(phenylsulfonyl)methylene] tetrahydrofuran **54**, produced *via* base-mediated cyclisation of hydroxyl propargylic sulfones (**Scheme 2.20**).[105] In all cases reported, (*E*)-exo-alkylidene tetrahydrofurans were isolated as the sole product in high yield (80–85%).[105] Similar (*Z*)-2-alkylidene tetrahydrofuran products have also been obtained from mercury(II)- and palladium(II)-mediated cyclisation of acetylenic alcohols and used as the key intermediates in prostacyclin PGI_2 synthesis.[106,107] Indeed, tetrahydrofurans are important structural units found in many biologically active molecules such as polyether antibiotics,[108] annonaceous acetogenins[109] and macrodiolides[110] and as a result the synthesis of substituted tetrahydrofurans has been the focus of many research efforts.[111-113] The generation of **54** *via* a carbenoid hyride transfer pathway (**Scheme 2.19**) thus offers an additional route to substituted tetrahydrofuran products with high *Z*-selectivity. Although low overall yields of **54** were recorded for the reactions of diazo sulfone **35**, the formation of increased levels of tetrahydrofuran product may be possible by examination of a wider range of substrates and catalysts for this transformation.



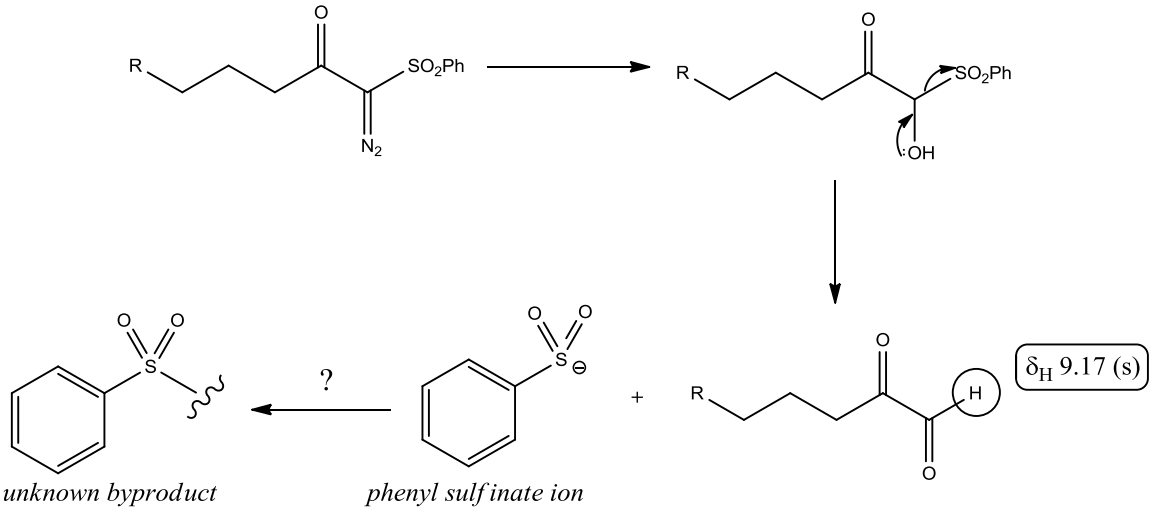
Scheme 2.20

In addition to the byproducts already described (**Figure 2.9** and **Scheme 2.19**), minor amounts (≤ 3% yield) of an unknown side product were also isolated from several of the reaction mixtures arising from the copper-catalysed reactions described in **Table 2.12** (and subsequent reactions in **Table 2.14**) following chromatographic purification (least polar fraction). This compound, which displayed identical spectroscopic features irrespective of the α-diazo-β-keto sulfone R substituent, showed distinctive multiplet signals in the region of δ_H 7.2–7.6 in the ^{1}H NMR spectrum, with no signals observed outside of this area indicating that this compound possesses only aromatic hydrogens. ^{13}C NMR analysis revealed the presence of two quaternary signals (δ_C 127.8 and 142.9) and six aromatic CH signals corresponding to ten aromatic CH carbons [δ_C 127.6 (2 × *C*H), 128.8 (2 × *C*H), 129.4 (2 × *C*H), 131.4, 133.6 and 136.6 (2 × *C*H)], suggesting the presence of two non-equivalent aromatic rings. This finding was reinforced by the observation of four individual doublet signals [δ_H 7.60 (*J* 8.7), 7.52 (*J* 8.4), 7.44 (*J* 8.7) and 7.25 (*J* 8.7)] in the analogous unknown compound arising from reaction of the *para*-bromophenylsulfonyl-substituted α-diazo-β-keto sulfone (see **Scheme 2.23** for structure). In the IR spectrum, signals were observed at 1448, 1326, 1145 and 1078 cm^{-1}, with the middle two signals presumed to represent asymmetric and symmetric sulfonyl stretches, respectively, while mass spectrometry analysis revealed major peaks at m/z (ES+) 261.4 and m/z (ES–) 157.3 and 173.3.

Possible structures considered for this unknown compound included phenylbenzenethiosulfonate,[114] benzene sulfonic acid,[115] diphenyl disulfide,[116] phenylsulfonyl chloride,[117] diphenyl sulfone,[118] and diphenyl disulfone,[119] however, the spectroscopic data for these compounds did not match that obtained from the analysis described above.

The tentatively proposed mechanism for the formation of the unknown aromatic compound is presented in **Scheme 2.21**. Accordingly, transformation of the O–H insertion byproduct to the corresponding aldehyde may occur *via* attack of the lone pair of electrons of the hydroxyl group resulting in generation of the phenylsulfinate anion. The formation of the aldehyde compound is indicated by the observation of a distinctive singlet at δ_H 9.17 in the ^{1}H NMR spectra of several of the crude reaction mixtures, in line with reports for similar dicarbonyl compounds in the literature.[120,121] Notably, in each instance that the unknown aromatic compound was isolated, the aldehyde signal at δ_H 9.17 was also observed in the ^{1}H NMR spectrum of the crude reaction mixture. This aldehyde signal was not observed in any fractions isolated following column chromatography. The phenylsulfinate anion thus generated is thought to react with an electrophilic species present in solution resulting in the formation of the unknown aromatic compound. Further studies are warranted to try to unambiguously establish the structure of this unknown byproduct.

Tentatively proposed mechanism



Scheme 2.21

The levels of enantioselectivity obtained for the copper-bis(oxazoline)-catalysed insertions (**Table 2.12**) were found to be both substrate- and catalyst-dependent. Highest asymmetric induction (up to 76% ee) was achieved for reactions of the phenyl-substituted diazo substrate **35** (**Table 2.12**, entries 9–20), with decreased enantiocontrol observed for

insertions with the other diazo substrates, largely in order of decreasing size of the R group (*i*-Pr > Et > Me ≈ Bn). This result is in line with previous findings by Hashimoto and co-workers, who also reported enhanced enantioselectivity for insertion into benzylic C–H bonds.[91] Choice of copper source was found to be particularly important in this study. Reactions in the presence of CuCl and $CuCl_2$ lead, in general, to poor levels of enantioselectivity (typically <10% ee), with a slight increase observed for insertion of α-diazo-β-keto sulfone **35** with ligand (4*R*,5*S*)-diPh **52** (**Table 2.12**, entry 17) and (3*S*,8*R*)-Ind **53** (**Table 2.12**, entry 18). In contrast, C–H insertions employing $Cu(OTf)_2$ and $Cu(MeCN)_4PF_6$ provided significantly higher asymmetric induction for all substrates tested. In particular, an increase to 76% ee and 71% ee for cyclisations of **35** in the presence of bis(oxazoline) (4*R*)-Ph **49,** and $Cu(OTf)_2$ and $Cu(MeCN)_4PF_6$, respectively, (**Table 2.12**, entries 16 and 15) was recorded, representing a vast improvement when contrasted with the corresponding CuCl and $CuCl_2$-catalysed reactions in which low asymmetric induction, 8% ee and 9% ee, respectively, was observed (**Table 2.12**, entries 13 and 14). Notably, the extent of enantiocontrol recorded for these reactions was considerably higher than those observed for insertions employing chiral rhodium-mandelate-derived catalysts (**Table 2.10**).

Throughout this study, the use of the ligands (4*R*)-Ph **49**, (4*R*)-Bn **50** and (4*R*,5*S*)-diPh **52**, with the same absolute stereochemistry, lead to cyclopentanone products of the same enantiomeric series, while bis(oxazolines) (4*S*)-*t*-Bu **51** and (3*S*,8*R*)-Ind **53**, which have the opposite absolute stereochemistry, as predicted lead consistently to the opposite enantiomeric series of cyclopentanones (**Figure 2.15**).

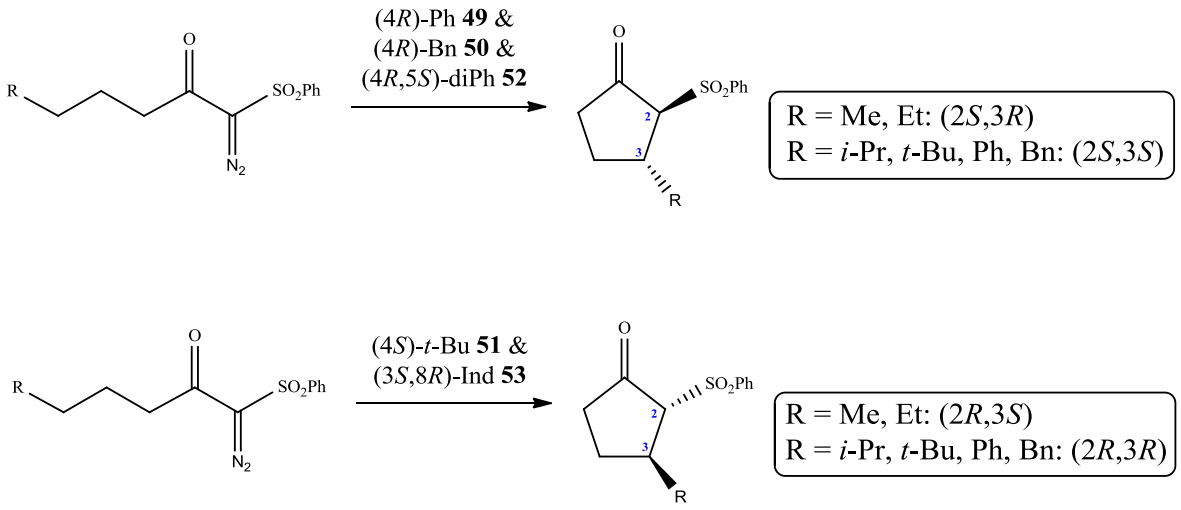


Figure 2.15

2.6.2 Investigation of additive effects

In an effort to improve upon the poor enantioselectivities obtained for C–H insertions in the presence of CuCl and $CuCl_2$ (**Section 2.6.1**), an examination of additive effects was next conducted. For this purpose, the effects of the additive NaBARF {BARF = tetrakis[3,5-bis (trifluoromethyl)phenyl] borate} were first examined. The borate anion $BARF^-$ (**Figure 2.16**) was first utilised in 1981 by Kobayashi and co-workers as a negatively charged phase transfer catalyst.[122] This anionic species behaves as an extremely weakly-coordinating anion owing to distribution of the negative charge over a large area of non-nucleophilic and chemically stable functional groups.[123] Salts of $BARF^-$, including sodium, potassium, silver and thallium compounds, have been employed in several transition metal-catalysed transformations, such as hydrogenation[124,125] and hydrovinylation[126,127] reactions, where they have been shown to enhance the activity of cationic catalyst species, resulting in improvements in reaction efficiencies and selectivities.

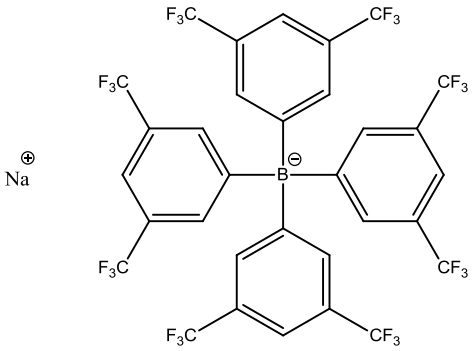


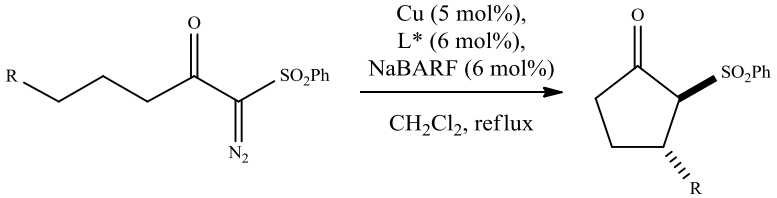
Figure 2.16

The use of NaBARF has previously been shown to enhance enantioselectivity in the copper-catalysed insertion of carbenoids into N–H and O–H bonds,[101,102] and in the copper-catalysed intramolecular Buchner reaction.[94] In addition, the presence of NaBARF has also been reported to result in improved efficiency and selectivity in [3+2] cycloadditions of α-aryldiazoesters with terminal alkenes,[128] and in another instance altered efficiency and regioselectivity in intermolecular C–H insertion reactions with ethyl diazoacetate.[129] At the beginning of this investigation an understanding of the mechanistic basis for such improvements in carbenoid transformations remained elusive, however, it was envisioned that employment of this borate additive in our copper-catalysed C–H insertions may have similar beneficial effects on reaction efficiency and selectivity.

2.6.2.1 C–H insertions in the presence of NaBARF

Copper-bis(oxazoline)-catalysed C–H insertions of α-diazo-β-keto phenylsulfones **1**, **32**–**36** in the presence of NaBARF are presented in **Table 2.14**.

Table 2.14 *Copper-bis(oxazoline)-catalysed C–H insertions of α-diazo-β-keto phenylsulfones with NaBARF*[a]



Entry	Diazo	Product	R	Cu	L*	C–H : Red : O–H[b]	Time (h)	Yield (%)[c]	ee (%)[d,e]
1	**1**	**2**	Me	CuCl	(4*R*)-Ph **49**	1 : 0.02 : 0.00	27	94	30 (2*S*, 3*R*)
2	**1**	**2**	Me	CuCl	(4*R*,5*S*)-diPh **52**	1 : 0.00 : 0.00	21	74	~0
3	**1**	**2**	Me	CuCl	(4*R*)-Bn **50**	1 : 0.03 : 0.01	3	62	58 (2*S*, 3*R*)
4	**1**	**2**	Me	$CuCl_2$	(3*S*,8*R*)-Ind **53**	1 : 0.02 : 0.03	2	74	66 (2*R*, 3*S*)
5	**1**	**2**	Me	CuCl	(4*S*)-*t*-Bu **51**	1 : 0.00 : 0.01	22	73	13 (2*R*, 3*S*)
6	**32**	**39**	Et	CuCl	(4*R*)-Ph **49**	1 : 0.00 : 0.00	6	97	29 (2*S*, 3*R*)
7	**32**	**39**	Et	CuCl	(4*R*,5*S*)-diPh **52**	1 : 0.01 : 0.00	21	76[f]	11 (2*S*, 3*R*)
8	**32**	**39**	Et	CuCl	(4*R*)-Bn **50**	1 : 0.02 : 0.00	15	70[f]	62 (2*S*, 3*R*)
9	**32**	**39**	Et	$CuCl_2$	(3*S*,8*R*)-Ind **53**	1 : 0.02 : 0.04	3	82[f]	71 (2*R*, 3*S*)
10	**32**	**39**	Et	CuCl	(4*S*)-*t*-Bu **51**	1 : 0.01 : 0.01	15	73[f]	28 (2*R*, 3*S*)
11	**33**	**40**	*i*-Pr	CuCl	(4*R*)-Ph **49**	1 : 0.06 : 0.00	4.5	54[f]	37 (2*S*, 3*S*)
12	**33**	**40**	*i*-Pr	CuCl	(4*R*,5*S*)-diPh **52**	1 : 0.00 : 0.00	21	65[g]	14 (2*S*, 3*S*)
13	**33**	**40**	*i*-Pr	CuCl	(4*R*)-Bn **50**	1 : 0.06 : 0.10	16	95[f]	60 (2*S*, 3*S*)
14	**33**	**40**	*i*-Pr	$CuCl_2$	(3*S*,8*R*)-Ind **53**	1 : 0.04 : 0.04	2	87[f]	75 (2*R*, 3*R*)
15	**33**	**40**	*i*-Pr	CuCl	(4*S*)-*t*-Bu **51**	1 : 0.10 : 0.04	24	55[f]	42 (2*R*, 3*R*)
16	**34**	**41**	*t*-Bu	$CuCl_2$	(4*R*)-Ph **49**	1 : 0.14 : 0.10[h]	2	84[j]	76 (2*S*, 3*S*)[i]
17	**34**	**41**	*t*-Bu	$CuCl_2$	(4*R*,5*S*)-diPh **52**	1 : 0.03 : 0.11[h]	2	76[j]	52 (2*S*, 3*S*)[i]
18	**34**	**41**	*t*-Bu	$CuCl_2$	(4*R*)-Bn **50**	1 : 0.08 : 0.03[h]	2	75	73 (2*S*, 3*S*)
19	**34**	**41**	*t*-Bu	$CuCl_2$	(3*S*,8*R*)-Ind **53**	1 : 0.02 : 0.01[h]	2	72	77 (2*R*, 3*R*)
20	**34**	**41**	*t*-Bu	$CuCl_2$	(4*S*)-*t*-Bu **51**	1 : 0.38 : 0.26[h]	2	62[j]	53 (2*S*, 3*S*)[i]
21	**35**	**42**	Ph	CuCl	(4*R*)-Ph **49**	1 : –[k] : 0.00	3.5	68	49 (2*S*, 3*S*)
22	**35**	**42**	Ph	$CuCl_2$	(4*R*)-Ph **49**	1 : –[k] : 0.05	2	69	57 (2*S*, 3*S*)
23	**35**	**42**	Ph	CuCl	(4*R*,5*S*)-diPh **52**	1 : –[k] : 0.03	22	82	58 (2*S*, 3*S*)
24[l]	**35**	**42**	Ph	CuCl	(4*R*,5*S*)-diPh **52**	1 : –[k] : 0.01	6	64	55 (2*S*, 3*S*)
25	**35**	**42**	Ph	$CuCl_2$	(4*R*,5*S*)-diPh **52**	1 : –[k] : 0.05	2	54	52 (2*S*, 3*S*)
26	**35**	**42**	Ph	CuCl	(4*R*)-Bn **50**	1 : –[k] : 0.01	19	62	82 (2*S*, 3*S*)
27	**35**	**42**	Ph	$CuCl_2$	(4*R*)-Bn **50**	1 : –[k] : 0.01	2	58	81 (2*S*, 3*S*)
28[m]	**35**	**42**	Ph	$CuCl_2$	(4*R*)-Bn **50**	1 : –[k] : 0.03	2	65	80 (2*S*, 3*S*)
29	**35**	**42**	Ph	CuCl	(3*S*,8*R*)-Ind **53**	1 : –[k] : 0.03	21	57	84 (2*R*, 3*R*)
30	**35**	**42**	Ph	$CuCl_2$	(3*S*,8*R*)-Ind **53**	1 : –[k] : 0.02	2	87	89 (2*R*, 3*R*)
31[l]	**35**	**42**	Ph	$CuCl_2$	(3*S*,8*R*)-Ind **53**	1 : –[k] : 0.10	2	53	86 (2*R*, 3*R*)
32	**35**	**42**	Ph	CuCl	(4*S*)-*t*-Bu **51**	1 : –[k] : 0.01	19	55	64 (2*R*, 3*R*)

33	**36**	**43**	Bn	CuCl	(4*R*)-Ph **49**	1 : 0.06 : 0.00	21	57	14 (2*S*, 3*S*)
34	**36**	**43**	Bn	CuCl	(4*R*,5*S*)-diPh **52**	1 : 0.06 : 0.00	21	46[f]	~0
35	**36**	**43**	Bn	CuCl	(4*R*)-Bn **50**	1 : 0.26 : 0.02	6	54[f]	57 (2*S*, 3*S*)
36	**36**	**43**	Bn	$CuCl_2$	(3*S*,8*R*)-Ind **53**	1 : 0.13 : 0.05[h]	3	78[j]	66 (2*S*, 3*S*)
37	**36**	**43**	Bn	CuCl	(4*S*)-*t*-Bu **51**	1 : 0.02 : 0.02	8	62[f]	33 (2*S*, 3*S*)

[a] Reactions conducted using the general procedure for copper-catalysed C–H insertion reactions (see **Section 4.2.9** for details).
[b] Ratio of C–H insertion : diazo reduction (Red): O–H insertion based on integration of the C(2)H doublet of the cyclopentanone product, the $C(1)H_2$ singlet of the β-keto sulfone and the δ_H 5.14–5.17 singlet of the O–H insertion product (see **Figure 2.9** for general structure), respectively, in the ^{1}H NMR spectra of the crude reaction mixtures.
[c] Yield of *trans*-cyclopentanone after column chromatography.
[d] Enantiopurity of *trans*-cyclopentanone determined by chiral stationary phase HPLC (see appendix I for details).
[e] Stereochemical assignments for **2**, **39**, **40**, **42** and **43** were made by comparison with previously reported rotation and HPLC data.[80,103] Absolute stereochemistry of **41** determined by single crystal analysis (see appendix I for details).
[f] Isolated product contains minor amount of β-keto sulfone (R = Et: **24**, *i*-Pr: **25**, *t*-Bu: **26**, Ph(*p*-Br): **70**, Bn: **28**).
[g] Unknown byproduct (colourless oil) isolated in ~30% yield after column chromatography.
[h] Unknown peaks observed in the ^{1}H NMR spectra of the crude reaction mixture.
[i] HPLC trace was complex, therefore value is tentatively assigned.
[j] Isolated product not fully clean.
[k] Ratio of β-keto sulfone **27** not determined due to overlap with the C(3)H signal of cyclopentanone **42**, but **27** is presumed to be present in low levels.
[l] 10 mol% copper, 12 mol% ligand, 12 mol% NaBARF.
[m] 12 mol% NaBARF.

Employment of NaBARF was found to have a positive effect on enantioselectivity, with significantly increased enantiocontrol observed compared to reactions in the presence of copper chloride and bis(oxazoline) ligand only (**Table 2.14** *vs.* **Table 2.12**). The dramatic improvements recorded are highlighted in **Figure 2.17** for CuCl-catalysed C–H insertions of α-diazo-β-keto sulfones **1**, **32**, **33**, **35** and **36** in the presence of the phenyl-substituted ligand (4*R*)-**49** and C–H insertions of diazo **35** with ligands (4*R*)-Ph **49**, 4(*R*)-Bn **50**, (4*R*,5*S*)-diPh **52** and (3*S*,8*R*)-Ind **53**. Thus, for all reactions examined, the addition of NaBARF to the catalytic mixture correlates to a considerable enhancement in enantiocontrol. In particular, dramatic increases to 82% ee (from 9% ee) and 89% ee (from 14% ee) were achieved for $CuCl_2$-catalysed cyclisations of **35** with bis(oxazolines) (4*R*)-Bn **50** and (3*S*,8*R*)-Ind **53**, respectively (**Table 2.14**, entries 27 and 30 *vs.* **Table 2.12**, entries 14 and 18)**.**

Comparison of enantioselectivities for CuCl-bis(oxazoline)-catalysed C–H insertions with and without NaBARF

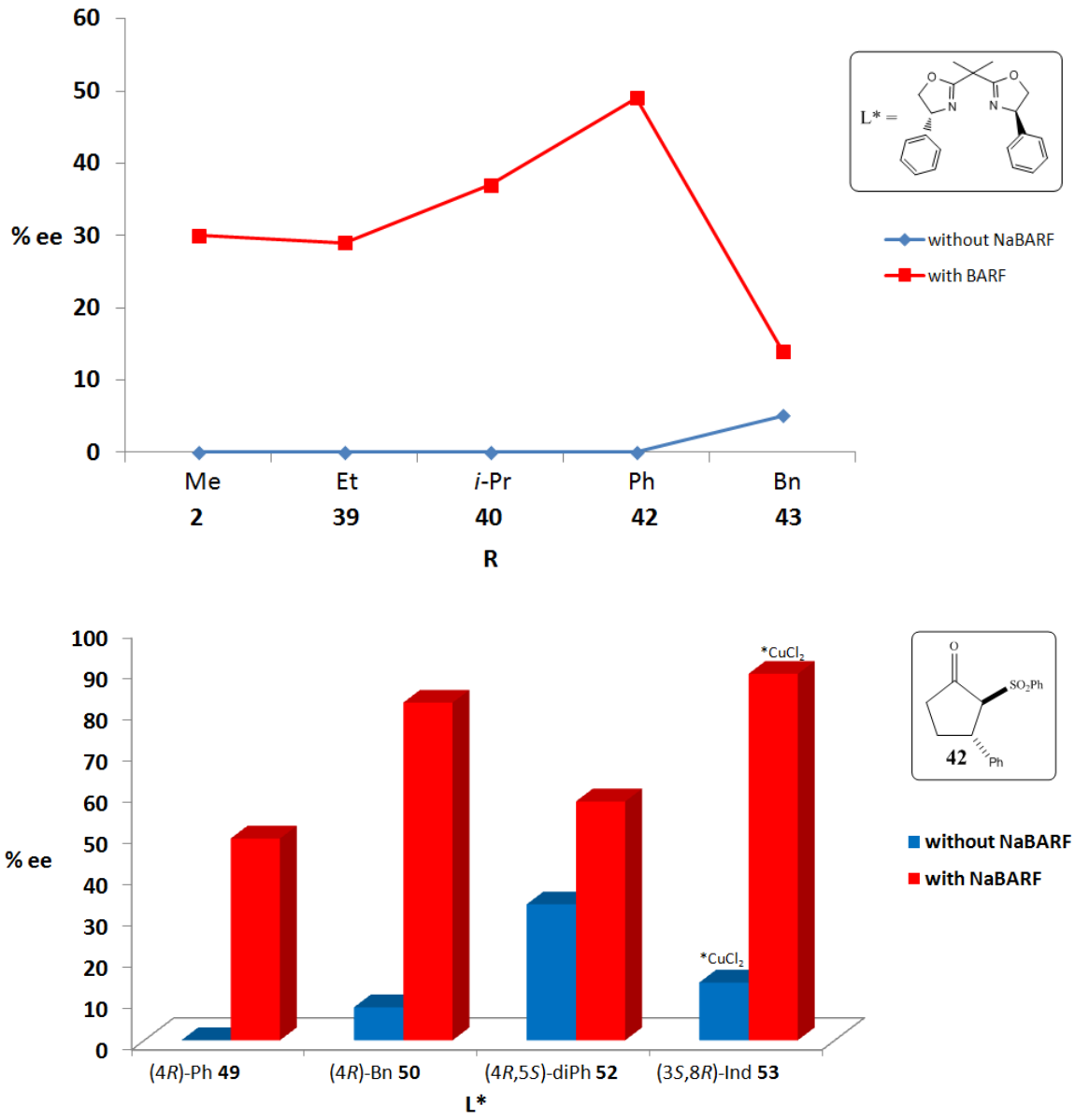


Figure 2.17

Interestingly, significantly reduced reaction times were observed for insertions in the presence of $CuCl_2$ in comparison to reactions employing CuCl. This effect is particularly evident in the reactions of α-diazo-β-keto sulfone **35** in which a dramatic decrease in reaction times to 2 h (from 22 h, 19 h and 21 h) was recorded for cyclisations in the presence of ligands (4*R*,5*S*)-diPh **52**, (4*R*)-Bn **50** and (3*S*,8*R*)-Ind **53**, respectively (**Table 2.14**, entry 23 *vs.* 25, 26 *vs.* 27 and 29 *vs.* 30). This observation is particularly interesting considering that copper(I) is known to be the active species for catalysis in carbenoid reactions.[7,130] The copper(II) complex is reduced to its active Cu(I) derivative by the diazo compound present in solution.[130] Thus, the decreased reaction times observed in

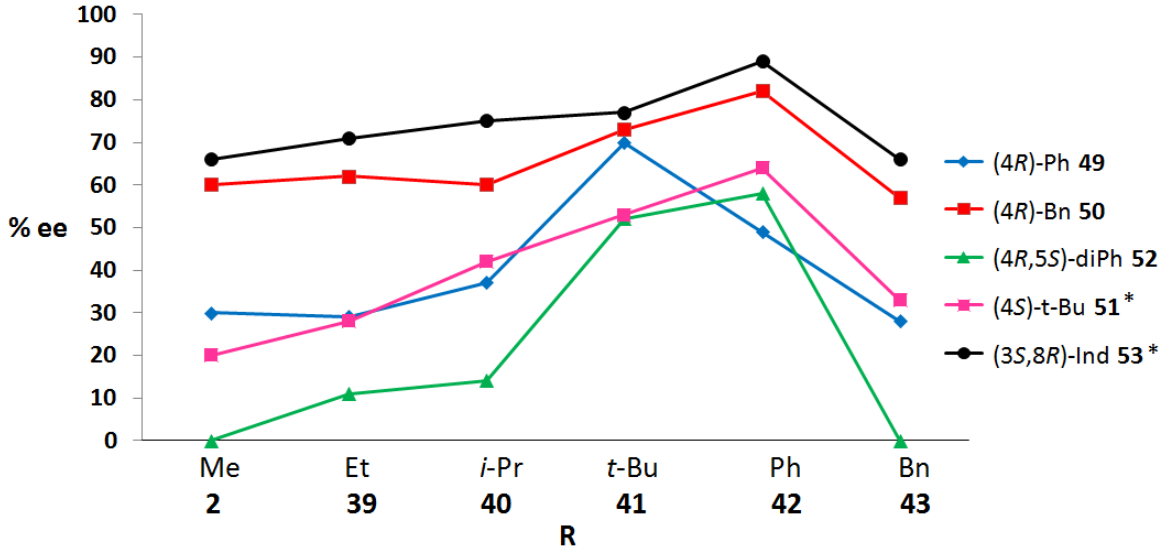
this work are likely due in part to the increased solubility of the copper(II) species in the reaction solvent. Notably, use of CuCl or $CuCl_2$ was found to lead to essentially the same outcome in terms of yield and enantioselectivity (**Table 2.14**, entry 21 *vs.* 22, 23 *vs.* 25, 26 *vs.* 27 and 29 *vs.* 30), therefore, for convenience $CuCl_2$ was adopted for the majority of subsequent cyclisations conducted in this project.

As summarised in **Figure 2.18**, a number of interesting trends can be seen in terms of the enantioselectivities obtained with the copper complexes derived from each of the bis(oxazoline) ligands **49**–**53**. The indane-derived bis(oxazoline) (3*S*,8*R*)-**53** was found to be the best-performing ligand, providing consistently high asymmetric induction across the range of diazo compounds examined (**Table 2.14**, entries 4, 9, 14, 19, 29, 30. 31 and 36). Enantioselectivity for this ligand was seen to peak at 89% ee (**Table 2.14**, entry 30) for reaction of the phenyl-substituted diazo substrate **35**. Indeed, with only one exception noted (**Table 2.14**, entry 16), cyclisation of **35** was observed to give the highest levels of enantioselectivity for all ligands tested. With the phenyl-substituted ligand (4*R*)-**49**, relatively consistent enantiocontrol is observed across the series of α-diazo-β-keto sulfones, typically around 30% ee, with enhanced enantioselectivity observed for insertion into the benzylic C–H bond (**Table 2.14**, entries 21 and 22). The benzyl-substituted ligand (4*R*)-**50** gives consistently good asymmetric induction in the region of 60% ee, relatively independent of the nature of the R group at the insertion site (**Table 2.14**, entries 3, 8, 13, 18 and 35). As was observed for ligand (4*R*)-Ph **49**, the enantioselectivity achieved with ligand (4*R*)-Bn **50** is increased (82% ee) in the formation of cyclopentanone **42** (**Table 2.14**, entries 26–28). In contrast, ligand (4*R*,5*S*)-**52**, which features a diphenyl substitution pattern, was found to proceed with modest enantiocontrol (52–58% ee) for only the phenyl- and *tert*-butyl-substituted substrates **35** (**Table 2.14**, entries 23–25) and **34** (**Table 2.14**, entry 17), respectively; for each of the other diazo sulfones, very little enantioselection was observed. With the *tert*-butyl-substituted ligand (4*S*)-**51**, a steady increase in enantiocontrol is noted on increasing the size of the R group adjacent to the C–H insertion site, indicating an important steric effect with this ligand. As before, best results for bis(oxazoline) (4*S*)-*t*-Bu **51** were achieved in the synthesis of the 3-phenylcyclopentanone **42** (**Table 2.14**, entry 32).

Thus, with most of the ligands in **Figure 2.18** a general increase in enantioselectivity is observed with increasing size of the R substituent at the site of insertion, reflecting a steric effect. The electronic effect associated with C–H insertion at the benzylic position of **35** is more powerful and generally leads to the highest levels of enantiocontrol across the series of bis(oxazolines). Results obtained with **36** (R = Bn) are comparable to those with **32** (R = Et), indicating that the benzyl substituent is essentially acting as a primary alkyl substituent without an additional effect of the aryl ring. As illustrated in **Figure 2.18**, the data recorded for C–H insertion adjacent to the *tert*-butyl substituent of **34** is somewhat out of line relative to the other diazo sulfone substrates, which may reflect the increased steric demand of the *tert*-butyl group.

However, there were challenges in accurately determining the % ee in this series, therefore, interpretation of this observation must be considered in this context.

Enantioselective CuCl-bis(oxazoline)-catalysed C–H insertions with NaBARF



**Reactions conducted with $CuCl_2$*

Figure 2.18

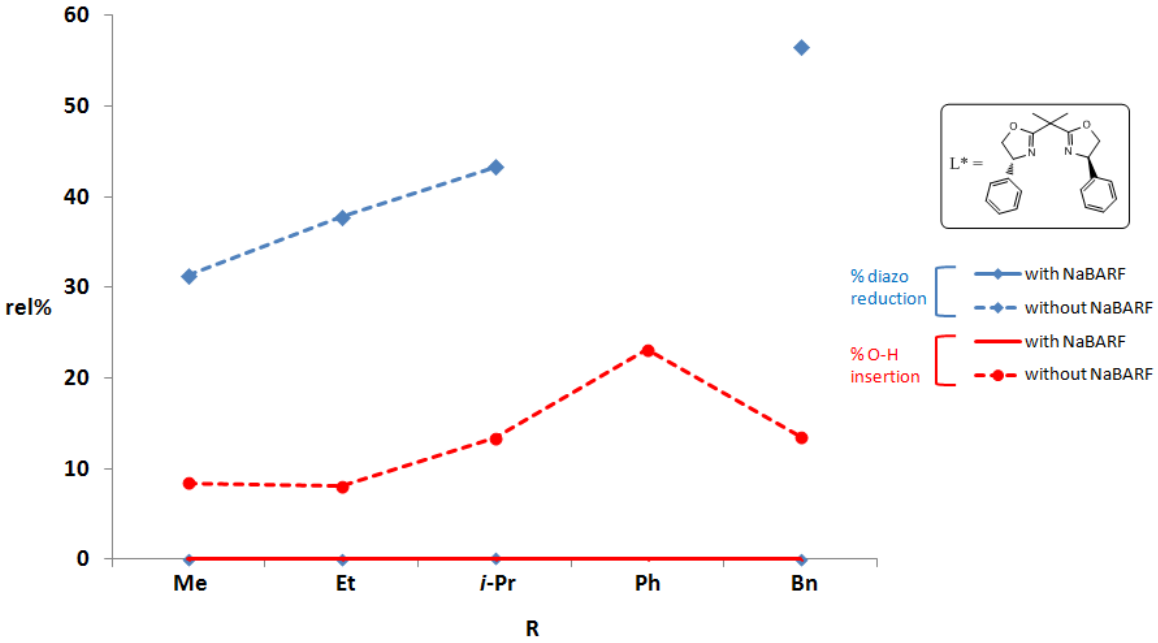
Comparison of the results obtained with ligands (4*R*)-Ph **49** and (4*R*,5*S*)-diPh **52** is also noteworthy. With substrates **1** (R = Me), **32** (R = Et)**, 33** (R = *i*-Pr) and **36** (R = Bn), the enantiocontrol using ligand (4*R*,5*S*)-diPh **52** is much less than that achieved using ligand (4*R*)-Ph **49**. Thus, the conformational impact of the additional Ph substituent and the alteration to an unsubstituted methylene bridge in ligand (4*R*,5*S*)-diPh **52** appears to orientate the ligand in a less favorable position in terms of asymmetric induction than can be achieved with the more conformationally mobile ligand (4*R*)-Ph **49**. The only exceptions to this pattern are observed with substrates **34** (R = *t*-Bu) and **35** (R = Ph), where 52–58% ee was achieved using ligand (4*R*,5*S*)-diPh **52** (**Table 2.14**, entries 17 and 23–25).

Investigation of the influence of doubling the catalyst concentration (**Table 2.14**, entries 24 *vs.* 23 and 31 *vs.* 30) and increase of NaBARF equivalents only to 12 mol% (**Table 2.14**, entry 28 *vs.* 27) for cyclisation of **35** interestingly led to essentially the same levels of enantiocontrol. Thus, addition of 5 mol% copper, 6 mol% ligand and 6 mol% NaBARF was employed as the standard catalyst loading for all subsequent C–H insertion reactions.

Yields obtained for copper-catalysed C–H insertions with NaBARF (**Table 2.14**) were generally good, averaging at 70% and, therefore, representing an increase with respect to reactions in the absence of NaBARF (**Table 2.12**), where yields of less than 60% were typically recorded. In general, cleaner ^{1}H NMR spectra were observed for the crude reaction mixtures of reactions with NaBARF versus the corresponding reactions

in the absence of NaBARF, with impurities commonly observed for the latter process. Thus, the presence of the additive appears to increase selectivity towards C–H insertion. Indeed, formation of competing O–H insertion and β-keto sulfone byproducts was found to be significantly reduced for CuCl- and $CuCl_2$-catalysed reactions employing NaBARF (**Table 2.14** *vs.* **Table 2.12**, entries 1, 3, 4, 6, 8–10, 13, 14, 17, 18 and 21); typical ratio of C–H insertion : O–H insertion reactions in the absence of NaBARF was 1 : 0.30, while ratio for corresponding reactions with NaBARF was 1 : 0.04. **Figure 2.19** highlights the observed differences in byproduct formation for CuCl-catalysed reactions with and without NaBARF.

Comparison of byproduct formation for CuCl-bis(oxazoline)-catalysed C–H insertions with and without NaBARF

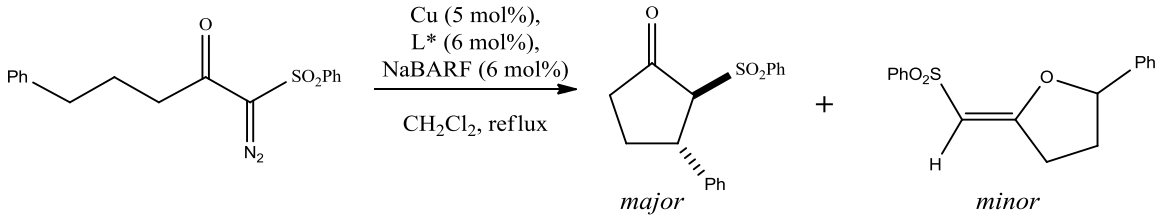


% relative to cyclopentanone formation as observed by integration of the ^{1}H NMR spectra of the crude reaction mixtures

Figure 2.19

Despite the dramatic influence of the additive species on the occurrence of competing intermolecular water insertion and diazo reduction, the addition of NaBARF to the catalytic mixture was found to have minimal impact on formation of the tetrahydrofuran byproduct **54** (**Table 2.15** and **Figure 2.20**) *e.g.* ratios of **42** : **54** were 1 : 0.16 (**Table 2.13**, entry 5) and 1 : 0.19 (**Table 2.13**, entry 9) for CuCl-catalysed insertion with ligand (4*R*)-Bn **50** and (4*R*,5*S*)-diPh **52**, respectively, in the absence of NaBARF and 1 : 0.10 (**Table 2.15**, entry 6) and 1 : 0.22 (**Table 2.15**, entry 3) for the corresponding insertions with NaBARF.

Table 2.15 *Formation of cyclopentanone **42** versus tetrahydrofuran **54** for reactions in the presence of NaBARF*[a]

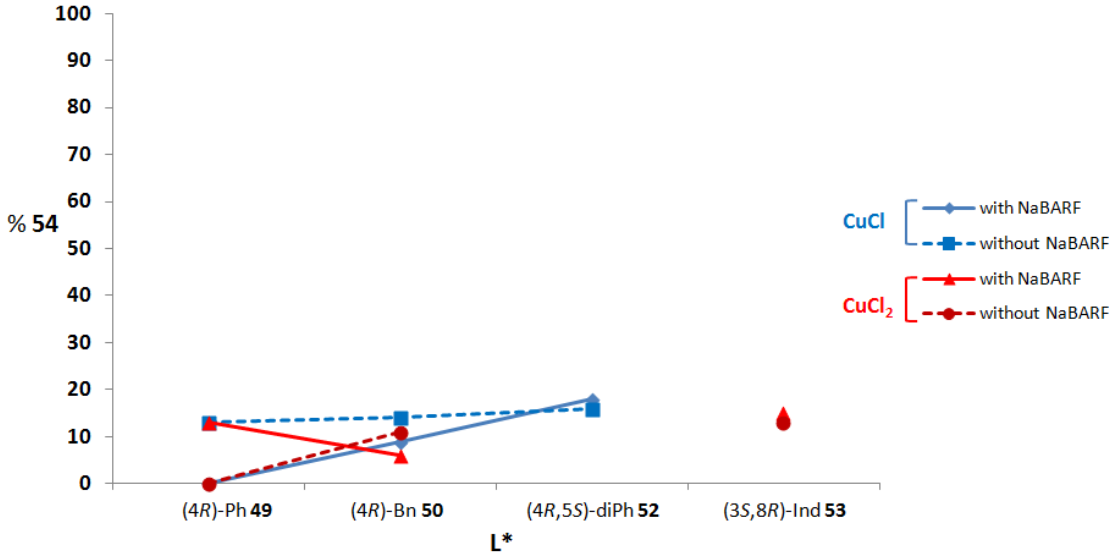


35 **42** **54**

Entry	Cu	L*	**42** : **54**[b]
1	CuCl	(4*R*)-Ph **49**	1 : 0.00
2	$CuCl_2$	(4*R*)-Ph **49**	1 : 0.15
3	CuCl	(4*R*,5*S*)-Ph **52**	1 : 0.22
4[c]	CuCl	(4*R*,5*S*)-Ph **52**	1 : 0.32
5	$CuCl_2$	(4*R*,5*S*)-Ph **52**	1 : 0.04
6	CuCl	(4*R*)-Bn **50**	1 : 0.10
7	$CuCl_2$	(4*R*)-Bn **50**	1 : 0.06
8[d]	$CuCl_2$	(4*R*)-Bn **50**	1 : 0.03
9	CuCl	(3*S*,8*R*)-Ind **53**	1 : 0.08
10	$CuCl_2$	(3*S*,8*R*)-Ind **53**	1 : 0.17
11[c]	$CuCl_2$	(3*S*,8*R*)-Ind **53**	1 : 0.15
12	CuCl	(4*S*)-*t*-Bu **51**	1 : 0.27

[a] Reactions conducted using the general procedure for copper-catalysed C–H insertion reactions (see **Section 4.2.9** for details).
[b] Ratios based on integration of the C(2)H doublet of **42** and the δ_H 5.62 singlet of **54** in the ^{1}H NMR spectra of the crude reaction mixtures.
[c] 10 mol% copper, 12 mol% ligand, 12 mol% NaBARF.
[d] 12 mol% NaBARF.

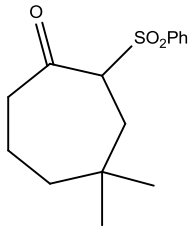
*Comparison of recorded levels of the tetrahydrofuran byproduct **54** for CuCl and $CuCl_2$-catalysed reactions of α-diazo-β-keto sulfone **35** with and without NaBARF*



(as observed by integration of the ^{1}H NMR spectra of the crude reaction mixtures)

Figure 2.20

Reactions with the *tert*-butyl-substituted diazo **34** were found to be more complex than those observed for synthesis with the other α-diazo-β-keto sulfones **1**, **32**, **33**, **35** and **36**. The presence of the sterically bulky *tert*-butyl group, therefore, appears to reduce chemoselectivity towards C–H insertion into the adjacent C(5) bond, allowing other processes to effectively compete with desired cyclopentanone synthesis. Such processes may include insertion into the C(7) methyl group, providing 4,4-dimethyl-2-(phenylsulfonyl)cycloheptanone (**Figure 2.21**), however, no analytically pure sample to confirm the presence of this byproduct was obtained. Indeed, the formation of this cycloheptanaone byproduct would be unusual considering the formation of seven-membered ring products has been previously reported only for insertions into highly activated C–H bonds.[131] As with the other diazo substrates, competing O–H insertion was also observed for reactions of **34**, as characterised by the appearance of a singlet at δ_H 5.17 in the ^{1}H NMR spectrum of the crude reaction mixture. Due to the complexity of the crude reaction mixture, purification of the desired cyclopentanone product **41** was often difficult and in some cases the final isolated product sample was not fully clean. As a result, enantioselectivity values for these samples (**Table 2.14**, entries 16, 17 and 20) are tentatively assigned.

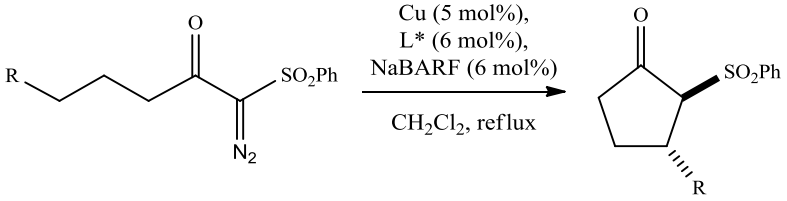


4,4-dimethyl-2-(phenylsulfonyl)cycloheptanone

Figure 2.21

Notably, in contrast to CuCl- and $CuCl_2$-catalysed insertions (**Table 2.14**), the presence of NaBARF was found to have little impact on the outcome of reactions employing $Cu(OTf)_2$ and $Cu(MeCN)_4PF_6$ as the copper source. As shown in **Table 2.16**, short reaction times, good yields, minimal competing O–H insertion and moderate to good enantioselectivities were recorded for $Cu(OTf)_2$- and $Cu(MeCN)_4PF_6$-catalysed reactions of α-diazo-β-keto sulfones **1**, **32**, **35** and **36**. These results largely parallel those previously observed for the corresponding reactions in the absence of NaBARF (**Table 2.16** *vs.* **Table 2.12**). Thus, as displayed in **Figure 2.22**, addition of the additive species in this case does not offer any significant improvements in terms of yield, chemoselectivity or enantiocontrol.

Table 2.16 *Copper-bis(oxazoline)-catalysed C–H insertions of α-diazo-β-keto phenylsulfones with NaBARF*[a]



Entry	Diazo	Product	R	Cu	L*	C–H : Red : O–H[b]	Time (h)	Yield (%)[c]	ee (%)[d,e]
1	**1**	**2**	Me	$Cu(MeCN)_4PF_6$	(4*R*)-Ph **49**	1 : 0.03 : 0.00[f]	2	69	21 (2*S*, 3*R*)
2	**32**	**39**	Et	$Cu(MeCN)_4PF_6$	(4*R*)-Ph **49**	1 : 0.01 : 0.00	1	49[g]	29 (2*S*, 3*R*)
3	**35**	**42**	Ph	$Cu(MeCN)_4PF_6$	(4*R*)-Ph **49**	1 : –[h] : 0.10	1	63	49 (2*S*, 3*S*)
4	**35**	**42**	Ph	$Cu(OTf)_2$	(4*R*)-Ph **49**	1 : –[h] : 0.00	2	64	49 (2*S*, 3*S*)
5	**35**	**42**	Ph	$Cu(MeCN)_4PF_6$	(4*R*)-Bn **50**	1 : –[h] : 0.00	2	87	60 (2*S*, 3*S*)
6	**35**	**42**	Ph	$Cu(OTf)_2$	(4*R*)-Bn **50**	1 : –[h] : 0.00	2	59	68 (2*S*, 3*S*)
7	**35**	**42**	Ph	$Cu(MeCN)_4PF_6$	(3*S*,8*R*)-Ind **53**	1 : –[h] : 0.00	3	75	78 (2*R*, 3*R*)
8	**35**	**42**	Ph	$Cu(OTf)_2$	(3*S*,8*R*)-Ind **53**	1 : –[h] : 0.00	2	65	88 (2*R*, 3*R*)
9	**36**	**43**	Bn	$Cu(MeCN)_4PF_6$	(4*R*)-Ph **49**	1 : 0.02 : 0.00	2	45[g]	32 (2*S*, 3*S*)

[a] Reactions conducted using the general procedure for copper-catalysed C–H insertion reactions (see **Section 4.2.9** for details).

[b] Ratio of C–H insertion : diazo reduction (Red) : O–H insertion based on integration of the C(2)H doublet of the cyclopentanone product, the $C(1)H_2$ singlet of the β-keto sulfone and the δ_H 5.14–5.17 singlet of the O–H insertion product, respectively, in the ^1H NMR spectra of the crude reaction mixtures.

[c] Yield of *trans*-cyclopentanone after column chromatography.

[d] Enantiopurity of *trans*-cyclopentanone determined by chiral stationary phase HPLC (see appendix I for details).

[e] Stereochemical assignments were made by comparison with previously reported rotation and HPLC data (see Appendix I for details).[103]

[f] Unknown singlet observed at δ_H 9.22 in the ^1H NMR spectrum of the crude reaction mixture.

[g] Isolated product contains minor amount of β-keto sulfone (R = Et: **24**, R = Bn: **28**).

[h] Ratio of β-keto sulfone **27** not determined due to overlap with the C(3)H signal of cyclopentanone **42**, but **27** is presumed to be present in low levels.

Comparison of yield, chemoselectivty and enantioselectivity for $Cu(MeCN)_4PF_6$-catalysed C–H insertions with and without NaBARF

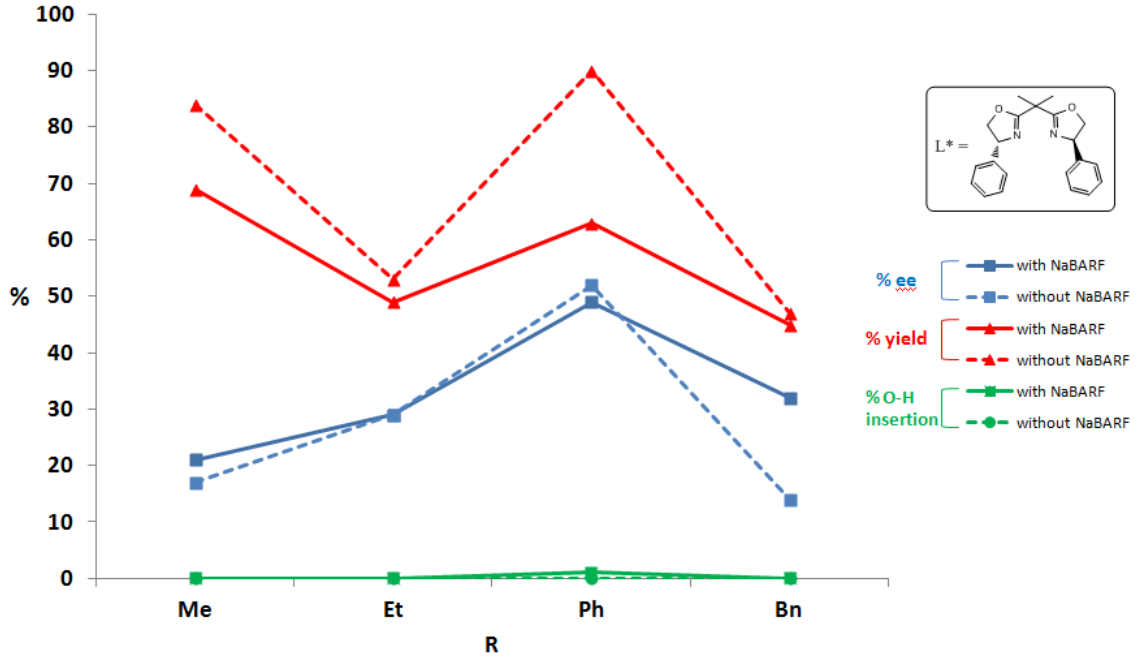
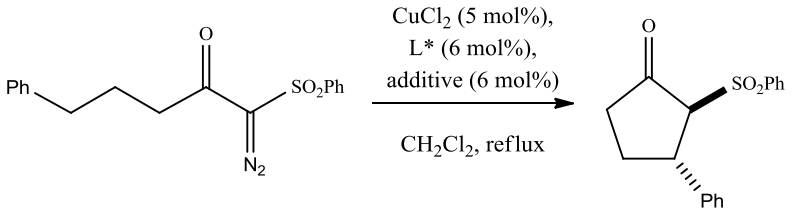


Figure 2.22

2.6.2.2 C–H insertions in the presence of a range of additive species

As previously stated, the mechanistic role that NaBARF plays in enhancing asymmetric induction in carbenoid insertion reactions has not been discussed in the literature. With this in mind, copper-catalysed C–H insertions in the presence of a range of additives were next examined in an effort to determine their role in such processes. For this purpose, the effects of nine different additives [NaBARF, $NaPF_6$, $NaB(C_6H_5)_4$, $NaBF_4$, KBARF, KPF_6, $LiPF_6$, AgBARF and $AgPF_6$] were investigated (**Table 2.18** and **Figure 2.23**). These additives were selected to enable investigation of the influence of both the nature of the metal cation and counteranion.

Table 2.18 *Copper-bis(oxazoline)-catalysed C–H insertions with various additives*[a]



35 **42**

Entry	Additive	Time (h)			Yield (%)[b]			ee (%)[c,d]		
	L*	**53**	**50**	**49**	**53**	**50**	**49**	(3*S*,8*R*)-**53**	(4*R*)-**50**	(4*R*)-**49**
1	–	21	21	30	62	57	48	14 (2*R*, 3*R*)	9 (2*S*, 3*S*)	10 (2*S*, 3*S*)
2	NaBARF	2	2	2	87	65	69	89 (2*R*, 3*R*)	79 (2*S*, 3*S*)	57 (2*S*, 3*S*)
3	$NaPF_6$	4	8	5	66	75	43	83 (2*R*, 3*R*)	76 (2*S*, 3*S*)	55 (2*S*, 3*S*)
4	$NaB(C_6H_5)_4$	5	36	20	77	77	71	25 (2*R*, 3*R*)	46 (2*S*, 3*S*)	15 (2*S*, 3*S*)
5	$NaBF_4$	20	35	20	63	56	53	11 (2*R*, 3*R*)	22 (2*S*, 3*S*)	7 (2*S*, 3*S*)
6	KBARF	2	2	2	59	67	80	91 (2*R*, 3*R*)	78 (2*S*, 3*S*)	49 (2*S*, 3*S*)
7	KPF_6	20	25	29	43	36	42	35 (2*R*, 3*R*)	56 (2*S*, 3*S*)	37 (2*S*, 3*S*)
8	$LiPF_6$	5	5	5	78	83	59	71 (2*R*, 3*R*)	78 (2*S*, 3*S*)	51 (2*S*, 3*S*)
9	AgBARF	2	2	2	89	80	71	52 (2*R*, 3*R*)	76 (2*S*, 3*S*)	45 (2*S*, 3*S*)
10	$AgPF_6$	2	20	2	81	78	80	77 (2*R*, 3*R*)	59 (2*S*, 3*S*)	53 (2*S*, 3*S*)

[a] Reactions conducted using the general procedure for copper-catalysed C–H insertion reactions (see **Section 4.2.9** for details).
[b] Yield of *trans*-cyclopentanone **42** after column chromatography.
[c] Enantiopurity determined by chiral stationary phase HPLC (see Appendix I for details).
[d] Stereochemical assignments for **42** were made by comparison with previously reported rotation and HPLC data (see Appendix I for details).[103]

A variety of sodium salts, (displaying varying solubilities in dichloromethane), was initially explored to determine their effects on enantioselectivity in the cyclisations of α-diazosulfone **35**. Enantioselectivities obtained in the presence of sodium hexafluorophosphate were found to largely parallel those achieved with NaBARF, although increased reaction times were recorded (**Table 2.18**, entry 3). Reactions with the remaining sodium salts, sodium tetraphenylborate and sodium tetrafluoroborate, displayed significantly decreased enantiocontrol, and considerably longer reaction times were required (**Table 2.18**, entries 4 and 5). From the results obtained for the C–H insertion reactions of α-diazosulfone **35** the following order of effect on enantioselectivity may be defined: $NaBF_4 < NaB(C_6H_5)_4 << NaPF_6 <$ NaBARF (**Figure 2.23**). This pattern is in line with results reported by Pfaltz and co-workers for studies of anion effects in asymmetric hydrogenation reactions employing iridium-phosphinooxazoline catalysts, in

which increased reaction rates and catalyst stability were observed in the presence of $BARF^-$ compared to other anionic species such as PF_6^- and BF_4^-.[124,125] Indeed a similar effect was also observed by Zhou and co-workers for asymmetric hydrovinylation reactions employing catalytic palladium complexes of chiral phosphoramidite and phosphate ligands.[126] In this previous work, improving reactivity and enantioselectivity were recorded for various counteranions in the order: $OTf^- < BF_4^- < PF_6^- < SbF_6^- < BARF^-$.

*Comparison of enantioselectivities for reaction of **35** in the presence of various additive species*

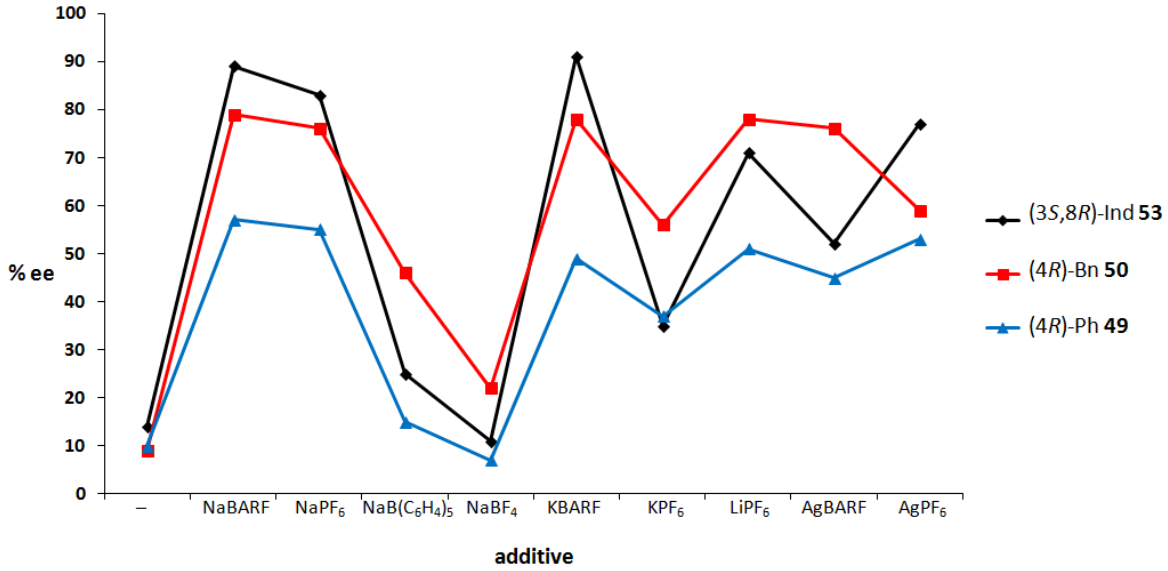


Figure 2.23

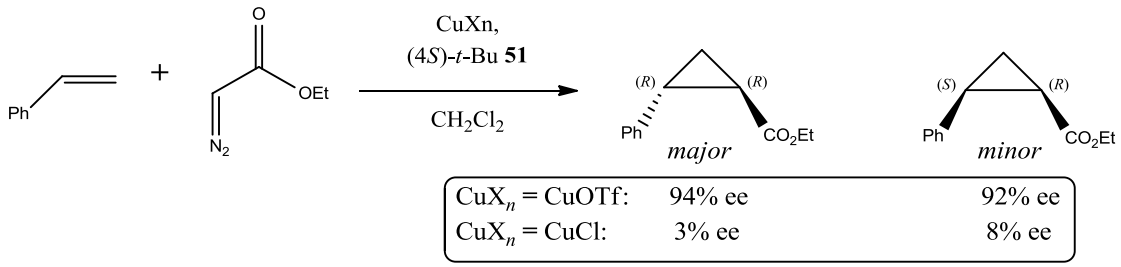
Reactions employing KBARF as an additive (**Table 2.18**, entry 6), were found to result in similar levels of enantioselectivity in comparison to C–H insertions in the presence of NaBARF (**Table 2.18**, entry 2), with reaction times and yields also seen to be generally in agreement. A slight increase in the level of enantioinduction achieved (91% ee) was recorded for the reaction in the presence of KBARF and the indane-derived ligand (3*S*,8*R*)-**53**. Notably, this result represents the highest level of asymmetric induction recorded to date for cyclopentanone synthesis *via* C–H insertion, proving superior to the previous record for rhodium-catalysed enantioselective cyclisations employing α-diazo-β-keto esters in which up to 80% ee was achieved.[5,92]

In contrast to reactions employing NaBARF and $NaPF_6$ as additives in which similar levels of enantioselectivity were recorded, a significant falloff in enantioselectivity was recorded for cyclisations in the presence of KPF_6 relative to the corresponding KBARF reactions (**Table 2.18**, entries 7 *vs.* 6). This decrease in asymmetric induction, as well as the considerable increase in reaction times, is believed to be a related to poor solubility of KPF_6 in the reaction solvent which may limit its effect in the C–H insertion process (accurate solubility data for the additive species in dichloromethane was not available in

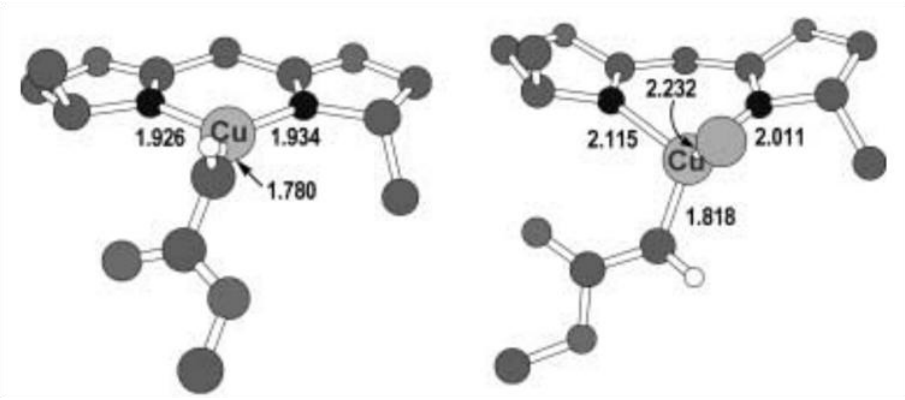
the literature, but it was clear when conducting these experiments that KPF_6 was noticeably less soluble). Despite a slight increase in reaction times, high levels of asymmetric induction were again observed for C–H insertions in the presence of $LiPF_6$ (**Table 2.18**, entry 8). Enantioselectivities obtained for these cyclisations were largely in line with those previously observed for reactions employing NaBARF, however, a decrease in enantioselectivity was recorded for insertion with ligand (3*S*,8*R*)-Ind **53** (**Table 2.18**, entries 2 *vs.* 8).

Use of the silver(I) salts AgBARF and $AgPF_6$ was also found to provide enhanced enantiocontrol relative to reactions with $CuCl_2$ and bis(oxazoline) ligand in the absence of an additive (**Table 2.18**, entries 9 and 10 *vs.* entry 1). Results obtained for these experiments did not follow the trends previously observed with the alkali metal salts as additives *e.g.* higher enantioselectivity observed with $AgPF_6$ (77% ee and 53% ee) versus AgBARF (52% ee and 45% ee) for insertions with the benzyl-substituted ligand (4*R*)-**50** and the phenyl-substituted ligand (4*R*)-**49**, respectively. These deviations may be due in part to the light sensitive nature of the silver(I) salts.

In studies by Fraile and co-workers examining the role of the counterion in copper-bis(oxazoline)-catalysed enantioselective cyclopropanation reactions, the presence of the chloride counteranion was shown to dramatically decrease enantioselectivity compared to reactions with the more weakly-coordinating triflate anion (**Scheme 2.22**).[132] Theoretical calculations subsequently conducted by Fraile revealed that the presence of the strongly-coordinating chloride ion results in significant geometric changes in the catalyst structure (**Figure 2.24**), with the result that the diastereomeric transition structures for the carbenoid insertion do not possess any clear steric interaction that allows for discrimination between the two prochiral faces of the carbene-carbon.[133]



Scheme 2.22



without Cl^- *with Cl^-*

Figure 2.24 *ref.*[134]

It has been suggested in earlier reports for other transformations that the primary function of NaBARF is the abstraction of chloride from the catalytic structure.[135-137] It was therefore envisaged that complete or partial abstraction of chloride by the 'naked' sodium ion of NaBARF occurs in the C–H insertion reactions of **35**, thereby altering the geometry of the catalytic complex resulting in higher levels of enantiocontrol. The observation of small amounts of an insoluble white solid in the reaction flask following reaction completion, found to be NaCl by PXRD analysis, supports this theory (**Figure 2.25**).

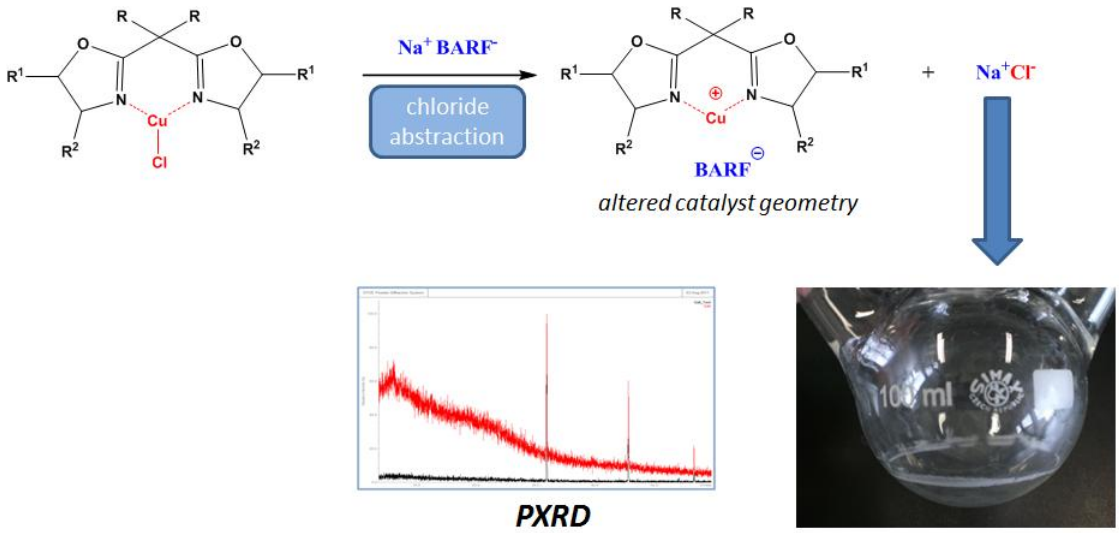


Figure 2.25

The results obtained in **Table 2.18** indicate that the nature of the counterion in the metal (Na, K, Li, Ag) additives only plays a role in terms of enantioselectivity in so far as it enables solubility of the group I cations. Thus, the key role of the additives is in generating a poorly-solvated 'naked' alkali metal cation in the dichloromethane solution.

Taking the above findings into account, replacement of $CuCl_2$ with a copper source possessing a more weakly-coordinating anion should lead to increased levels of enantioselectivity for our C–H insertion reactions. Such an effect has been previously observed by Zhou and co-workers for copper-catalysed carbenoid insertions into Si–H bonds in which enantioselectivites in excess of 90% ee were recorded for reactions in the presence of $Cu(MeCN)_4PF_6$ and $Cu(OTf)_2$ without addition of NaBARF.[138] In this project, insertion reactions of diazosulfone **35** with the weakly coordinating $Cu(MeCN)_4PF_6$ and $Cu(OTf)_2$ salts (**Table 2.12**, entries 2, 5, 7, 11, 12, 15, 16, 19, 20 and 22) were previously found to result in significantly higher levels of enantiocontrol compared to CuCl and $CuCl_2$-catalysed reactions (**Table 2.18**, entry 1 and **Table 2.12**, entries 1, 3, 4, 6, 8–10, 13, 14, 17, 18, 21), although failing to reach the levels recorded for cyclisations in the presence of NaBARF (**Table 2.18**, entry 2 and **Table 2.14**). This outcome is consistent with $BARF^-$ being much less coordinating than both PF_6^- and OTf^-.[123]

We have previously observed (**Figure 2.19**) that the presence of NaBARF in the catalytic mixture results in a significant decrease in chemoselectivity towards O–H insertion for CuCl-catalysed reactions. In this context, interesting trends in terms of chemoselectivity for C–H insertion versus O–H insertion into adventitious water were seen in the cyclisations of α-diazo-β-keto sulfone **35** described in **Table 2.18**. Depending on the nature of the additive species, varying amounts of O–H insertion products were observed in the $CuCl_2$-catalysed reactions (**Figure 2.26**). Significantly, with only one exception noted [KPF_6 and (4*R*)-Bn **50**], all additives tested were found to lead to reduced levels of O–H insertion compared to reactions in which no additive was present. Therefore, potentially the 'naked' metal ions are also behaving as water scavengers, complexing any adventitious water in the medium and thereby decreasing O–H insertion. In general the BARF salts (Na^+, K^+ and Ag^+) were observed to provide the highest levels of chemoselectivity compared to the other additive species examined, however, this trend was not absolute *e.g.* decreased O–H insertion was observed for reaction with $AgPF_6$ and (3*S*,8*R*)-Ind **53** versus corresponding reactions in the presence of NaBARF, KBARF and AgBARF.

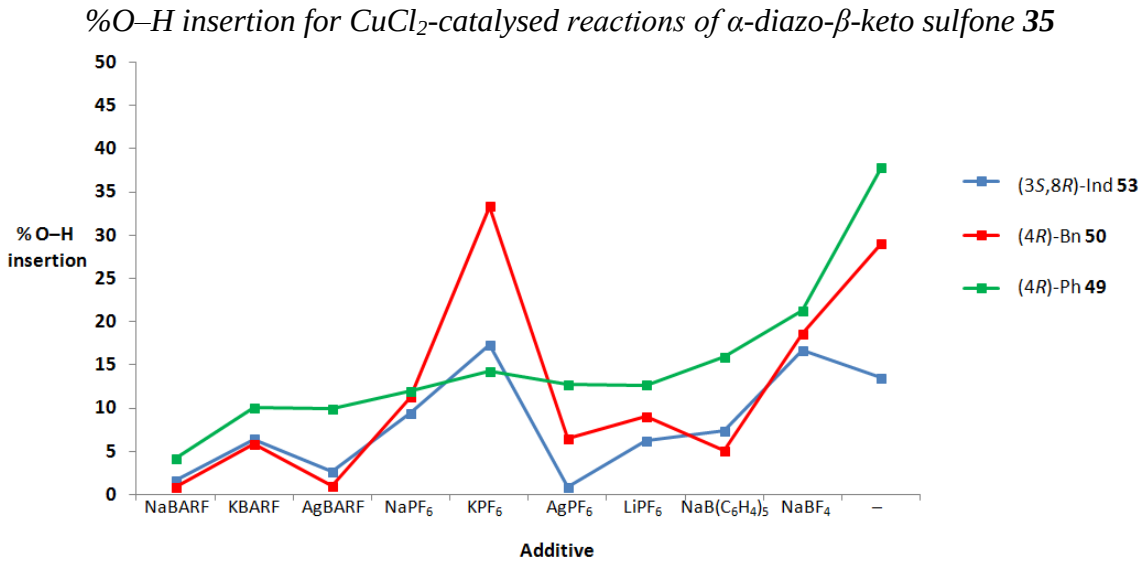
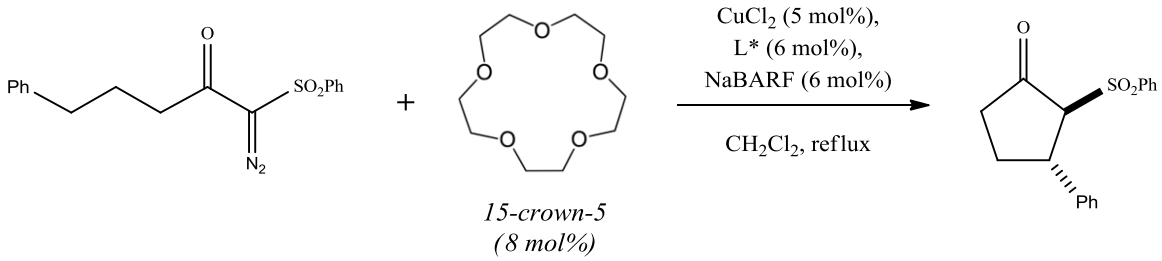


Figure 2.26

In order to confirm the key role that the metal ion (Na^+, K^+, Li^+, Ag^+) plays in enhancing the efficiency and enantioselectivity of the C–H insertion reactions of α-diazosulfone **35**, a number of experiments were conducted with NaBARF in the presence of 15-crown-5 (**Table 2.19**). 8 mol% Crown ether was employed in these reactions providing a slight excess relative to NaBARF (6 mol%). Crown ethers are widely recognized as strong binding agents for metal ions, with 15-crown-5 known to have a particular high affinity for sodium cations.[139] Addition of 15-crown-5 to our catalytic system comprising $CuCl_2$, bis(oxazoline) ligand and NaBARF was found to have a significant detrimental effect on both the time required to achieve reaction completion and the level of enantioselectivity obtained (**Table 2.19**, entries 1–3). Through crown ether-mediated complexation of the sodium cation, chloride abstraction is prevented with the result that the copper-bis(oxazoline) complex can no longer adopt a geometry leading to efficient asymmetric induction. Thus, the presence of the crown ether negates the enhancement of enantioselectivity previously observed for insertions employing NaBARF, thereby confirming the key role of the sodium cation in this effect.

Table 2.19 *C–H insertions in the presence of 15-crown-5*[a]



35 **42**

Entry	L*	Time (h)	Yield (%)[b]	ee (%)[c,d]	Time (h)	Yield (%)[b]	ee (%)[c,d]
		Reactions with 15-crown-5			**Reactions without 15-crown-5**		
1	(3*S*, 8*R*)-Ind **53**	20	63	25 (2*R*, 3*R*)	2	87	89 (2*R*, 3*R*)
2	(4*R*)-Bn **50**	48	50	28 (2*S*, 3*S*)	2	58	81 (2*S*, 3*S*)
3	(4*R*)-Ph **49**	20	62	20 (2*S*, 3*S*)	2	69	57 (2*S*, 3*S*)

[a] Reactions conducted using the general procedure for copper-catalysed C–H insertion reactions (see **Section 4.2.9** for details).
[b] Yield of *trans*-cyclopentanone **42** after column chromatography.
[c] Enantioputiry determined by chiral stationary phase HPLC (see Appendix I for details).
[d] Stereochemical assignments were made by comparison with previously reported rotation and HPLC data (see Appendix I for details).[103]

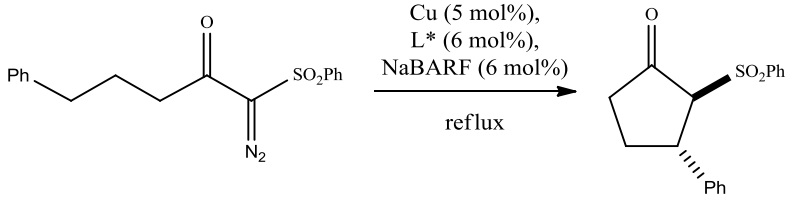
2.6.3 Investigation of reaction conditions

2.6.3.1 Investigation of solvent effects

Asymmetric transformations are often governed by many subtle factors including choice of reaction solvent and reaction temperature. To this end, we next wished to investigate the effect of variation of solvent on the copper-bis(oxazoline)-catalysed C–H insertion reactions of α-diazo-β-keto sulfones (**Table 2.20**). Three solvents were chosen for this purpose; dichloromethane (DCM), toluene and dichloroethane (DCE). All three solvent systems are commonly employed in both rhodium- and copper-catalysed C–H insertions in the literature.[57,59] CuCl-catalysed reaction of α-diazo-β-keto sulfone **35** in refluxing dichloromethane in the presence of bis(oxazoline) (4*R*,5*S*)-diPh **52** and NaBARF was found to provide cyclopentanone **42** in high yield (82%) and moderate enantioselectivity (58% ee), albeit with a long reaction time (22 h) (**Table 2.20**, entry 1). Change of solvent to the higher boiling toluene resulted in a significantly decreased reaction time (4 h), however, a reduction enantiocontrol (32% ee) was also observed (**Table 2.20**, entry 2 *vs.* 1). Short reaction time (2 h) and moderate asymmetric induction (51% ee) were recorded for employment of dichloroethane as solvent in the CuCl-catalysed cyclisation of **35** (**Table 2.20**, entry 3 vs. 1).

Increase of reaction temperature has previously been shown to be associated with a corresponding decrease in enantiocontrol in several literature examples of rhodium- and copper-catalysed insertion reactions.[6,140-143] Indeed, it is generally accepted that enantioselectivity in chiral processes increases with decreasing temperature.[144,145] Thus, the decrease in enantioselectivity observed for employment of toluene as reaction solvent (**Table 2.20**, entry 2 *vs.* 1) was not unexpected. Surprisingly, however, increase of temperature for reaction in dichloroethane was found to lead to only a modest decrease in enantiocontrol (**Table 2.20**, entry 3 vs. 1). As was previously observed (**Table 2.14**), CuCl- and $CuCl_2$-catalysed insertions provided very similar outcomes in terms of enantioselectivty (**Table 2.20**, entry 1 *vs.* 4 and entry 3 *vs.* 5).

Table 2.20 *Investigation of solvent effects for C–H insertions of α-diazo-β-keto sulfone* ***35***[a]



35 **42**

Entry	Cu	L*	Solvent	b.p (°C)	**42** : **54** : **46**[b]	Time (h)	Yield **42** (%)[c]	ee **42** (%)[d,e]
1	CuCl	(4*R*,5*S*)-diPh **52**	DCM	40	1 : 0.03 : 0.00	22	82	58 (2*S*, 3*S*)
2	CuCl	(4*R*,5*S*)-diPh **52**	toluene	111	1 : 0.00 : 0.00[f]	4	66	32 (2*S*, 3*S*)
3	CuCl	(4*R*,5*S*)-diPh **52**	DCE	84	1 : 0.17 : 0.01[f]	2	70[g]	51 (2*S*, 3*S*)
4	$CuCl_2$	(4*R*,5*S*)-diPh **52**	DCM	40	1 : 0.04 : 0.05	2	54	52 (2*S*, 3*S*)
5	$CuCl_2$	(4*R*,5*S*)-diPh **52**	DCE	84	1 : 0.06 : 0.04[f]	2	47	51 (2*S*, 3*S*)

[a] Reactions conducted using the general procedure for copper-catalysed C–H insertion reactions (see **Section 4.2.9** for details).

[b] Ratio of C–H insertion : alkene formation : O–H insertion based on integration of the C(2)H doublet of cyclopentanone **42** product, the δ_H 5.62 singlet of **54** and the δ_H 5.14 singlet of the O–H insertion product **46**, respectively, in the ^{1}H NMR spectra of the crude reaction mixtures.

[c] Yield of *trans*-**42** after column chromatography.

[d] Enantiopurity determined by chiral stationary phase HPLC (see appendix I for details).

[e] Stereochemical assignments were made by comparison with previously reported rotation and HPLC data (see Appendix I for details).[103]

[f] Unknown peaks (minor) observed in the ^{1}H NMR spectrum of the crude reaction mixture.

[g] Isolated product not fully clean.

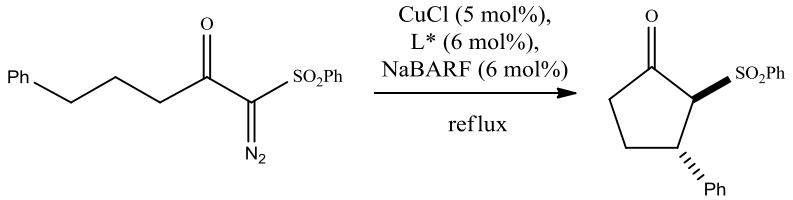
Yields obtained for the copper-catalysed reactions in the solvent study were moderate to good, ranging from 47% for the $CuCl_2$-catalysed reaction in dichloroethane (**Table 2.20**, entry 5) to 82% for the CuCl-catalysed cyclisation of **35** in dichloromethane (**Table 2.20**, entry 1). Significantly, cleaner ^{1}H NMR spectra were recorded for the crude reaction mixtures arising from cyclisations in dichloromethane, with minor amounts of unknown byproducts observed for reactions in toluene and dichloroethane, presumably due to

higher reaction temperatures. For this reason, the use of dichloromethane as reaction solvent was continued for all subsequent insertion reactions in this project.

2.6.3.2 Investigation of catalyst complexation time

The copper-bis(oxazoline)-catalysed C–H insertion reactions described thus far have involved pre-generation of the catalytic species for 1.5 h prior to dropwise addition of the α-diazo-β-keto sulfone substrate, in-line with literature procedures.[101,102] In order to investigate the significance of this catalyst pre-generation period a number of experiments were conducted examining variations in complexation time and diazo addition (**Table 2.21**).

Table 2.21 *Investigation of catalyst complexation time for C–H insertions of α-diazo-β-keto sulfone **35**[a]*



35 **42**

Entry	L*	Solvent	Complexation time (h)[b]	**42** : **54** : **46**[c]	Time (h)	Yield **42** (%)[d]	ee **42** (%)[e,f]
1	(4*R*,5*S*)-diPh **52**	DCM	1.5	1 : 0.03 : 0.00	22	82	58 (2*S*, 3*S*)
2	(4*R*,5*S*)-diPh **52**	toluene	1.5	1 : 0.00 : 0.00[g]	4	66	32 (2*S*, 3*S*)
3	(4*R*,5*S*)-diPh **52**	DCM	0[h]	1 : 0.12 : 0.04	21	64	33 (2*S*, 3*S*)
4	(4*R*,5*S*)-diPh **52**	toluene	0[h]	1 : 0.00 : 0.00[g]	6	46	20 (2*S*, 3*S*)
5	(4*R*,5*S*)-diPh **52**	DCM	0	1 : 0.25 : 0.01	16	62	55 (2*S*, 3*S*)
6	(4*R*,5*S*)-diPh **52**	DCM	24	1 : 0.07 : 0.05	2	71	50 (2*S*, 3*S*)

[a] Reactions conducted using the general procedure for copper-catalysed C–H insertion reactions (see **Section 4.2.9** for details).

[b] Catalyst complexation time prior to dropwise addition of α-diazo-β-keto sulfone **35**.

[c] Ratio of C–H insertion : alkene formation : O–H insertion based on integration of the C(2)H doublet of cyclopentanone **42** product, the δ_H 5.62 singlet of **54** and the δ_H 5.14 singlet of the O–H insertion product **46**, respectively, in the ^{1}H NMR spectra of the crude reaction mixtures.

[d] Yield of *trans*-**42** after column chromatography.

[e] Enantiopurity determined by chiral stationary phase HPLC (see appendix I for details).

[f] Stereochemical assignments were made by comparison with previously reported rotation and HPLC data (see Appendix I for details).[103]

[g] Unknown peaks (minor) observed in the ^{1}H NMR spectrum of the crude reaction mixture.

[h] All-in-one addition of α-diazo-β-keto sulfone **35** and catalyst prior to reflux.

An all-in-one addition strategy was first examined involving simultaneous addition of the catalytic components (CuCl, ligand **52** and NaBARF) and α-diazo-β-keto sulfone **35** to

the reaction flask followed by heating (**Table 2.21**, entries 3 and 4). Reaction times and yields were largely unaffected by this variation from standard procedures, however, a decrease in enantioselectivity was recorded for both the dichloromethane and toluene reactions (**Table 2.21**, entry 3 *vs.*1 and entry 4 *vs.* 2). In contrast, when CuCl, (4*R*,5*S*)-diPh **52** and NaBARF were mixed and brought directly to reflux, followed by immediate dropwise addition of diazo sulfone **35** (**Table 2.21**, entry 5) similar results were recorded in terms of reaction time and enantioselectivity compared to cyclisation with the standard 1.5 h catalyst pre-generation period, however, increased formation of alkene **54** was observed (**Table 2.21**, entry 5 *vs.* 1). Extension of the pre-complexation time to 24 h resulted in a slight decrease in asymmetric induction, however, a much faster cyclisation was observed (**Table 2.21**, entry 6 *vs.* 1). Thus, as the modified procedures examined offered no apparent advantage over the standard protocol adopted to date, 1.5 h was deemed to be the optimal complexation time for C–H insertions of α-diazo-β-keto sulfones and use of this procedure was continued for subsequent experiments.

Rationalising the results from **Table 2.21** provides an insight into the formation of the enantioselective catalyst species in our C–H insertion reactions. Comparison of entries 5 and 1 highlights that the enantioselective catalyst complex is formed very quickly when the copper, ligand and additive are heated to reflux, with essentially the same asymmetric induction observed with or without a 1.5 h pre-complexation time. In contrast, as shown in **Table 2.21**, entry 3, when all species are added together prior to heating to reflux, reduced enantioselectivity is recorded showing that the most enantioselective catalyst species is not formed on mixing at room temperature. Interestingly, comparison of entries 1 versus 5, while showing similar enantioselectivity, display a noticeable difference in chemoselectivity with substantially more of the tetrahydrofuran byproduct **54** formed in the experiment without the pre-complexation reflux. This may indicate that a different copper species present initially preferentially forms **54** through hydride abstraction, however, this observation warrants exploration with a wider range of ligands and substrates.

Interestingly, in a related project (**Table 2.1**),[11] increased byproduct formation and lower isolated thiopyran product yields were recorded for reactions in which catalyst pre-generation was conducted versus reactions employing the all-in-one addition method. Choice of catalyst preparation procedure did not appear to impact on enantioselectivity for this related C–H insertion process.

2.7 Examination of α-diazo-β-keto sulfone substrate modification

The enantioselective C–H insertion reactions described thus far have employed α-diazo-β-keto phenylsulfones as substrates. Highest asymmetric induction (91% ee) has been achieved for insertions into the benzylic C–H bond of diazo sulfone **35**, suggesting the presence of the phenyl group plays a key role in permitting highly stereoselective cyclopentanone synthesis. In order to gain a better understanding of the relationship

between substrate structure and enantioselectivity, we next wished to evaluate the significance of the phenyl rings present at both the sulfone substituent and adjacent to the C–H insertion site on the stereochemical outcome of our C–H insertion reactions. For this purpose, modification of the phenylsulfone moiety and alteration of the electronic properties of the aromatic ring adjacent to the methylene group undergoing insertion were examined (**Figure 2.27**).

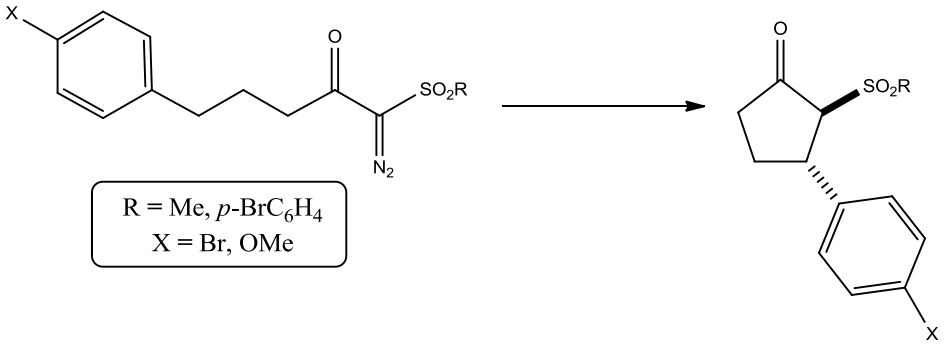
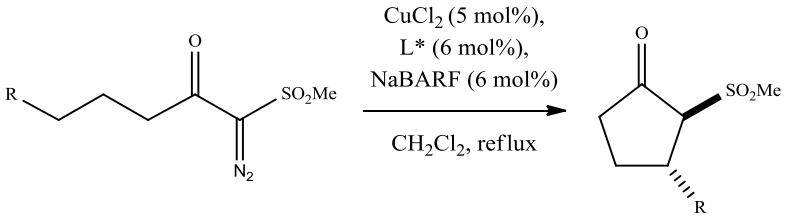


Figure 2.27

2.7.1 Investigation of modifications to the sulfone substituent

Examination of C–H insertions employing α-diazo-β-keto methylsulfone substrates was first conducted. The modified diazo compounds **37** (R = Me) and **38** (R = Ph) were prepared as previously described (**Section 2.2** and **Section 2.3**) and cyclised to provide access to the 2-methylsulfonyl cyclopentanones **44** and **45**, respectively. Enantioselective $CuCl_2$-bis(oxazoline)-catalysed reactions of **37** and **38** in the presence of NaBARF are displayed in **Table 2.22**.

Table 2.22 *Copper-bis(oxazoline)-catalysed C–H insertions of α-diazo-β-keto methylsulfones*[a]



Entry	Diazo	Product	R	L*	Time (h)	C–H : UBP : Red : O–H[b]	Yield (%)[c]	ee (%)[d,e]
1	**37**	**44**	Me	(4*R*)-Ph **49**	5	1 : 0.21 : 0.01 : 0.02	88[f]	16 (2*S*, 3*R*)
2	**37**	**44**	Me	(4*R*)-Bn **50**	5	1 : 0.90 : 0.06 : 0.05	83[f]	46 (2*S*, 3*R*)
3	**37**	**44**	Me	(4*S*)-*t*-Bu **51**	5	1 : 0.01 : 0.00 : 0.03	95[f]	28 (2*S*, 3*R*)
4	**37**	**44**	Me	(4*R*,5*S*)-Ph **52**	5	1 : 0.16 : 0.06 : 0.06	77	16 (2*S*, 3*R*)
5	**37**	**44**	Me	(3*S*,8*R*)-Ind **53**	5	1 : 0.80 : 0.04 : 0.06	87[f]	49 (2*R*, 3*S*)
6	**38**	**45**	Ph	(4*R*)-Ph **49**	2	1 : 0.90 : –[i] : 0.04[h]	82[g]	9 (2*R*, 3*R*)
7	**38**	**45**	Ph	(4*R*)-Bn **50**	2	1 : 0.12 : –[i] : 0.02[h]	90	70 (2*S*, 3*S*)
8	**38**	**45**	Ph	(4*S*)-*t*-Bu **51**	2	1 : 0.20 : –[i] : 0.03[h]	71	33 (2*R*, 3*R*)
9	**38**	**45**	Ph	(4*R*,5*S*)-Ph **52**	2	1 : 2.39 : –[i] : 0.02[h]	60[j]	~0
10	**38**	**45**	Ph	(3*S*,8*R*)-Ind **53**	2	1 : 0.12 : –[i] : 0.02[h]	89	62 (2*R*, 3*R*)

[a] Reactions conducted using the general procedure for copper-catalysed C–H insertions (see **Section 4.2.9** for details).
[b] Ratio of C–H insertion : unknown byproduct (UBP) formation : diazo reduction (Red) : O–H insertion based on integration of the C(2)*H* doublet of the cyclopentanone product, the δ_H 3.32 singlet of the UBP, the δ_H 4.02 singlet of β-keto sulfone **29** and the δ_H 5.06–5.12 singlet of the O–H insertion product (R = Me: **55**, R = Ph: **56**), respectively, in the ^{1}H NMR spectra of the crude reaction mixture.
[c] Yield of *trans*-cyclopentanone after column chromatography.
[d] Enantiopurity of *trans*-cyclopentanone determined by chiral stationary phase HPLC (see appendix I for details).
[e] Stereochemical assignments for **44** were made by comparison to previously reported rotation and chiral HPLC data.[20] Absolute stereochemistry of **45** determined by single crystal analysis (see appendix I for details).
[f] Isolated product contains minor amount of unknown byproduct(s).
[g] Unknown byproduct also isolated in ~10% yield.
[h] Unknown peaks observed in the ^{1}H NMR spectrum of the crude reaction mixture.
[i] Ratio not determined due to overlap of the δ_H 4.02 singlet of β-keto sulfone **30** with the C(2)*H* doublet of **45**, but **30** is presumed to be present in low levels.
[j] Isolated product not fully clean.

Replacement of the phenylsulfonyl moiety adjacent to the diazo group with a methylsulfonyl group was found to have a dramatic effect on enantioselectivity in the C–H insertions under investigation (**Figure 2.28**). In general, considerably reduced asymmetric induction was recorded for reactions of the α-diazo methylsulfones **37** and **38** compared to reactions with the corresponding α-diazo phenylsulfones **1** and **35**, although two exceptions to this trend were observed for insertion of **37** (**Table 2.22**, entries 3 and 4 *vs.* **Table 2.14**, entries 2 and 5), albeit with modest enantiopurities. As was previously noted for cyclisations with α-diazo-β-keto phenylsulfones **1** and **35**, the benzyl ligand (4*R*)-**50** and the indane-derived bis(oxazoline) (3*S*,8*R*)-**53** were found to provide the highest levels of enantiocontrol for synthesis of the cyclopentanones **44** and

45 (**Table 2.22**, entries 2, 5, 7 and 10). Interestingly, in two instances (**Table 2.22**, entries 3 and 6) the opposite enantiomer to that observed for the corresponding phenylsulfonyl derivatives (**Table 2.14**, entries 5 and 22) was found to be in excess. This indicates that the change of the sulfone substituent results in a significant alteration in transition state geometry, to the extent that enantiomeric preference is reversed for synthesis of the products **44** and **45** in the presence of the ligands (4*S*)-*t*-Bu **51** and (4*R*)-Ph **49**, respectively. This observation is significant in enhancing our understanding of the mechanistic aspects of the enantioselective C–H insertion process (see **Section 2.9** for discussion).

Comparison of enantioselectivities for copper-bis(oxazoline)-catalysed C–H insertions of α-diazo-β-keto methylsulfones versus phenylsulfones

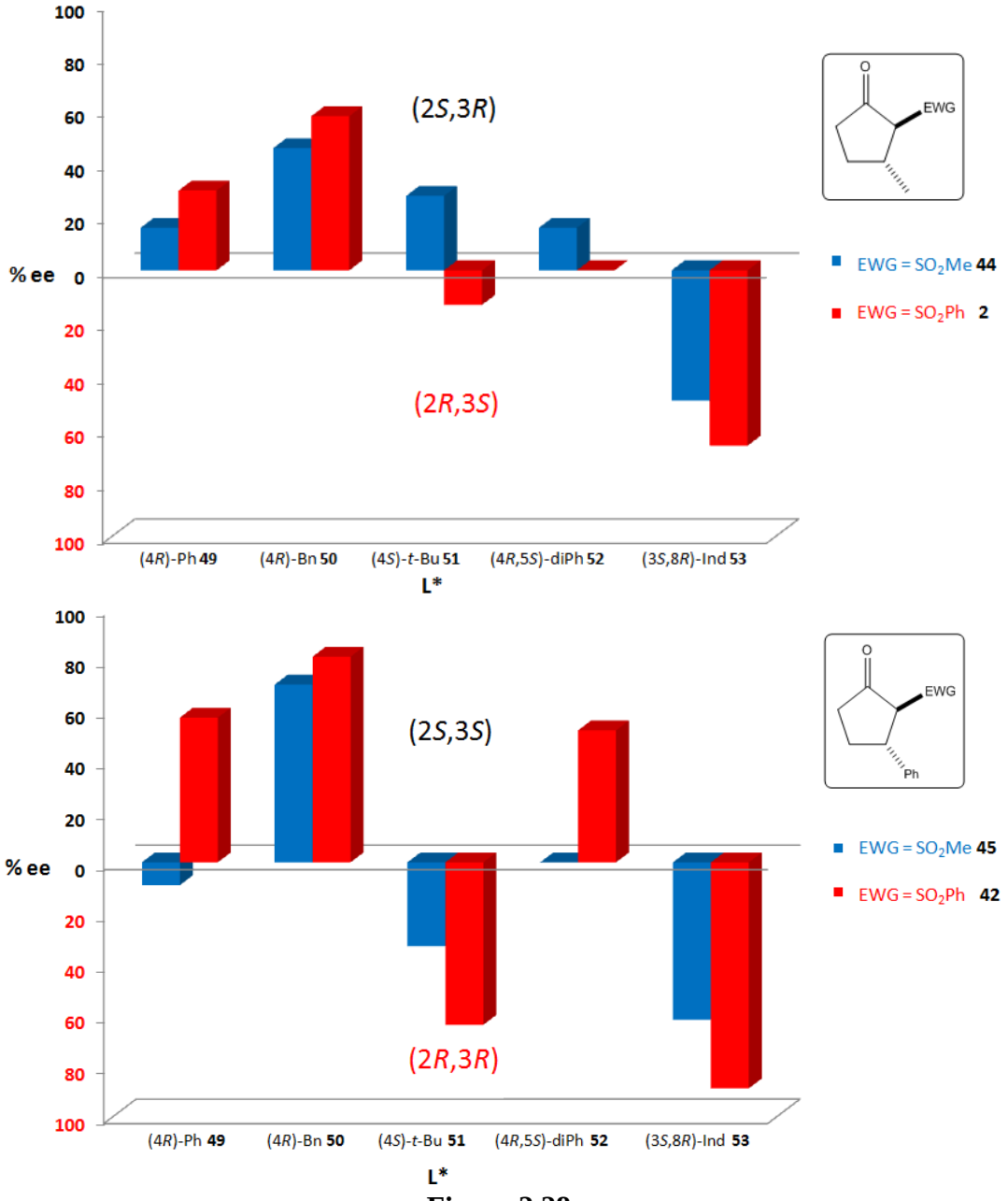
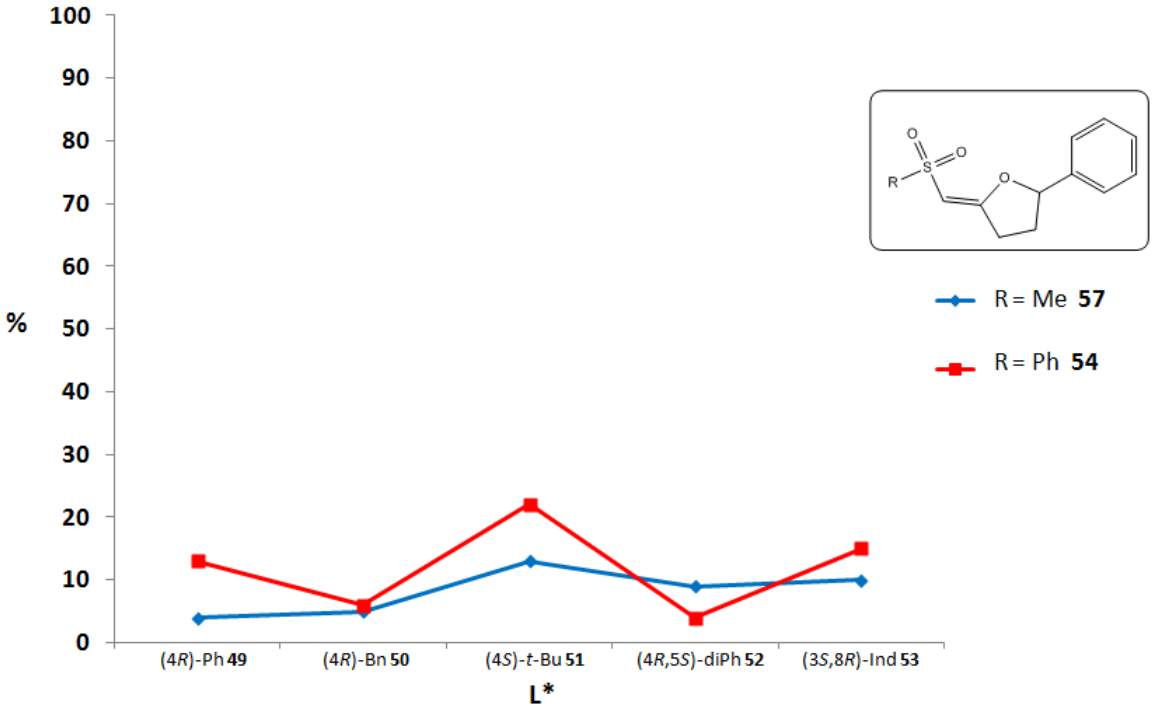


Figure 2.28

In addition to the observed effects on enantioselectivity discussed above, change from the phenylsulfonyl to methylsulfonyl group was found to result in reduced chemoselectivity towards intramolecular C–H insertion. Thus, increased levels of byproducts were observed in the ^{1}H NMR spectra of the crude reaction mixtures obtained from the experiments described in **Table 2.22**. Such byproducts included 1-hydroxy-1-(methylsulfonyl)heptan-2-one **55** and 1-hydroxy-1-(methylsulfonyl)-5-phenylpentan-2-one **56** arising from O–H insertion of **37** and **38**, respectively, 1-(methylsulfonyl) hexan-2-one **29** and 1-(methylsulfonyl)-5-phenylpentan-2-one **30** resulting from reduction of the diazo moieties of **37** and **38**, respectively, and 2-[(methylsulfonyl)methylene]-5-phenyltetrahydrofuran **57**, formed by intramolecular nucleophilic attack of the enolic oxygen at the benzylic position of the phenyl-substituted diazo **38**, as previously discussed in **Section 2.6.1**. Levels of **57** observed in the ^{1}H NMR spectra of the crude product mixtures for reactions of **38** (**Table 2.22**, entries 6–10) were largely in line with those previously observed for formation of **54** in corresponding cyclisations of α-diazo-β-keto phenylsulfone **35** (**Figure 2.29**).



**% relative to cyclopentanone formation as determined by integration of the ^{1}H NMR spectrum of the crude reaction mixtures*

Figure 2.29

The ^{1}H NMR spectrum of the crude reaction mixture from the $CuCl_2$-catalysed reaction of **37** in the presence of (3*S*,8*R*)-Ind **53** and NaBARF (**Table 2.22**, entry 5) is presented in **Figure 2.30**. The spectrum shows minor signals for the byproducts **29** and **55**, however, the presence of several other unidentified byproduct peaks are also noted. In particular, major signals (~40% relative to cyclopentanone **44**) are observed at δ_H 2.71 and 3.32 (UBP in **Table 2.22**), meaning byproduct formation is occurring to a significant level. The unknown singlet signals were also observed in the ^{1}H HMR spectrum of the product **44** isolated after column chromatography. These signals were no longer observed by ^{1}H

NMR analysis of a sample of **44** stored for approximately 1 month at low temperature, suggesting the unknown byproduct formed is an unstable compound. Observation of these unknown singlet signals were not previously recorded for cyclisations with α-diazo-β-keto phenylsulfone substrates. C–H insertion into the methylsulfonyl group is not thought to have occurred as such a byproduct would be characterised by distinctive multiplet signals in the region of δ_H 3.5–4.5, representing the methylene protons of the episulfone ring. It is possible that the unknown byproduct signals observed in **Figure 2.30** may represent a methyl sulfonyl compound analogous to the 'unknown aromatic compound' previously described for reactions of α-diazo-β-keto phenylsulfones (**Scheme 2.21**), however, no evidence to support this theory was obtained in this project.

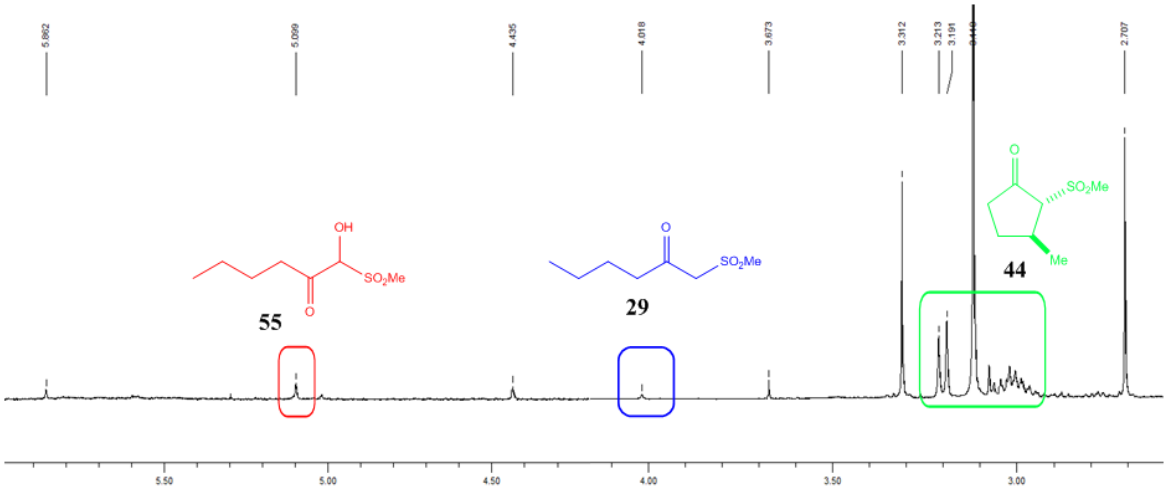
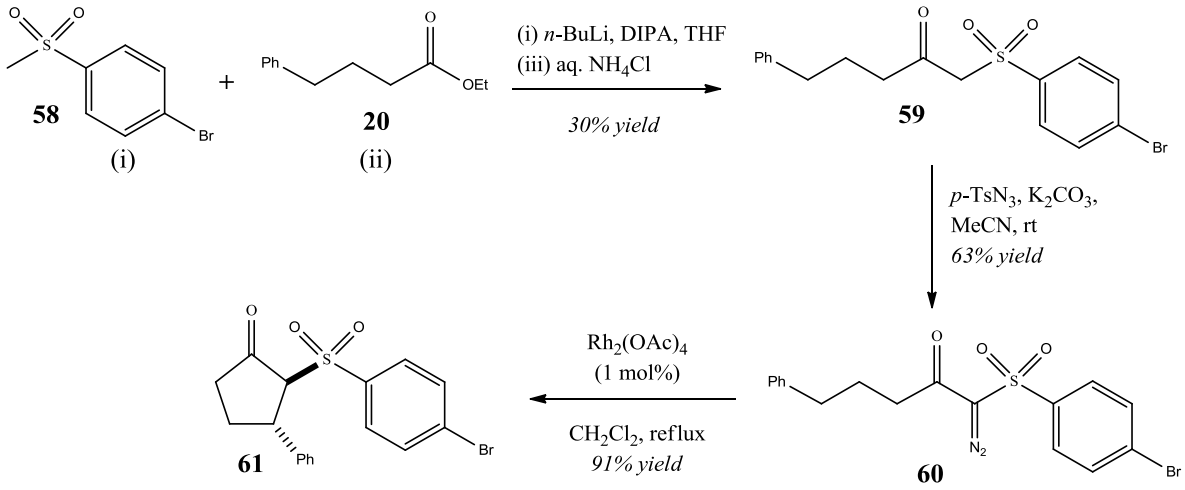


Figure 2.30 *δ_H (400 MHz, $CDCl_3$)*

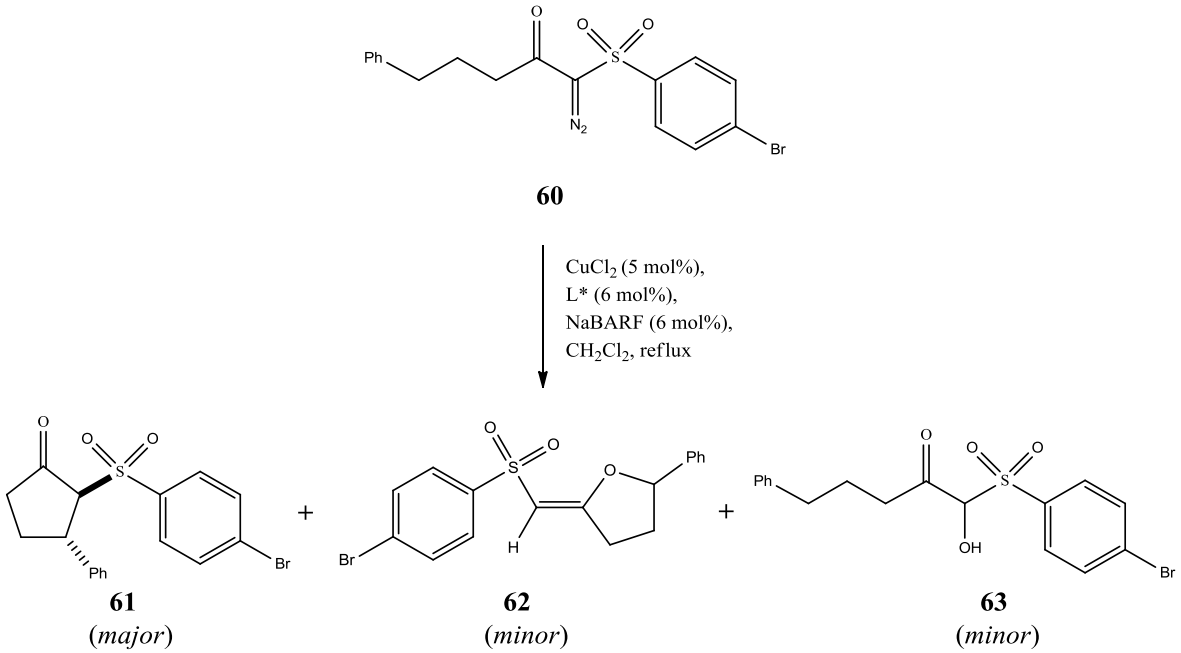
It was clear from the results discussed above that the presence of the phenyl ring at the sulfone substituent plays a key role in chemo- and enantiocontrol in the C–H insertion reactions of α-diazo-β-keto sulfones. Therefore, we next wished to assess the impact of modification of the electronic properties of this aromatic ring. For this purpose, a novel diazo compound possessing a *para*-bromophenylsulfonyl group was prepared (**Scheme 2.23**). Synthesis began from commercially available 4-bromothioanisole which was converted to the corresponding sulfone **58** by oxidation with hydrogen peroxide. Reaction of **58** with ethyl 4-phenylbutanoate **20** and lithium diisopropylamide in THF provided 1-(4-bromophenyl)sulfonyl-5-phenylpentan-2-one **59** which was converted to its diazo derivative **60** by treatment with *p*-tosyl azide **31** and potassium carbonate as previously described (**Section 2.3**). Cyclisation of 1-diazo-1-(4-bromophenyl)sulfonyl-5-phenylpentan-2-one **60** with rhodium(II) acetate produced the novel cyclopentanone 2-(4-bromophenyl)sulfonyl-3-phenylcyclopentanone **61** as a racemic mixture for use in chiral stationary phase HPLC analysis. The synthesis and behaviour of each of the compounds in **Scheme 2.23** mirrored very closely the parent series in the absence of the bromine substituent, except for the first step of the sequence in which a slightly decreased yield (30%) was recorded.



Scheme 2.23

$CuCl_2$-bis(oxazoline)-catalysed C–H insertions of α-diazo-β-keto 4-bromophenylsulfone **60** are presented in **Table 2.23**. Interestingly, the introduction of an electron-withdrawing substituent (Br) on the phenylsulfonyl ring was found to have little or no effect on efficiencies, yields and levels of enantioselectivity achieved for cyclopentanone synthesis (**Figure 2.31**). This would seem to suggest that the primary influence of the phenylsulfonyl ring on enantiocontrol is a steric one, although further experiments examining a wider range of modifications at the sulfone site are required to fully validate this view.

Table 2.23 *Copper-bis(oxazoline)-catalysed C–H insertions of α-diazo-β-keto 4-bromophenylsulfone* ***60***[a]



Entry	L*	Time (h)	**61** : **62** : **63**[b,c]	Yield **61** (%)[d]	ee **61** (%)[e,f]
1	(4*R*)-Ph **49**	2	1 : 0.30 : 0.03[g]	77	47 (2*S*, 3*S*)
2	(4*R*)-Bn **50**	2	1 : 0.12 : 0.03	62	83 (2*S*, 3*S*)
3	(4*S*)-*t*-Bu **51**	18	1 : 0.32 : 0.11	71	68 (2*R*, 3*R*)
4	(4*R*,5*S*)-Ph **52**	2	1 : 0.26 : 0.04[g]	49	53 (2*S*, 3*S*)
5	(3*S*,8*R*)-Ind **53**	2	1 : 0.19 : 0.04	47	87 (2*R*, 3*R*)

[a] Reactions conducted using the general procedure for copper-catalysed C–H insertion reactions (see **Section 4.2.9** for details).

[b] Ratio of C–H insertion : alkene formation : O–H insertion based on integration of the C(2)*H* doublet of cyclopentanone **61**, the δ_H 5.62 singlet of **62** and the δ_H 5.14 singlet of **63**, respectively, in the ^{1}H NMR spectra of the crude reaction mixtures.

[c] Ratio of β-keto sulfone **59** formation not determined due to overlap of the C(1)H_2 signal of **59** with the C(3)H signal of cyclopentanone **61**.

[d] Yield of *trans*-cyclopentanone **61** after column chromatography.

[e] Enantiopurity determined by chiral stationary phase HPLC (see appendix I for details).

[f] Absolute stereochemistry of **61** determined by single crystal analysis (see appendix I for details).

[g] Unknown peaks observed in the ^{1}H NMR spectrum of the crude reaction mixture.

*Comparison of enantioselectivities for copper-bis(oxazoline)-catalysed C–H insertions of α-diazo-β-keto phenylsulfone **35** versus α-diazo-β-keto 4-bromophenylsulfone **60***

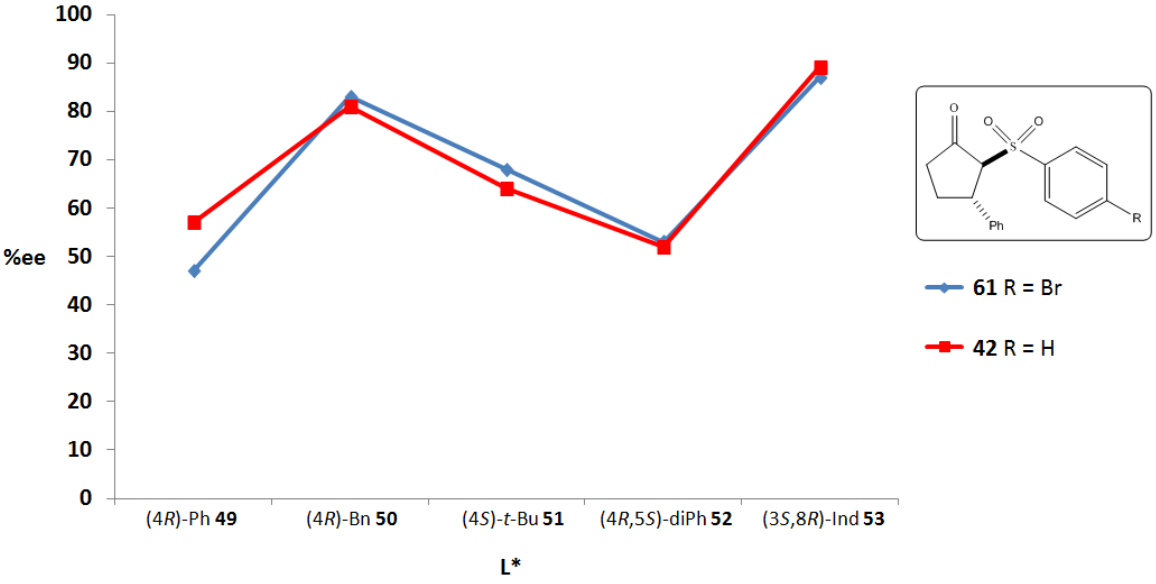


Figure 2.31

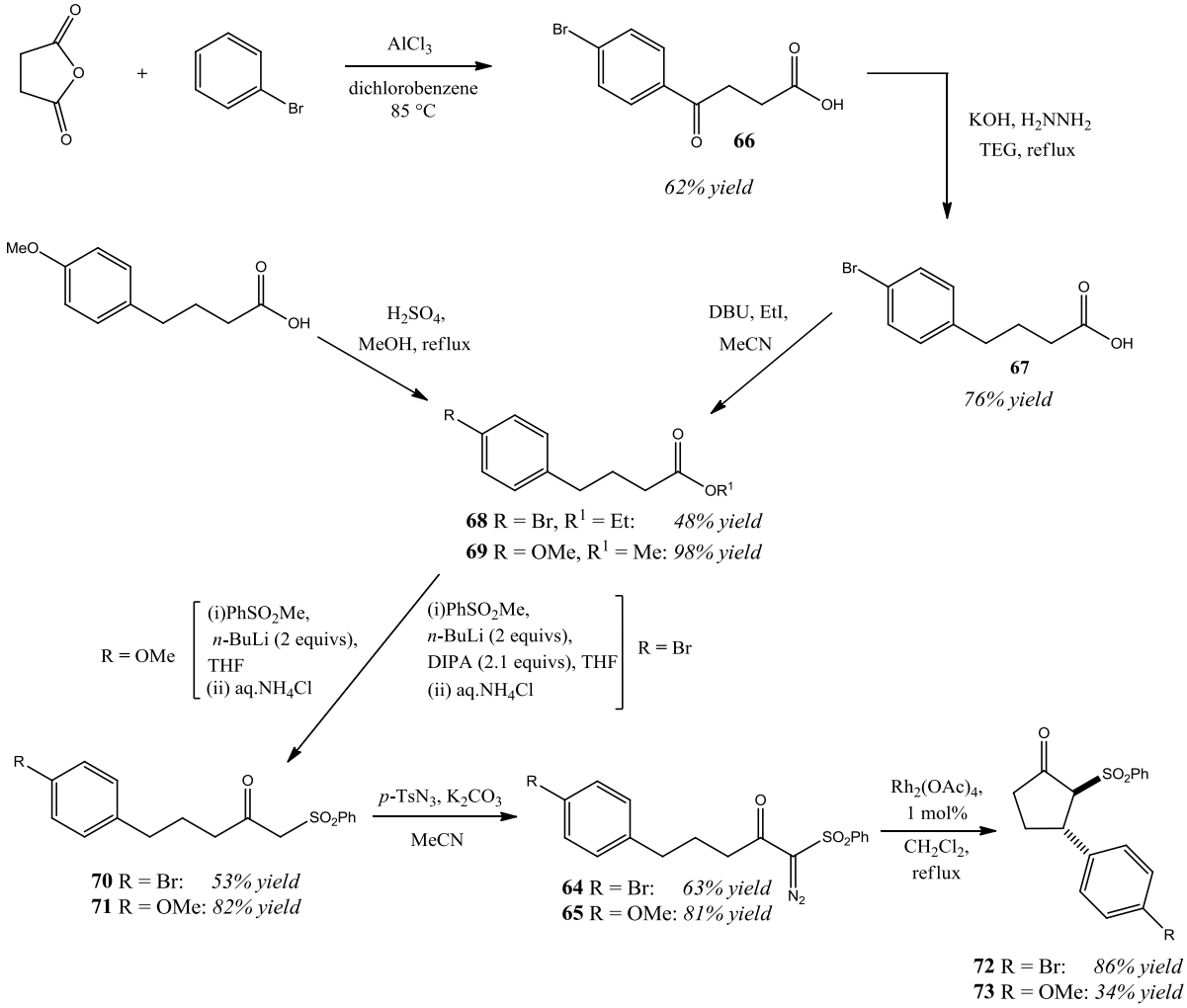
As was previously observed for reactions of 1-diazo-1-phenylsulfonyl-5-phenylpentan-2-one **35**, intramolecular alkylidene THF formation and O–H insertion were found to compete with C–H insertion. Thus, minor amounts of 2-[(4-bromophenylsulfonyl)methylene]-5-phenyl tetrahydrofuran **62** and 1-[(4-bromophenyl)sulfonyl]-1-hydroxy-5-phenylpentan-2-one **63** were noted in the ^{1}H NMR spectra of the crude reaction mixtures in **Table 2.23**. Observed byproducts levels were largely in line with levels recorded for reactions of the non-brominated diazo derivative **35**.

2.7.2 Investigation of modifications to the phenyl ring adjacent to the C–H insertion site

As previously discussed (**Section 2.4**), C–H insertion reactions occur *via* a mechanism involving complexation of the electron-deficient α-diazo carbon with the electron density in the target C–H bond. As a result, modification of electronic properties at the target C–H bond should in theory affect the outcome of the C–H insertion reaction. In order to investigate this effect, two novel α-diazo-β-keto sulfone substrates were targeted: 1-diazo-5-(4-bromophenyl)-1-phenylsulfonylpentan-2-one **64** and 1-diazo-5-(4-methoxyphenyl)-1-phenylsulfonylpentan-2-one **65**, featuring electron-withdrawing and electron-donating groups, respectively, at the *para* position of the phenyl ring.

The diazo compounds **64** and **65** were prepared as outlined in **Scheme 2.24**. Synthesis of carboxylic acid **67** was previously described in the literature and was prepared following these reported procedures.[146-148] Accordingly, synthesis of **64** began with the Friedel-Crafts reaction of bromobenzene and succinic anhydride with aluminium trichloride in

1,2-dichlorobenzene to give 4-(4-bromophenyl)-4-oxobutanoic acid **66** in 62% yield. This was followed by Wolff-Kishner reduction of the ketone moiety of **66** using the Huang-Minlon procedure,[148] providing the carboxylic acid **67** in good yield (76%). Conversion to the corresponding previously described ester derivative **68**[149] was achieved by reaction of **67** with DBU and ethyl iodide in acetonitrile. The Fischer esterification procedure was initially attempted for the synthesis of **68**, however, as was previously observed for preparation of the *tert*-butyl-substituted ester **18**, this was not a viable synthetic route due to formation of a large amount of an unknown byproduct. Notably, the unidentified byproduct formed in the reaction of **67** was identical by ^{1}H NMR analysis to the byproduct observed for the reaction of the *tert*-butyl-substituted carboxylic acid **16** (**Figure 2.5**). Employment of the Fischer procedure was successfully used for the esterification of commercially available 4-(4-methoxyphenyl)butanoic acid, providing access to the previously described ester methyl 4-(4-methoxyphenyl)butanoate **69**[150] in high yield (98%).



Scheme 2.24

The esters **68** and **69** were subsequently transformed to the corresponding sulfone (**70** and **71**) and diazo (**64** and **65**) compounds (**Scheme 2.24**) using similar procedures to those reported for synthesis of the unsubstituted phenyl derivatives **27** and **35** (**Section 2.2.6** and **Section 2.3**). Lithium diisopropylamide was used in place of *n*-butyllithium for the synthesis of 5-(4-bromophenyl)-1-phenylsulfonylpentan-2-one **70** to avoid lithium-halogen exchange. Rhodium(II) acetate-catalysed cyclisation of the α-diazo-β-keto sulfones **64** (R = Br) and **65** (R = OMe) provided the novel cyclopentanones **72** and **73**, respectively. Both products were isolated exclusively as *trans*-isomers, with no evidence for formation of *cis*-**72** or *cis*-**73** observed in the ^{1}H NMR spectra of the crude reaction mixtures. The crude reaction mixture obtained for synthesis of *para*-bromo-substituted **72** was relatively clean, with approximately 12% O–H insertion product also observed.

In contrast, a complex mixture of crude products was observed in the ^{1}H NMR spectrum for reaction of the *p*-methoxyphenyl diazo **65** (**Figure 2.32**). Such products included those arising from competing O–H insertion (**74**), intramolecular attack of the enolic oxygen at the benzylic site [(*Z*)-**75**] and hydride abstraction (*trans*-**76**).

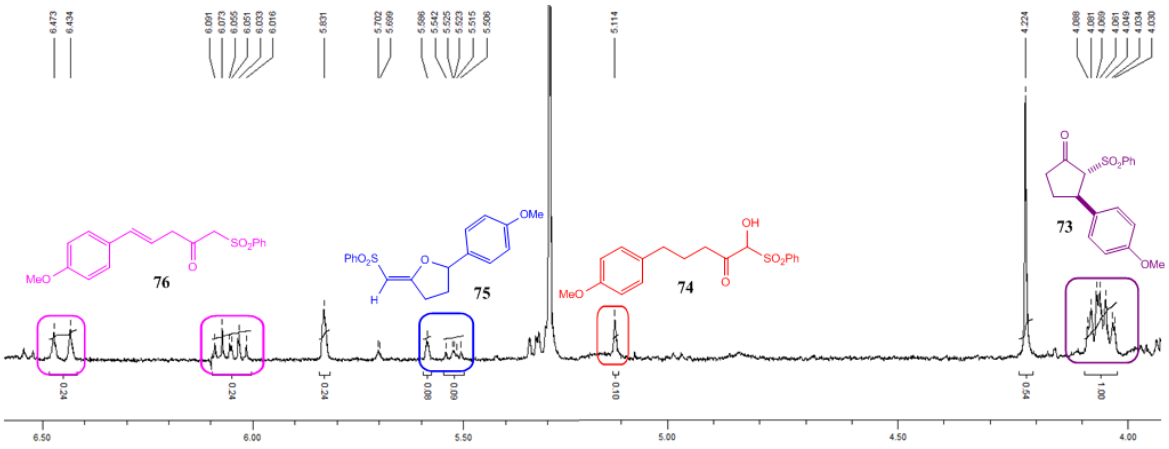


Figure 2.32 δ_H *(400 MHz, CDCl$_3$)*

The observed decreased chemoselectivity towards C–H insertion is surprising given that increase of electron density at the target C–H insertion site might be expected to result in increased reactivity towards the electron-deficient carbenoid carbon. Rationalisation of the altered chemoselectivity may be achieved by examination of the mechanism for C–H insertion. Two important events are involved in the transition state for the crucial C–H insertion step; hydride transfer from the alkane to the carbenoid carbon and catalyst dissociation/formation of a new C–C bond. C–H insertion is widely known to be a concerted process,[7,58,59] however, as reported by Nakamura and co-workers in 2002,[78] the C–C bond formation lags behind the hydride transfer, meaning that C–H bond activation/C–C bond formation occurs in a nonsynchronous concerted manner (**Figure 2.33**). Taking this into account, the presence of the electron-donating *para*-methoxy substituent on the diazo substrate **65** is believed to enhance the extent of hydride transfer

relative to C–H insertion due to stabilisation of the cationic carbon in **TS-II**, resulting in increased byproduct formation *via* the hydride transfer route.

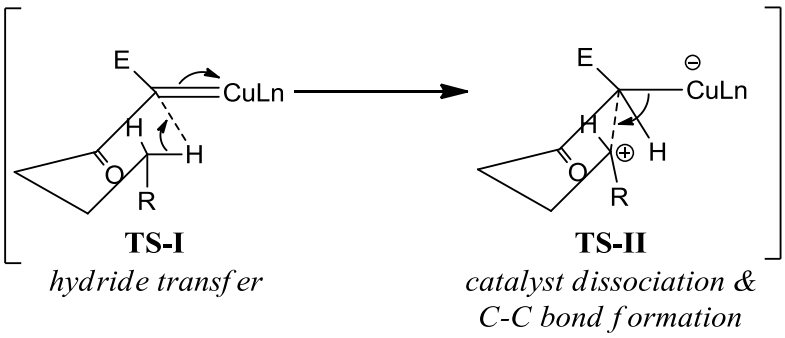
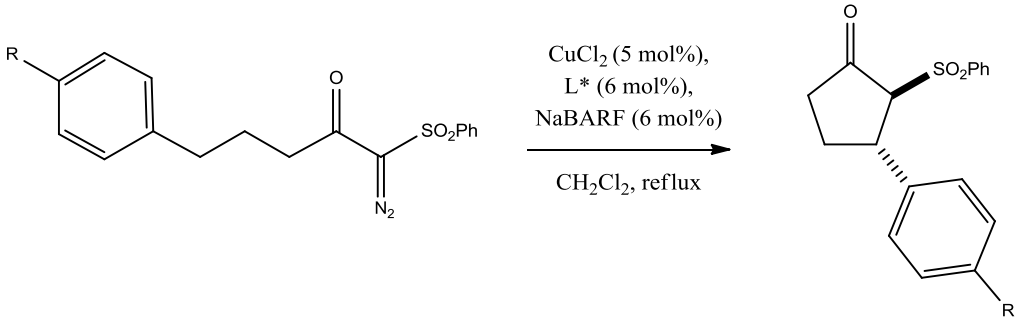


Figure 2.33

Copper-bis(oxazoline)-catalysed C–H insertions of the electronically modified α-diazo-β-keto sulfones **64** and **65** are presented in **Table 2.24**. The impact of electronic effects on the chemoselectivity of the α-diazo-β-keto sulfone transformations was again evident (**Figure 2.34**). While the introduction of an electron-withdrawing halide substituent (R = Br) on the phenyl ring was found to result in largely similar byproduct patterns to reactions with the unmodified diazo substrate **35** (R = H), a dramatic shift in chemoselectivity towards intramolecular tetrahydrofuran formation was observed for reactions of the *para*-methoxyphenyl-substituted diazo sulfone **65**. For each of the copper-catalysed reactions examined (**Table 2.24**, entries 6–10) a large excess of **75** was observed relative to cyclopentanone **73**. This is in agreement with the mechanism earlier proposed (**Scheme 2.19**) for formation of **75** and related compounds; the increase in electron density contributed by the *para*-methoxy substituent favours carbocation formation through complete hydride transfer relative to the more concerted C–H insertion pathway. Subsequent intermolecular attack of the carbocationic centre by the enolic oxygen leads to formation of the tetrahydrofuran ring.

Table 2.24 *Copper-bis(oxazoline)-catalysed C–H insertions of electronically modified α-diazo-β-keto sulfones*[a]



Entry	Diazo	Product	R	L*	Time (h)	C–H : THF : O–H[b]	Yield (%)[c]	ee (%)[d,e]
1	**64**	**72**	Br	(4*R*)-Ph **49**	3	1 : 0.01 : 0.17[f]	69	39 (2*S*,3*S*)
2	**64**	**72**	Br	(4*R*)-Bn **50**	5	1 : 0.09 : 0.04	86	67 (2*S*,3*S*)
3	**64**	**72**	Br	(4*S*)-*t*-Bu **51**	4	1 : 0.18 : 0.14	73	59 (2*R*,3*R*)
4	**64**	**72**	Br	(4*R*,5*S*)-diPh **52**	2	1 : 0.02 : 0.04[f]	65	49 (2*S*,3*S*)
5	**64**	**72**	Br	(3*S*,8*R*)-Ind **53**	6	1 : 0.04 : 0.08	60	87 (2*R*,3*R*)
6	**65**	**73**	OMe	(4*R*)-Ph **49**	2	1 : 3.71[g] : 0.03	25[h]	49 (2*S*,3*S*)
7	**65**	**73**	OMe	(4*R*)-Bn **50**	2	1 : 8.69[g] : 0.07	20[h]	71 (2*S*,3*S*)
8	**65**	**73**	OMe	(4*S*)-*t*-Bu **51**	2	1 : 8.11[g] : 0.25	10[h]	58 (2*R*,3*R*)
9	**65**	**73**	OMe	(4*R*,5*S*)-diPh **52**	2	1 : 4.98[g] : 0.11	26[h]	59 (2*S*,3*S*)
10	**65**	**73**	OMe	(3*S*,8*R*)-Ind **53**	2	1 : 8.80[g] : 0.06	19[h]	88 (2*R*,3*R*)
11[i]	**35**	**42**	H	(4*R*)-Ph **49**	2	1 : 0.15 : 0.05	69	57 (2*S*,3*S*)
12[i]	**35**	**42**	H	(4*R*)-Bn **50**	2	1 : 0.06 : 0.01	58	81 (2*S*,3*S*)
13[i]	**35**	**42**	H	(4*S*)-*t*-Bu **51**[j]	19	1 : 0.27 : 0.01	55	64 (2*R*,3*R*)
14[i]	**35**	**42**	H	(4*R*,5*S*)-diPh **52**	2	1 : 0.04 : 0.05	54	52 (2*S*,3*S*)
15[i]	**35**	**42**	H	(3*S*,8*R*)-Ind **53**	2	1 : 0.17 : 0.02	87	89 (2*R*,3*R*)

[a] Reactions conducted using the general procedure for copper-catalysed C–H insertion reactions (see **Section 4.2.9** for details).

[b] Ratio of C–H insertion : THF formation : O–H insertion based on integration of the C(2)*H* doublet of the cyclopentanone product, the δ_H 5.59–5.64 singlet of the THF byproduct (R = Br: **77**, R = OMe: **75**, R = H: **54**) and the δ_H 5.14 singlet of the O–H insertion byproduct, respectively, in the ^{1}H NMR spectra of the crude reaction mixtures.

[c] Yield of *trans*-cyclopentanone after column chromatography.

[d] Enantiopurity of *trans*-cyclopentanone determined by chiral stationary phase HPLC (see appendix I for details).

[e] Absolute stereochemistry of cyclopentanone **72** determined by single crystal analysis (see appendix I for details). Absolute stereochemistry of **73** and **42** determined by comparison to previously reported polarimetry and chiral HPLC data.

[f] Unknown peaks (minor) observed in the ^{1}H NMR spectrum of the crude reaction mixture.

[g] Mixture of (*Z*)-**75** (major) and (*E*)-**75** (minor) observed in the ^{1}H NMR spectrum of the crude reaction mixture (see **Table 2.25** for exact ratios).

[h] Isolated product contains minor amount (<10%) of (*E*)-**75**.

[i] Reproduced from **Table 2.14**.

[j] Reaction catalysed by CuCl.

Comparison of byproduct formation for copper-bis(oxazoline)-catalysed C–H insertions of electronically modified α-diazo-β-keto phenylsulfones

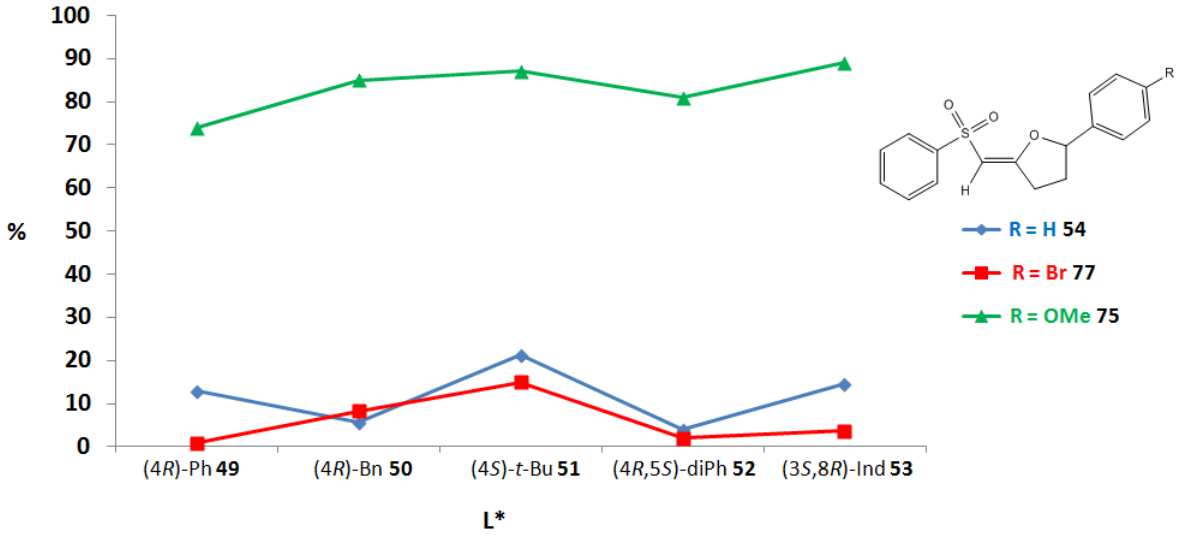
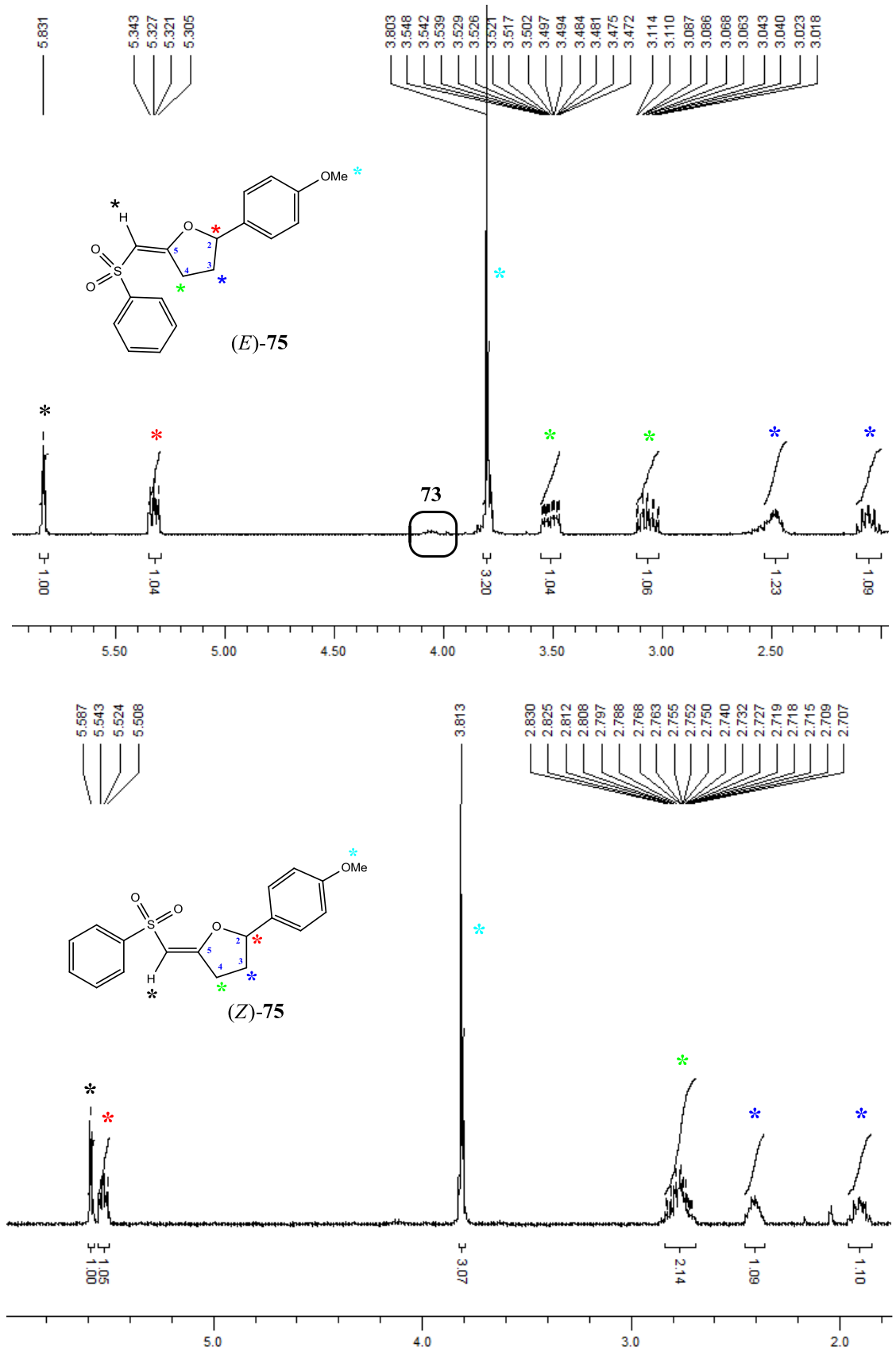


Figure 2.34

Interestingly, a mixture of *Z*- and *E*-isomers of **75** was observed in the ^{1}H NMR spectra of the crude reaction mixtures for reactions of α-diazo-β-keto sulfone **65** [for (*Z*)-**75** : (*E*)-**75** ratios see **Table 2.25**]. While the *Z*-isomer of the tetrahydrofuran-derived byproduct had been routinely observed for the copper-catalysed reactions of phenyl-substituted diazo substrates (**35** and **38**) examined to date, the corresponding *E*-isomer had not been observed. The ^{1}H NMR spectrum of (*E*)-**75**, isolated from reaction in the presence of (4*R*)-Ph **49** (**Table 2.24**, entry 6), is presented in **Figure 2.35**. The novel byproduct (*E*)-**75** was characterised by distinctive singlet and triplet peaks at δ_H 5.32 and 5.83, representing the alkene and C(2)*H* protons, respectively. The *E*-geometry about the double bond results in pronounced changes in signal pattern for the C(4)H_2 protons relative to the corresponding methylene signal (δ_H 2.68–2.86, m) in the ^{1}H NMR spectrum of (*Z*)-**75**. Thus, the C(4)H_2 protons of (*E*)-**75** are observed further downfield than the C(4)H_2 protons of (*Z*)-**75** and as individual multiplet signals, due presumably to interaction with the contiguous phenylsulfonyl moiety resulting in a characteristic diastereotopic splitting pattern. The stereochemistry of (*Z*)-**75** was assigned by comparison to the analogous THF derivative **54** (stereochemistry of **54** confirmed by X-ray crystallography, see **Scheme 2.19**). High resolution mass spectrometry (HRMS) analysis confirmed the presence of the molecular ion of both (*Z*)-**75** and (*E*)-**75** (see **Section 4.2.9** for details).



Note: aromatic signals and some peak picking omitted for the purpose of clarity.

Figure 2.35 δ_H *(400 MHz, $CDCl_3$)*

In contrast to the dramatic effects on chemoselectivity described above, the introduction of electron-withdrawing and electron-donating substituents onto the *para* position of the phenyl ring of the diazo substrate was found to have mimimal effect on enantiocontrol (**Figure 2.36**). With only one exception noted (**Table 2.24**, entry 9 *vs.* 14), a slight decrease in enantioselectivity was recorded for reactions of the bromo- and methoxy-substituted α-diazo-β-keto sulfones **64** and **65**, respectively, relative to cyclisations with the corresponding unsubstituted diazo compound **35**. This outcome is in agreement with previous reports by Hashimoto and co-workers who also observed reduced levels of asymmetric induction for rhodium(II)-catalysed C–H insertion reactions of α-diazo-β-keto esters featuring electron-withdrawing (Br, 70% ee) and electron-donating (OMe, 57% ee) groups on the *para* position of the phenyl ring, relative to reactions with the unsubstituted diazo substrate (76% ee) (**Table 1.2**, entries 6–8).[5] In the same study, cyclopentanone synthesis was achieved with 80% enantiopurity for reaction of an α-diazo substrate possessing a triflate substituent at the *para* position (**Table 1.2**, entry 9). The triflate moiety is a much stronger deactivator by comparison to bromine and thus, as increased enantioselectivity was observed with the triflate-substituted substrate, the synthesis and exploration of α-diazo-β-keto sulfones featuring strongly electron-withdrawing substituents, *e.g.* CF_3SO_3, NO_2, may be warranted in future projects in this area. Indeed, improvements in both yield and enantiocontrol have been recorded for intermolecular C–H insertions with electron deficient aryl diazoacetate precursors.[151-154]

Comparison of enantioselectivities for $CuCl_2$-catalysed C–H insertion reactions of electronically modified α-diazo-β-keto sulfones

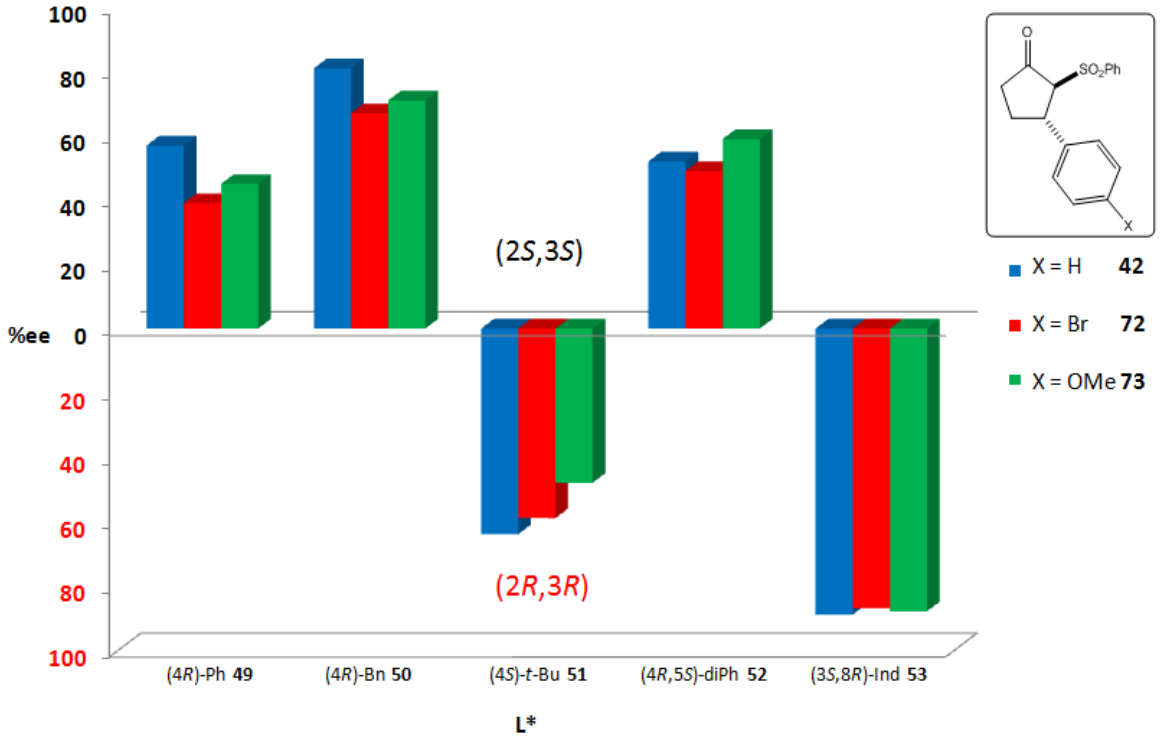
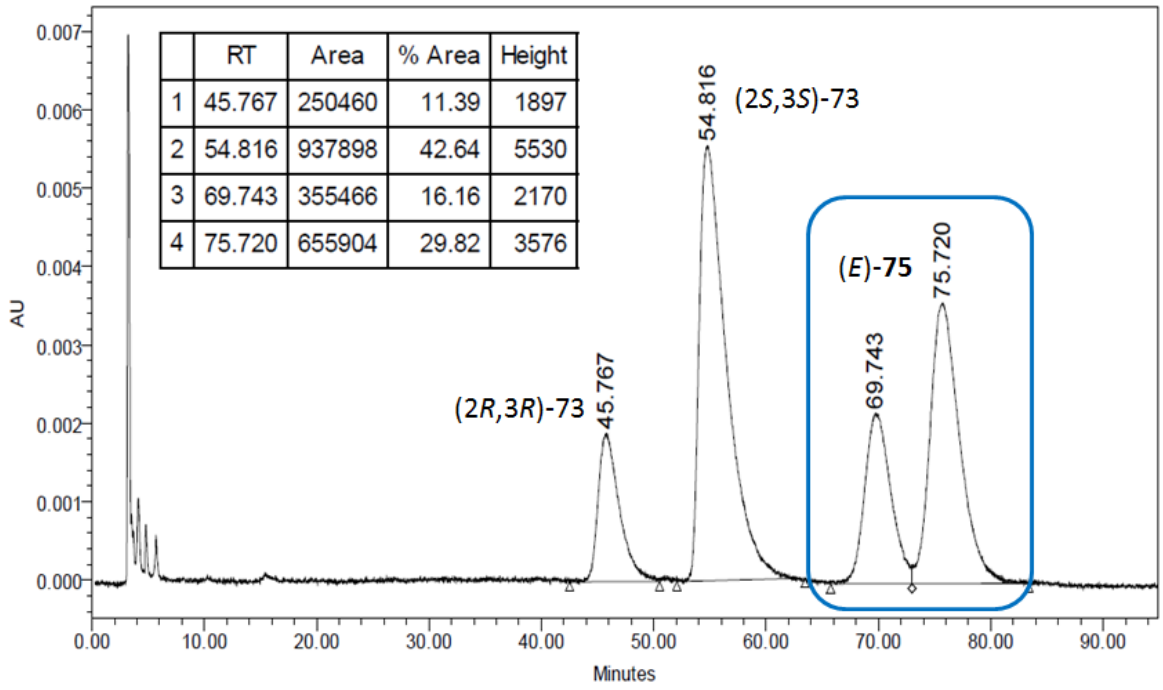


Figure 2.36

The samples of cyclopentanone **73** isolated from the experiments described in **Table 2.24** also contained minor amounts of (*E*)-**75** owing to co-elution of these compounds by column chromatography. Thus, when developing methods for the determination of enantiopurity of **73** by chiral stationary phase HPLC analysis, efforts were also made to achieve efficient separation of the enantiomers of (*E*)-**75**. As displayed in **Figure 2.37**, this was indeed achieved, albeit without full baseline separation, allowing the enantiopurities obtained for the copper-catalysed synthesis of (*E*)-**75** to be tentatively assigned (**Table 2.25**).



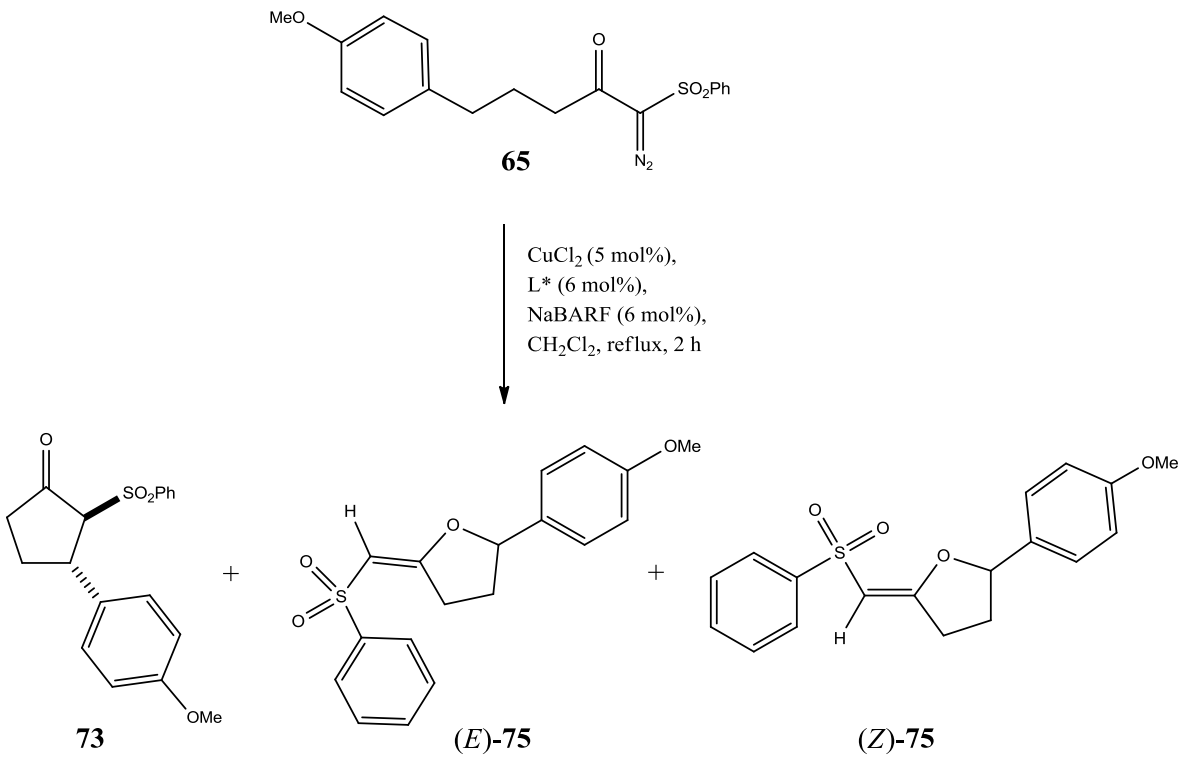
isolated from reaction of **65 in the presence of $CuCl_2$, (4R,5S)-diPh **52** and NaBARF (**Table 2.24**, entry 9).*

Figure 2.37

Significantly, for the first time in this project, evidence was observed (**Table 2.25**) for the influence of the chiral catalytic complex on the formation of THF products *via* the hydride abstraction pathway. In each of the copper-bis(oxazoline)-catalysed reactions of α-diazo-β-keto sulfone **65** examined some extent of asymmetric induction was observed by chiral HPLC analysis, ranging from ~6% ee for reaction in the presence of (4*R*)-Ph **49** (**Table 2.25**, entry 1) to ~43% for cyclisation with the benzyl-substituted ligand (4*R*)-**50** (**Table 2.25**, entry 2). Indeed, the copper catalyst-mediated formation of (*E*)-**75** was also evident by examination of the observed enantiomeric series pattern; thus, as was previously observed for cyclopentanone synthesis (**Figure 2.15**), the use of ligands (4*S*)-*t*-Bu **51** and (3*S*,8*S*)-Ind **53**, with the same absolute stereochemistry, lead to the same enantiomeric series for (*E*)-**75** (**Table 2.25**, entries 3 and 5), while the opposite enantiomer of (*E*)-**75** was found to be in excess for reactions in the presence of the (4*R*)-substituted ligands **49**, **50** and **52**, which have the opposite absolute stereochemistry (**Table 2.25**, entries 1, 2 and 4).

Although not isolated for reactions in the presence of the other bis(oxazoline) ligands, a sample of (*Z*)-**75** obtained from the $CuCl_2$-catalysed reaction of **65** with (4*R*,5*S*)-diPh **52** displayed a specific rotation value of $[\alpha]_D^{20}$ –10.95 (*c* 0.3, CH_2Cl_2) when subjected to polarimetry analysis, suggesting some extent of asymmetric induction had also occured for the formation of the *Z*-isomer of **75**. Determination of enantiopurity by chiral stationary phase HPLC analysis was not undertaken for this compound.

Table 2.25 *Enantioselectivities for the copper-catalysed synthesis of* (E)-***75***[a]



Entry	L*	**73** : (*E*)-**75** : (*Z*)-**75**[b]	Yield **73** & (*E*)-**75** (%)[c]	ee (*E*)-**75** (%)[d,e]
1	(4*R*)-Ph **49**	1 : 1.16 : 2.55	55	6[f]
2	(4*R*)-Bn **50**	1 : 0.16 : 8.53	20	43[f]
3	(4*S*)-*t*-Bu **51**	1 : 0.06 : 8.05	10	8[g]
4	(4*R*,5*S*)-diPh **52**	1 : 0.07 : 4.91	26	30[f]
5	(3*S*,8*R*)-Ind **53**	1 : 0.06 : 8.74	19	25[g]

[a] Reactions conducted using the general procedure for copper-catalysed C–H insertion reactions (see **Section 4.2.9** for details).

[b] Ratio of C–H insertion : (*E*)-THF formation : (*Z*)-THF formation based on integration of the C(2)*H* doublet of cyclopentanone **73**, the δ_H 5.83 singlet of (*E*)-**75** and the δ_H 5.59 singlet of (*Z*)-**75**, respectively, in the ^{1}H NMR spectra of the crude reaction mixtures.

[c] Yield of *trans*-**73** and (*E*)-**75** after column chromatography.

[d] Enantiopurity of (*E*)-**75** determined by chiral stationary phase HPLC (see appendix I for details).

[e] Baseline separation not achieved, therefore, values are tentatively assigned.

[f] Second peak in the HPLC trace in the major peak.

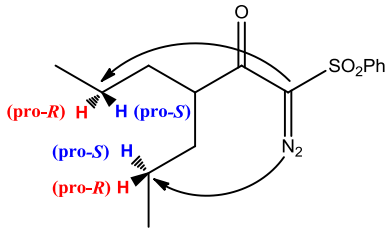
[g] Opposite enantiomer in excess: first peak in the HPLC trace is the major peak.

Previous chiral stationary phase HPLC analysis of a recrystallised sample of tetrahydrofuran (*Z*)-**54** had revealed a 50 : 50 mixture of enantiomers *i.e.* no asymmetric induction (**Section 2.6.1**, see Appendix II for HPLC trace). As a result, and owing to the minor amounts of sample typically obtained, determination of enantiopurity of the THF byproducts obtained from subsequent cyclisation reactions was not conducted. However, given the observation of asymmetric induction for the synthesis (*E*)-**75**, it is probable that some extent of enantiocontrol may also have occurred for the earlier syntheses of the THF byproducts **54**, **57**, **62** and **77**.

The observation of asymmetric induction for the synthesis of (*E*)-**75** and (*Z*)-**75** is particularly interesting considering the literature precedent for the application of similar alkylidene tetrahydrofuran products as key intermediates in the synthesis of prostacyclin PGI_2.[106,107] Indeed, tetrahydrofuran derivatives are widely found in many natural products of biological interest.[112] Thus, further exploration of this reaction is warranted in future projects, with the aim of identifying a broader range of substrates and catalysts for the production of novel enantioenriched alkylidene THF products.

2.7.3 Investigation of diastereocontrol

As part of our investigations into the effects of substrate modification on stereoselectivty in intramolecular C–H insertion reactions, an additional novel α-diazo-β-keto sulfone substrate **78** was prepared. Control of stereochemistry in this substrate is more complex as both the site of insertion and the selection of the pro-chiral hydrogen at the methylene group must be controlled (**Figure 2.38**).

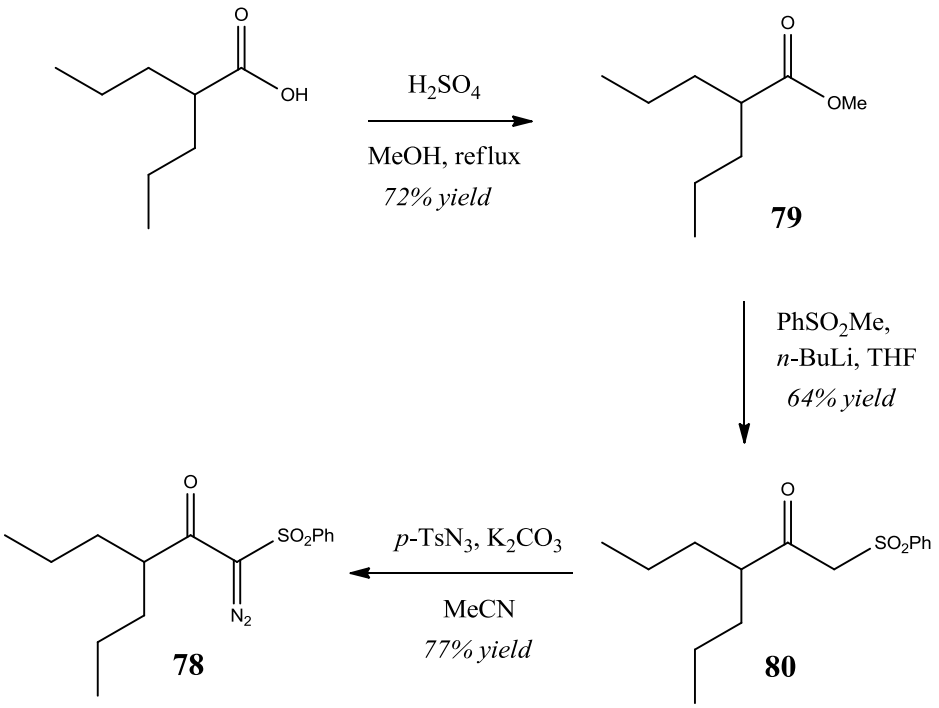


78

Figure 2.38

1-Diazo-1-phenylsulfonyl-3-propylhexan-2-one **78** was prepared using methods previously outlined for the synthesis of α-diazo-β-keto sulfones **1**, **32**–**38** (**Section 2.2** and **Section 2.3**) Accordingly, commercially available valproic acid was transformed to methyl valproate **79**, a known compound,[155] using Fischer esterification (**Scheme 2.25**). Reaction of **79** with the anion of methyl phenyl sulfone **21** (generated using *n*-butyllithium) provided 1-phenylsulfonyl-3-propylhexan-2-one **80** in 64% yield. Synthesis of 1-diazo-1-phenylsulfonyl-3-propylhexan-2-one **78** was then achieved by diazo transfer employing *p*-tosyl azide **31** and potassium carbonate (**Scheme 2.25**). β-Keto sulfone **78**

and α-diazo-β-keto sulfone **80** are novel compounds and were thus fully characterised (see **Section 4.2.7** and **Section 4.2.8** for details). The efficiency of the sulfone and diazo syntheses was essentially comparable to those observed for earlier preparations of related β-keto sulfones **23**–**30** (**Table 2.6**) and their diazo derivatives **1**, **32**–**38** (**Table 2.8**).



Scheme 2.25

Rhodium(II) acetate-catalysed C–H insertion of α-diazo-β-keto sulfone **78** in refluxing dichloromethane provided access to cyclopentanone **81**. This novel product possesses three stereogenic centres, therefore, the formation of four diastereomers, each present as a pair of enantiomers, is possible (**Figure 2.39**). The relative stereochemistry assigned to each enantiomeric pair is shown in **Figure 2.39**.

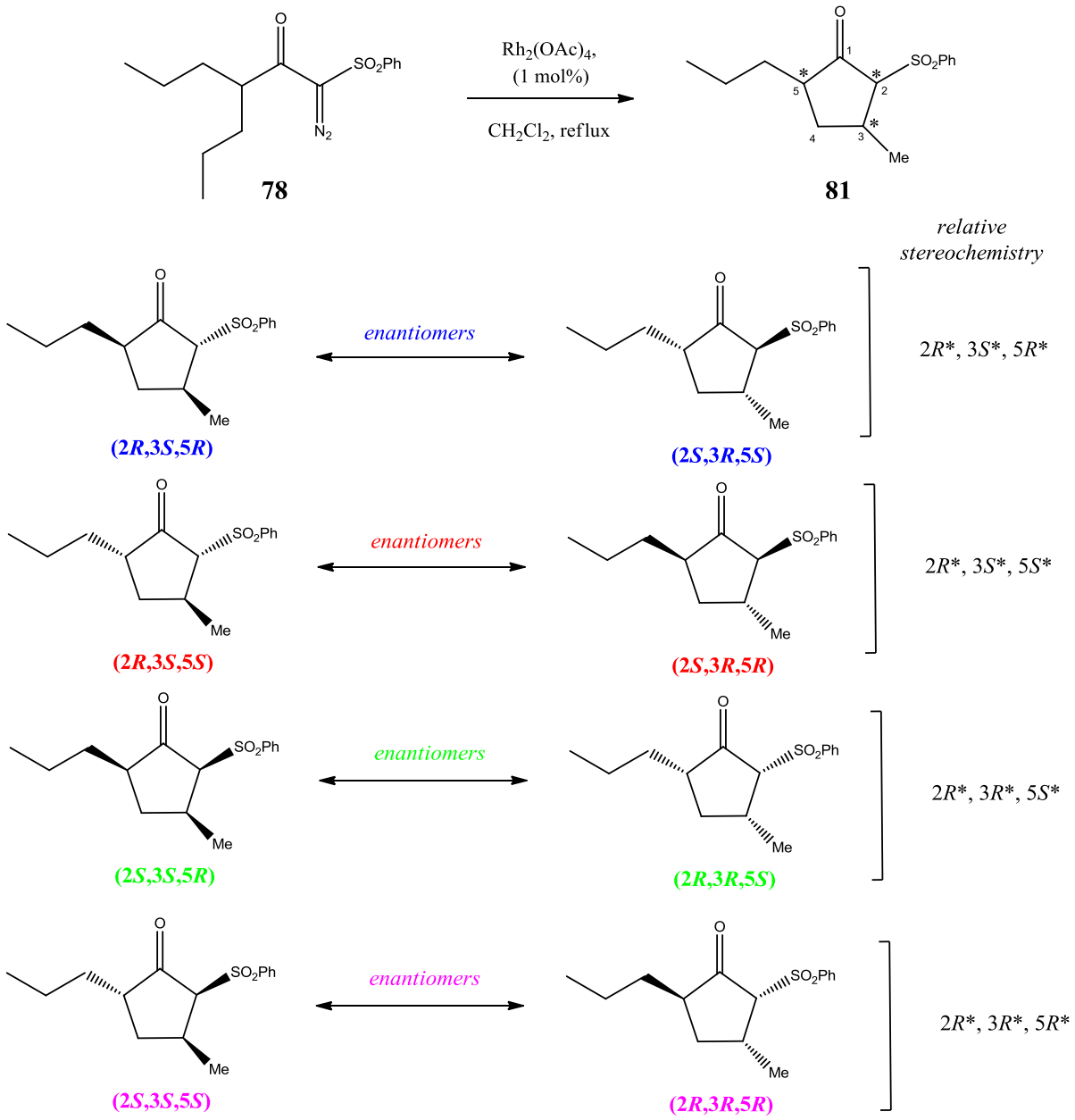


Figure 2.39

Signals for all four diastereoisomers were observed in the ^{1}H NMR spectrum for the crude reaction mixture resulting from the rhodium(II)-catalysed reaction of **78** [**Figure 2.40** (a)]. A 1.00 : 4.87 : 1.96 : 3.21 ratio of diastereoisomers was recorded, meaning some level of diastereoselection is seen in the C–H insertion process. The observed diastereocontrol indicates that the carbenoid does not insert indiscriminately into each of the two methylene units, but instead selectively inserts at one of the two possible sites presumably due to conformational features of the transition state for insertion.[72,156,157] The doublet signals at δ_H 3.71 and 3.84 were not observed in the ^{1}H NMR spectrum of the product sample isolated after column chromatography. These signals were, therefore, assigned to (2*R**,3*R**,5*S**)-**81** and (2*R**,3*R**,5*R**)-**81** which possess *cis* stereochemistry at

C2 and C3, in line with previous trends for exclusive isolation of *trans*-cyclopentanones following chromatographic purification (**Section 2.4** and **Section 2.5**). Two product fractions were isolated following purification by column chromatography, both containing a mixture of (2*R**,3*S**,5*R**)-**81b** and (2*R**,3*S**,5*S**)-**81a** in differing ratios [the ^{1}H NMR spectrum for one product fraction is displayed in **Figure 2.40** (b)].

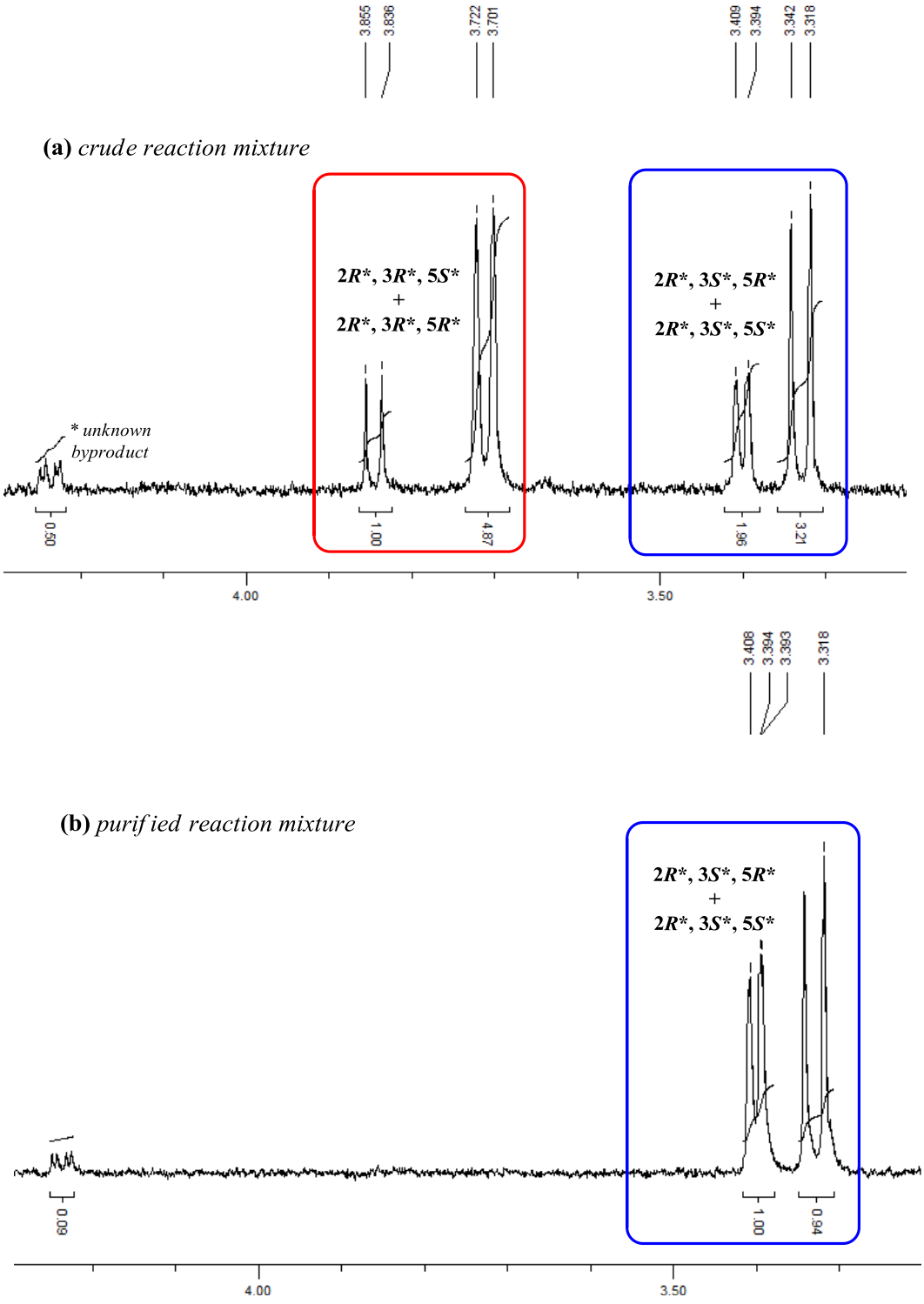


Figure 2.40 δ_H *(400 MHz, $CDCl_3$)*

An unknown doublet of doublets signal (J = 7.2/2.4) was also observed at δ_H 4.24 in the ^{1}H NMR spectrum of the crude racemic reaction mixture, indicating the occurrence of competing reaction processes. Removal of this unknown byproduct *via* column chromatography proved difficult, meaning minor quantities were often present in the final isolated product samples. One possible structure considered for this byproduct was the cyclohexanone derivative shown in **Figure 2.41**, derived from C–H insertion into the primary C–H bond rather than the secondary C–H bond. While insertion into primary C–H bonds is not generally favoured, isolated examples have been seen in our research team in previous projects.[11,80] Comparison of the spectral features with those of structurally related compounds prepared by O'Riordan[80] indicate that this is not likely to be the compound responsible for the signal observed at δ_H 4.24.

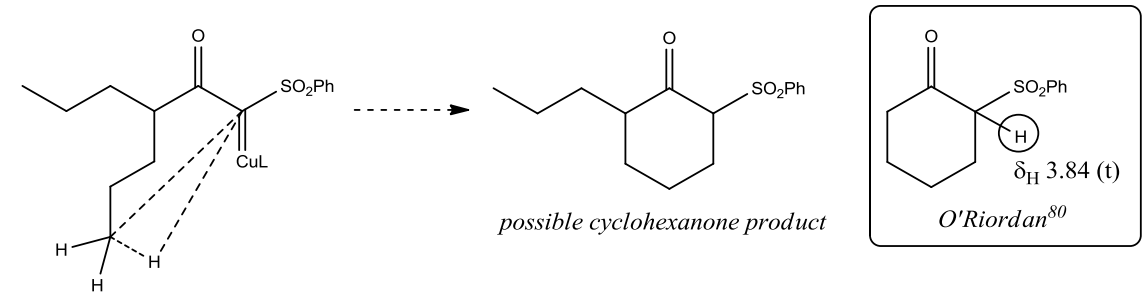
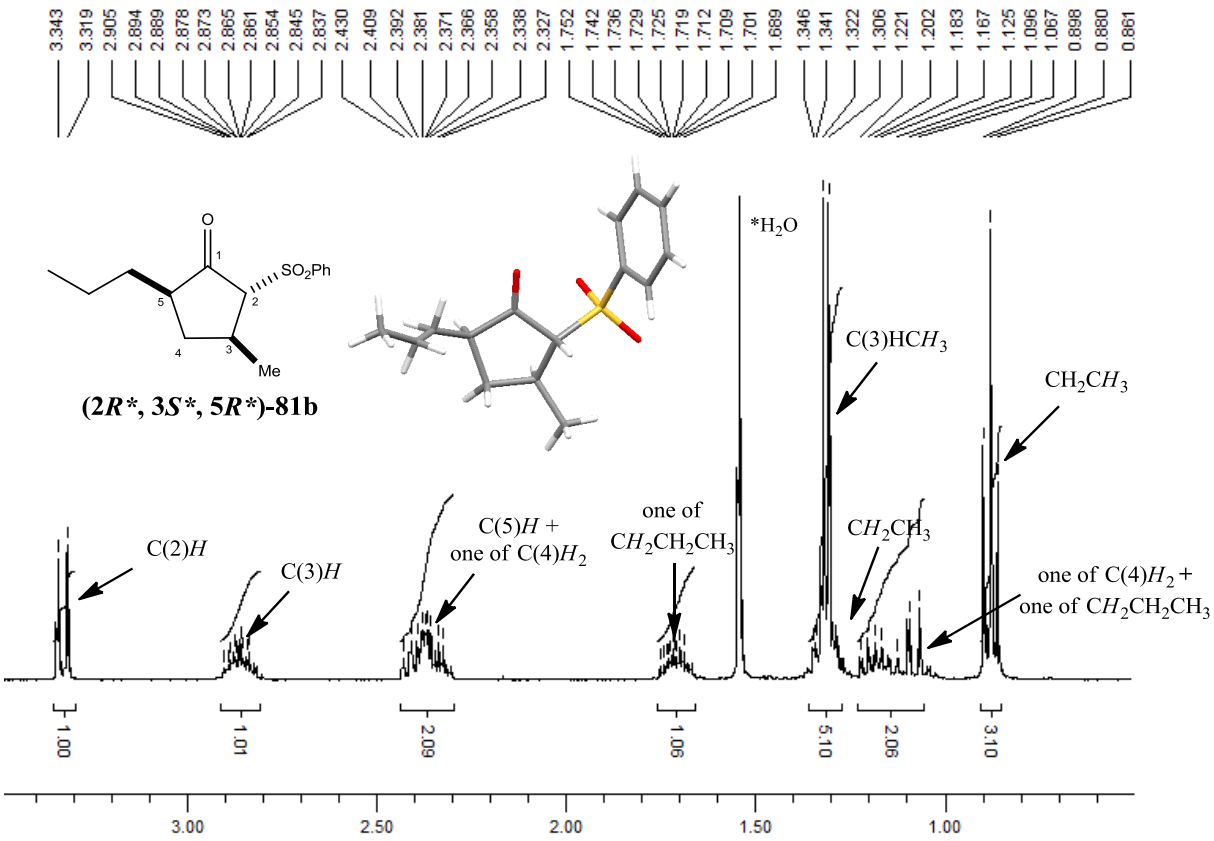


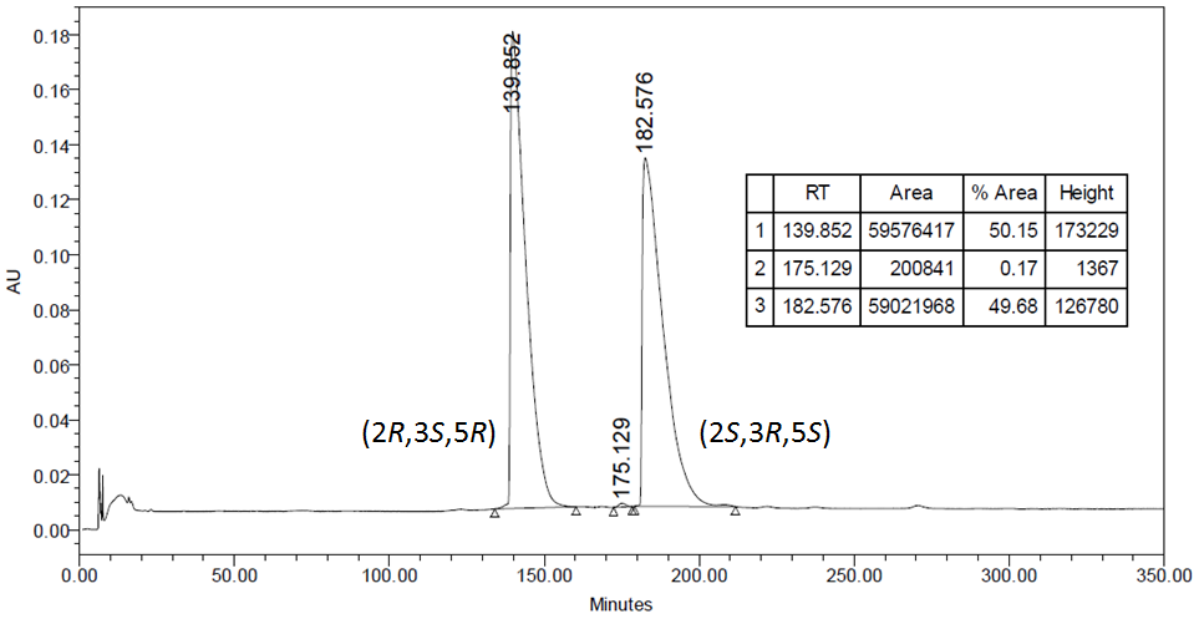
Figure 2.41

C–H insertion of α-diazo-β-keto sulfone **78** catalysed by Cu(OTf)$_2$ was next examined. As was noted for previous copper-catalysed reactions, the presence of cyclopentanone products possessing exclusively *trans* stereochemistry across the C2–C3 bond was recorded. Thus, a 1 : 2.6 mixture of isomers was observed [later identified as (2*R**,3*S**,5*S**)-**81a** : (2*R**,3*S**,5*R**)-**81b**] in the ^{1}H NMR spectrum of the crude reaction mixture for the Cu(OTf)$_2$-catalysed cyclisation, as determined by integration of the doublet signals at δ_H 3.40 and 3.33, respectively. Careful purification *via* column chromatography, employing a 0–10% gradient mixture of ethyl acetate in hexane as eluent, allowed separation of the two diastereomers in individual fractions, thus permitting individual spectroscopic analysis of both (2*R**,3*S**,5*R**)-**81b** and (2*R**,3*S**,5*S**)-**81a** [**Figure 2.42**, (a) and (b)]. Assignment of the spectroscopic features of (2*R**,3*S**,5*R**)-**81b** and (2*R**,3*S**,5*S**)-**81a** was aided by COSY and HETCOR experiments. Determination of the relative stereochemistry of an isolated sample of **81b** was later achieved by single crystal analysis of enantioenriched cyclopentanone **81b** obtained from copper-bis(oxazoline)-catalysed reactions of **78**. The relative stereochemistry of **81a** was also assigned on the basis of this structure.



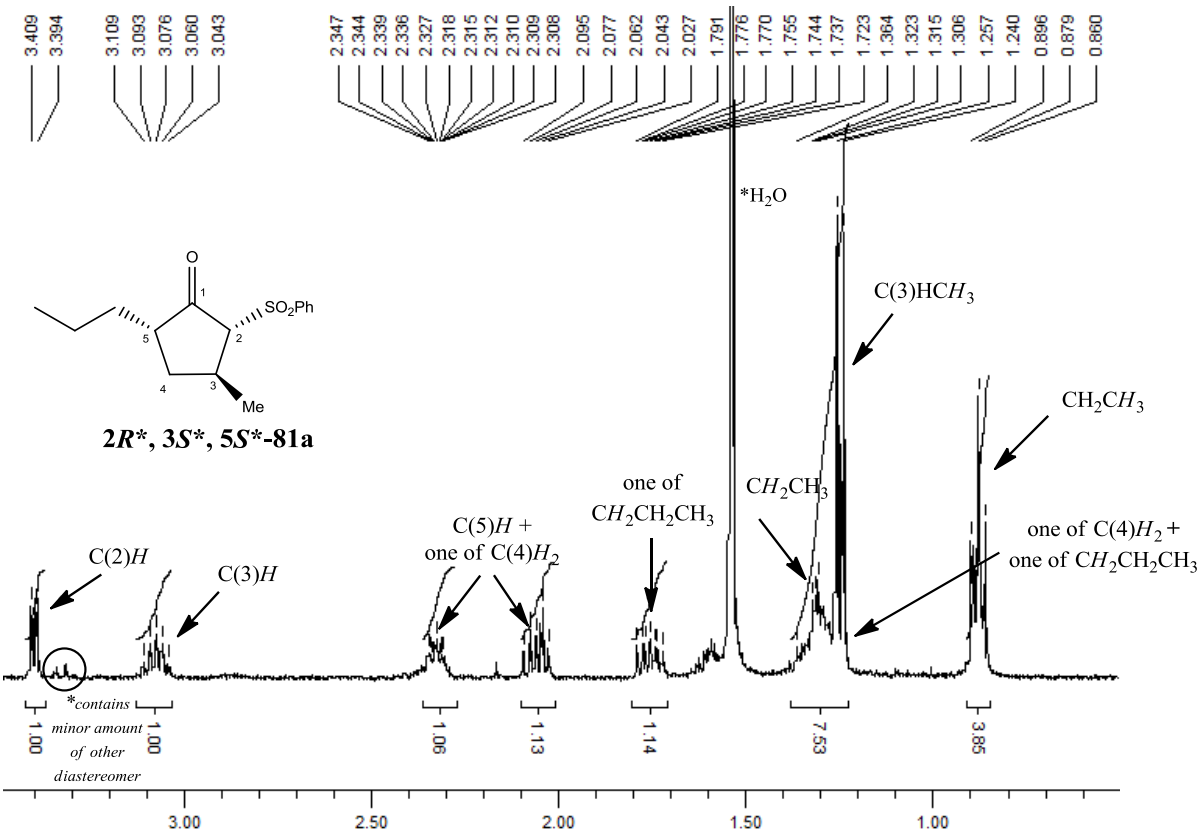
Note: aromatic signals and some peak picking omitted for the purpose of clarity.

δ_H (400 MHz, $CDCl_3$)



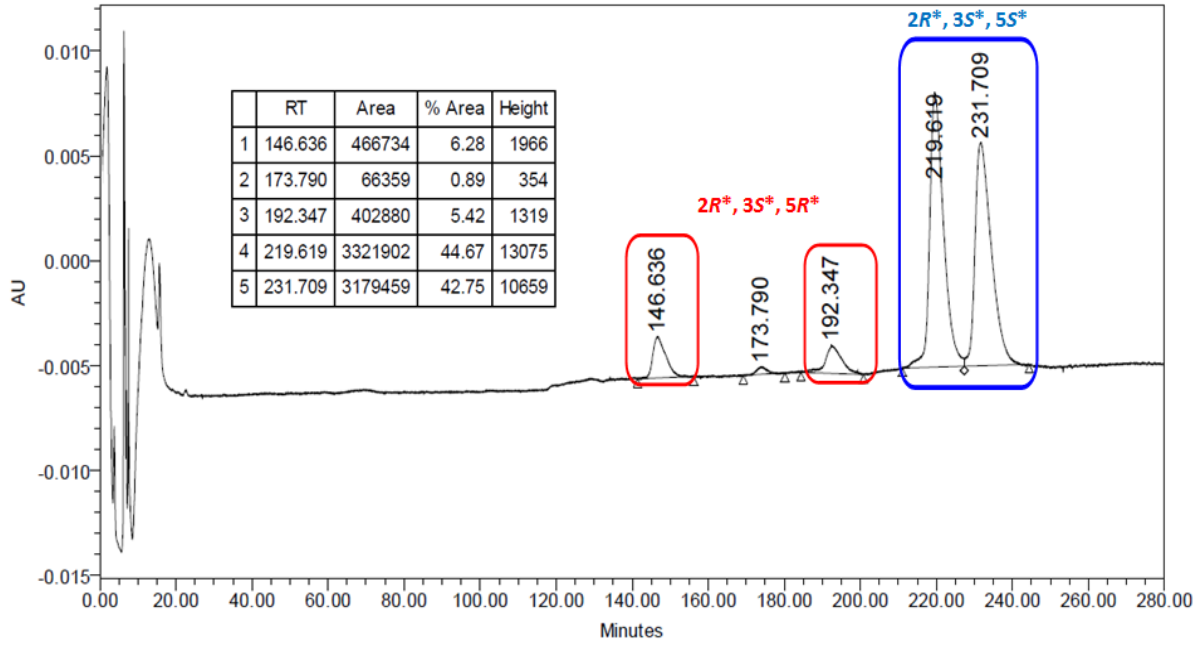
**for chiral HPLC conditions see Appendix I*

Figure 2.42 (a)



Note: aromatic signals and some peak picking omitted for the purpose of clarity.

δ_H *(400 MHz, $CDCl_3$)*



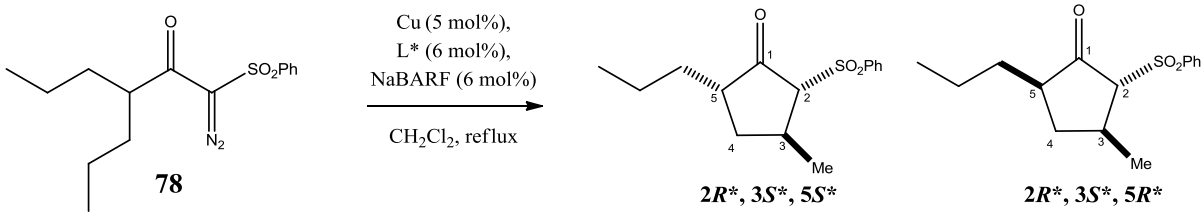
	RT	Area	% Area	Height
1	146.636	466734	6.28	1966
2	173.790	66359	0.89	354
3	192.347	402880	5.42	1319
4	219.619	3321902	44.67	13075
5	231.709	3179459	42.75	10659

**for chiral HPLC conditions see Appendix I*

Figure 2.42 (b)

Enantioselective $CuCl_2$-catalysed C–H insertion reactions of 1-diazo-1-phenylsulfonyl-3-propylhexan-2-one **78** in the presence of our portfolio of commercially available bis(oxazolines) are presented in **Table 2.26**. For all reactions examined, preferential formation of (2*R**,3*S**,5*R**)-**81b** over (2*R**,3*S**,5*S**)-**81a** was recorded. Little or no competing byproduct formation was observed in the ^{1}H NMR spectra of the crude reaction mixtures arising from the copper-catalysed reactions, with the exception of the unknown doublet of doublets signal at δ_H 4.24 which was observed in minor quantities (<5%).

Table 2.26 *Copper-catalysed C–H insertion reactions of 1-diazo-1-phenylsulfonyl-3-propylhexan-2-one* ***78***[a]



Entry	Copper	Ligand	Additive	Time (h)	**81a** : **81b**[b]	Yield (%)[b]	ee **81a** (%)[d]	ee **81b** (%)[d,e]
1	$Cu(OTf)_2$	–	–	4	1 : 2.6	87	–	–
2	$CuCl_2$	(4*R*)-Ph **49**	NaBARF	12	1 : 1.4	93	~0	14 (2*R*,3*S*,5*R*)
3	$CuCl_2$	(4*R*)-Bn **50**	NaBARF	4	1 : 2.1	95	64	63 (2*R*,3*S*,5*R*)
4	$CuCl_2$	(4*S*)-*t*-Bu **51**	NaBARF	10	1 : 2.9	99	35	19 (2*R*,3*S*,5*R*)
5	$CuCl_2$	(4*R*,5*S*)-diPh **52**	NaBARF	2	1 : 1.6[f]	89	~0	13 (2*R*,3*S*,5*R*)
6	$CuCl_2$	(3*S*,8*R*)-Ind **53**	NaBARF	3	1 : 1.7	99	75	59 (2*S*,3*R*,5*S*)

[a] Reactions conducted using the general procedure for copper-catalysed C–H insertion reactions (see **Section 4.2.9** for details).
[b] Ratios based on integration of the C(2)H signals from the ^{1}H NMR spectra of the crude products.
[c] Yield of **81a** and **81b** following column chromatography.
[d] Enantiopurity determined by chiral stationary phase HPLC (see appendix I for details).
[e] Absolute stereochemistry assigned by single crystal analysis (see appendix I for details).
[f] ~2% O–H insertion byproduct observed in the ^{1}H NMR spectrum of the crude reaction mixture (characterised by singlet at δ_H 5.12).

The enantiomers of (2*R**,3*S**,5*R**)-**81b** and (2*R**,3*S**,5*S**)-**81a** were successfully resolved by chiral stationary phase HPLC analysis employing a Chiralpak® OJ-H column (for details of HPLC conditions see appendix I). Single crystal analysis of the diastereomerically pure compound **81b**, obtained from reaction in the presence of (3*S*,8*R*)-Ind **53** , followed by chiral HPLC analysis of the isolated crystal was conducted to determine the absolute stereochemistry corresponding to each HPLC peak of (2*R**,3*S**,5*R**)-**81b** (see appendix I for full details). Single crystal analysis to determine the absolute stereochemistry corresponding to each HPLC peak of (2*R**,3*S**,5*S**)-**81a** is pending.

As was observed for earlier reactions of α-diazo-β-keto sulfones **1**, **32**–**36**, the indane-derived and benzyl-substituted bis(oxazolines) (3*S*,8*R*)-**53** and (4*R*)-**50**, respectively, were found to provide the highest levels of enantiocontrol, with up to 75% ee recorded for the synthesis of **81a** in the presence of the former ligand (**Table 2.26**, entry 6). In contrast, very little enantioselection was recorded for reactions of **78** in the presence of (4*R*)-Ph **49** and (4*R*,5*S*)-diPh **52** (**Table 2.26**, entries 2 and 5). A slight improvement in enantioselectivity was observed for cyclisation with the *tert*-butyl-substituted ligand (4*S*)-**51** (**Table 2.26**, entry 4). Curiously, in contrast to previous trends (**Figure 2.15**), the *tert*-butyl-substituted ligand (4*S*)-*t*-Bu **51** was found to provide cyclopentanone **81b** with the opposite stereochemistry to that obtained for the analogous reaction in the presence of (3*S*,8*R*)-Ind **53** (**Figure 2.43**). Significantly, as shown in **Figure 2.43** the results obtained for C–H insertions reactions of **78** displayed in **Table 2.26** are largely similar to those obtained for the analogous copper-bis(oxazoline)-catalysed cyclisations of α-diazo-β-keto sulfone **1** (**Table 2.14**, entries 1–5). Thus, the extra stereogenic centre present in cyclopentanone **81** does not appear to impact the overall enantiocontrol for this process.

*Comparison of enantioselectivities for $CuCl_2$-catalysed C–H insertion reactions of 1-diazo-1-phenylsulfonyl-3-propylhexan-2-one **78** versus 1-diazo-1-phenylsulfonyl hexan-2-one **1***

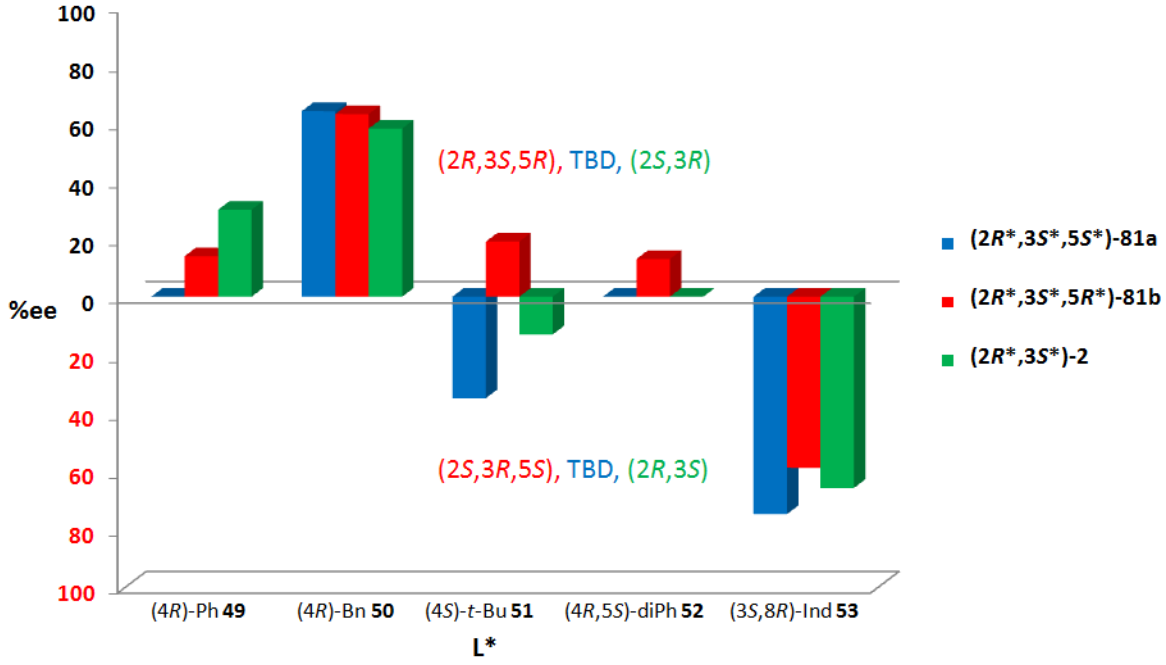


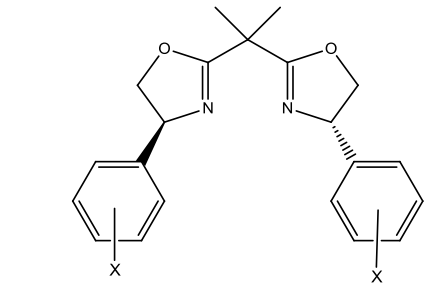
Figure 2.43

The overall outcome of this study demonstrated a moderate selectivity in terms of which of the two of the propyl chains in **Figure 2.38** is the site of insertion. This is likely to be conformationally controlled with a preference for the transition state in which the additional propyl chain is pseudo-equatorial leading to the major isomer.[72,156,157] More interestingly, in terms of enantiocontrol, the outcome in terms of insertion into the pro-chiral C–H bonds in **Figure 2.38** is practically unaffected by the presence of the additional stereogenic centre, with the trends in **Figure 2.43** displaying essentially the

same overall features as seen for the analogous cyclopentanone **2** which does not bear the extra n-propyl substituent. The implication of this is that the presence of the chiral copper catalyst does not result in selective insertion into one of the two pendant alkyl chains, but instead this feature is entirely conformationally controlled. A discussion of the theoretical transition states associated with the C–H insertion reactions of **78** and rationalisation of the observed stereoselectivity is included in **Section 2.9**.

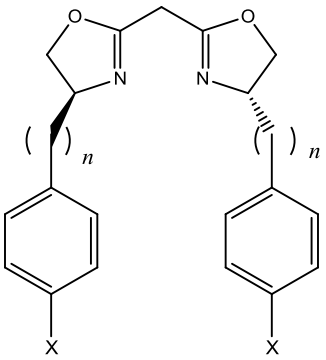
2.8 Synthesis of bis(oxazoline) ligands and investigation of effects on enantiocontrol

Since their introduction in 1989, many novel C_2-symmetric bis(oxazoline) ligands encompassing a vast array of structural features have been reported in the literature.[95,96] Included in these structures are a wide range of variations in aryl substituents of phenyl- and benzyl-substituted ligands. As shown in **Figure 2.44**, compounds prepared to date have featured largely methoxy, alkyl (X = Me, *t*-Bu) and halide (X = Cl, Br) substitution patterns. Additionally, Desimoni,[158] Itagaki[159] and Rutjes[160,161] have reported naphthyl- and anthryl-derived ligands.

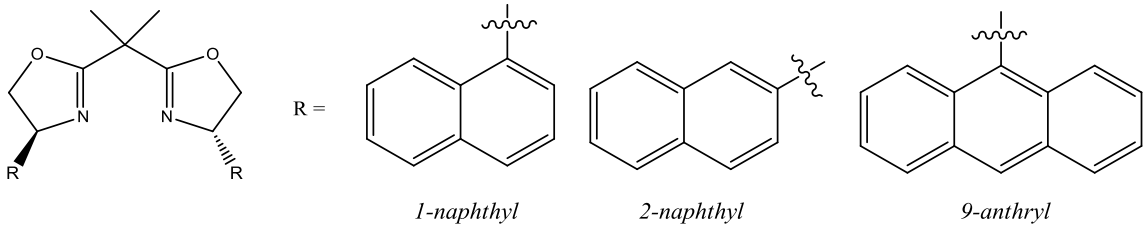


X = 4-OMe[162]
X = 4-Br[163]
X = 2-OMe[164]
X = 4-*t*-Bu[165]
X = 4-Me[166]
X = 4-CF_3[165]
X = 3,4-diOMe[167]

X = 4-Cl[162]
X = 4-Ph[163]
X = 2-OMe, 5-Cl[164]
X = 2-OMe, 5-*t*-Bu[164]
X = 2-$(CH_2)_2$Cl, 5-*t*-Bu[164]
X = 2,4,6-triMe[167]
X = H: **49**



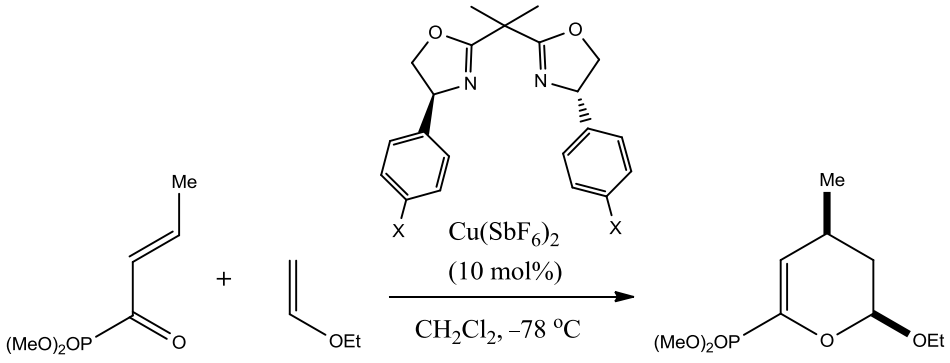
n = 0, X = O-*t*-Bu[168]
n = 0, X = OCH_2Ph[168]
n = 0, X = OCF_3[168]
n = 1, X = OMe[168]
n = 1, X = OCH_2Ph[168]
n = 1, X = $OCH_2CH{=}CH_2$[169]
n = 1, X = H: **50**



1-naphthyl *2-naphthyl* *9-anthryl*

Figure 2.44

The importance of electronic effects in asymmetric catalysis has been increasingly recognised.[170,171] Indeed, substituents on ligands that are situated remote from the active metal centre can significantly influence the enantioselectivity and rate of a reaction. Several examples to this effect have been described for bis(oxazoline)-catalysed reactions in the literature *e.g.* electron-withdrawing groups were shown to enhance the reaction rate and induce higher levels of enantioselectivity in the asymmetric hydrosilyation of simple ketones,[172] in asymmetric cyclopropanation reactions of alkenes[173] and in asymmetric reductive aldol reactions[174] catalysed by Rh-PyBOX, Ru-PyBOX and Rh-PhBOX catalysts, respectively. Evans and co-workers investigated the contribution of electronic effects on enantioselectivity for copper-catalysed hetero-Diels-Alder reactions by incorporation of both electron-donating and electron-withdrawing substituents in the *para*-position of the bis(oxazoline) phenyl ring (**Scheme 2.26**).[162] It was found that the level of asymmetric induction remained the same when a *para*-hydrogen was replaced by a *para*-methoxy group (93% ee), while a slight decrease was observed for reactions with a chlorine atom (89% ee) at the *para* position. The influence of the electronic properties of ligands has also been described for C–H insertion reactions with rhodium carboxylate and carboxamidate catalysts. In general, electron-withdrawing ligands were found to generate a more reactive carbenoid that undergoes bond formation through an earlier transition state, resulting in reduced selectivity.[7,70,175]



Scheme 2.26

The steric influence of catalysts may also contribute to the stereochemical outcome of asymmetric transformations.[158,160,161] As outlined in **Figure 2.45**,[161] positive and negative effects on enantioselectivity may result for increased steric demand of the aryl substituent of bis(oxazoline) ligands depending on the reaction under investigation; the 1-Np-BOX ligand was shown to provide the highest enantioselectivity (74% ee) for the $Mg(OTf)_2$-catalysed tandem oxa-Michael addition-Friedel-Crafts alkylation reaction, with a slight decrease in enantiocontrol observed for reactions in the presence of the Ph-BOX (65% ee) and 2-Np-BOX (62% ee) ligands [**Figure 2.45**, (a)]. Despite the increased steric demand of the 9-Ant-BOX, the use of this ligand in combination with $Mg(OTf)_2$ resulted in a dramatic decrease in asymmetric induction (20% ee). In contrast, a significant increase to

45% ee was observed for the hetero-Diels-Alder reaction in the presence of 9-Ant-BOX relative to corresponding reactions with the Ph-BOX (13% ee) and 1-Np-BOX (19% ee) ligands [**Figure 2.45**, (b)]. Similar levels of enantioselectivity were recorded for the Ph-BOX- (24% ee), 1-Np-BOX- (19% ee) and 2-Np-BOX-catalysed (31% ee) Mukaiyama aldol reactions [**Figure 2.45**, (c)]. Despite the use of X-ray crystallography to acquire more details on the exact geometry of the copper-aryl-BOX complexes, Rutjes and co-workers could not find a conclusive explanation for the observed dependency of the stereochemical outcome of the reactions examined on a particular ligand.

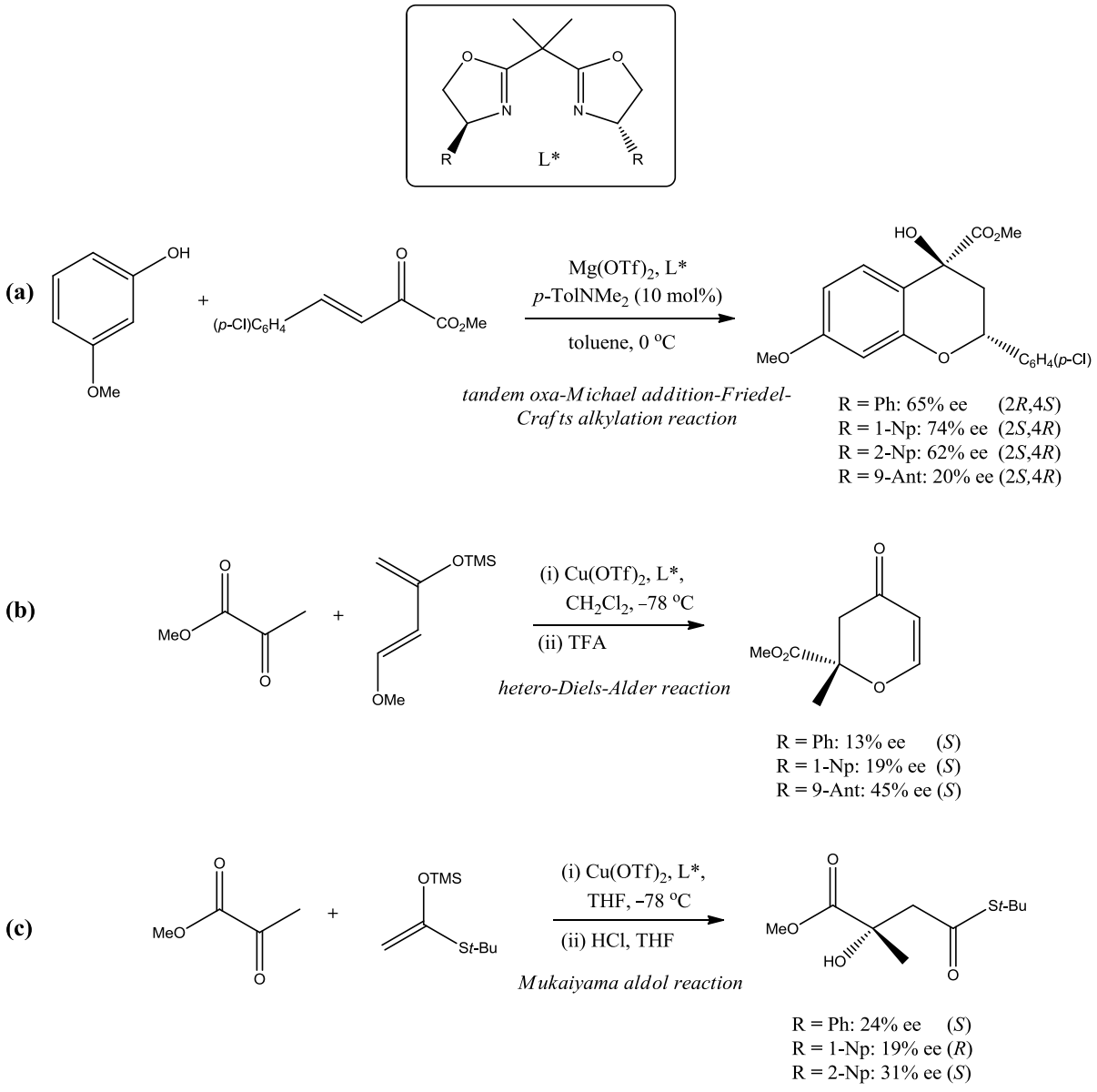
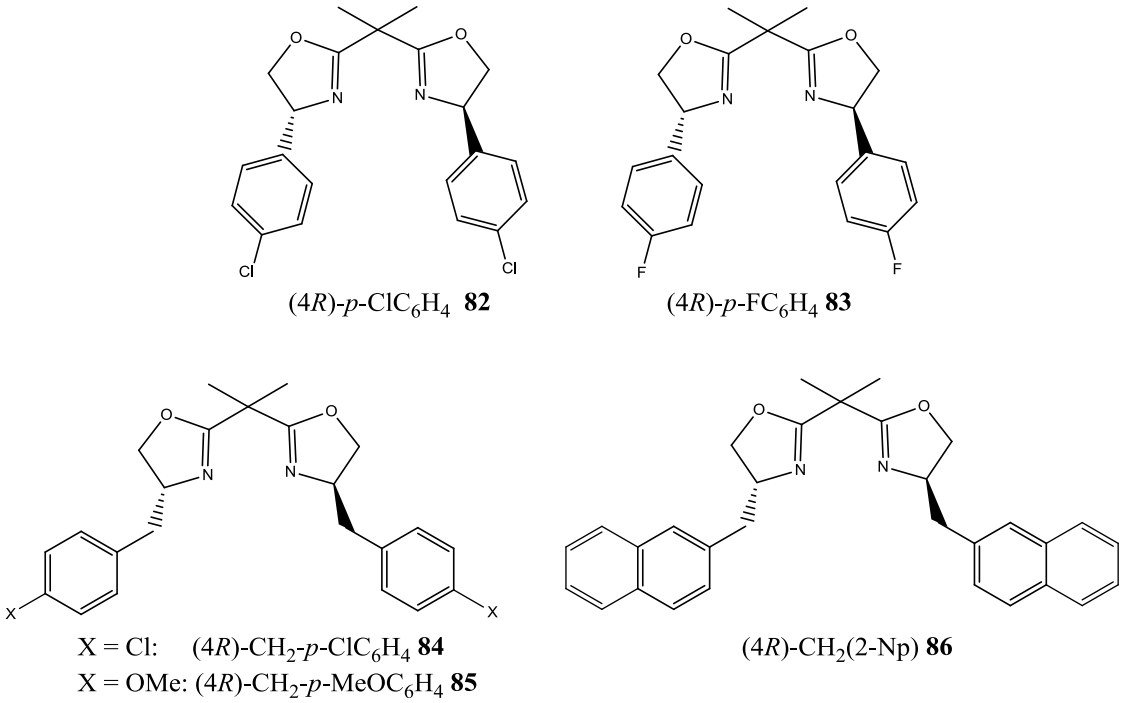


Figure 2.45

Taking the above reports into account, we envisaged that alterations of the electronic and steric properties of the substituents on the aryl ring on the bis(oxazoline) scaffold should modulate asymmetric induction and consequently, the preparation of five ligands was

targeted (**Figure 2.46**), exploring modifications to both the phenyl- and benzyl-substituted bis(oxazoline) series. In particular, we hoped to gain a greater insight into the key ligand properties which govern enantiocontrol in the copper-catalysed C–H insertions under investigation, and thereby allow for better informed and more logical catalyst design in future research projects in this area. The ultimate objective of this work was to use the information obtained to design a generally applicable catalyst-ligand system.



Note: shorthand ligand names used for convenience

Figure 2.46

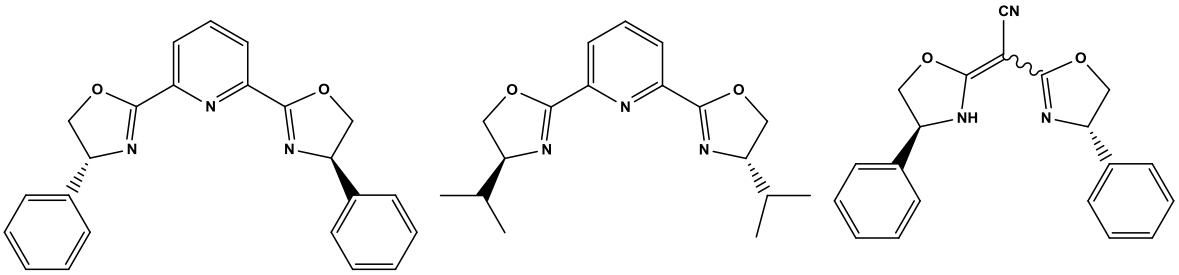
The phenyl-substituted ligands (4*R*)-**82** and (4*R*)-**83** were previously prepared in this research group in a project examining asymmetric induction in the intramolecular Buchner reaction of α-diazoketones.[176] In this earlier work, inclusion of inductively electron-withdrawing chlorine and fluorine substituents on the phenyl ring was found to have little or no effect on enantioselectivity, with minimum effects on catalyst reactivity also recorded. It was found in this case that the stereochemical outcome of the aromatic addition reaction was governed more by the electronic nature of the aryl ring on the α-diazoketone substrate.

The benzyl-substituted bis(oxazoline) (4*R*)-**50** has displayed a particular propensity for highly enantioselective cyclopentanone syntheses in the C–H insertion reactions described thus far in this research project. Fine-tuning of the catalyst scaffold of (4*R*)-Bn **50** was, therefore, a logical choice considering the potential for further enhancing the enantioselectivity of this ligand. In addition, synthesis of benzyl-substituted ligand structures (derived from phenylalaninol analogues) is inherently easier than the synthesis of the analogous phenyl-substituted bis(oxazolines) due to risk of racemisation of the more labile stereogenic centre starting from substituted phenylglycines, an occurrence

which had proved problematic in previous bis(oxazoline) syntheses with phenylglycine-derived substrates.[176] Three novel benzyl-substituted ligands (**84**, **85** and **86**) were prepared in this study, allowing investigation of the impact of both electron-withdrawing effects (X = Cl) and electron-donating effects (X = MeO) and examination of steric effects *via* the introduction of a bulky naphthalene substituent.

Note: while chlorine is inductively electron-withdrawing it can also donate electron density through resonance effects.

Investigation of the influence of ligand structure on enantiocontrol was also extended to include application of the commercially available pyridine-bis(oxazolines) **87** and **88** and the semicorrin ligand **89** (**Figure 2.47**).



Py-(4*R*)-Ph **87** Py-(4*S*)-*i*-Pr **88** CN-(4*S*)-Ph **89**

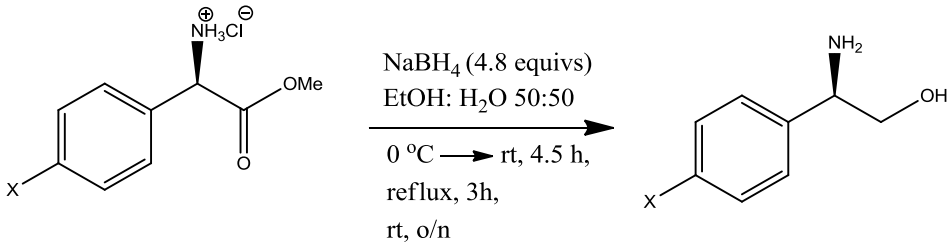
Note: shorthand ligand names used for convenience

Figure 2.47

2.8.1 Synthesis of bis(oxazoline) ligands

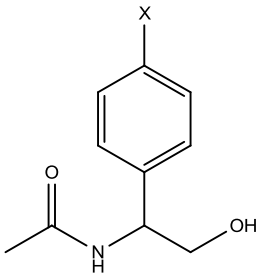
Synthesis of the phenyl-substituted bis(oxazolines) (4*R*)-**82** (previously described by Evans[162]) and (4*R*)-**83** (previously described by O'Keeffe;[176] not reported in the literature) was first conducted using the synthetic strategy previously adopted by O'Keeffe.[176] Accordingly, (*R*)-4-chlorophenylglycine methyl ester hydrochloride[177] and (*R*)-fluorophenylglycine methyl ester hydrochloride[177] were transformed to the corresponding enantiopure amino alcohols (*R*)-**90** and (*R*)-**91** in the presence of $NaBH_4$ following methodology outlined by Meyers (**Table 2.27**).[178]

Table 2.27 *Synthesis of amino alcohols* ***90*** *and* ***91***



Entry	X	Amino alcohol	Yield (%)	$[\alpha]_D^T$
1	Cl	**90**	70	–41.2 (*c* 0.69, 18 °C, $CHCl_3$)
				lit.[176] –40.1 (*c* 0.69, 18 °C, $CHCl_3$)
2	F	**91**	74	–47.1 (*c* 0.79, 20 °C, $CHCl_3$)
				lit.[176] –46.2 (*c* 0.79, 20 °C, $CHCl_3$)

Work-up procedures employed by O'Keeffe for this reaction involved extraction of the crude product mixture with ethyl acetate. In this project, such a strategy was found to result in the formation of significant amounts of the tentatively assigned *N*-acetyl side product *N*-[1-(4-halophenyl)-2-hydroxyethyl)acetamide (**Figure 2.48**), characterised by signals at δ_H 6.14 (1H, bs, N*H*), 5.03–5.09 (1H, m, C*H*CH_2OH), 3.89 (2H, d, *J* 3.2, CHC*H*$_2$OH), 2.05 (3H, s, $COCH_3$), in line with literature reports for similar compounds.[179,180] This side product most likely results from *N*-acetylation through reaction of the primary amine with ethyl acetate. Ethyl acetate was, therefore, replaced with diethyl ether for purification of subsequent reduction reactions, providing access to the desired amino alcohols (*R*)-**90** and (*R*)-**91** in excellent purity and good yield (**Table 2.27**).



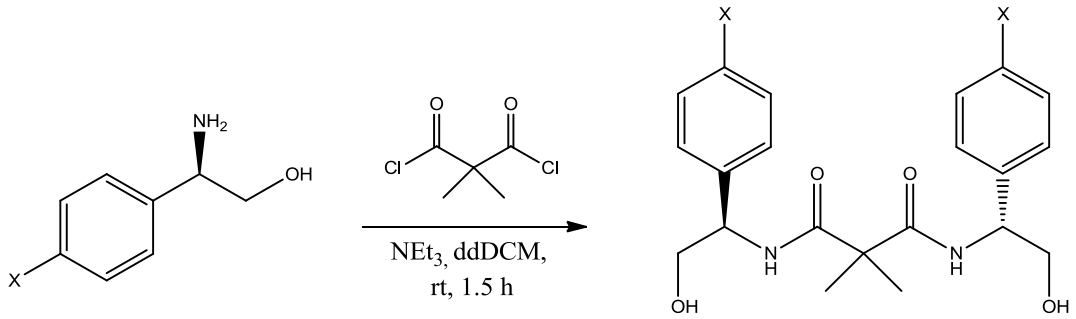
N-[1-(4-halophenyl)-2-hydroxyethyl]acetamide

Figure 2.48

Acylation of the amino alcohols (*R*)-**90** and (*R*)-**91** was next conducted *via* reaction with triethylamine and 0.5 equivalents dimethylmalonyl chloride **92**, which functions to introduce two methyl groups on the spacer carbon of the bis(oxazoline) skeleton, providing the analogous bisamides (*R*)-**93** and (*R*)-**94** (**Table 2.28**). Yields obtained for synthesis of the bisamides were poor (35%) for both the chlorine and fluorine products (**Table 2.28**, entry 1 and 2), representing significantly lower values than those reported by

O'Keeffe (73% for **93** and 80% for **94**).[176] It is suspected that loss of yield may have occurred due to formation of bisamide salts following addition of aqueous hydrochloric acid to the reaction mixture and resulting loss of product during aqueous extractions. Careful monitoring of pH during work-up procedures is, therefore, warranted for future bisamide syntheses *via* this method. Challenges with solubility may also have contributed to low product yields. Varying amounts of triethylamine hydrochloride salt were typically observed in the ^{1}H NMR spectra of the isolated products. Accordingly, the crude bisamides (*R*)-**93** and (*R*)-**94** were triturated in water for approximately 15 minutes followed by filtration of the suspension and rinsing with hexane to remove the triethylamine side-product.

Table 2.28 *Synthesis of bisamides **93** and **94***

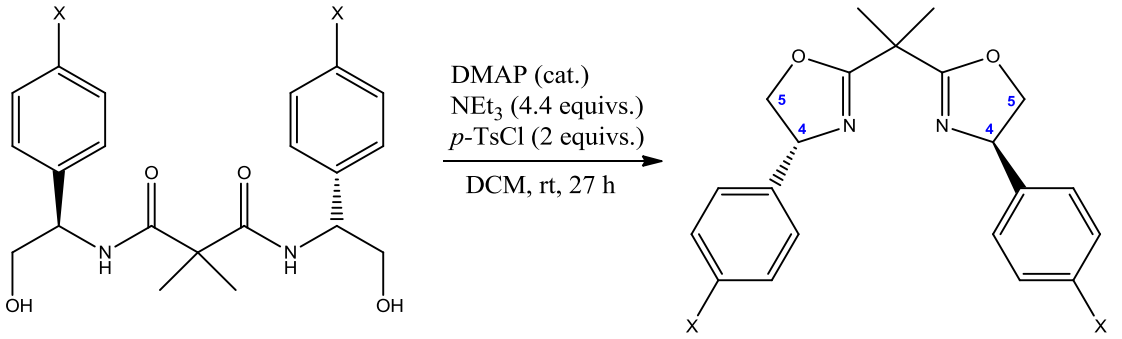


Entry	X	Amino alcohol	Bisamide	Yield (%)[a]
1	Cl	**90**	**93**	35
2	F	**91**	**94**	35

[a] Yield of bis(oxazoline) following column chromatography.

Finally, the oxazoline ring-forming step was achieved by treatment of the bisamides (*R*)-**93** and (*R*)-**94** with *p*-tosyl chloride and triethylamine in the presence of a catalytic quantity of 4-(dimethylamino)pyridine (DMAP) following the procedure described by Evans and employed earlier by O'Keeffe.[176,181] This affects the *in situ* formation of the bis(tosylate), which undergoes cyclisation to give the desired bis(oxazolines) (4*R*)-**82** and (4*R*)-**83** in good yields (**Table 2.29**, entry 1 and 2) in the same range as those previously reported by Evans and O'Keeffe.[176,181] Column chromatography on silica gel, using diethyl ether and hexane as eluent, was employed to purify the crude bis(oxazolines). TLC analysis proved troublesome as the bis(oxazolines) products were not UV active and could only be visualised by staining with potassium permanganate solution and in practice several rounds of chromatography were often required to remove all impurities present. Nonetheless, (*R*)-**82** and (*R*)-**83** were successfully isolated in analytically pure form and critically, specific rotations for these compounds compared favourably with literature data.[176]

Table 2.29 *Synthesis of bis(oxazoline) ligands* ***82*** *and* ***83***

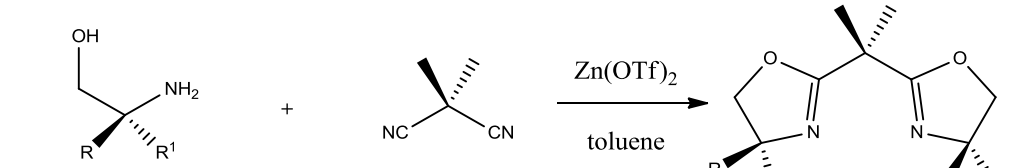


Entry	X	Bisamide	Bis(oxazoline)	Yield (%)	$[\alpha]_D^{20}$
1	Cl	**93**	**82**	67	+133.0[a] (*c* 0.37, CH_2Cl_2) lit.[176] +169.0 (*c* 0.37, CH_2Cl_2) lit.[162] –141.0 (*c* 7.4, CH_2Cl_2, *S*-**82**)
2	F	**94**	**83**	75	+130.3 (*c* 0.30, $CHCl_3$) lit.[176] +125.7 (*c* 0.30, $CHCl_3$)

[a] Bis(oxazoline) **82** was found to be >98% enantiopure by chiral stationary phase HPLC analysis (see appendix for details).

Spectral characteristics for the *para*-chlorophenyl- and *para*-fluorophenyl-substituted bis(oxazolines) (4*R*)-**82** and (4*R*)-**83**, respectively, were in line with previous reports.[162,176] The protons at C5 of the oxazoline ring are diastereotopic due to the adjacent chiral centre at C4 and each proton appears as a doublet of doublets due to ABX splitting with each other (AB) and the C4 proton (X). Similarly, a doublet of doublets signal is also observed for the C4 proton.

When subsequently commencing synthesis of the benzyl-substituted ligands **84**, **85** and **86**, an alternative synthetic route was sought due to the poor yields obtained for preparation of the bisamides and difficulties encountered when purifying the bis(oxazolines), both of which contributed to a poor overall product recovery for the synthetic sequence. Many routes have been identified in the literature by which amino alcohols can be used for the construction of the bis(oxazoline) framework.[95,182] In 2005, García and co-workers described an efficient and general one-pot method for the synthesis of chiral bis(oxazoline) ligands catalysed by zinc triflate (**Scheme 2.27**).[183] This was an attractive procedure for our desired ligand syntheses as the requirement for bisamide synthesis was circumvented and, therefore, the synthetic pathway to the final bis(oxazoline) product was reduced by one step. In addition, yields of typically 90% or greater were reported for reactions with a wide variety of different chiral amino alcohols without the need for product purification *via* column chromatography.



R^1 = H and R = Ph, CH_2Ph, *i*-Pr, *t*-Bu, Me, indanyl.
R^1 = Me and R = Ph.

75-100% yield

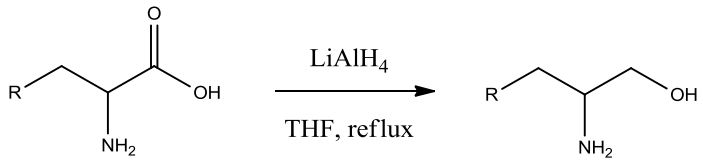
Scheme 2.27

In order to prepare the desired benzyl-substituted ligands, access to the enantiopure phenylalaninol derivatives **95** (R = *p*-ClC_6H_4), **96** (R = *p*-$MeOC_6H_4$) and **97** (R = 2-Np) was first required. Reduction of the commercially available 4-chlorophenylalanine, 4-methoxyphenylalanine and 2-naphthylalanine starting materials was initially attempted using the $NaBH_4$ procedure employed for synthesis of the phenylglycine-derived amino alcohols (*R*)-**90** and (*R*)-**91**, however, no reduction product was obtained, likely due to poor solubility of the amino acid substrates in the ethanol/water solvent system. Several other reduction methods were subsequently trialed including $NaBH_4$/iodine reduction in tetrahydrofuran (THF)[184] and transformation of the carboxylic acid moiety to a mixed anhydride *via* treatment with *N*-methylmorpholine and ethyl chloroformate, followed by $NaBH_4$ reduction in methanol,[185] however, again little or no amino alcohol formation was observed. Reduction of the phenylalanine-substituted amino acids was next attempted with $LiAlH_4$ using the procedure described by Hilmersson.[186] This method, involving slow addition of the amino acid substrates to a mixture of the hydride in THF followed by overnight reflux of the resulting solution, proved successful, allowing access to the desired amino alcohols in high yield and without the need for further purification (**Table 2.30**). Spectral characteristics for **95**, **96** and **97** were in agreement with previously reported data,[168,187-189] however, specific rotation values were available only for (*S*)-**96**.

Note: literature precedent exists for the use of both $NaBH_4$ and $LiAlH_4$ for the reduction of both phenylalanine and phenylglycine derivatives with excellent retention of enantiopurity.[168,185,190]

The targeted benzyl-substituted bis(oxazolines) **84**, **85** and **86** are novel compounds. Thus, as no literature data was available to confirm the enantiopurity of the novel ligands by comparison of specific rotation values, synthesis of both enantiomers of **84**, **85** and **86** and thus, the corresponding amino alcohols **95**, **96** and **97** (**Table 2.30**), was undertaken to allow determination of enantiopurity of the final bis(oxazoline) ligands by chiral stationary phase HPLC analysis.

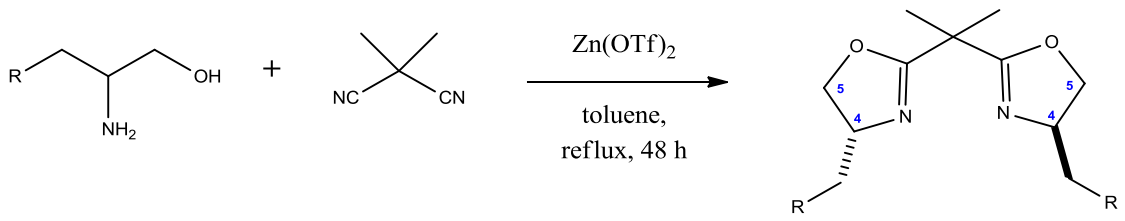
Table 2.30 *Synthesis of amino alcohols* ***95***, ***96*** *and* ***97***



Entry	R	Amino alcohol	Yield (%)	$[\alpha]_D^{20}$
1	*p*-ClC_6H_4	(*S*)-**95**	78	–12.4 (*c* 0.99, CH_2Cl_2)
2	*p*-ClC_6H_4	(*R*)-**95**	99	+13.0 (*c* 0.99, CH_2Cl_2)
3	*p*-$MeOC_6H_4$	(*S*)-**96**	72	–19.0 (*c* 0.99, CH_2Cl_2)
				lit.[168] –15.0 (*c* 0.99, CH_2Cl_2)
4	*p*-$MeOC_6H_4$	(*R*)-**96**	95	+17.1 (*c* 0.99, CH_2Cl_2)
5	2-Np	(*S*)-**97**	91	–15.8 (*c* 0.99, CH_2Cl_2)
6	2-Np	(R)-**97**	98	+17.6 (*c* 0.99, CH_2Cl_2)

With the required enantiopure chiral amino alcohols (*S*)-**95**, (*R*)-**95**, (*S*)-**96**, (*R*)-**96**, (*S*)-**97** and (*R*)-**97** now in hand, synthesis of the corresponding bis(oxazolines) (*S*)-**84**, (*R*)-**84**, (*S*)-**85**, (*R*)-**85**, (*S*)-**86** and (*R*)-**86**, respectively, was next conducted using the one-pot method reported by García and co-workers (**Scheme 2.27**).[183] Accordingly, the phenylalanine-derived amino alcohol substrates were reacted with 2,2-dimethylmalononitrile in the presence of a stoichiometric amount of zinc triflate. Following heating of the reaction mixture under reflux in toluene for 48 h and subsequent brine and aqueous sodium bicarbonate washes, the bis(oxazoline) products were obtained in good yields and excellent purity (**Table 2.31**). Chromatographic purification was, therefore, unnecessary thus avoiding the difficulties previously encountered during column chromatography of (*R*)-**82** and (*R*)-**83** owing to the poor UV activity of the bis(oxazoline) products. Purification by recrystallisation was, however, required for the synthesis of (*S*)-**85** and (*S*)-**86** due to the presence of baseline impurities in the isolated product samples (**Table 2.31**, entries 3 and 5).

Table 2.31 *Synthesis of bis(oxazoline)* ***84****,* ***85*** *and* ***86***



Entry	R	Bis(oxazoline)	Yield (%)	$[\alpha]_D^{20}$
1	*p*-ClC_6H_4	(*S*)-**84**	70	–46.0 (*c* 0.30, $CHCl_3$)
2	*p*-ClC_6H_4	(*R*)-**84**	55	+53.5 (*c* 0.30, $CHCl_3$)
3	*p*-$MeOC_6H_4$	(*S*)-**85**	60[a]	–33.5 (*c* 0.30, $CHCl_3$)
4	*p*-$MeOC_6H_4$	(*R*)-**85**	74	+25.7 (*c* 0.30, $CHCl_3$)
5	2-Np	(*S*)-**86**	41[a]	–34.7 (*c* 0.30, $CHCl_3$)
6	2-Np	(*R*)-**86**	61	+33.7 (*c* 0.30, $CHCl_3$)

[a] Yield of bis(oxazoline) following recrystallisation in a 4 : 1 mixture of hexane : DCM.

The bis(oxazolines) (*S*)-**84**, (*R*)-**84**, (*S*)-**86** and (*R*)-**86** were obtained as white solids, while the corresponding *para*-methoxyphenyl derivatives (*S*)-**85** and (*R*)-**85** were isolated as light yellow oils. HRMS was employed to characterise the molecular ions of the novel ligand structures (see **Section 4.8.3** for details). The benzyl-substituted bis(oxazolines) were characterised in the ^1H NMR spectra by doublet of doublet signals at approximately δ_H 3.97 and 4.16, representing the individual diastereotopic protons at C5 which exist in an ABX splitting pattern with the C4 proton as was previously observed for the phenyl-substituted ligands (*R*)-**82** and (*R*)-**83**. A similar signal pattern was observed for the diastereotopic benzylic protons which also undergo ABX splitting with the C4 proton resulting in two doublet of doublet signals in the region of δ_H 2.60–3.22. Characteristic aromatic signals were also detected; two doublets for the *para*-chloro and *para*-methoxy-substituted bis(oxazolines) **84** and **85**, respectively, and a singlet at δ_H 7.61 confirming the 2-naphthlene substitution pattern of **86** (**Figure 2.49**).

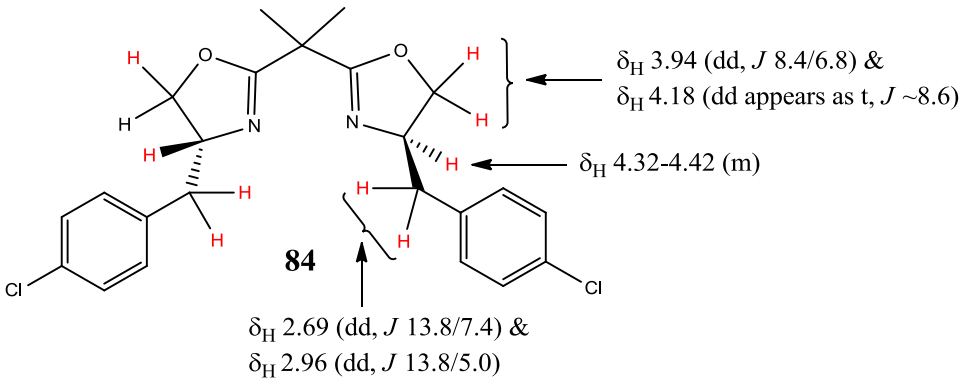


Figure 2.49

The enantiopurity of each of the bis(oxazoline) products **84**, **85** and **86** was determined by chiral stationary phase HPLC analysis. In all cases, the synthesised ligands were found to have enantiopurities ≥97% ee. The absolute stereochemistry of the novel bis(oxazolines) (*S*)-**84**, (*R*)-**84**, (*S*)-**86** and (*R*)-**86** was determined by single crystal analysis (**Figure 2.50**), thus confirming the retention of stereochemistry imparted by the commercially available D- and L-phenylalanine starting materials. Single crystal analysis of (*S*)-**85** and (*R*)-**85** was not possible as these products were isolated as oils. However, as retention of stereochemistry was observed for the corresponding *para*-chlorophenyl- and 2-naphthyl-substituted ligands (*S*)-**84**, (*R*)-**84**, (*S*)-**86** and (*R*)-**86**, we were confident that analogous assignment of absolute stereochemistry for the *para*-methoxy bis(oxazolines) (*S*)-**85** and (*R*)-**85** was justified.

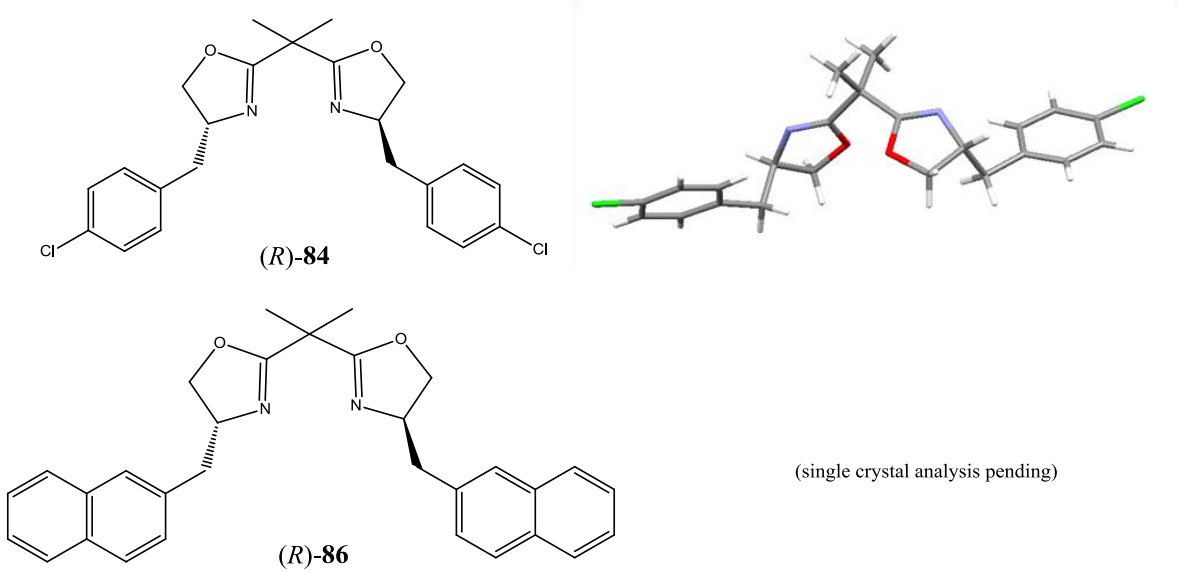
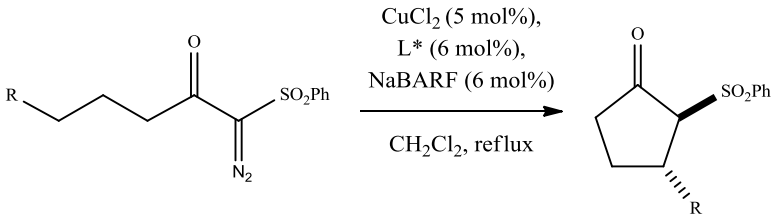


Figure 2.50

2.8.2 C–H insertion reactions with modified bis(oxazoline) ligands

C–H insertions employing the prepared modified bis(oxazoline) ligands (4*R*)-*p*-ClC_6H_4 **82**, (4*R*)-*p*-FC_6H_4 **83**, (4*R*)-CH_2-*p*-ClC_6H_4 **84**, (4*R*)-CH_2-*p*-$MeOC_6H_4$ **85** and (4*R*)-CH_2(2-Np) **86** were next conducted in an effort to further understand the role played by the phenyl ring on the ligand structures in influencing enantioselectivity. The results obtained for these reactions are collated below in **Table 2.32**. Yields recorded for the $CuCl_2$-catalysed reactions were generally good, ranging from 54% (**Table 2.32**, entry 25) to 98% (**Table 2.32**, entries 2, 7 and 13). As was previously observed for reactions with the commercially available phenyl and benzyl bis(oxazolines) (4*R*)-**49** and (4*R*)-**50**, respectively, competition between C–H insertion, diazo reduction and O–H insertion was found to occur, resulting in the formation of minor quantities of byproducts as observed in the ^{1}H NMR spectra of the crude reaction mixtures. Levels of byproducts formed were largely in line with those observed for the corresponding reactions in the presence of (4*R*)-Ph **49** and (4*R*)-Bn **50**.

Table 2.32 *C–H insertion reactions with modified bis(oxazoline) ligands*[a]



Entry	Diazo	Product	R	L*	Time (h)	C–H : Red : O–H[b]	Yield (%)[c]	ee (%)[d,e]
1	**1**	**2**	Me	(4*R*)-*p*-ClC_6H_4 **82**	2	1 : 0.03 : 0.05	94	24 (2*S*, 3*R*)
2	**1**	**2**	Me	(4*R*)-*p*-FC_6H_4 **83**	2	1 : 0.07 : 0.05	98	31 (2*S*, 3*R*)
3	**1**	**2**	Me	(4*R*)-CH_2-*p*-ClC_6H_4 **84**	2	1 : 0.04 : 0.04	95	62 (2*S*, 3*R*)
4	**1**	**2**	Me	(4*R*)-CH_2-*p*-$MeOC_6H_4$ **85**	4	1 : 0.01 : 0.02	98	61 (2*S*, 3*R*)
5	**1**	**2**	Me	(4*R*)-CH_2(2-Np) **86**	2	1 : 0.00 : 0.04	77	53 (2*S*, 3*R*)
6	**32**	**39**	Et	(4*R*)-*p*-ClC_6H_4 **82**	2	1 : 0.04 : 0.03	84[f]	37 (2*S*, 3*R*)
7	**32**	**39**	Et	(4*R*)-*p*-FC_6H_4 **83**	2	1 : 0.03 : 0.03	98[f]	36 (2*S*, 3*R*)
8	**32**	**39**	Et	(4*R*)-CH_2-*p*-ClC_6H_4 **84**	2	1 : 0.10 : 0.05[g]	88[h]	68 (2*S*, 3*R*)
9	**32**	**39**	Et	(4*R*)-CH_2-*p*-$MeOC_6H_4$ **85**	2	1 : 0.04 : 0.04	93[f]	60 (2*S*, 3*R*)
10	**32**	**39**	Et	(4*R*)-CH_2(2-Np) **86**	2	1 : 0.01 : 0.05[g]	87[f]	56 (2*S*, 3*R*)
11	**33**	**40**	*i*-Pr	(4*R*)-*p*-ClC_6H_4 **82**	2	1 : 0.01 : 0.01	78[f]	42 (2*S*, 3*S*)
12	**33**	**40**	*i*-Pr	(4*R*)-*p*-FC_6H_4 **83**	2	1 : 0.06 : 0.04	62	42 (2*S*, 3*S*)
13	**33**	**40**	*i*-Pr	(4*R*)-CH_2-*p*-ClC_6H_4 **84**	2	1 : –[i] : 0.03	98	63 (2*S*, 3*S*)
14	**33**	**40**	*i*-Pr	(4*R*)-CH_2-*p*-$MeOC_6H_4$ **85**	2	1 : 0.06 : 0.00[j]	93	56 (2*S*, 3*S*)
15	**33**	**40**	*i*-Pr	(4*R*)-CH_2(2-Np) **86**	2	1 : 0.25 : 0.10[g]	76[f]	48 (2*S*, 3*S*)
16	**34**	**41**	*t*-Bu	(4*R*)-*p*-ClC_6H_4 **82**	2	1 : 0.06 : 0.05[j]	90[h]	77 (2*S*, 3*S*)
17	**34**	**41**	*t*-Bu	(4*R*)-*p*-FC_6H_4 **83**	2	1 : 0.52 : 0.14[j]	67[h]	74 (2*S*, 3*S*)[k]
18	**35**	**42**	Ph	(4*R*)-*p*-ClC_6H_4 **82**	2	1 : –[l] : 0.05[j]	83[h]	51 (2*S*, 3*S*)
19	**35**	**42**	Ph	(4*R*)-*p*-FC_6H_4 **83**	3	1 : –[l] : 0.13[j]	57	64 (2*S*, 3*S*)
20	**35**	**42**	Ph	(4*R*)-CH_2-*p*-ClC_6H_4 **84**	2	1 : –[l] : 0.03	92	77 (2*S*, 3*S*)
21	**35**	**42**	Ph	(4*R*)-CH_2-*p*-$MeOC_6H_4$ **85**	2	1 : –[l] : 0.03	91	75 (2*S*, 3*S*)
22	**35**	**42**	Ph	(4*R*)-CH_2(2-Np) **86**	2	1 : –[l] : 0.03	95	70 (2*S*, 3*S*)
23	**35**	**42**	Ph	Py-(4*R*)-Ph **87**	20	1 : –[l] : 0.07[j]	59	~0
24	**35**	**42**	Ph	Py-(4*R*)-*i*-Pr **88**	5	1 : –[l] : 0.07	77	32 (2*R*, 3*R*)
25	**35**	**42**	Ph	CN-(4*R*)-Ph **89**	20	1 : –[l] : 0.09	54	17 (2*R*, 3*R*)
26	**64**	**72**	Ph(*p*-Br)	(4*R*)-*p*-ClC_6H_4 **82**	2	1 : 0.15 : 0.12[j]	82[h]	45 (2*S*, 3*S*)
27	**64**	**72**	Ph(*p*-Br)	(4*R*)-*p*-FC_6H_4 **83**	2	1 : 0.07 : 0.07	89[h]	54 (2*S*, 3*S*)
28	**64**	**72**	Ph(*p*-Br)	(4*R*)-CH_2-*p*-ClC_6H_4 **84**	2	1 : 0.01 : 0.04	90	68 (2*S*, 3*S*)
29	**64**	**72**	Ph(*p*-Br)	(4*R*)-CH_2-*p*-$MeOC_6H_4$ **85**	2	1 : 0.01 : 0.04	83	64 (2*S*, 3*S*)
30	**36**	**43**	Bn	(4*R*)-*p*-ClC_6H_4 **82**	2	1 : 0.12 : 0.03[j]	59[f]	31 (2*S*, 3*S*)
31	**36**	**43**	Bn	(4*R*)-*p*-FC_6H_4 **83**	2	1 : 0.13 : 0.07	74[h]	34 (2*S*, 3*S*)

32	**36**	**43**	Bn	(4*R*)-CH_2-*p*-ClC_6H_4 **84**	2	1 : 2.40 : 0.01[j]	86[f]	60 (2*S*, 3*S*)
33	**36**	**43**	Bn	(4*R*)-CH_2-*p*-$MeOC_6H_4$ **85**	2	1 : 0.18 : 0.04	66[f]	55 (2*S*, 3*S*)
34	**36**	**43**	Bn	(4*R*)-CH_2(2-Np) **86**	2	1 : 0.40 : 0.51[j]	69[f]	42 (2*S*, 3*S*)

[a] Reactions conducted using the general procedure for copper-catalysed C–H insertion reactions (see **Section 4.2.9** for details).

[b] Ratio of C–H insertion : diazo reduction (Red) : O–H insertion based on integration of the C(2)*H* doublet of the cyclopentanone product, the C(1)H singlet of the β-keto sulfone byproduct and the C(1)H singlet of the O–H insertion product (see **Figure 2.9** for general structures), respectively, in the ^{1}H NMR spectra of the crude reaction mixture.

[c] Yield of *trans*-cyclopentanone after column chromatography.

[d] Enantiopurity of *trans*-cyclopentanone determined by chiral stationary phase HPLC (see appendix I for details).

[e] Stereochemical assignments for **2**, **39**, **40**, **42** and **43** were made by comparison with previously reported rotation and HPLC data.[20,80] Absolute stereochemistry of **41** and **72** determined by single crystal analysis (see appendix I for details).

[f] Isolated product contains minor amount of β-keto sulfone (R = Et: **24**, *i*-Pr: **25**, *t*-Bu: **26**, Ph(*p*-Br): **70**, Bn: **28**).

[g] Unknown singlet observed at δ_H 9.22 in the ^{1}H NMR spectrum of the crude reaction mixture.

[h] Isolated product not fully clean.

[i] Not determined due to overlap with unknown impurity peak.

[j] Unknown peaks observed in the ^{1}H NMR spectrum of the crude reaction mixture.

[k] Chiral HPLC trace was complex, therefore, value is tentatively assigned.

[l] Ratio of β-keto sulfone (Red) **27** not determined due to overlap with the C(3)H signal of cyclopentanone **42**, but **27** is presumed to be present in low levels.

Comparison of enantioselectivities for copper-catalysed C–H insertion reactions with modified phenyl-substituted bis(oxazoline) ligands

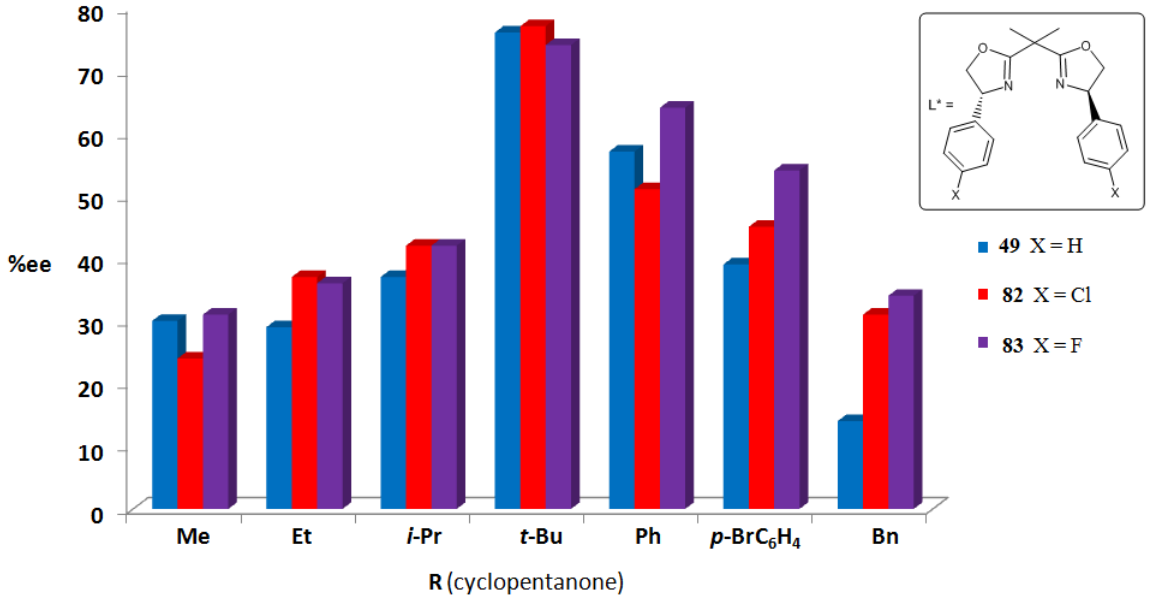


Figure 2.51

Comparison of enantioselectivities for copper-catalysed C–H insertion reactions with modified benzyl-substituted bis(oxazoline) ligands

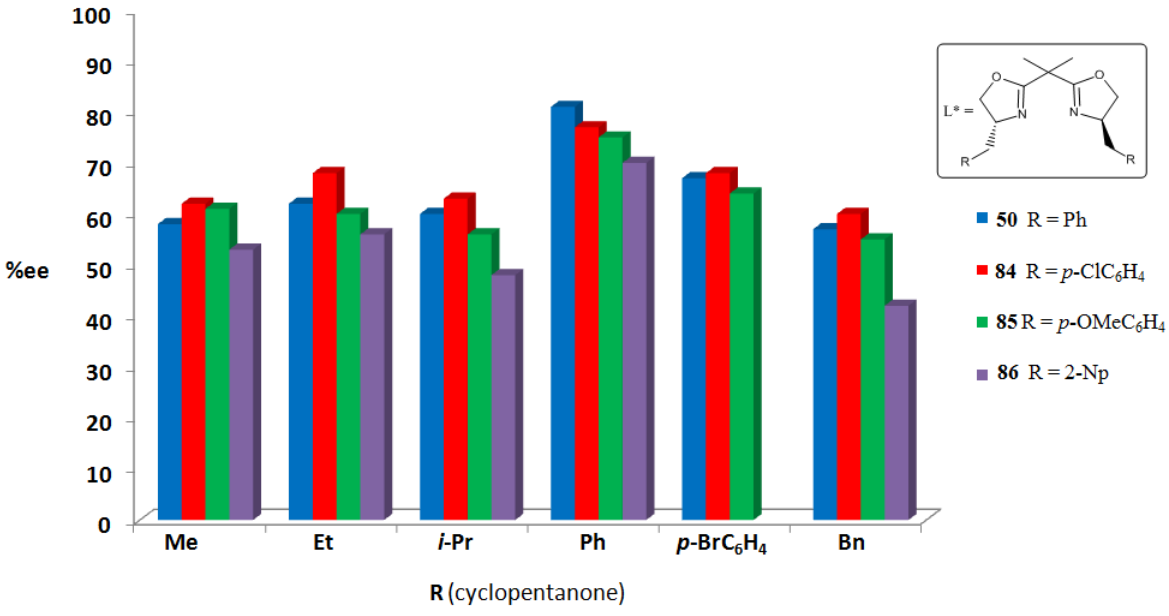
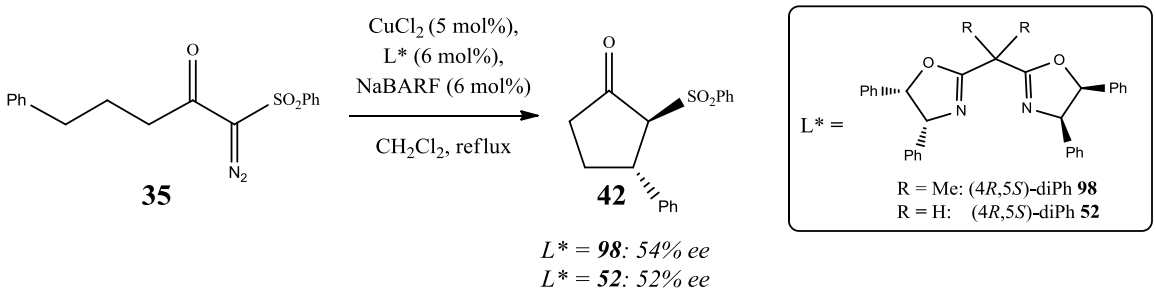


Figure 2.52

The inclusion of electron-withdrawing substituents (X = Cl, F) on the phenyl ring of (4*R*)-**49** was found to have minimal effect on enantiocontrol in the cyclisation reactions of α-diazo-β-keto sulfones **1** (R = Me), **32** (R = Et), **33** (R = *i*-Pr), **34** (R = *t*-Bu), and **35** (R = Ph) (**Figure 2.51**). This outcome is in line with previous observations by O'Keeffe for application of (4*R*)-*p*-ClC_6H_4 **82** and (4*R*)-*p*-FC_6H_4 **83** in the Buchner reaction of α-diazoketones.[176] For C–H insertions with the *para*-bromophenyl- and benzyl-substituted diazo substrates **64** and **36**, respectively, a slight increase in asymmetric induction was noted for employment of the modified ligand structures in the order X =H **49** < X = Cl **82** < X = F **83**. Cyclisations with the *para*-methoxyphenyl-substituted diazo **65** in the presence of the modified bis(oxazoline) ligands were not attempted due to the low chemoselectivity towards C–H insertion observed for reactions with **65** (**Table 2.24**, entries 6–10).

A similar outcome was observed for reactions with the electronically modified benzyl-substituted bis(oxazolines) (4*R*)-CH_2-*p*-ClC_6H_4 **84** and (4*R*)-CH_2-*p*-$MeOC_6H_4$ **85**. Thus, alteration of the electronic nature of the benzyl-ligand structure was found to have minimal impact on enantioselectivity for all α-diazo-β-keto sulfone substrates examined (**Figure 2.52**). Notably, decreased levels of enantiocontrol were recorded for insertions in the presence of (4*R*)-CH_2(2-Np) **86** which features an increased steric demand of the aryl moiety of the benzyl-ligand scaffold relative to reactions with ligand (4*R*)-Bn **50**. Increase of ligand steric bulk, therefore, appears to correlate to a decrease in asymmetric induction, however, examination of further benzyl-ligand modifications *e.g.* R = CH_2(1-Np), CH_2(9-Ant), is required to validate this finding.

Examination of enantiocontrolling effects at the ligand bridgehead position was also conducted. C–H insertions of diazo **35** with the commercially available PyBOX ligands **87** (~0% ee) and **88** (32% ee) and the semicorrin ligand **89** (17% ee) resulted in significantly reduced asymmetric induction compared to reaction with ligand (4*R*)-Ph **49** (57% ee) (**Table 2.32**, entries 23–25 *vs.* **Table 2.14**, entry 22). Thus, the bis(oxazoline) ligand framework is more effective in terms of enantiocontrol for our α-diazo-β-keto sulfone C–H insertion reactions. In order to further investigate the importance of the bridgehead substituents on the bis(oxazoline) scaffold, reaction of diazo **35** in the presence of (4*R*,5*S*)-diPh **98**, featuring a dimethyl substitution pattern at the bridgehead position, was also carried out (**Scheme 2.28**). This ligand was synthesised in our research group by Aoife Ring[191] using the zinc triflate-mediated method described by García.[183] Interestingly, alteration of ligand structure in this way was found to have little effect on enantiocontrol. Previous literature reports have shown that increased steric bulk at the carbon connecting the oxazoline rings generally correlates to an increase in enantiocontrol,[95,182,192,193] therefore, further modifications at this position (R = Et,[194] *i*-Pr,[192] *i*-Bu,[195] Bn[196]) may lead to enhanced enantioselectivity in the C–H insertion reactions of **35** and other α-diazo-β-keto sulfone substrates.



L = **98**: 54% ee*
L = **52**: 52% ee*

Scheme 2.28

2.9 Transition state studies of enantioselective copper-catalysed C–H insertion reactions of α-diazo-β-keto sulfones

Reports of enantioselective copper-catalysed C–H insertion reactions in the literature are sparse, and as a result a detailed mechanistic understanding of such processes has lagged behind that of corresponding rhodium-catalysed transformations, of which many mechanistic studies have been conducted.[59,71,76,197-200] Therefore, in an effort to gain a better insight into the mechanism of enantiocontrol in copper bis(oxazoline)-catalysed insertions, an attempt to rationalise the transition states for this process was undertaken. If achieved, a detailed knowledge of the steps that control the stereochemistry of the insertion products should aid in the identification and design of more efficient catalyst systems for future studies.

Copper-catalysed cyclopropanation of alkenes with diazoacetates was one of the first asymmetric reactions described employing bis(oxazoline) ligands.[201-203] Much work has been conducted to elucidate the mechanism of this carbenoid transformation and an examination of results obtained is worthwhile as background for understanding the key features of copper bis(oxazoline)-catalysed C–H insertion reactions. Pflatz and co-workers proposed an early model in 1988 for cyclopropanation that was later extended by theoretical studies conducted by Fraile and co-workers to rationalise the stereochemical outcome of this reaction.[133,204] The postulated mechanism involves initial formation of the carbenoid (ligand)Cu=$CHCO_2Me$ complex (**Figure 2.53**)[133] followed by approach of the alkene substrate and direct carbene insertion into the double bond. The active species in the cyclopropanation reaction is the monomeric copper(I)-ligand complex. According to the model, the substituents on the carbene of this complex adopt positions perpendicular to the plane spanned by the copper-bis(oxazoline) moieties. This geometry is thought to arise due to steric factors, avoiding interactions of the ester with the R groups of the ligand.[205]

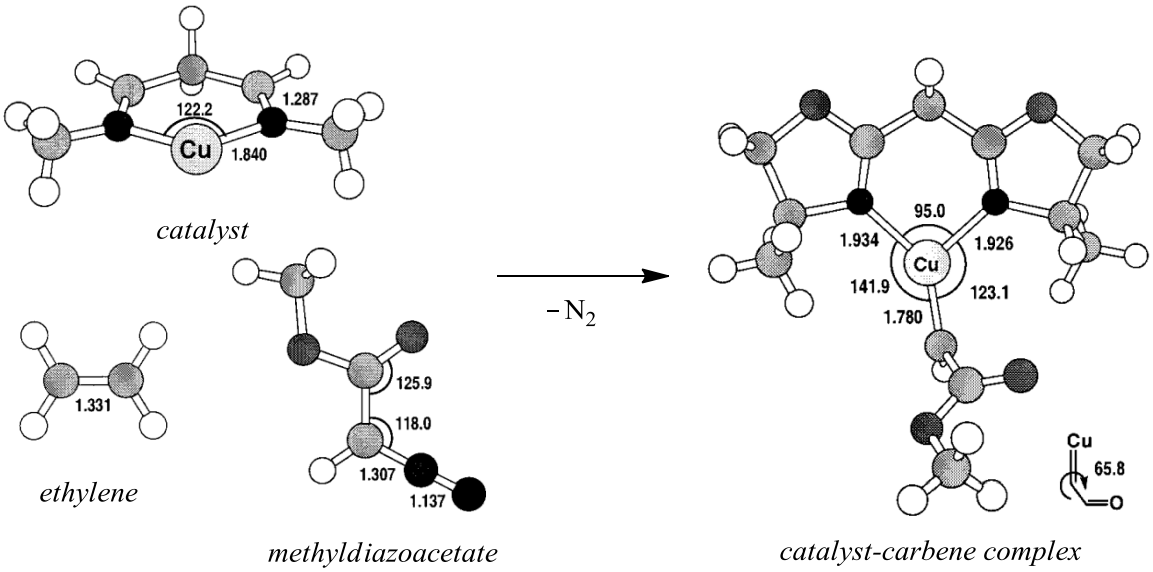
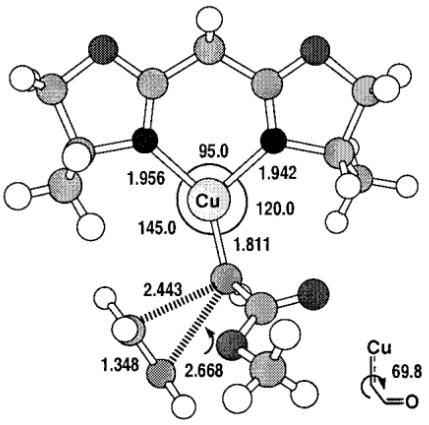
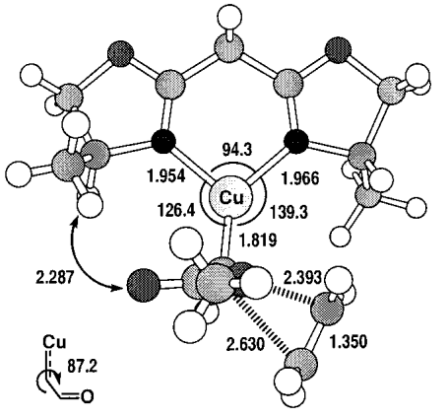


Figure 2.53 *adapted from ref.*[133]

Subsequent alkene attack may result in two possible diastereomeric transition structures, arising from approach of the alkene molecule to the *Re* and *Si* stereofaces of the plane defined by the Cu=C–C arrangement, each leading to different configurations (*R* or *S*) at C(1) of the cyclopropane product. The two transition structures and the asymmetric induction model are displayed in **Figure 2.54**.[133] The main steric interaction responsible for enantioselectivity has been determined to be that between the carbonyl oxygen atom of the ester and the substituent on one of the stereogenic carbon atoms of the bis(oxazoline) ligand. A short distance (2.287 Å) is observed between these two groups for ethylene attack to the *Si* face, meaning the alternative *Re* attack is preferred. Although not shown in **Figure 2.54** (R^1 and R^2 = H), the *cis*/*trans* selectivity of the final cyclopropane products is determined by the steric interaction between the carbene ester group and the substituents on the prochiral carbon of the double bond, with bulky ester groups generally required to achieve good diastereoselectivity. The prochiral alkene carbon is thought to be too remote from the bis(oxazoline) ligand for any efficient asymmetric induction from the ligand to occur.



alkene attack to Re *face*
(favoured)



alkene attack to Si face
(disfavoured)

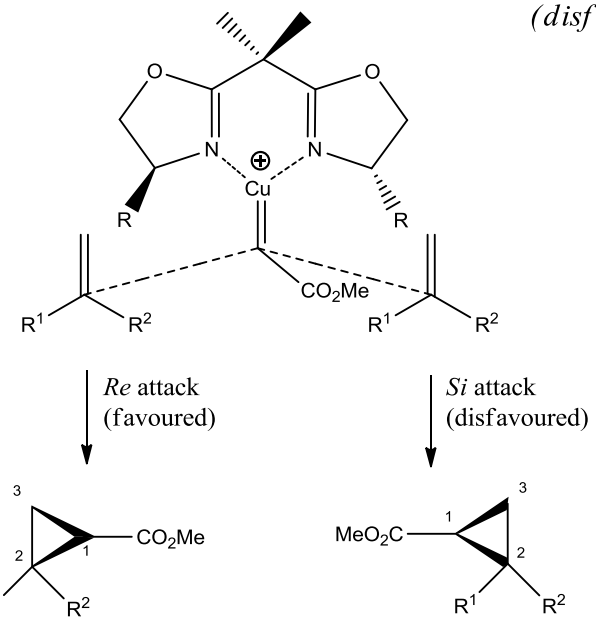


Figure 2.54 *adapted from ref.*[133]

As proposed in theoretical studies on diastereo- and enantioselective rhodium-catalysed C–H insertions, an *n*-membered ring formation reaction proceeds *via* an [n+1]-membered cyclic transition state involving the transferred hydrogen atom.[206] Accordingly, in our system, cyclopentanone formation is proposed to occur *via* a six-membered transition state in a pseudo-chair conformation. Four chair-like transition states are possible, each leading to one of the four possible enantiomeric products (**Figure 2.55**).

*Note: in the following analysis we assume that the copper-ligand complex is more sterically demanding than the sulfonyl substituent, and therefore occupies the pseudo-equatorial position as illustrated in **Figure 2.55** and **Figure 2.56**.*

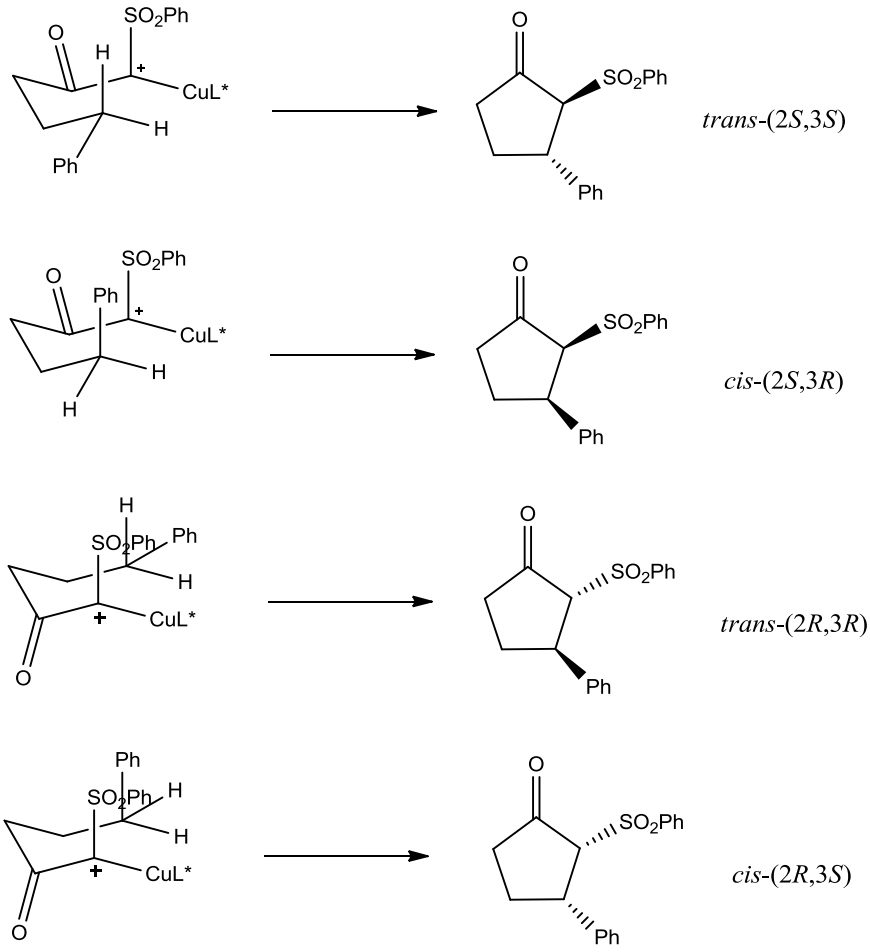


Figure 2.55

Exclusive *trans*-cyclopentanone formation was observed for copper-bis(oxazoline)-catalysed C–H insertions in this project, although epimerisation of the less thermodynamically favoured *cis*-cyclopentanone cannot be unambiguously ruled out. This observation is rationalised on the basis of the transition states displayed in **Figure 2.55**, as the diaxial substituents [leading to *cis*-(2*S*,3*R*) and *cis*-(2*R*,3*S*)] would be disfavoured due to 1,3-steric interactions, thereby favouring formation of the alternative *trans*-cyclopentanone products *via* a diequatorial arrangement of the copper species and R group substituent in the transition state (**Figure 2.56**).

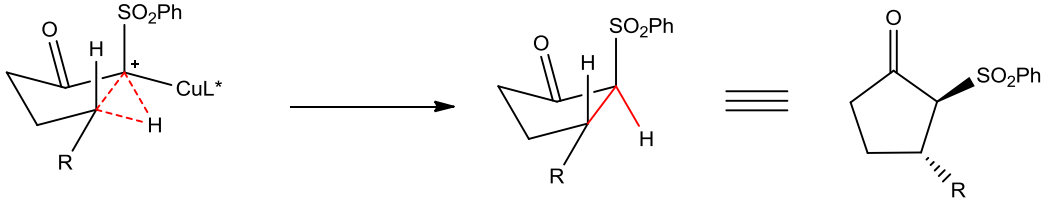


Figure 2.56

A mixture of *cis*- and *trans*-cyclopentanones were observed for rhodium-catalysed C–H insertion. This finding may be due to the increased length of the carbon-rhodium bond versus the carbon-copper bond in the transition state model, owing to the larger van der Waal radius of the former metal. This means that the sulfone group and the rhodium complex may be in equilibrium at the equatorial position and, therefore, a less diastereoselective C–H insertion occurs (**Figure 2.57**).

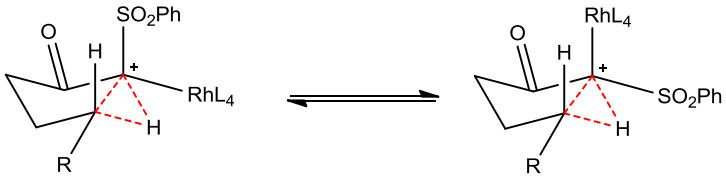


Figure 2.57

A similar rationalisation can be applied to explain the observed stereoselectivities recorded for the C–H insertion reactions of 1-diazo-1-phenylsulfonyl-3-propylhexan-2-one **78** (**Section 2.7.3**). A 1.00 : 4.87 : 1.96 : 3.21 ratio of diastereoisomers was was observed in the ^{1}H NMR spectrum of the crude reaction mixture for the rhodium(II) acetate-catalysed reaction of **78** (**Figure 2.39**). The latter two values (1.96 : 3.21) were found to correspond to (2*R**,3*S**,5*S**)-**81a** and (2*R**,3*S**,5*R**)-**81b**, respectively. Thus, (2*R**,3*S**,5*R**)-**81b**, which is formed *via* the transition state with no unfavourable 1,3-diaxial interactions was found to be in excess (**Figure 2.58**). Similar 1,3-diaxial interactions are observed in the transition states leading to both *cis*-diastereoisomers of **81**: 2*R**3*R**,5*S** and 2*R**,3*R**,5*R** (**Figure 2.58**), which are less thermodynamically favourable relative to the corresponding *trans* isomers and are therefore, not observed in the ^{1}H NMR spectrum of the product mixture isolated followed chromatographic purification (**Figure 2.40**). A 1.00 : 4.87 ratio of *cis*-diastereoisomers was observed for the rhodium(II) acetate-catalysed reaction of **78.** Although unambiguous assignment of the relative stereochemistry of these diastereoisomers cannot be made as the *cis*-cyclopentanone products were not isolated, presumably the minor diastereoisomer is (2*R**,3*R**,5*S**)-**81** owing to the occurrence of two 1,3-diaxial interactions in the transition state leading to this product (**Figure 2.58**). In the copper-catalysed reactions of **78**, an excess of (2*R**,3*S**,5*R**)-**81b** over (2*R**,3*S**,5*S**)-**81a** was observed in the ^{1}H NMR spectra of the crude reaction mixtures for each of the cyclisations examined (**Table 2.25**). Again, this outcome is accounted for by the steric strain resulting from 1,3-diaxial interactions between the n-propyl and sulfonyl substituents in the transition states leading to **81a** (**Figure 2.58**).

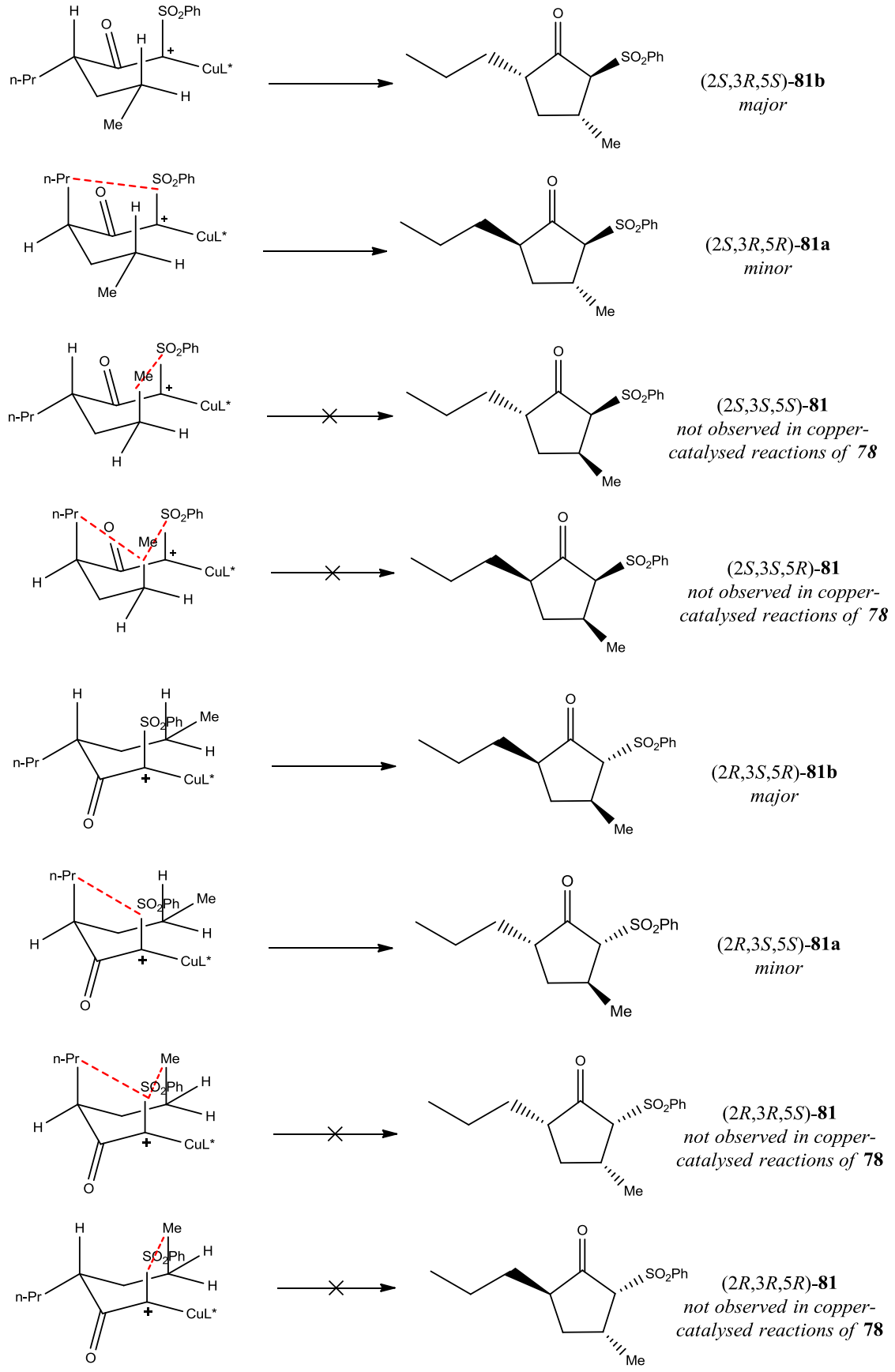

(2S,3R,5S)-81b
major
(2S,3R,5R)-81a
minor
(2S,3S,5S)-81
not observed in copper-catalysed reactions of 78
(2S,3S,5R)-81
not observed in copper-catalysed reactions of 78
(2R,3S,5R)-81b
major
(2R,3S,5S)-81a
minor
(2R,3R,5S)-81
not observed in copper-catalysed reactions of 78
(2R,3R,5R)-81
not observed in copper-catalysed reactions of 78

Figure 2.58

Over-interpretation of the different outcomes in terms of diastereocontrol for the copper- and rhodium-mediated systems must be undertaken with caution. In general, rhodium-catalysed C–H insertions occur very quickly (~0.5 h) and are essentially complete following dropwise addition of the α-diazo sulfone substrate, while extended heating (≥2 h) is generally required to bring the corresponding copper-catalysed reactions to completion. Thus, while *cis*-cyclopentanone formation may occur in the initial C–H insertion step, epimerisation to the more thermodynamically stable *trans*-isomer can be envisaged. Indeed evidence for this epimerisation has been seen in this work (**Table 2.11**) and by other researchers in the team.[11]

Unlike achiral rhodium and copper complexes, the two faces of a chiral carbene complex are no longer equivalent. Thus, as shown in **Figure 2.59**, there are two possible approaches of the reacting C–H bond (**A** and **B**). For each approach, the R group of the diazo precursor can be either *cis* or *trans* with respect to the sulfone substituent bonded to the carbene carbon. Accordingly, diastereoselectivity (as discussed above) is controlled by insertion into either of the two pro-chiral hydrogen atoms (as determined by the steric influence of the diazo R substituent, **Figure 2.55**), while enantioselectivity is governed by the facial selectivity of the carbenoid to which the reacting C–H bond approaches (as determined by the ligand R^1 substituents). Enantiocontrol thus occurs in a similar manner to that reported for asymmetric cyclopropanation reactions, where enantioselectivity is determined by approach of the alkene substrate to either the *Re* or *Si* face of the carbene carbon.

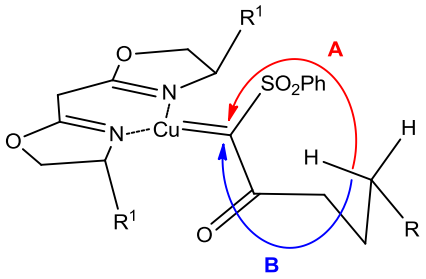


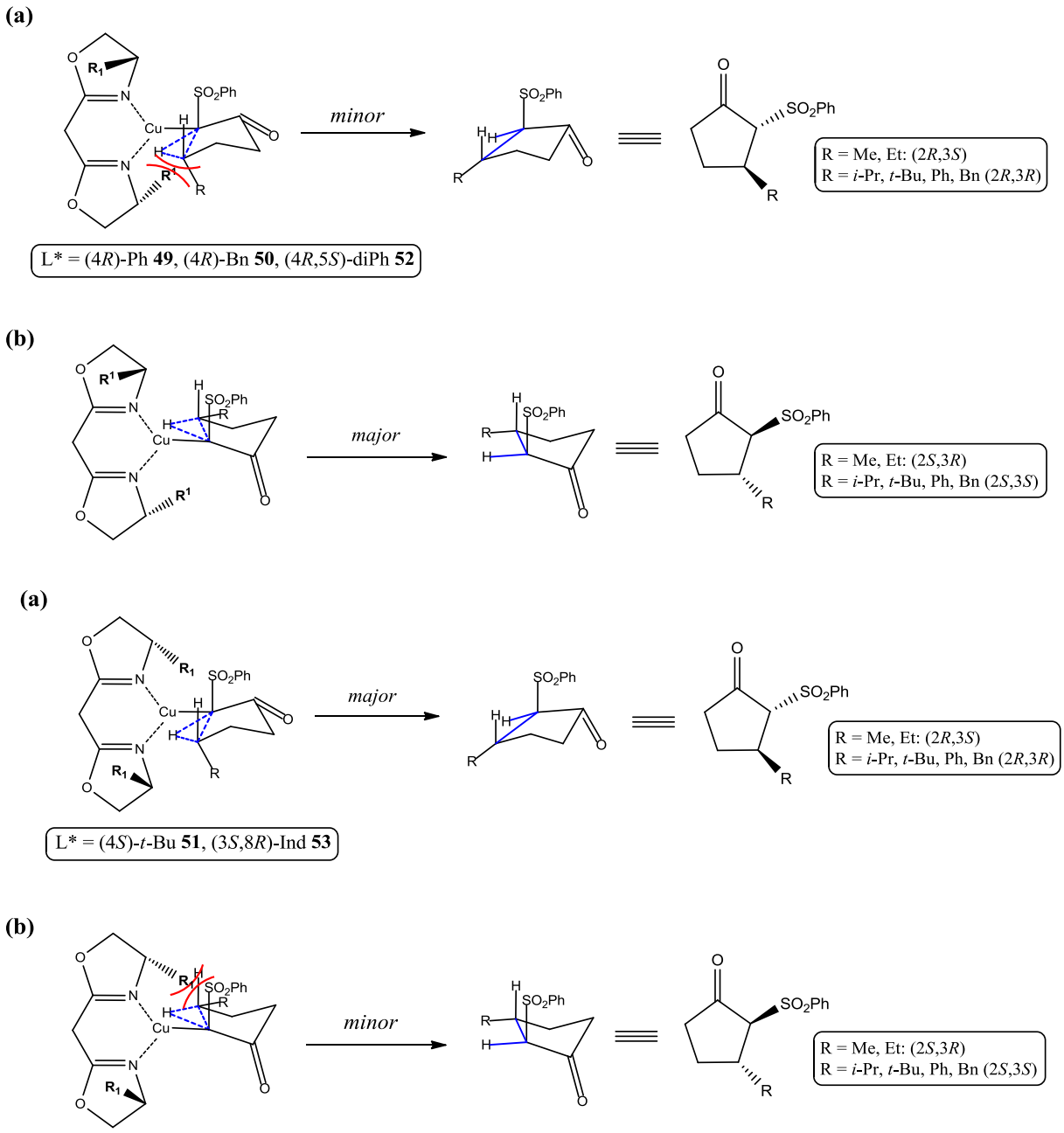
Figure 2.59

Rationalisation of the basis for the observed enantioselectivities in the C–H insertions of α-diazo-β-keto sulfones recorded in this project (**Figure 2.18**) may be achieved by examination of the transition states presented in **Figure 2.60**. Moderate levels of asymmetric induction were typically recorded for reactions in the presence of (4*R*)-Ph **49**. Change to the benzyl-substituted ligand (4*R*)-Bn **50** resulted in increased levels of enantiocontrol, presumably because the latter ligand positions the aryl ring in a better position for interaction with the diazo substrate, resulting in decreased cyclopentanone formation *via* the "minor" reaction pathway depicted in **Figure 2.60** (a). Interestingly, reactions in the presence of the diphenyl-substituted ligand (4*R*,5*S*)-diPh **52** typically resulted in significantly reduced enantiocontrol relative to reactions with (4*R*)-Ph **49**. Thus, the conformational impact of the additional phenyl substituent in the disubstituted

ligand (4*R*,5*S*)-diPh **52** appears to orientate the phenyl ring in a less favourable orientation in terms of asymmetric induction than can be achieved with the more conformationally mobile ligand (4*R*)-Ph **49**, although exceptions to this trend were observed for two diazo substrates (R = *t*-Bu, Ph).

Largely similar levels of enantioselectivity were observed for C–H insertions in the presence of (4*R*)-Ph **49** and (4*S*)-*t*-Bu **51**. This outcome is particularly important in enhancing our understanding of ligand effects for this process. Thus, it is evident that the influence of the R^1 substituent of the bis(oxazoline) is mainly steric as no significant impact in terms of asymmetric induction is observed when the aryl ring is present at the position adjacent to nitrogen. This finding is further reinforced by the observation of comparable levels of enantiocontrol for reactions of α-diazo-β-keto sulfones **34** (R = *t*-Bu) and **35** (R = Ph) and the fact that minimal impact on enantioselectivity was recorded for diazo substrates **64** and **65** which feature electronically-modified phenyl rings (**Figure 2.36**).

Interestingly, the enantiocontrol observed in the C–H insertion reactions of α-diazo-β-keto sulfone **78**, displayed in **Figure 2.43**, can be rationalised in essentially the same manner as that applied for synthesis of the disubstituted cyclopentanones **2**, **39**–**43**, illustrating that the pendant alkyl chain and the resulting stereogenic centre has no fundamental impact on the enantioselective C–H insertion. The diastereocontrol in this series is essentially conformationally controlled (see **Section 2.7.3** for discussion).



**the structures displayed above are designed to show the favourable and unfavourable steric interactions leading to the major and minor cyclopentanone products, respectively, however, these structures may not accurately represent the transition state geometries leading to C–H insertion.*

Figure 2.60

Highest levels of asymmetric induction in this project were achieved for reactions employing the indane-derived bis(oxazoline) (3*S*,8*R*)-Ind **53** which is characterised by a rigid ligand structure. It is apparent therefore, that the aryl ring in this ligand is positioned in a very favourable position for enantiocontrol, with up to 91% ee achieved for C–H insertion with α-diazo-β-keto sulfone **35** (R = Ph). As the combination of ligand (3*S*,8*R*)-**53** and substrate **35** provided the best result in terms of asymmetric induction in this project, this system was chosen for further modelling studies conducted in conjuction

with Dr. Noel O'Boyle in University College Cork. The results obtained from this study are presented in **Figure 2.61**.

*Note: In the structures in **Figure 2.61**, the geometry of the chiral ligand, the Cu, the carbene C, as well as the two ligand atoms adjacent to the carbene C, are all taken from a DFT calculation at the B3LYP/3-21G level of theory [but using 6-31G(d,p) for the Cu and S] using the Gaussian09 software. The geometry of the remaining atoms was prepared interactively by optimising with the UFF forcefield with the Avogadro software.*

As shown in **Figure 2.61** (a), unfavourable steric interactions between the ligand aryl system and the diazo substrate result in the formation of only minor quantities of the (2*S*,3*S*) isomer of cyclopentanone **42**. The transition state leading to *cis*-(2*R*,3*S*)-**42** [**Figure 2.61**, (b)] is also characterised by unfavourable steric interactions, and thus this isomer is not observed in the ^{1}H NMR spectrum of the initial crude product mixture for this reaction. In contrast, no such steric interaction is observed for the transition state presented in **Figure 2.61** (c) in which the phenyl group is in a pseudo-equatorial position, thereby avoiding interaction with the ligand indane ring and accounting for the significant preference for cyclopentanone formation *via* this transition state.

In the structures depicted in **Figure 2.61**, the phenylsulfone moiety is seen to reside in a position roughly perpendicular to the plane occupied by the bis(oxazoline) ligand. In this research, replacement of the phenylsulfone group with a methylsulfone substituent resulted in decreased levels of enantiocontrol and in two instances a reversal of enantiomeric preferences (**Figure 2.28**). Thus, the presence of the aryl ring in the latter group does impact on the stereochemical outcome of the C–H insertion reaction, presumably through 1,3-steric interactions with the diazo R group (**Figure 2.55**), which would be more unfavourable for the phenyl-substituted sulfone versus the methylsulfone, although interactions with the ligand structure cannot be ruled out. Notably, similar trends in terms of enantioselectivity have also been observed by Hashimoto and co-workers who reported increased levels of asymmetric induction for increasing size of the ester alkoxy substituent in studies examining the C–H insertion reactions of α-diazo-β-keto esters (**Table 1.2**).[91,92] Further modelling studies examining cyclisations of the methylsulfonyl-substituted substrates **37** and **38**, and indeed diazo compounds featuring a wider range of sulfone substituents (*e.g.* SO_2t-Bu, SO_2Np), are required to fully probe the influence of the sulfone substituent.

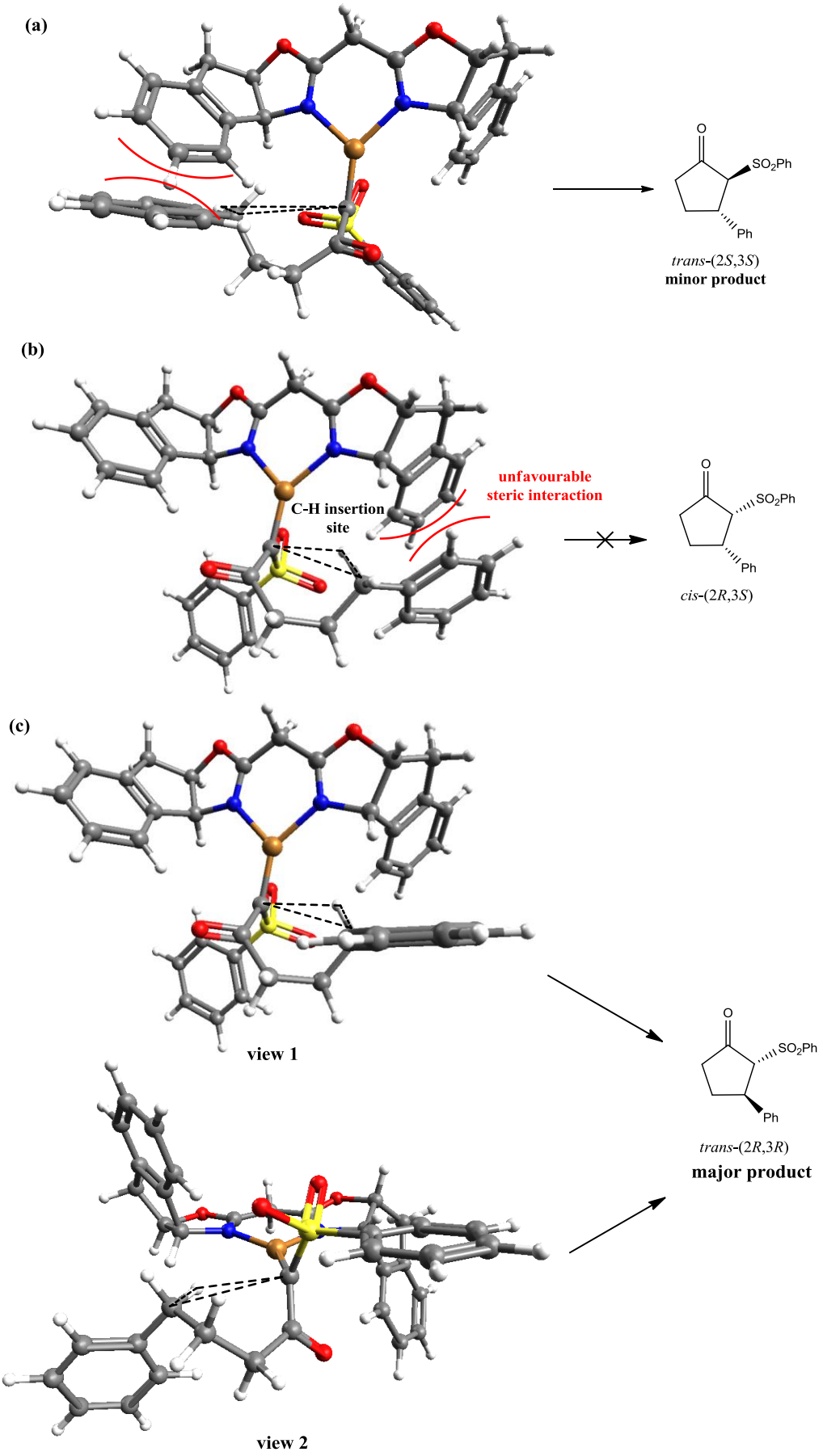

(a)
O
SO2Ph
Ph
trans-(2S,3S)
minor product
(b)
unfavourable
steric interaction
C-H insertion
site
O
SO2Ph
Ph
cis-(2R,3S)
(c)
view 1
O
SO2Ph
Ph
trans-(2R,3R)
major product
view 2

Figure 2.61

It should be noted that in the above discussion of the transition states for copper-bis(oxazoline)-catalysed C–H insertions, the effect of the metal counterion and the additive species has not been included. Two principal geometries are possible for tetracoordinated bis(oxazoline) complexes, namely, tetrahedral and square-planar. Copper(II)-halide complexes with bis(oxazolines), which was the main catalyst type investigated in this project, are known to be considerably more distorted towards a square-planar geometry.[98] As shown in **Figure 2.62**,[98] the chlorine ligands orientate themselves away from the ligand quadrants blocked by the sterically demanding R^1 substituents. Notably, the degree of distortion away from the ideal tetrahedral geometry has been shown to increase with increasing steric bulk of the ligand R^1 substituent.[98] Complexes possessing either tetrahedral or square-planar geometry have been found, in certain cases (mostly hetero-Diels Alder reactions), to display opposite selectivity,[207-214] however, in this project cyclopentanones with the opposite sense of asymmetric induction were obtained for reactions in the presence of (4*S*)-*t*-Bu **51** and (4*R*)-Ph **49** (**Figure 2.15**), highlighting the mechanistic differences between C–H insertion and other copper-bis(oxazoline)-catalysed processes.

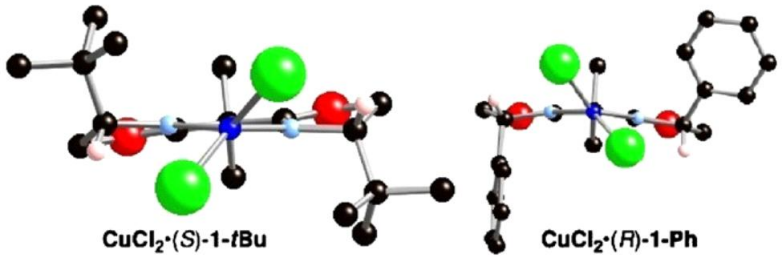


Figure 2.62 *ref.*[98]

The effect of the additive species has previously been discussed in Section **2.6.2.2**. Dramatic increases in enantioselectivity were recorded for CuCl- and $CuCl_2$-catalysed C–H insertions in the presence of NaBARF compared to reactions in which no additive was present (**Figure 2.17**). This increase was rationalised by changes in the geometry of the catalyst structure (**Figure 2.24**) resulting from complete or partial abstraction of chloride by the 'naked' sodium ion of NaBARF (**Figure 2.25**). The presence of NaBARF in the reaction mixture has not been accounted for in the structures presented in **Figure 2.61**, therefore, further detailed examination of the transition states for C–H insertion including the influence of the additive species on catalyst geometry is warranted in future studies to provide a more accurate representation of this process. In reality, in the transition states in **Figure 2.61**, association of chloride with the copper appears to reduce the levels of enantiocontrol through variation of the nature of the catalytic complex.

2.10 Conclusions

In this work, the synthesis and C–H insertion of a range of α-diazo-β-keto sulfones, including seven novel compounds (**33**, **34**, **36**, **60**, **64**, **65** and **81**), has been described. Cyclisations of α-diazo-β-keto sulfone substrates were conducted in the presence of a range of achiral and chiral rhodium and copper catalysts, with particular emphasis on the use of chiral copper complexes, which have not been widely exploited for C–H insertion reactions in the literature. Significantly, the results obtained in this study represent the highest enantioselectivities (up to 91% ee) reported to date for cyclopentanone synthesis *via* C–H insertion and indeed are the only example in the literature of asymmetric copper-catalysed synthesis of α-sulfonyl cyclopentanones. The influence of various additive species on the C–H insertion process was also explored. The borate additives NaBARF and KBARF were found to be the most effective species for permitting highly enantioselective syntheses with short reaction times and minimal byproduct formation. Notably, direct evidence of the mechanistic role of the additive in enantioselective C–H insertion reactions has been reported for the first time.

The impact of substrate and ligand structure was also examined *via* the preparation of several novel α-diazo-β-keto sulfones and bis(oxazoline) compounds. From the results collected it is apparent that enantiocontrol for this process is more sensitive to changes in steric bulk at the C–H insertion site than to alteration of the electronic properties at this position. Modification of the electronic nature of the aryl ring of the ligand was also found to have minimal impact on enantiocontrol, however, increased steric demand of the aryl moiety of the ligand scaffold did lead to decreased asymmetric induction. Importantly, rationalisation of the basis of enantioselectivity has been achieved *via* examination of the theoretical transition states for the C–H insertion process, while further analysis is required to fully rationalise the observed trends based on ligand structure.

In addition to the observed effects on enantioselectivity, interesting trends were also recorded in this project in terms of chemoselectivity. A number of reaction pathways were found to compete with carbenoid C–H insertion, including those leading to O–H insertion and diazo reduction byproducts. Byproduct formation *via* hydride transfer was also observed for reactions of phenyl-substituted diazo substrates, providing the alkylidene tetrahydrofuran byproduct (*Z*)-**54** and the analogous novel compounds (*Z*)-**57**, (*Z*)-**62**, (*Z*)-**77**, (*Z*)-**75** and (*E*)-**75**, with some sense of asymmetric induction observed for synthesis of the latter two compounds. Significantly, the formation of alkylidene tetrahydrofuran byproducts *via* this mechanistically interesting reaction pathway has not previously been reported in the literature.

2.11 References

1. Carey, J. S.; Laffan, D.; Thomson, C.; Williams, M. T. *Org. Biomol. Chem.* **2006**, *4*, 2337-2347.
2. Sweet, M. J. *Berkeley Technology Law Journal* **2009**, *24*, 129-147.
3. Kennedy, M.; McKervey, M. A.; Maguire, A. R.; Roos, G. H. P. *J. Chem. Soc., Chem. Commun.* **1990**, 361-362.
4. Maguire, A. R. *Ph.D. Thesis, NUI* **1989**.
5. Hashimoto, S.-i.; Wantanabe, N.; Ikegami, S. *Synlett* **1994**, *1994*, 353-355.
6. Minami, K.; Saito, H.; Tsutsui, H.; Nambu, H.; Anada, M.; Hashimoto, S.-i. *Adv. Synth. Catal.* **2005**, *347*, 1483-1487.
7. Doyle, M.; McKervey, M.; Ye, T. *Modern Catalytic Methods for Organic Synthesis with Diazo Compounds: From Cyclopropanes to Ylides*; Wiley: New York, **1998**.
8. Müller, P.; Bolea, C. *Molecules* **2001**, *6*, 258-266.
9. Fraile, J. M.; Garcia, J. I.; Mayoral, J. A.; Roldan, M. *Org. Lett.* **2007**, *9*, 731-733.
10. Flynn, C. J.; Elcoate, C. J.; Lawrence, S. E.; Maguire, A. R. *J. Am. Chem. Soc.* **2010**, *132*, 1184-1185.
11. Flynn, C. J. *Ph.D. Thesis, NUI* **2011**.
12. Regitz, M. *Angew. Chem., Int. Ed.* **1967**, *6*, 733-749.
13. Corey, E. J.; Chaykovsky, M. *J. Am. Chem. Soc.* **1965**, *87*, 1345-1353.
14. Bordwell, F. G.; Boutan, P. J. *J. Am. Chem. Soc.* **1957**, *79*, 717-722.
15. Truce, W. E.; Bannister, W. W.; Knospe, R. H. *J. Org. Chem.* **1962**, *27*, 2821-2828.
16. Bordwell, F. G.; Harrelson, J. A.; Zhang, X. *J. Org. Chem.* **2002**, *56*, 4448-4450.
17. Lygo, B. *Synlett* **1992**, *1992*, 793-795.
18. Honma, M.; Sawada, T.; Fujisawa, Y.; Utsugi, M.; Watanabe, H.; Umino, A.; Matsumura, T.; Hagihara, T.; Takano, M.; Nakada, M. *J. Am. Chem. Soc.* **2003**, *125*, 2860-2861.
19. Eisch, J. J.; Dua, S. K.; Behrooz, M. *J. Org. Chem.* **1985**, *50*, 3674-3676.
20. Kelleher, L. *Ph.D. Thesis, NUI* **1998**.
21. O'Keeffe, E. *Ph.D. Thesis, NUI* **2002**.
22. Yoon, N. M.; Pak, C. S.; Brown Herbert, C.; Krishnamurthy, S.; Stocky, T. P. *J. Org. Chem.* **1973**, *38*, 2786-2792.
23. Pouchert, C. J.; Behnke, J. *The Aldrich Library of ^{13}C and ^{1}H FT NMR spectra* Milwaukee Aldrich Chemical **1993**.
24. Berkenbusch, T.; Brückner, R. *Tetrahedron* **1998**, *54*, 11461-11470.
25. Idenix Pharmaceuticals, I. **2009**, US2009/60866 A60861.
26. Shao, X.-B.; Jiang, X.-K.; Zhu, S.-Z.; Li, Z.-T. *Tetrahedron* **2004**, *60*, 9155-9162.
27. Kryshtal, G. V.; Zhdankina, G. M.; Zlotin, S. G. *Russ. Chem. Bull., Int. Ed.* **2004**, *53*, 652-658.
28. Nečas, D.; Turský, M.; Kotora, M. *J. Am. Chem. Soc.* **2004**, *126*, 10222-10223.
29. Sattar, F. A.; Darley, D. J.; Politano, F.; Woodman, T. J.; Threadgill, M. D.; Lloyd, M. D. *Chem. Commun.* **2010**, *46*.
30. Zhang, L.; He, W.; Liang, Y.; Cui, Y. *Science in China Series B: Chemistry* **2009**, *52*, 937-942.
31. Krapcho, A. P.; Weimaster, J. F.; Eldridge, J. M.; Jahngen, E. G. E.; Lovey, A. J.; Stephens, W. P. *J. Org. Chem.* **1978**, *43*, 138-147.
32. Krapcho, A. P. *Arkivoc* **2007**, *ii*, 1-53.
33. *Toyama Chemical Co., Ltd.*; US6384065 B1, **2002**.

34. Rao, C. G. *Org. Prep. Proced. Int.* **1980**, *12*, 225-228.
35. Balog, M.; Abé, C.; Kálai, T.; Steinhoff, H.-J.; Jekő, J.; Hideg, K. *Synthesis* **2007**, *2007*, 1663-1670.
36. Regitz, M., Maas, G. *Diazo Compounds, Properties and Synthesis*; Academic Press: London, **1986**.
37. Curphey, T. J. *Org. Prep. Proc. Int.* **1981**, *13*, 112-115.
38. Bollinger, F. W.; Tuma, L. D. *Synlett* **1996**, *1996*, 407-413.
39. Doyle, M. P.; Dorow, R. L.; Terpstra, J. W.; Rodenhouse, R. A. *J. Org. Chem.* **1985**, *50*, 1663-1666.
40. Hazen, G. G.; Weinstock, L. M.; Connell, R.; Bollinger, F. W. *Synth. Commun.* **1981**, *11*, 947-956.
41. Maas, G. *Angew. Chem., Int. Ed.* **2009**, *48*, 8186-8195.
42. Taber, D. F.; Ruckle, R. E.; Hennessy, M. J. *J. Org. Chem.* **1986**, *51*, 4077-4078.
43. Khare, A. B.; McKenna, C. E. *Synthesis* **1991**, *1991*, 405,406.
44. Hendrickson, J. B.; Wolf, W. A. *J. Org. Chem.* **1968**, *33*, 3610-3618.
45. Hatch, C. E.; Baum, J. S.; Takashima, T.; Kondo, K. *J. Org. Chem.* **1980**, *45*, 3281-3285.
46. Davies, H. M. L.; Cantrell, W. R.; Romines, K. R.; Baum, J. S. *Org. Synth.* **1992**, *70*, 93.
47. Goddard-Borger, E. D.; Stick, R. V. *Org. Lett.* **2007**, *9*, 3797-3800.
48. Cavender, C. J.; Shiner, V. J. *J. Org. Chem.* **1972**, *37*, 3567-3569.
49. Katritzky, A. R.; El Khatib, M.; Bol'shakov, O.; Khelashvili, L.; Steel, P. J. *J. Org. Chem.* **2010**, *75*, 6532-6539.
50. Harned, A. M.; Sherrill, W. M.; Flynn, D. L.; Hanson, P. R. *Tetrahedron* **2005**, *61*, 12093-12099.
51. Green, G. M.; Peet, N. P.; Metz, W. A. *J. Org. Chem.* **2001**, *66*, 2509-2511.
52. Lombardo, L.; Mander, L. N. *Synthesis* **1980**, 368-370.
53. Kitamura, M.; Tashiro, N.; Okauchi, T. *Synlett* **2009**, *2009*, 2943,2944.
54. Suárez, J. R.; Trastoy, B.; Pérez-Ojeda, M. E.; Marín-Barrios, R.; Chiara, J. L. *Adv. Synth. Catal.* **2010**, *352*, 2515-2520.
55. Chiara, J. L.; Suárez, J. R. *Adv. Synth. Catal.* **2011**, *353*, 575-579.
56. Koskinen, A. M. P.; Munoz, L. *J. Chem. Soc., Chem. Commun.* **1990**, 652-653.
57. Slattery, C. N.; Ford, A.; Maguire, A. R. *Tetrahedron* **2010**, *66*, 6681-6705.
58. Doyle, M. P.; Duffy, R.; Ratnikov, M.; Zhou, L. *Chem. Rev.* **2010**, *110*, 704-724.
59. Davies, H. M. L.; Beckwith, R. E. J. *Chem. Rev.* **2003**, *103*, 2861-2904.
60. Ye, T.; McKervey, M. A. *Chem. Rev.* **1994**, *94*, 1091-1160.
61. Taber, D. F.; Ruckle, R. E. *J. Am. Chem. Soc.* **1986**, *108*, 7686-7693.
62. Taber, D. F.; Petty, E. H. *J. Org. Chem.* **1982**, *47*, 4808-4809.
63. Taber, D. F.; Raman, K. *J. Am. Chem. Soc.* **1983**, *105*, 5935-5937.
64. Taber, D. F.; Ruckle, R. E. *Tetrahedron Lett.* **1985**, *26*, 3059-3062.
65. Monteiro, H. J. *Tetrahedron Lett.* **1987**, *28*, 3459-3462.
66. Davies, H.; Dick, A.; Yu, J.-Q., Shi, Z., Eds.; Springer Berlin / Heidelberg: 2010; Vol. 292, p 303-345.
67. Doyle, M. P.; Dyatkin, A. B. *J. Org. Chem.* **1995**, *60*, 3035-3038.
68. Davies, H. M. L.; Hansen, T.; Hopper, D. W.; Panaro, S. A. *J. Am. Chem. Soc.* **1999**, *121*, 6509-6510.
69. Diaz-Requejo, M. M.; Belderrain, T. R.; Nicasio, M. C.; Trofimenko, S.; Perez, P. J. *J. Am. Chem. Soc.* **2002**, *124*, 896-897.
70. Doyle, M. P.; Westrum, L. J.; Wolthuis, W. N. E.; See, M. M.; Boone, W. P.; Bagheri, V.; Pearson, M. M. *J. Am. Chem. Soc.* **1993**, *115*, 958-964.

71. Davies, H. M. L.; Hansen, T.; Churchill, M. R. *J. Am. Chem. Soc.* **2000**, *122*, 3063-3070.
72. Doyle, M. P.; Taunton, J.; Pho, H. Q. *Tetrahedron Lett.* **1989**, *30*, 5397-5400.
73. Doyle, M. P.; Davies, S. B.; May, E. J. *J. Org. Chem.* **2001**, *66*, 8112-8119.
74. Taber, D. F.; You, K. K.; Rheingold, A. L. *J. Am. Chem. Soc.* **1996**, *118*, 547-556.
75. Davies, H. M. L. *Eur. J. Org. Chem.* **1999**, *1999*, 2459-2469.
76. Timmons, D. J.; Doyle, M. P. *J. Organomet. Chem.* **2001**, *617-618*, 98-104.
77. Doyle, M. P.; Duffy, R.; Ratnikov, M.; Zhou, L. *Chem. Rev.* **2009**.
78. Nakamura, E.; Yoshikai, N.; Yamanaka, M. *J. Am. Chem. Soc.* **2002**, *124*, 7181-7192.
79. Taber, D. F.; Petty, E. H.; Raman, K. *J. Am. Chem. Soc.* **1985**, *107*, 196-199.
80. O'Riordan, N. B. *Ph.D. Thesis, NUI* **2001**.
81. Maguire, A. R.; Kelleher, L. L. *Tetrahedron Lett.* **1997**, *38*, 7459-7462.
82. Ballini, R.; Bosica, G.; Mecozzi, T. *Tetrahedron* **1997**, *53*, 7341-7346.
83. Cox, G. G.; Moody, C. J.; Austin, D. J.; Padwa, A. *Tetrahedron* **1993**, *49*, 5109-5126.
84. Cox, G. G.; Miller, D. J.; Moody, C. J.; Sie, E.-R. H. B.; Kulagowski, J. J. *Tetrahedron* **1994**, *50*, 3195-3212.
85. Buck, R. T.; Coe, D. M.; Drysdale, M. J.; Ferris, L.; Haigh, D.; Moody, C. J.; Pearson, N. D.; Sanghera, J. B. *Tetrahedron: Asymmetry* **2003**, *14*, 791-816.
86. Mountjoy, B. W. *Ph.D. Thesis, NUI* **1998**.
87. Pirrung, M. C.; Zhang, J.; Lackey, K.; Sternbach, D. D.; Brown, F. *J. Org. Chem.* **1995**, *60*, 2112-2124.
88. Coughlan, N. M. M. *Ph.D. Thesis, NUI* **1999**.
89. Satoh, T.; Mizu, Y.; Kawashima, T.; Yamakawa, K. *Tetrahedron* **1995**, *51*, 703-710.
90. Bozhenkov, G. V.; Leckovskaya, G. G.; Larina, L. I.; Ushakov, P. E.; Dolgushin, G. V.; Mirskova, A. N. *Russ. J. Org. Chem.* **2004**, *40*, 1583-1592.
91. Hashimoto, S.-i.; Watanabe, N.; Ikegami, S. *Tetrahedron Lett.* **1990**, *31*, 5173-5174.
92. Hashimoto, S.-i.; Watanabe, N.; Sato, T.; Shiro, M.; Ikegami, S. *Tetrahedron Lett.* **1993**, *34*, 5109-5112.
93. O'Keeffe, S.; Harrington, F.; Maguire, A. R. *Synlett* **2007**, *2007*, 2367-2370.
94. O'Neill, S.; O'Keeffe, S.; Harrington, F.; Maguire, A. R. *Synlett* **2009**, *2009*, 2312-2314.
95. Desimoni, G.; Faita, G.; Jorgensen, K. A. *Chem. Rev.* **2006**, *106*, 3561-3651.
96. Hargaden, G. i. C.; Guiry, P. J. *Chem. Rev.* **2009**, *109*, 2505-2550.
97. Lim, H.-J.; Sulikowski, G. A. *J. Org. Chem.* **1995**, *60*, 2326-2327.
98. Rasappan, R.; Laventine, D.; Reiser, O. *Coord. Chem. Rev.* **2008**, *252*, 702-714.
99. Fraile, J. M.; García, J. I.; Mayoral, J. A. *Coord. Chem. Rev.* **2008**, *252*, 624-646.
100. Rechavi, D.; Lemaire, M. *Chem. Rev.* **2002**, *102*, 3467-3494.
101. Liu, B.; Zhu, S.-F.; Zhang, W.; Chen, C.; Zhou, Q.-L. *J. Am. Chem. Soc.* **2007**, *129*, 5834-5835.
102. Chen, C.; Zhu, S.-F.; Liu, B.; Wang, L.-X.; Zhou, Q.-L. *J. Am. Chem. Soc.* **2007**, *129*, 12616-12617.
103. Maguire, A. R.; Kelleher, L. L.; Ferguson, G. *J. Mol. Catal. B: Enzymatic* **1996**, *1*, 115-126.
104. Smith, M. R.; Blake, A. J.; Hayes, C. J.; Stevens, M. F. G.; Moody, C. J. *J. Org. Chem.* **2009**, *74*, 9372-9380.
105. Dai, W.-M.; Lee, M. Y. H. *Tetrahedron* **1998**, *54*, 12497-12512.

106. Riediker, M.; Schwartz, J. *J. Am. Chem. Soc.* **1982**, *104*, 5842-5844.
107. Suzuki, M.; Yanagisawa, A.; Noyori, R. *J. Am. Chem. Soc.* **1988**, *110*, 4718-4726.
108. Faul, M. M.; Huff, B. E. *Chem. Rev.* **2000**, *100*, 2407-2474.
109. Zeng, L.; Ye, Q.; Oberlies, N. H.; Shi, G.; Gu, Z.-M.; He, K.; McLaughlin, J. L. *Nat. Prod. Rep.* **1996**, *13*.
110. Kang, E. J.; Lee, E. *Chem. Rev.* **2005**, *105*, 4348-4378.
111. Alvarez, E.; Candenas, M.-L.; Perez, R.; Ravelo, J. L.; Delgado Martin, J. *Chem. Rev.* **1995**, *95*, 1953-1980.
112. Taryn L.B, B. *Tetrahedron* **1987**, *43*, 3309-3362.
113. Chen, C.-H.; Kuan, T.-C.; Lu, K.-J.; Hou, D.-R. *Org. Biomol. Chem.* **2010**, *8*.
114. Sobhani, S.; Aryanejad, S.; Maleki, M. F. *Synlett* **2011**, *2011*, 319-322.
115. French, D. C.; Crumrine, D. S. *J. Org. Chem.* **1990**, *55*, 5494-5496.
116. Oba, M.; Tanaka, K.; Nishiyama, K.; Ando, W. *J. Org. Chem.* **2011**, *76*, 4173-4177.
117. Bahrami, K. *Synlett* **2011**, *2011*, 2671,2674.
118. Yang, H.; Li, Y.; Jiang, M.; Wang, J.; Fu, H. *Chem.-Eur. J.* **2011**, *17*, 5652-5660.
119. Liu, Y.; Zhang, Y. *Tetrahedron Lett.* **2003**, *44*, 4291-4294.
120. Rosowsky, A.; Chen, K. K. N. *J. Org. Chem.* **1973**, *38*, 2073-2077.
121. Inc., P. 2000.
122. Kobayashi, H.; Sonoda, T.; Iwamoto, H.; Yoshimura, M. *Chem. Lett.* **1981**, 579-580.
123. Krossing, I.; Raabe, I. *Angew. Chem., Int. Ed.* **2004**, *43*, 2066-2090.
124. Smidt, S. P.; Zimmermann, N.; Studer, M.; Pfaltz, A. *Chem.-Eur. J.* **2004**, *10*, 4685-4693.
125. Blackmond, D. G.; Lightfoot, A.; Pfaltz, A.; Rosner, T.; Schnider, P.; Zimmermann, N. *Chirality* **2000**, *12*, 442-449.
126. Shi, W.-J.; Xie, J.-H.; Zhou, Q.-L. *Tetrahedron: Asymmetry* **2005**, *16*, 705-710.
127. Zhang, Q.; Zhu, S.-F.; Qiao, X.-C.; Wang, L.-X.; Zhou, Q.-L. *Adv. Synth. Catal.* **2008**, *350*, 1507-1510.
128. Park, E. J.; Kim, S. H.; Chang, S. *J. Am. Chem. Soc.* **2008**, *130*, 17268-17269.
129. Fructos, M. R.; de Fremont, P.; Nolan, S. P.; Diaz-Requejo, M. M.; Perez, P. J. *Organometallics* **2006**, *25*, 2237-2241.
130. Salomon, R. G.; Kochi, J. K. *J. Am. Chem. Soc.* **1973**, *95*, 3300-3310.
131. Sarabia, F.; López-Herrera, F. J. *Tetrahedron Lett.* **2001**, *42*, 8805-8809.
132. Fraile, J. M.; García, J. I.; Mayoral, J. A.; Tarnai, T. *J. Mol. Catal. A: Chem.* **1999**, *144*, 85-89.
133. Fraile, J. M.; García, J. I.; Martínez-Merino, V.; Mayoral, J. A.; Salvatella, L. *J. Am. Chem. Soc.* **2001**, *123*, 7616-7625.
134. Fraile, J. M.; García, J. I.; Gil, M. J.; Martínez-Merino, V.; Mayoral, J. A.; Salvatella, L. *Chem.-Eur. J.* **2004**, *10*, 758-765.
135. Zhu, S.-F.; Xie, J.-B.; Zhang, Y.-Z.; Li, S.; Zhou, Q.-L. *J. Am. Chem. Soc.* **2006**, *128*, 12886-12891.
136. Rosenberg, M. L.; Vlašaná, K. r.; Gupta, N. S.; Wragg, D.; Tilset, M. *J. Org. Chem.* **2011**, *76*, 2465-2470.
137. Krumper, J. R.; Gerisch, M.; Suh, J. M.; Bergman, R. G.; Tilley, T. D. *J. Org. Chem.* **2003**, *68*, 9705-9710.
138. Zhang, Y.-Z.; Zhu, S.-F.; Wang, L.-X.; Zhou, Q.-L. *Angew. Chem., Int. Ed.* **2008**, *47*, 8496-8498.
139. Hiraoka, M. *Crown Ethers and Analogous Compounds*; Elsevier, 1992.

140. Zhu, S.-F.; Chen, C.; Cai, Y.; Zhou, Q.-L. *Angew. Chem., Int. Ed.* **2008**, *47*, 932-934.
141. Watanabe, N.; Ohtake, Y.; Hashimoto, S.-i.; Shiro, M.; Ikegami, S. *Tetrahedron Lett.* **1995**, *36*, 1491-1494.
142. Takahashi, T.; Tsutsui, H.; Tamura, M.; Kitagaki, S.; Nakajima, M.; Hashimoto, S. *Chem. Commun.* **2001**, 1604-1605.
143. Davies, H. M. L.; Hansen, T. *J. Am. Chem. Soc.* **1997**, *119*, 9075-9076.
144. *Asymmetric Synthesis*; Wiley-Interscience: New York, 1987.
145. Morrison, J. D.; Mosher, H. S. *Asymmetric Organic Reactions*; Prentice-Halls: Englewood Cliffs, 1971.
146. Heller, D. P.; Goldberg, D. R.; Wu, H.; Wulff, W. D. *Can. J. Chem.* **2006**, *84*, 1487-1503.
147. Chackal-Catoen, S.; Miao, Y.; Wilson, W. D.; Wenzler, T.; Brun, R.; Boykin, D. W. *Bioorg. Med. Chem.* **2006**, *14*, 7434-7445.
148. Huang, M. *J. Am. Chem. Soc.* **1946**, *68*, 2487-2488.
149. Allergan Sales, I. P. *US6344561 B2* **2002**.
150. Vieira, T. O.; Green, M. J.; Alper, H. *Org. Lett.* **2006**, *8*, 6143-6145.
151. Reddy, R. P.; Lee, G. H.; Davies, H. M. L. *Org. Lett.* **2006**, *8*, 3437-3440.
152. Davies, H. M. L.; Jin, Q. *Tetrahedron: Asymmetry* **2003**, *14*, 941-949.
153. Davies, H. M. L.; Stafford, D. G.; Hansen, T. *Org. Lett.* **1999**, *1*, 233-236.
154. Davies, H. M. L.; Yang, J. *Adv. Synth. Catal.* **2003**, *345*, 1133-1138.
155. Madder, A.; Sebastian, S.; Haver, D. V.; Clercq, P. J. D.; Maskill, H. *J. Chem. Soc., Perkin Trans. 2* **1997**, *12*, 2787-2793.
156. Doyle, M. P.; Pieters, R. J.; Taunton, J.; Pho, H. Q.; Padwa, A.; Hertzog, D. L.; Precedo, L. *J. Org. Chem.* **1991**, *56*, 820-829.
157. Doyle, M. P.; Shanklin, M. S.; Oon, S. M.; Pho, H. Q.; Van der Heide, F. R.; Veal, W. R. *J. Org. Chem.* **1988**, *53*, 3384-3386.
158. Crosignani, S.; Desimoni, G.; Faita, G.; Righetti, P. *Tetrahedron* **1998**, *54*, 15721-15730.
159. Itagaki, M.; Masumoto, K.; Yamamoto, Y. *J. Org. Chem.* **2005**, *70*, 3292-3295.
160. van Lingen, Hester L.; van de Mortel, Jeroen K. W.; Hekking, Koen F. W.; van Delft, Floris L.; Sonke, T.; Rutjes, Floris P. J. T. *Eur. J. Org. Chem.* **2003**, *2003*, 317-324.
161. van Lingen, H. L.; van Delft, F. L.; Storcken, R. P. M.; Hekking, K. F. W.; Klaassen, A.; Smits, J. J. M.; Ruskowska, P.; Frelek, J.; Rutjes, F. P. J. T. *Eur. J. Org. Chem.* **2005**, *2005*, 4975-4987.
162. Evans, D. A.; Johnson, J. S.; Olhava, E. J. *J. Am. Chem. Soc.* **2000**, *122*, 1635-1649.
163. Cattoën, X.; Pericàs, M. A. *Tetrahedron* **2009**, *65*, 8199-8205.
164. Cong-Dung Le, J.; Pagenkopf, B. L. *Org. Lett.* **2004**, *6*, 4097-4099.
165. Kato, K.; Matsuba, C.; Kusakabe, T.; Takayama, H.; Yamamura, S.; Mochida, T.; Akita, H.; Peganova, T. y. A.; Vologdin, N. V.; Gusev, O. V. *Tetrahedron* **2006**, *62*, 9988-9999.
166. Endeshaw, M. M.; Bayer, A.; Hansen, L. K.; Gautun, O. R. *Eur. J. Org. Chem.* **2006**, *2006*, 5249-5259.
167. Kusakabe, T.; Kato, K.; Takaishi, S.; Yamamura, S.; Mochida, T.; Akita, H.; Peganova, T. y. A.; Vologdin, N. V.; Gusev, O. V. *Tetrahedron* **2008**, *64*, 319-327.
168. V. Caplar; Z. Raza; D. Katalenic; Zinic, M. *Croatica Chemica Acta* **2003**, *76*, 23-36.

169. Bayardon, J.; Sinou, D. *Tetrahedron: Asymmetry* **2005**, *16*, 2965-2972.
170. Jacobsen, E. N.; Zhang, W.; Guler, M. L. *J. Am. Chem. Soc.* **1991**, *113*, 6703-6704.
171. Benaglia, M.; Benincori, T.; Mussini, P.; Pilati, T.; Rizzo, S.; Sannicolò, F. *J. Org. Chem.* **2005**, *70*, 7488-7495.
172. Nishiyama, H.; Yamaguchi, S.; Kondo, M.; Itoh, K. *J. Org. Chem.* **1992**, *57*, 4306-4309.
173. Park, S.-B.; Murata, K.; Matsumoto, H.; Nishiyama, H. *Tetrahedron: Asymmetry* **1995**, *6*, 2487-2494.
174. Shiomi, T.; Ito, J.-i.; Yamamoto, Y.; Nishiyama, H. *Eur. J. Org. Chem.* **2006**, *2006*, 5594-5600.
175. Padwa, A.; Austin, D. J. *Angew. Chem., Int. Ed.* **1994**, *33*, 1797-1815.
176. O'Keeffe, S. *Ph.D. Thesis, NUI* **2007**.
177. *Purchased from SinoChem Qingdao Co. Ltd. China* **2005**.
178. Meyers, A. I.; Williams, D. R.; Erickson, G. W.; White, S.; Druelinger, M. *J. Am. Chem. Soc.* **1981**, *103*, 3081-3087.
179. Lewanowicz, A.; Lipiński, J.; Siedlecka, R.; Skarżewski, J.; Baert, F. *Tetrahedron* **1998**, *54*, 6571-6586.
180. Matsui, T.; Kondo, T.; Nishita, Y.; Itadani, S.; Nakatani, S.; Omawari, N.; Sakai, M.; Nakazawa, S.; Ogata, A.; Mori, H.; Terai, K.; Kamoshima, W.; Ohno, H.; Obata, T.; Nakai, H.; Toda, M. *Bioorg. Med. Chem.* **2002**, *10*, 3757-3786.
181. Evans, D. A.; Peterson, G. S.; Johnson, J. S.; Barnes, D. M.; Campos, K. R.; Woerpel, K. A. *J. Org. Chem.* **1998**, *63*, 4541-4544.
182. Desimoni, G.; Faita, G.; Jørgensen, K. A. *Chem. Rev.* **2011**, *111*, PR284-PR437.
183. Cornejo, A.; Fraile, J. M.; García, J. I.; Gil, M. J.; Martínez-Merino, V.; Mayoral, J. A.; Pires, E.; Villalba, I. *Synlett* **2005**, *2005*, 2321,2324.
184. McKennon, M. J.; Meyers, A. I.; Drauz, K.; Schwarm, M. *J. Org. Chem.* **1993**, *58*, 3568-3571.
185. Kokotos, G. *Synthesis* **1990**, *1990*, 299,301.
186. Granander, J.; Sott, R.; Hilmersson, G. *Tetrahedron* **2002**, *58*, 4717-4725.
187. Lazer, E. S.; Miao, C. K.; Wong, H.-C.; Sorcek, R.; Spero, D. M.; Gilman, A.; Pal, K.; Behnke, M.; Graham, A. G. *J. Med. Chem.* **1994**, *37*, 913-923.
188. Bosch, M. P.; Campos, F.; Niubó, I.; Rosell, G.; Díaz, J. L.; Brea, J.; Loza, M. I.; Guerrero, A. *J. Med. Chem.* **2004**, *47*, 4041-4053.
189. Combret, Y.; Duflos, J.; Dupas, G.; Bourguignon, J.; Quéguiner, G. *Tetrahedron: Asymmetry* **1993**, *4*, 1635-1644.
190. Di Marzo, V.; Ligresti, A.; Morera, E.; Nalli, M.; Ortar, G. *Bioorg. Med. Chem.* **2004**, *12*, 5161-5169.
191. Ring, A.; Maguire, A. R. *unpublished results*.
192. Denmark, S. E.; Stiff, C. M. *J. Org. Chem.* **2000**, *65*, 5875-5878.
193. Köhler, V.; Mazet, C.; Toussaint, A.; Kulicke, K.; Häussinger, D.; Neuburger, M.; Schaffner, S.; Kaiser, S.; Pfaltz, A. *Chem.-Eur. J.* **2008**, *14*, 8530-8539.
194. Murakata, M.; Tsutsui, H.; Hoshino, O. *Org. Lett.* **2000**, *3*, 299-302.
195. Denmark, S. E.; Nakajima, N.; Nicaise, O. J. C.; Faucher, A.-M.; Edwards, J. P. *J. Org. Chem.* **1995**, *60*, 4884-4892.
196. Burguete, M. I.; Fraile, J. M.; García, J. I.; García-Verdugo, E.; Luis, S. V.; Mayoral, J. A. *Org. Lett.* **2000**, *2*, 3905-3908.
197. Hansen, J.; Autschbach, J.; Davies, H. M. L. *J. Org. Chem.* **2009**, *74*, 6555-6563.
198. Bonge, H. T.; Hansen, T. *Eur. J. Org. Chem.* **2010**, *2010*, 4355-4359.
199. Bonge, H. T.; Hansen, T. *Tetrahedron Lett.* **2010**, *51*, 5378-5381.

200. Hansen, J.; Davies, H. M. L. *Coord. Chem. Rev.* **2008**, *252*, 545-555.
201. Evans, D. A.; Woerpel, K. A.; Hinman, M. M.; Faul, M. M. *J. Am. Chem. Soc.* **1991**, *113*, 726-728.
202. Lowenthal, R. E.; Abiko, A.; Masamune, S. *Tetrahedron Lett.* **1990**, *31*, 6005-6008.
203. Lowenthal, R. E.; Masamune, S. *Tetrahedron Lett.* **1991**, *32*, 7373-7376.
204. Fritschi, H.; Leutenegger, U.; Pfaltz, A. *Helv. Chim. Acta* **1988**, *71*, 1553-1565.
205. Straub, B. F.; Hofmann, P. *Angew. Chem., Int. Ed.* **2001**, *40*, 1288-1290.
206. Naohiko Yoshikai, E. N. *Adv. Synth. Catal.* **2003**, *345*, 1159-1171.
207. Thorhauge, J.; Roberson, M.; Hazell, R. G.; Jørgensen, K. A. *Chem.-Eur. J.* **2002**, *8*, 1888-1898.
208. Johannsen, M.; Joergensen, K. A. *J. Org. Chem.* **1995**, *60*, 5757-5762.
209. Johannsen, M.; Anker Jørgensen, K. *Tetrahedron* **1996**, *52*, 7321-7328.
210. Yao, S.; Johannsen, M.; Audrain, H.; Hazell, R. G.; Jørgensen, K. A. *J. Am. Chem. Soc.* **1998**, *120*, 8599-8605.
211. Desimoni, G.; Faita, G.; Righetti, P. P. *Tetrahedron Lett.* **1996**, *37*, 3027-3030.
212. Audrain, H.; Jørgensen, K. A. *J. Am. Chem. Soc.* **2000**, *122*, 11543-11544.
213. Evans, D. A.; Tregay, S. W.; Burgey, C. S.; Paras, N. A.; Vojkovsky, T. *J. Am. Chem. Soc.* **2000**, *122*, 7936-7943.
214. Audrain, H.; Thorhauge, J.; Hazell, R. G.; Jørgensen, K. A. *J. Org. Chem.* **2000**, *65*, 4487-4497.

ucc
Coláiste na hOllscoile Corcaigh, Éire
University College Cork, Ireland

CORA
Cork Open Research Archive
Cartlann Taighde Oscailte Chorcaí

Slattery, C. N. 2012. *Investigation of catalyst effects in enantioselective copper- and rhodium-mediated transformations of a-diazocarbonyl compounds*. PhD Thesis, University College Cork.

Please note that Chapters 3-4 (pp.197-252) are unavailable due to a restriction requested by the author.

CORA Cork Open Research Archive http://cora.ucc.ie

Appendices

Appendix I *Chiral stationary phase HPLC and polarimetry data*

- All chiral stationary phase HPLC analysis was conducted at room temperature unless otherwise stated.

- Samples for chiral stationary phase HPLC analysis were prepared at a concentration of ~1 mg/mL.

- Injection volume was 10 μl for all compounds unless otherwise stated.

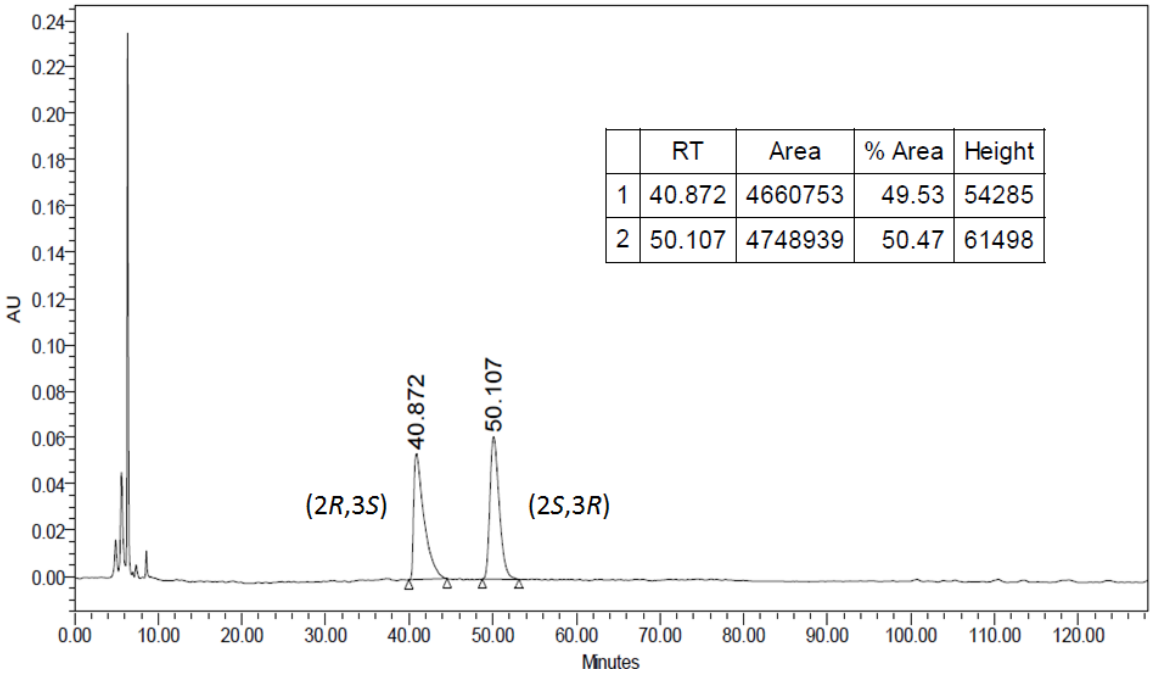
- Notably, the retention times can change per injection (particularly for long run times), however, the elution sequence of enantiomers remains the same.

- Stereochemical assignments of known cyclopentanone products were made by comparison to previously reported polarimetry, and chiral stationary phase HPLC data (where known).

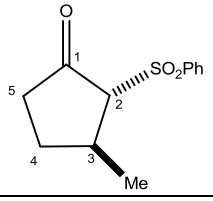
- The absolute stereochemistry of novel cyclopentanone products was assigned by single crystal analysis and chiral stationary phase HPLC analysis of the isolated single crystal.

- Wherever feasible, the crystals employed for X-ray diffraction to determine absolute stereochemistry were subsequently analysed by chiral stationary phase HPLC to unambiguously confirm the absolute stereochemistry corresponding to each HPLC peak. In some instances the detection of the weak signals from the single crystal proved challenging.

(±)-*trans*-2-Phenylsulfonyl-3-methylcyclopentanone 2



	RT	Area	% Area	Height
1	40.872	4660753	49.53	54285
2	50.107	4748939	50.47	61498

Compound	Column	Flow (mL/min)	λ Max (nm)	Mobile phase (hexane : IPA)	Retention time	
					Enantiomer	min
	Chiralcel OD-H	1.0	210	90 : 10	(2*R*, 3*S*)	40
					(2*S*, 3*R*)	50

(–)-(2*R*, 3*S*)-2-Phenylsulfonyl-3-methylcyclopentanone **2**:

$[\alpha]_D^{20}$ –21.8 (*c* 0.5, CH_2Cl_2, 20% ee)

Isolated from reaction of **1 in the presence of Rh_2(S-*Mand*)$_4$ (**Table 2.10**, entry 1).*

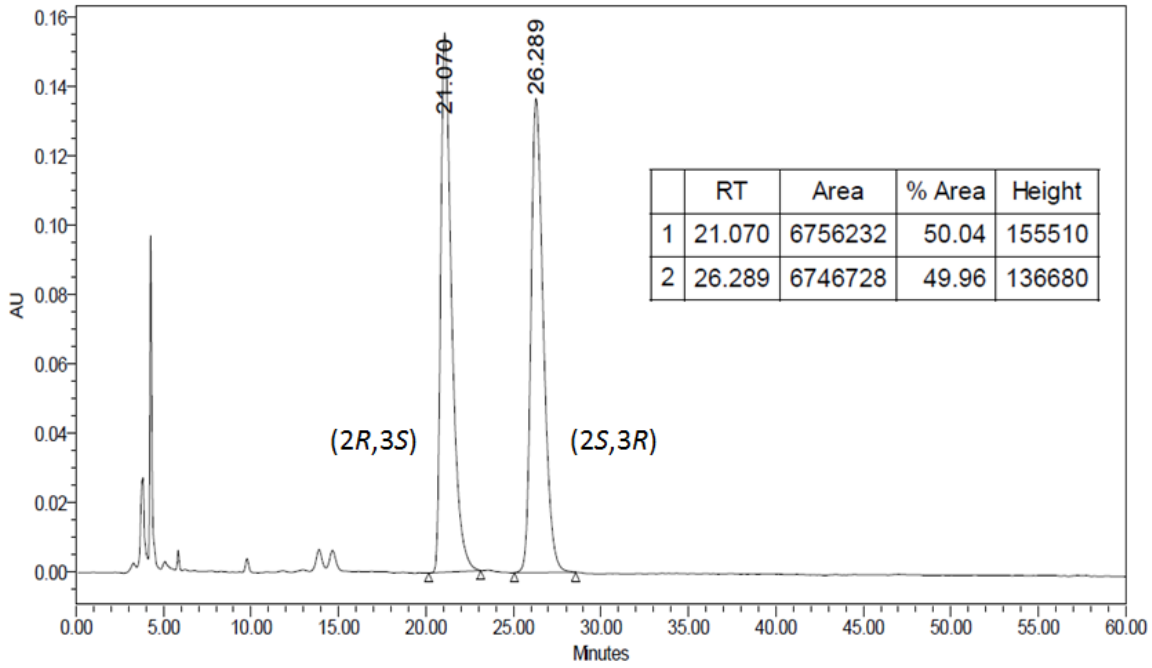
(+)-(2*S*, 3*R*)-2-Phenylsulfonyl-3-methylcyclopentanone **2**:

$[\alpha]_D^{20}$ +71.7 (*c* 0.5, CH_2Cl_2, 61% ee)

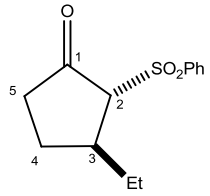
Isolated from reaction of **1 in the presence of $CuCl_2$,* (4R)-***85*** *and NaBARF (**Table 2.32**, entry 4).*

lit.[1,2]: $[\alpha]_D^{20}$ +69.8 (*c* 1.0, CH_2Cl_2, >95% ee)

(±)-*trans*-2-Phenylsulfonyl-3-ethylcyclopentanone 39



	RT	Area	% Area	Height
1	21.070	6756232	50.04	155510
2	26.289	6746728	49.96	136680

Compound	Column	Flow (mL/min)	λ Max (nm)	Mobile phase (hexane : IPA)	Retention time	
					Enantiomer	min
	Chiralcel OD-H	1.0	210	90 : 10	(2*R*, 3*S*)	22
					(2*S*, 3*R*)	27

(–)-(2*R*, 3*S*)-2-Phenylsulfonyl-3-ethylcyclopentanone **39**:

$[\alpha]_D^{20}$ –68.6 (*c* 0.5, CH_2Cl_2, 71% ee)

Isolated from reaction of **32 in the presence of $CuCl_2$,* (3S,8R)-*Ind **53** and NaBARF (**Table 2.14**, entry 9).*

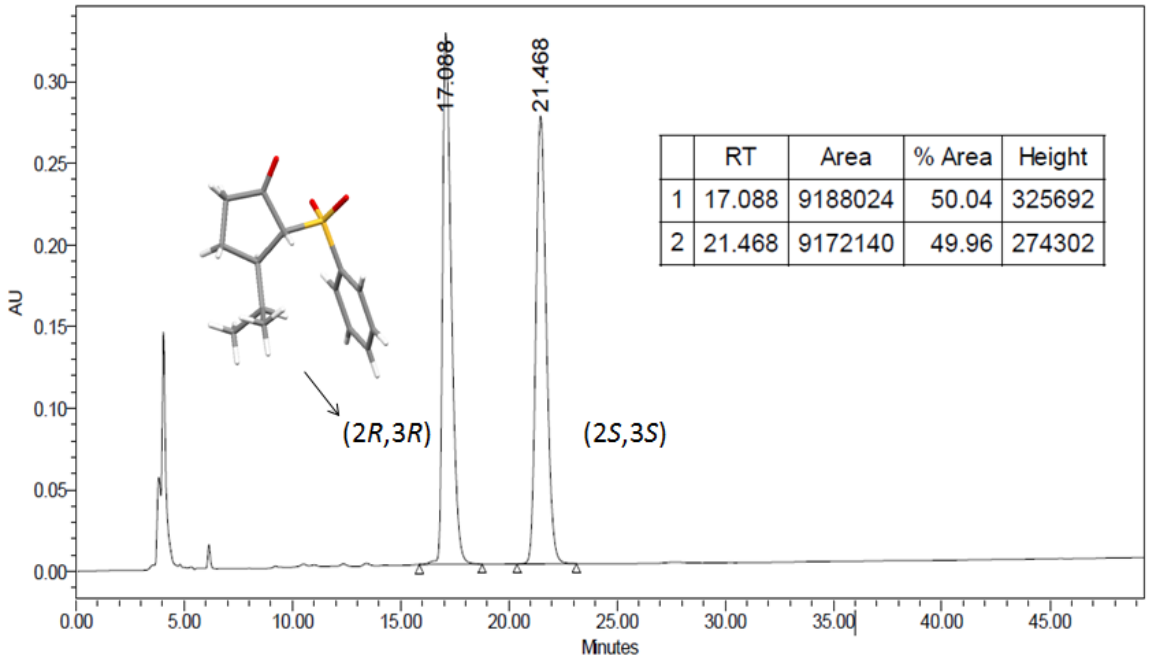
(+)-(2*S*, 3*R*)-2-Phenylsulfonyl-3-ethylcyclopentanone **39**:

$[\alpha]_D^{20}$ +17.0 (*c* 0.5, CH_2Cl_2, 29% ee)

Isolated from reaction of **32 in the presence of $Cu(MeCN)_4PF_6$ (**Table 2.12**, entry 5).*

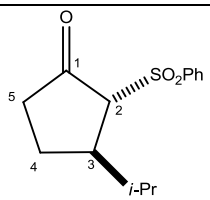
lit.[1,2]: $[\alpha]_D^{20}$ +78.1 (*c* 2.8, CH_2Cl_2, >95% ee)

(±)-*trans*-2-Phenylsulfonyl-3-*i*-propylcyclopentanone 40



	RT	Area	% Area	Height
1	17.088	9188024	50.04	325692
2	21.468	9172140	49.96	274302

*Note: single crystal isolated from sample of **40** obtained from reaction of **33** in the presence of $CuCl_2$,* (3S,8R)*-Ind **53** and NaBARF (**Table 2.14**, entry 14): 75% ee* (2R,3R)*. Chiral HPLC analysis of single crystal of **40** was attempted, however, no signal was observed.*

Compound	Column	Flow (mL/min)	λ Max (nm)	Mobile phase (hexane : IPA)	Retention time	
					Enantiomer	min
	Chiralpak OJ-H	1.0	218	70 : 30	(2*R*, 3*R*)	17
					(2*S*, 3*S*)	22

(–)-(2*R*, 3*R*)-2-Phenylsulfonyl-3-*i*-propylcyclopentanone **40**:

$[\alpha]_D^{20}$ –23.7 (*c* 0.5, CH_2Cl_2, 42% ee)

Isolated from reaction of **33 in the presence of CuCl,* (4S)-t-*Bu **51** and NaBARF (**Table 2.14**, entry 15).*

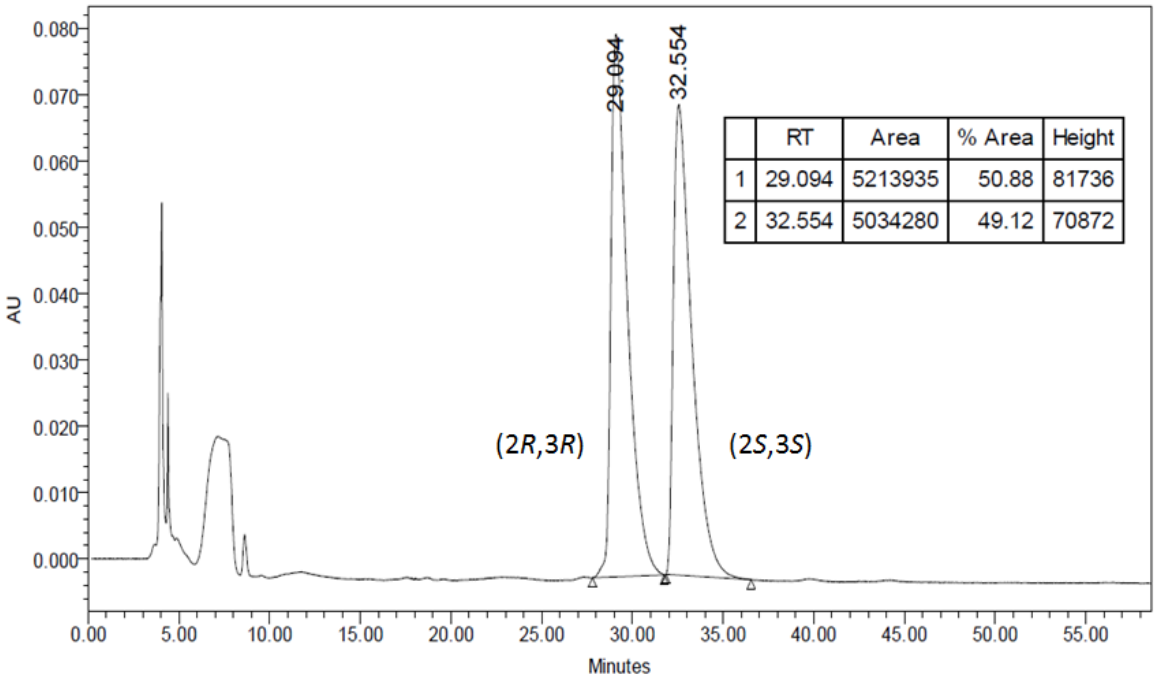
(+)-(2*S*, 3*S*)-2-Phenylsulfonyl-3-*i*-propylcyclopentanone **40**:

$[\alpha]_D^{20}$ +38.0 (*c* 0.5, CH_2Cl_2, 60% ee)

Isolated from reaction of **33 in the presence of CuCl,* (4R)-*Bn **50** and NaBARF (**Table 2.14**, entry 13).*

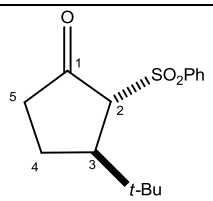
Lit.[3]: $[\alpha]_D^{20}$ +56.1 (*c* 1.0, $CHCl_3$, 91% ee)

(±)-trans-2-Phenylsulfonyl-3-*t*-butylcyclopentanone 41



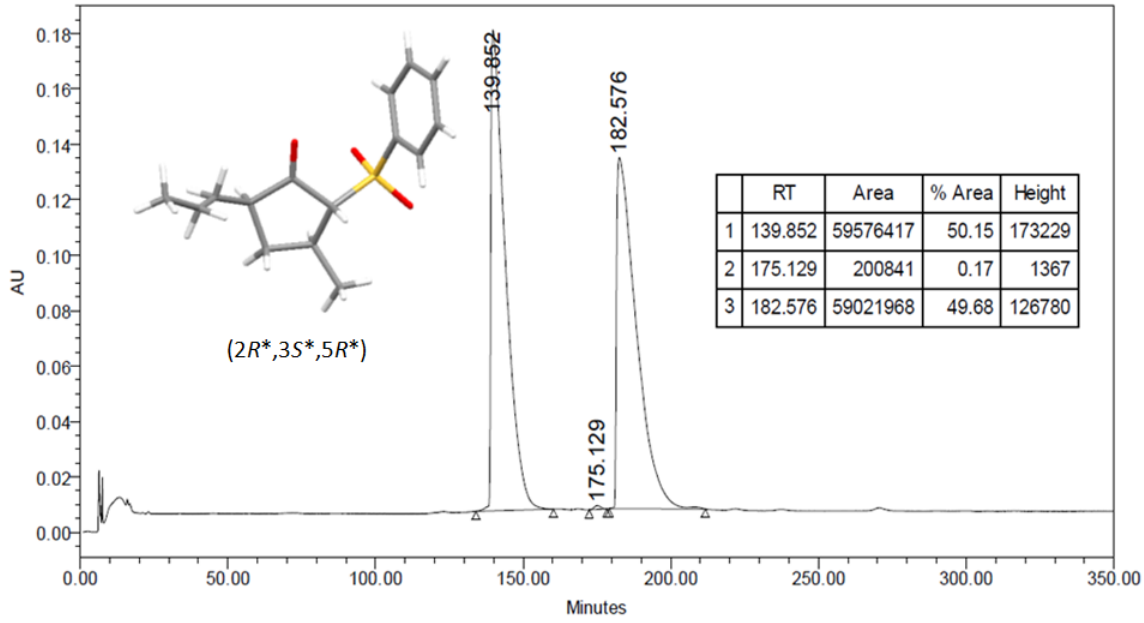
	RT	Area	% Area	Height
1	29.094	5213935	50.88	81736
2	32.554	5034280	49.12	70872

*Note: single crystal analysis for this compound is pending. Assignment of absolute stereochemistry of **41** was made by comparison to chiral HPLC data and ligand trends for analogous cyclopentanone structures.*

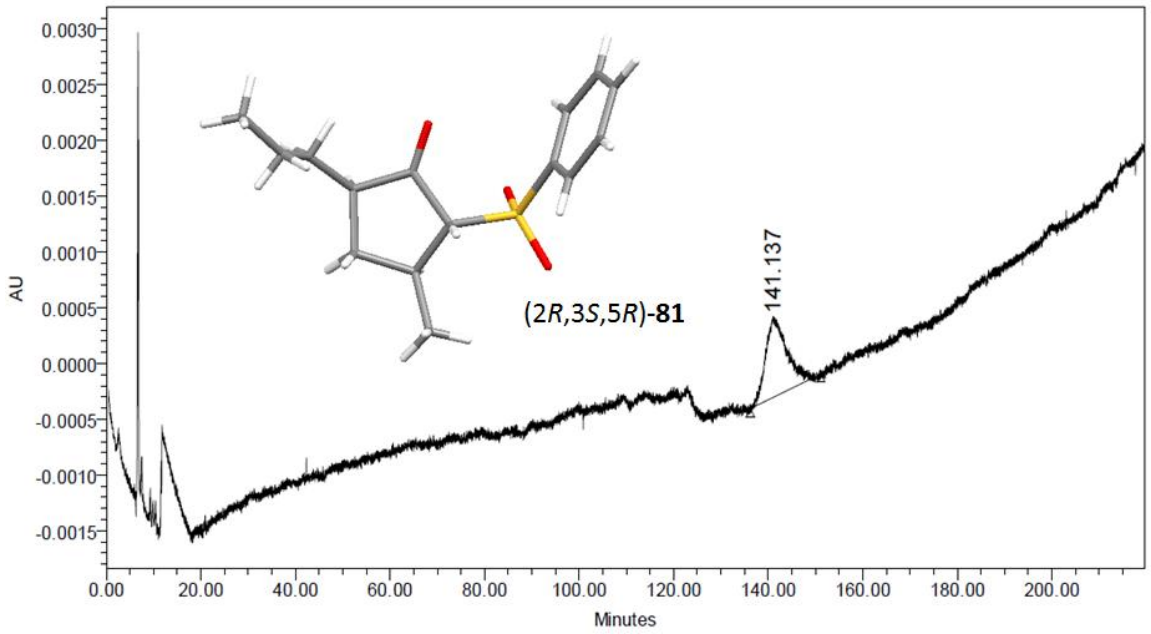
Compound	**Column**	**Flow (mL/min)**	**λ Max (nm)**	**Mobile phase (hexane : IPA)**	**Retention time**	
					Enantiomer	**min**
	Chiralcel OD-H	0.8	224	99 : 1	(2*R*, 3*R*)	29
					(2*S*, 3*S*)	33

*Note: isolated samples of **41** were of insufficient purity to obtain accurate rotation values.*

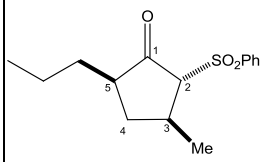
(±)-*trans*-3-methyl-2-phenylsulfonyl-5-propylcyclopentanone 81

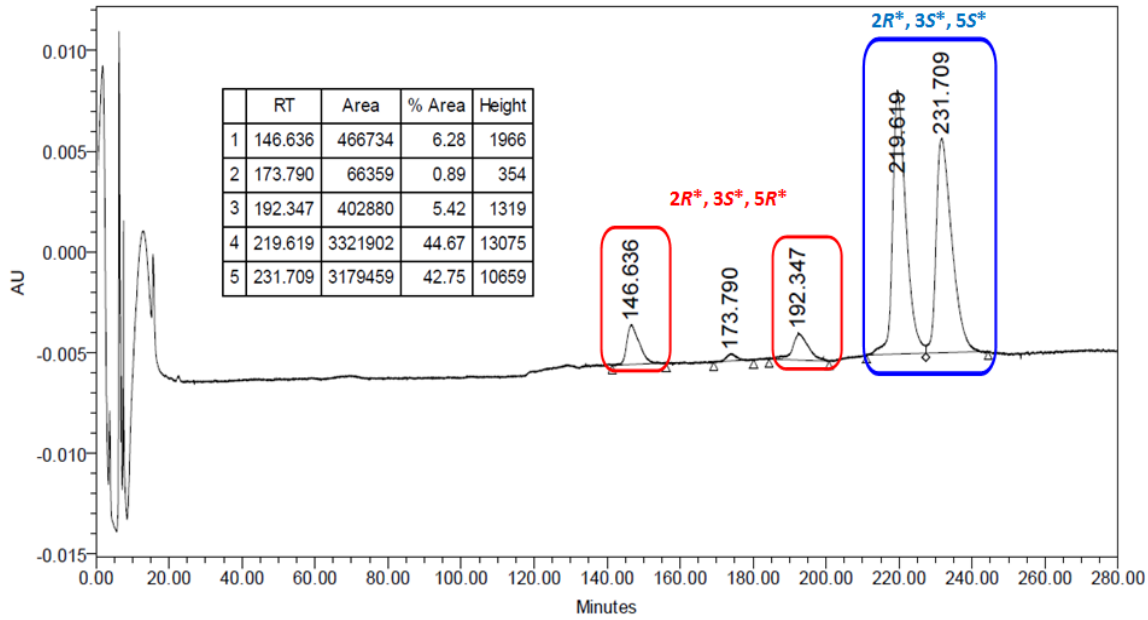


	RT	Area	% Area	Height
1	139.852	59576417	50.15	173229
2	175.129	200841	0.17	1367
3	182.576	59021968	49.68	126780

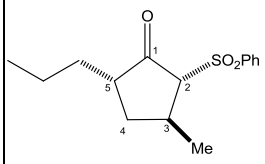


*Note: single crystal isolated from sample of **81b** obtained from reaction of **78** in the presence of $CuCl_2$,* (3S,8R)-*Ind **53** and NaBARF (**Table 2.26**, entry 6): 59% ee* (2R,3S,5R).

Compound	Column	Flow (mL/min)	λ Max (nm)	Mobile phase (hexane : IPA)	Retention time	
					Enantiomer	min
	Chiralcel OJ-H	0.5	222	*gradient* **0 min:** 99.7 : 0.3 **340 min:** 98 : 2	(2*R*,3*S*,5*R*)	140
					(2*S*,3*R*,5*S*)	183



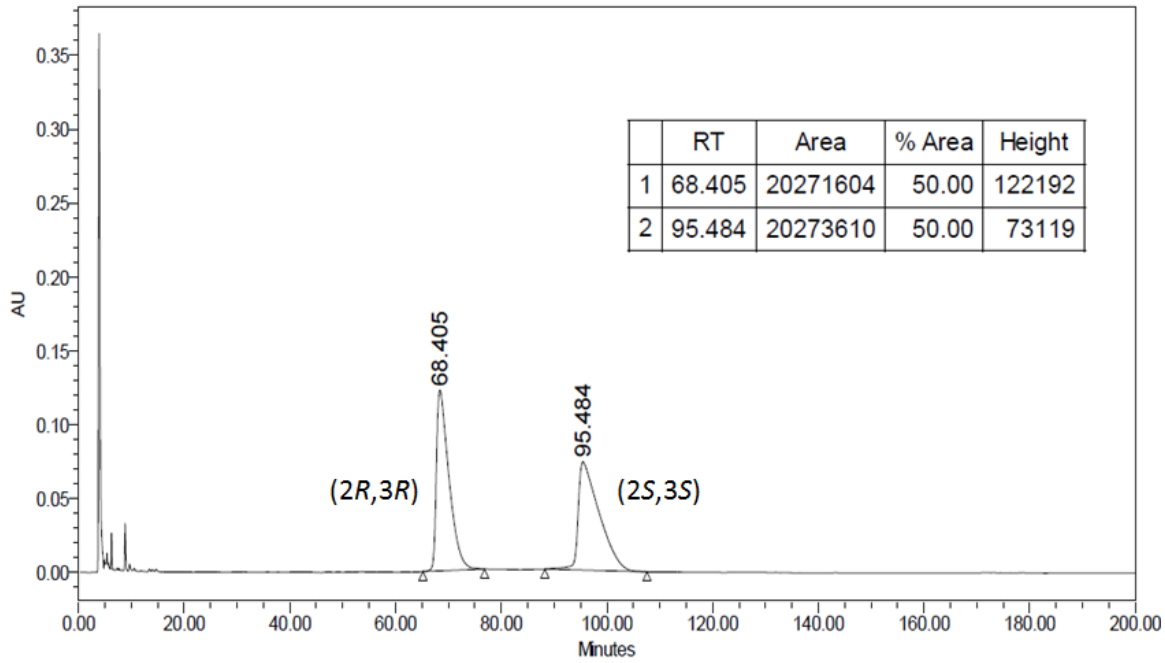
	RT	Area	% Area	Height
1	146.636	466734	6.28	1966
2	173.790	66359	0.89	354
3	192.347	402880	5.42	1319
4	219.619	3321902	44.67	13075
5	231.709	3179459	42.75	10659

Compound	**Column**	**Flow (mL/min)**	**λ Max (nm)**	**Mobile phase (hexane : IPA)**	**Retention time**	
					Enantiomer	**min**
	Chiralcel OJ-H	0.5	222	*gradient* **0 min:** 99.7 : 0.3 **100 min:** 99.7 : 0.3 **340 min:** 98 : 2	TBD	220
					TBD	232

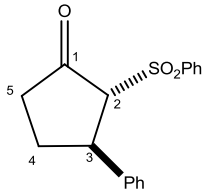
Single crystal analysis for (2R*,3S*,5S*)-**81a** *is pending.*

*Note: for each of the asymmetric copper-catalysed reactions examined (**Table 2.26**), cyclopentanone **81** was isolated as a mixture of diastereomers following column chromatography therefore, measurement of rotation values was not conducted.*

(±)-*trans*-2-Phenylsulfonyl-3-phenylcyclopentanone 42



	RT	Area	% Area	Height
1	68.405	20271604	50.00	122192
2	95.484	20273610	50.00	73119

Compound	Column	Flow (mL/min)	λ Max (nm)	Mobile phase (hexane : IPA)	Retention time	
					Enantiomer	min
	Chiralpak OJ-H	1.0	217	60 : 40	(2*R*, 3*R*)	68
					(2*S*, 3*S*)	95

(–)-(2*R*, 3*R*)-2-Phenylsulfonyl-3-phenylcyclopentanone **42**:

$[\alpha]_D^{20}$ –67.5 (*c* 0.5, CH_2Cl_2, 89% ee)

Isolated from reaction of **35 in the presence of $CuCl_2$,* (3S,8R)-*Ind **53** and NaBARF (**Table 2.14**, entry 30).*

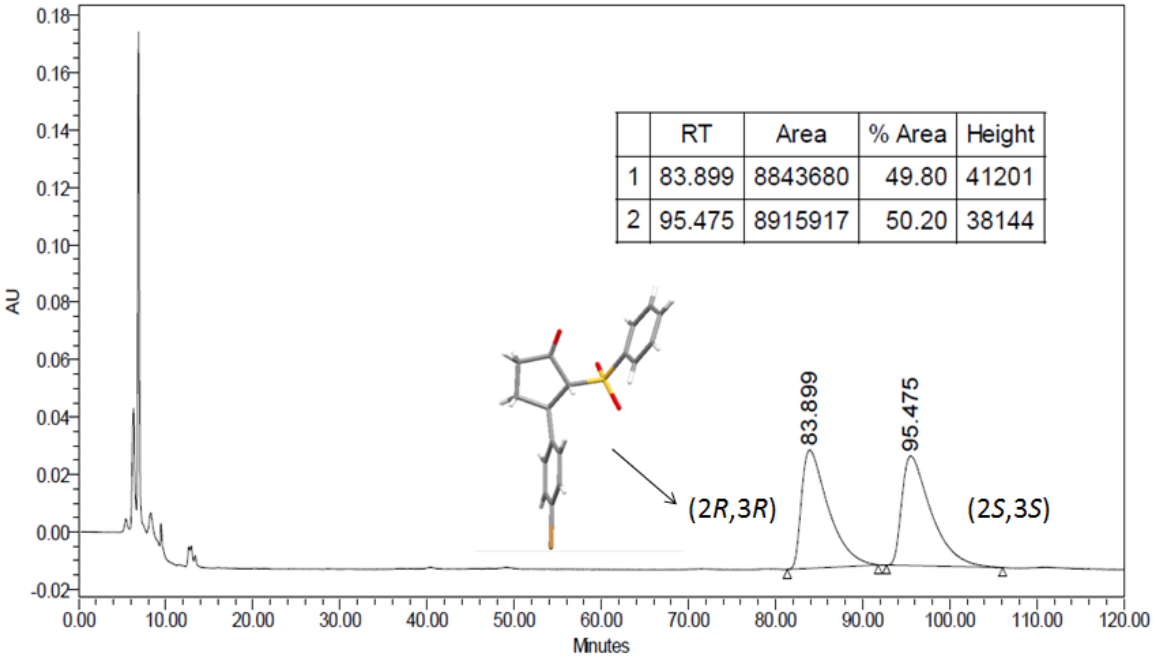
(+)-(2*S*, 3*S*)-2-Phenylsulfonyl-3-phenylcyclopentanone **42**:

$[\alpha]_D^{20}$ +19.1 (*c* 0.5, CH_2Cl_2, 23% ee)

Isolated from reaction of **35 in the presence of Rh_2(S-Phpa)$_4$.H_2O (**Table 2.10**, entry 17).*

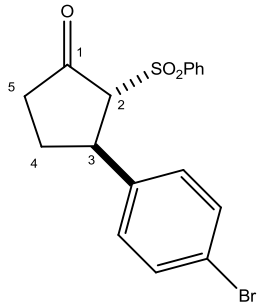
lit.[1,2]: $[\alpha]_D^{20}$ +43.8 (*c* 2.0, CH_2Cl_2, 86% ee)

(±)-*trans*-2-Phenylsulfonyl-3-(4-bromophenyl)cyclopentanone 72



	RT	Area	% Area	Height
1	83.899	8843680	49.80	41201
2	95.475	8915917	50.20	38144

*Note: single crystal isolated from sample of **72** obtained from reaction of **64** in the presence of $CuCl_2$,* (3S,8R)*-Ind **53** and NaBARF (**Table 2.24**, entry 5): 87% ee* (2R,3R)*. Chiral HPLC analysis of single crystal of **72** was attempted, however, no signal was observed.*

Compound	Column	Flow (mL/min)	λ Max (nm)	Mobile phase (hexane : IPA)	Retention time	
					Enantiomer	min
	Chiralcel OD-H	0.5	218	90 : 10	(2*R*, 3*R*)	84
					(2*S*, 3*S*)	96

(–)-(2*R*, 3*R*)-2-Phenylsulfonyl-3-(4-bromophenyl)cyclopentanone **72**:

$[\alpha]_D^{20}$ –57.2 (*c* 0.5, CH_2Cl_2, 87% ee)

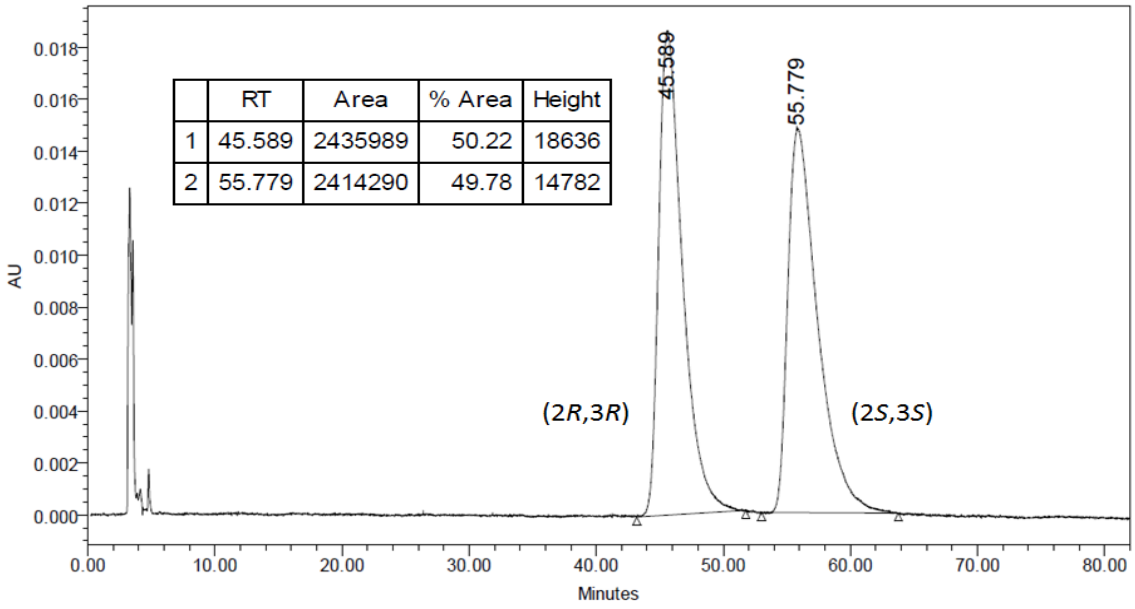
Isolated from reaction of **64 in the presence of $CuCl_2$,* (3S,8R)*-Ind **53** and NaBARF (**Table 2.24**, entry 5).*

(+)-(2*S*, 3*S*)-2-Phenylsulfonyl-3-(4-bromophenyl)cyclopentanone **72**:

$[\alpha]_D^{20}$ +49.0 (*c* 0.5, CH_2Cl_2, 67% ee)

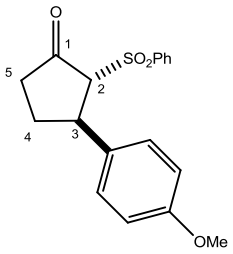
Isolated from reaction of **64 in the presence of $CuCl_2$,* (4R)*-Bn **50** and NaBARF (**Table 2.24**, entry 2).*

(±)-*trans*-2-[(4-Methoxyphenyl)sulfonyl]-3-phenylcyclopentanone 73

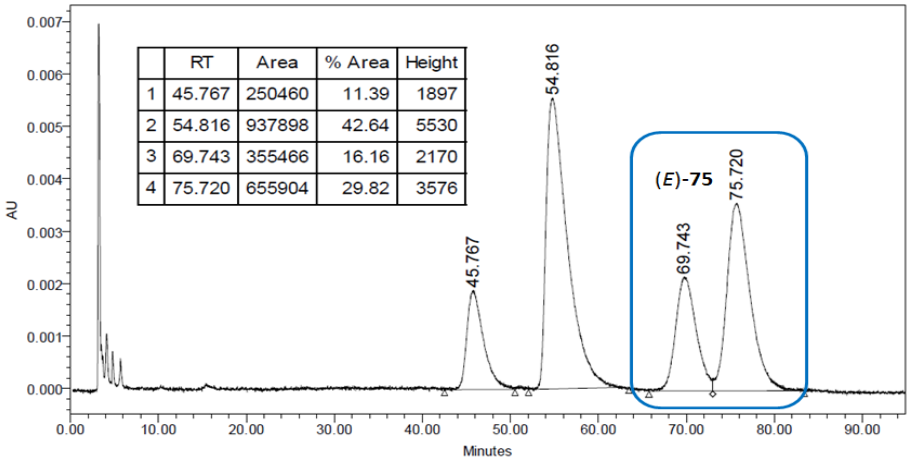


	RT	Area	% Area	Height
1	45.589	2435989	50.22	18636
2	55.779	2414290	49.78	14782

*Note: single crystal analysis of **73** was not conducted. Assignment of absolute stereochemistry and elution sequence of enantiomers for this compound was made by comparison to assignments for the related phenyl-substituted cyclopentanones **42**, **72** and **61**.*

Compound	Column	Flow (mL/min)	λ Max (nm)	Mobile phase (hexane : IPA)	Retention time	
					Enantiomer	min
	Chiralcel OD-H	1	221	90 : 10	(2*R*, 3*R*)	46
					(2*S*, 3*S*)	56

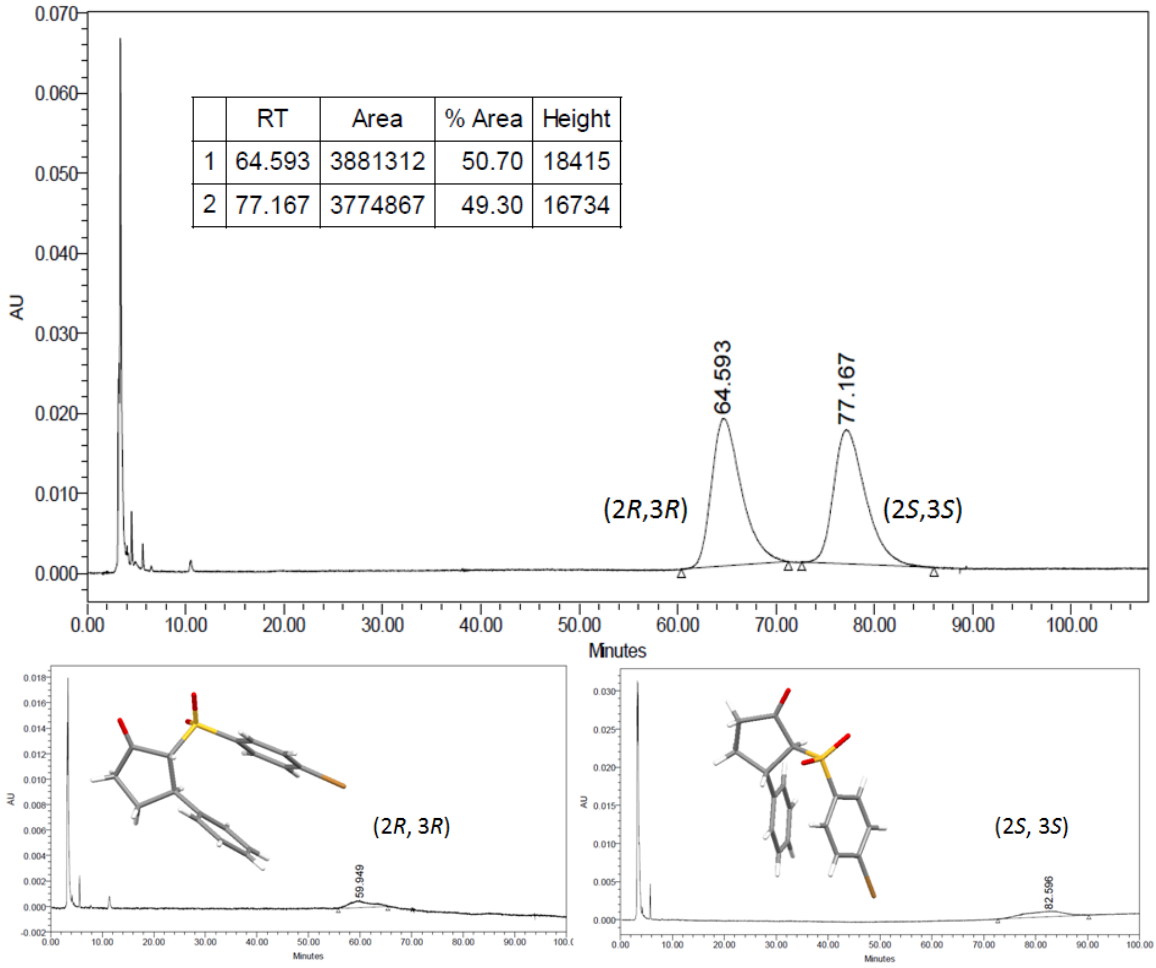
Note: samples of **73** isolated after column chromatography contained minor amount of (*E*)-**75**, therefore measurement of specific rotation values was not conducted. Separation of the enantiomeric peaks of (*E*)-**75** was also achieved using the HPLC conditions described above (see below). Optimal visualisation of the enantiomers of (*E*)-**75** was achieved at λ max = 245 nm.

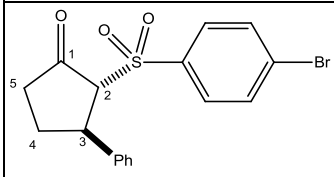


	RT	Area	% Area	Height
1	45.767	250460	11.39	1897
2	54.816	937898	42.64	5530
3	69.743	355466	16.16	2170
4	75.720	655904	29.82	3576

isolated from reaction of **65 in the presence of $CuCl_2$, (4R,5S)-diPh **52** and NaBARF (**Table 2.24**, entry 9).*

(±)-*trans*-2-[(4-Bromophenyl)sulfonyl]-3-phenylcyclopentanone 61



Compound	Column	Flow (mL/min)	λ Max (nm)	Mobile phase (hexane : IPA)	Retention time	
					Enantiomer	min
	Chiralpak OJ-H	1.0	231	30 : 70	(2*R*, 3*R*)	65
					(2*S*, 3*S*)	77

(–)-(2*R*, 3*R*)-2-[(4-bromophenyl)sulfonyl]-3-cyclopentanone **61**:

$[\alpha]_D^{20}$ –76.3 (*c* 0.5, CH_2Cl_2, 87% ee)

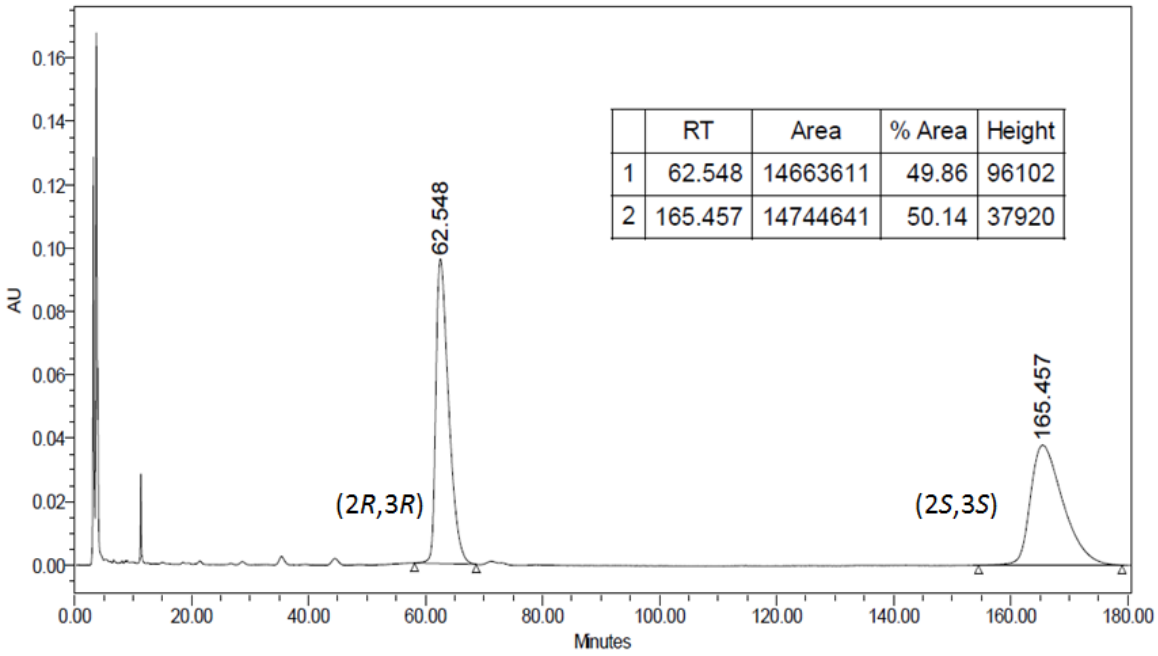
Isolated from reaction of **60 in the presence of $CuCl_2$,* (3S,8R)-*Ind **53** and NaBARF (**Table 2.23**, entry 5).*

(+)-(2*S*, 3*S*)-2-[(4-bromophenyl)sulfonyl]-3-cyclopentanone **61**:

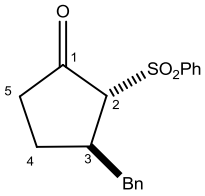
$[\alpha]_D^{20}$ +59.9 (*c* 0.5, CH_2Cl_2, 83% ee)

Isolated from reaction of **60 in the presence of $CuCl_2$,* (4R)-*Bn **50** and NaBARF (**Table 2.23**, entry 2).*

(±)-*trans*-2-Phenylsulfonyl-3-benzylcyclopentanone 43



	RT	Area	% Area	Height
1	62.548	14663611	49.86	96102
2	165.457	14744641	50.14	37920

Compound	Column	Flow (mL/min)	λ Max (nm)	Mobile phase (hexane : IPA)	Retention time	
					Enantiomer	min
	Chiralpak AS-H	1.0	210	90 : 10	(2*R*, 3*R*)	71
					(2*S*, 3*S*)	202

(–)-(2*R*, 3*R*)-2-Phenylsulfonyl-3-benzylcyclopentanone **43**:

$[\alpha]_D^{20}$ –39.0 (*c* 0.5, CH_2Cl_2, 66% ee)

Isolated from reaction of **36 in the presence of $CuCl_2$,* (3S,8R)-*Ind **53** and NaBARF (**Table 2.14**, entry 36).*

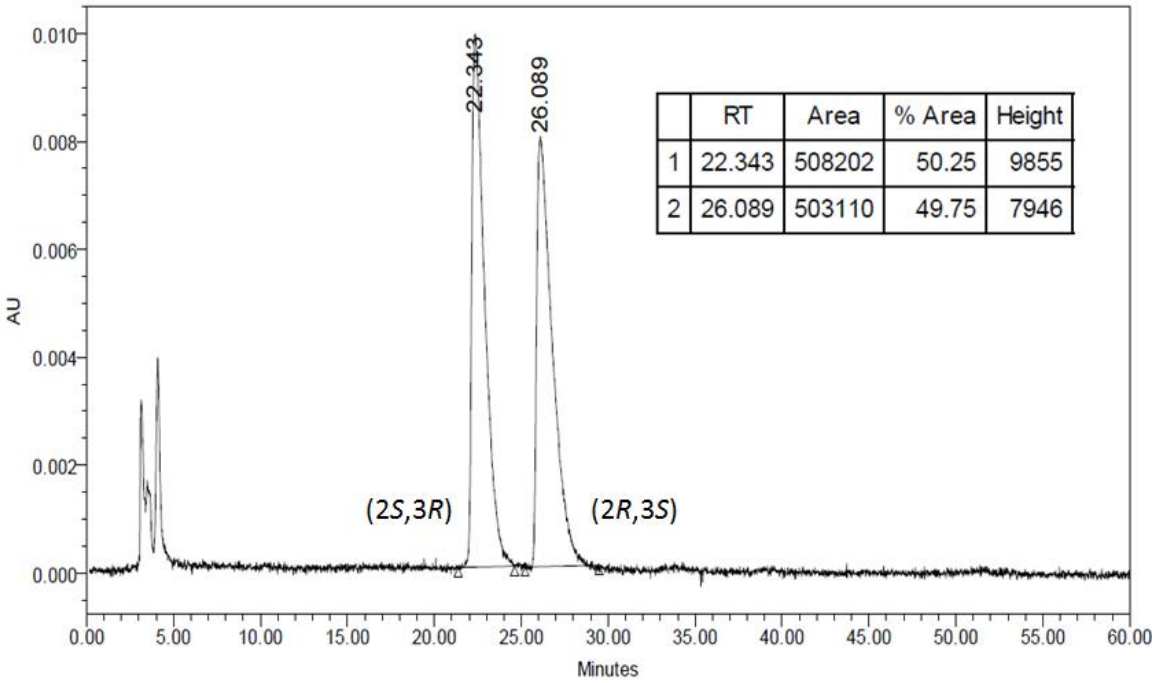
(+)-(2*S*, 3*S*)-2-Phenylsulfonyl-3-benzylcyclopentanone **43**:

$[\alpha]_D^{20}$ +37.1 (*c* 0.5, CH_2Cl_2, 55% ee)

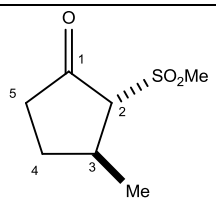
Isolated from reaction of **36 in the presence of $CuCl_2$,* (4R)-***85** and NaBARF (**Table 2.32**, entry 33).*

lit.[4]: $[\alpha]_D^{20}$ +55.6 (*c* 1.0, $CHCl_3$, 98% ee)

(±)-*trans*-2-(Methylsulfonyl)-3-methylcyclopentanone 44



	RT	Area	% Area	Height
1	22.343	508202	50.25	9855
2	26.089	503110	49.75	7946

Compound	Column	Flow (mL/min)	λ Max (nm)	Mobile phase (hexane : IPA)	Retention time	
					Enantiomer	min
	Chiralcel OD-H	1.0	312	90 : 10	(2*S*, 3*R*)	23
					(2*R*, 3*S*)	26

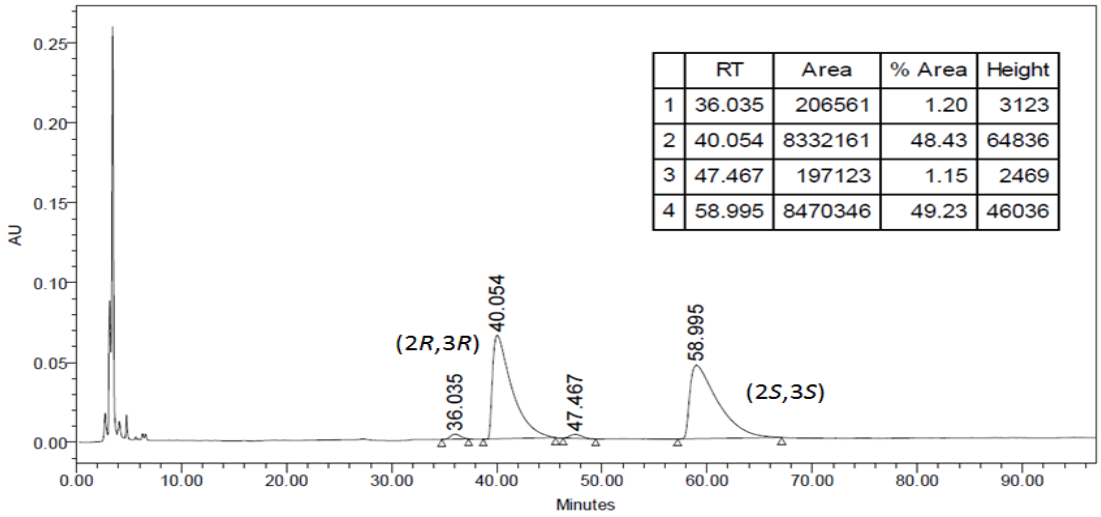
(+)-(2*S*, 3*R*)-2-(Methylsulfonyl)-3-methylcyclopentanone **44**:

$[\alpha]_D^{20}$ +14.8 (*c* 0.4, CH_2Cl_2, 16% ee)

Isolated from reaction of **37 in the presence of $CuCl_2$,* (4R,5S)-***52*** *and NaBARF (**Table 2.22**, entry 4).*

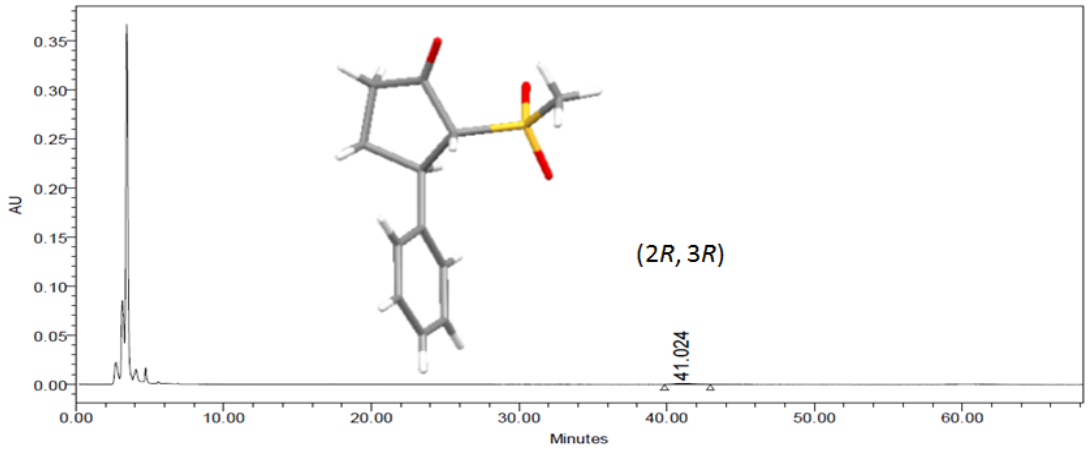
lit.[1,2]: $[\alpha]_D^{20}$ +5.6 (*c* 7.7, CH_2Cl_2, 10% ee)

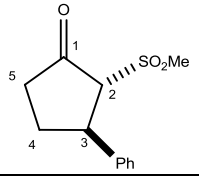
(±)-*trans*-2-(Methylsulfonyl)-3-phenylcyclopentanone 45



	RT	Area	% Area	Height
1	36.035	206561	1.20	3123
2	40.054	8332161	48.43	64836
3	47.467	197123	1.15	2469
4	58.995	8470346	49.23	46036

Note: two unknown peaks (50 : 50) were observed in the HPLC trace of 2-(methylsulfonyl)-3-phenylcyclopentanone ***45*** *at 36 and 47 minutes. These peaks were observed for both rhodium- and copper-catalysed reactions of* ***38****.*



Compound	Column	Flow (mL/min)	λ Max (nm)	Mobile phase (hexane : IPA)	Retention time	
					Enantiomer	min
	Chiralpak OJ-H	1.0	213	90 : 10	(2*R*, 3*R*)	40
					(2*S*, 3*S*)	59

(–)-(2*R*, 3*R*)-2-(Methylsulfonyl)-3-phenylcyclopentanone **45**:

$[\alpha]_D^{20}$ –20.7 (*c* 0.3, CH_2Cl_2, 62% ee)

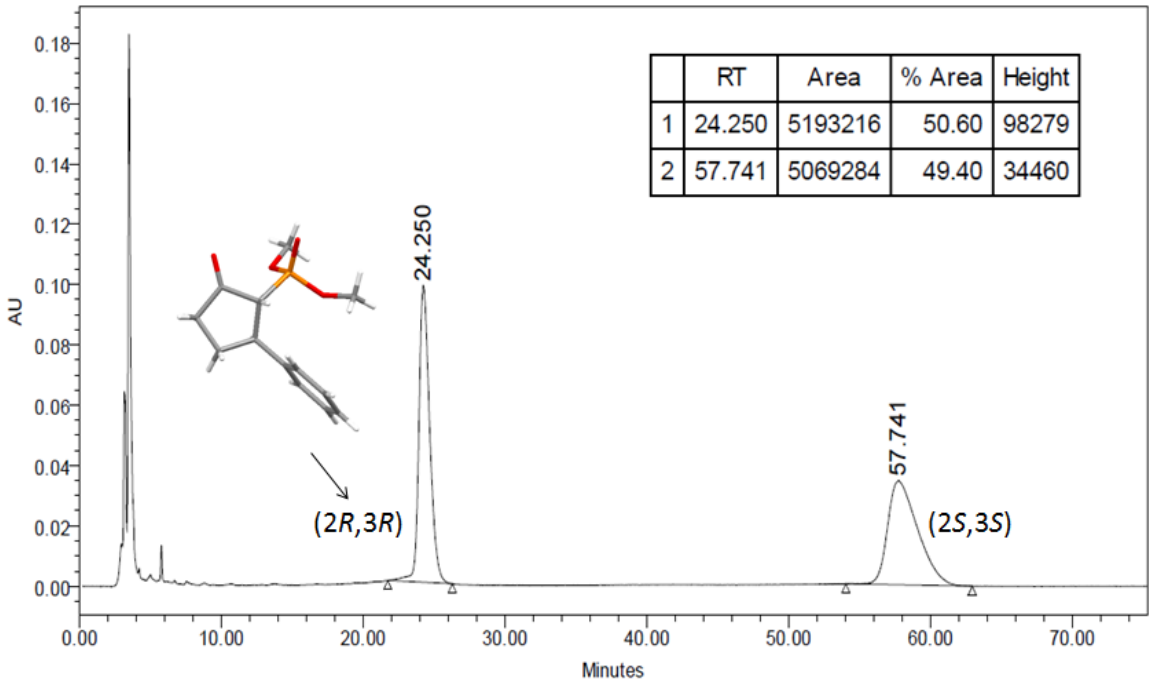
Isolated from reaction of* ***38* *in the presence of* $CuCl_2$, (3S,8R)-*Ind* ***53*** *and NaBARF (****Table 2.22****, entry 10).*

(+)-(2*S*, 3*S*)-2-(Methylsulfonyl)-3-phenylcyclopentanone **45**:

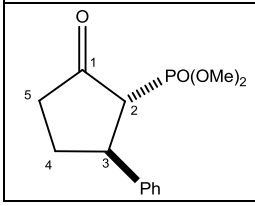
$[\alpha]_D^{20}$ +20.7 (*c* 0.3, CH_2Cl_2, 70% ee)

Isolated from reaction of* ***38* *in the presence of* $CuCl_2$, (4R)-*Bn* ***50*** *and NaBARF (****Table 2.22****, entry 7).*

(±)-*trans*-2-Dimethoxyphosphoryl-3-phenylcyclopentanone 101



*Note: single crystal isolated from sample of **101** obtained from reaction of **99** in the presence of $CuCl_2$,* (3S,8R)*-Ind **53** and NaBARF (**Table 3.1**, entry 1): 32% ee* (2R,3R)*. Chiral HPLC analysis of single crystal of **101** was attempted, however, no signal was observed.*

Compound	Column	Flow (mL/min)	λ Max (nm)	Mobile phase (hexane : IPA)	Retention time	
					Enantiomer	min
	Chiralpak OJ-H	1.0	215	80 : 20	(2*R*, 3*R*)	24
					(2*S*, 3*S*)	58

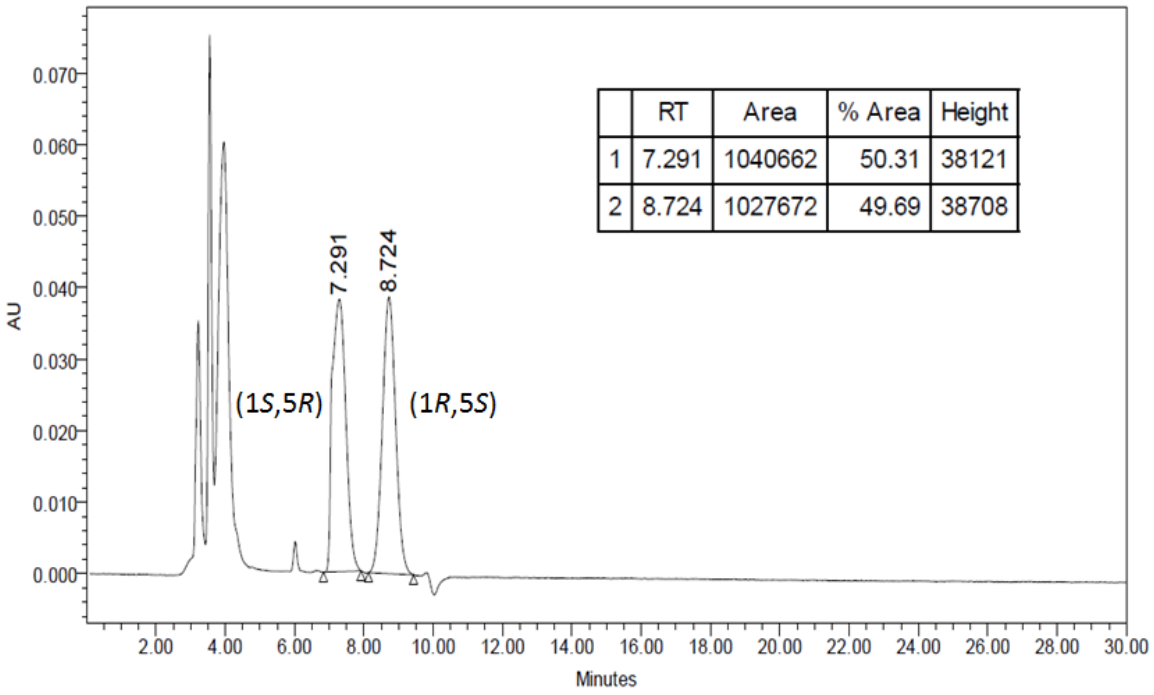
(+)-(2*S*, 3*S*)-2-Dimethoxyphosphoryl-3-phenylcyclopentanone **101**:

$[\alpha]_D^{20}$ +64.1 (*c* 0.5, CH_2Cl_2, 28% ee)

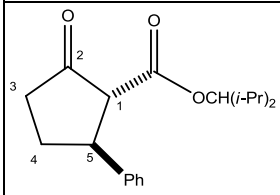
Isolated from reaction of **99 in the presence of $CuCl_2$ and* (4R)*-Bn **50** (**Table 3.3**, entry 4).*

Note: Enantioenriched sample of (2*R*,3*R*)-**101** obtained from reaction of **99** in the presence of $CuCl_2$, (3*S*,8*R*)-Ind **53** and NaBARF (**Table 3.3**, entry 1) was of insufficient purity to obtain an accurate rotation value.

(±)-*trans*-2,4-Dimethylpentan-3-yl 2-oxo-5-phenylcyclopentanecarboxylate 104



	RT	Area	% Area	Height
1	7.291	1040662	50.31	38121
2	8.724	1027672	49.69	38708

Compound	Column	Flow (mL/min)	λ Max (nm)	Mobile phase (hexane : IPA)	Retention time	
					Enantiomer	min
	Chiralpak OJ-H	1.0	218	90 : 10	(1*S*, 5*R*)	7
					(1*R*, 5*S*)	9

A sample of **104** isolated from cyclisation of **103** in the presence of $CuCl_2$, (3*S*,8*R*)-Ind **53** and NaBARF (**Table 3.5**, entry 1, 65% ee) was hydrolysed and decarboxylated to provide 3-phenylcyclopentanone **115** (see **Section 4.5.5** for details), which was used to determine which enantiomer was in excess by comparison to literature rotation values for **115**.

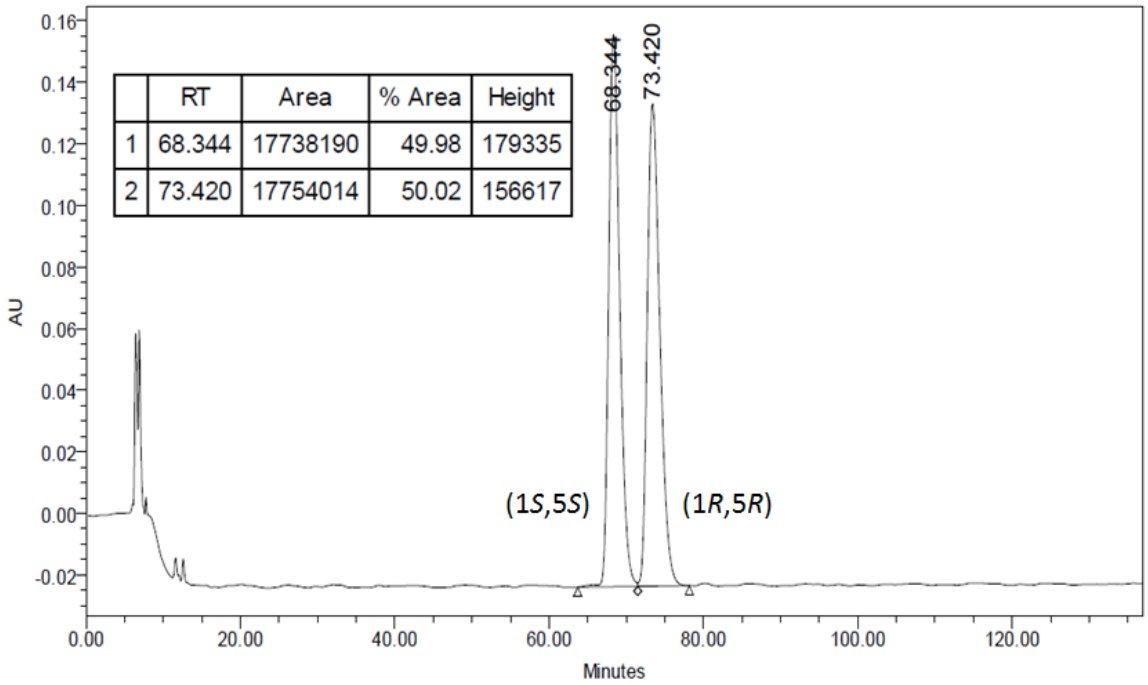
(–)-(*S*)-3-Phenylcyclopentanone **115**:

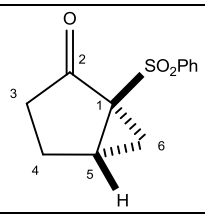
$[\alpha]_D^{20}$ –44.6 (*c* 0.77, $CHCl_3$, 65% ee)

(+)-(*R*)-3-Phenylcyclopentanone **115**:

lit.[5]: $[\alpha]_D^{20}$ +65.4 (*c* 1.06, $CHCl_3$, 60% ee)

(±)-1-(Phenylsulfonyl)bicyclo[3.1.0]hexan-2-one 117



Compound	Column	Flow (mL/min)	λ Max (nm)	Mobile phase (hexane : IPA)	Retention time	
					Enantiomer	min
	Chiralpak AS-H	0.5	215	80 : 20	(1*S*, 5*S*)	66
					(1*R*, 5*R*)	71

(+)-(1*S*, 5*S*)-1-Phenylsulfonyl-2-oxobicyclo[3.1.0]hexane **117**:

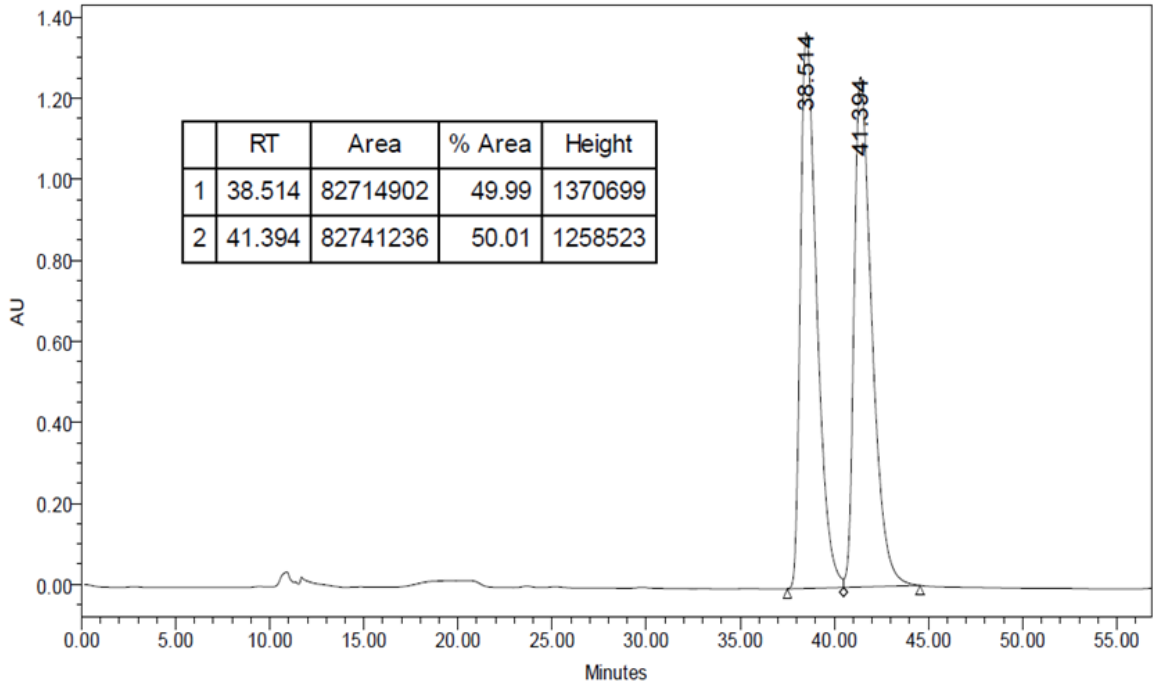
$[\alpha]_D^{23.5}$ +20.7 (*c* 0.6, $CHCl_3$, 61% ee)

Isolated from reaction of **116 in the presence of $Cu(OTf)_2$ and* (4R)-*Bn **50** (**Table 3.7**, entry 2).*

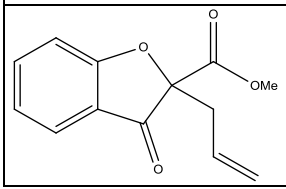
(–)-(1*R*, 5*R*)-1-Phenylsulfonyl-2-oxobicyclo[3.1.0]hexane **117**:

lit.[6]: $[\alpha]_D^{23.5}$ –62.1 (*c* 0.6, $CHCl_3$, 100% ee)

(±)-*trans*-2-Allyl-2-methoxycarbonyl-2,3-dihydrofuran-3-one 121



	RT	Area	% Area	Height
1	38.514	82714902	49.99	1370699
2	41.394	82741236	50.01	1258523

Compound	Column	Flow (mL/min)	λ Max (nm)	Mobile phase (hexane : IPA)	Retention time	
					Enantiomer	min
	Chiralcel OD-H	0.3	210	99 : 1	TBD	38
					TBD	41

(–)-2-Allyl-2-methoxycarbonyl-2,3-dihydrofuran-3-one **121**:

$[\alpha]_D^{20}$ –66.7 (*c* 0.5, CH_2Cl_2, 48% ee)

Isolated from reaction of **120 in the presence of Rh_2(R-p-*ClMand*)$_4$ (**Table 3.10**, entry 8).*

$[\alpha]_D^{20}$ –31.2 (*c* 0.5, CH_2Cl_2, 26% ee)

Isolated from reaction of **120 in the presence of $CuCl_2$, (4R,5S)-*diPh* **52** and NaBARF (**Table 3.9**, entry 10).*

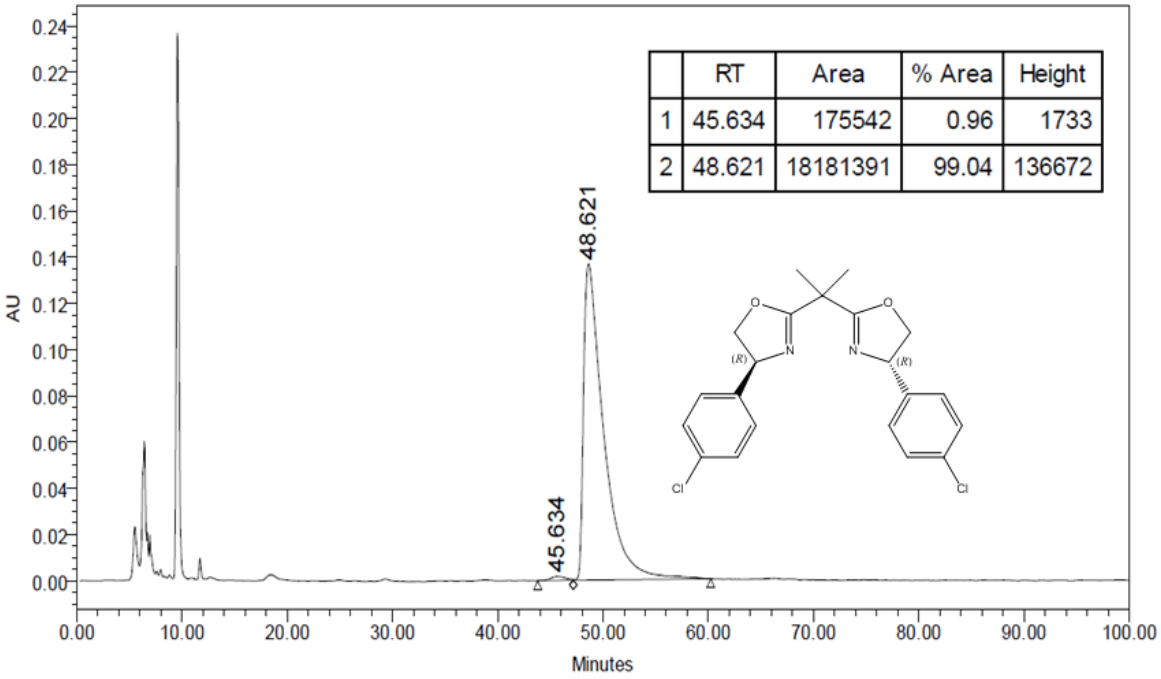
(+)-2-Allyl-2-methoxycarbonyl-2,3-dihydrofuran-3-one **121**:

$[\alpha]_D^{20}$ +51.0 (*c* 0.5, CH_2Cl_2, 37% ee)

Isolated from reaction of **120 in the presence of Rh_2(S-*Mand*)$_4$ (**Table 3.10**, entry 3).*

Note: specific rotation values for **121** not reported in the literature, however, Hodgson[7] had reported that reactions of **120** with Rh_2(*S*-PTTL)$_4$ provide (–)-**121** while reactions with Rh_2(*R*-BNP)$_4$ provide (+)-**121**. Single crystal analysis of **121** to determine absolute stereochemistry has yet to be conducted.

(*R*)-2,2-bis{-[4-(4-Methoxyphenyl)-1,3-oxazolinyl]}propane 82

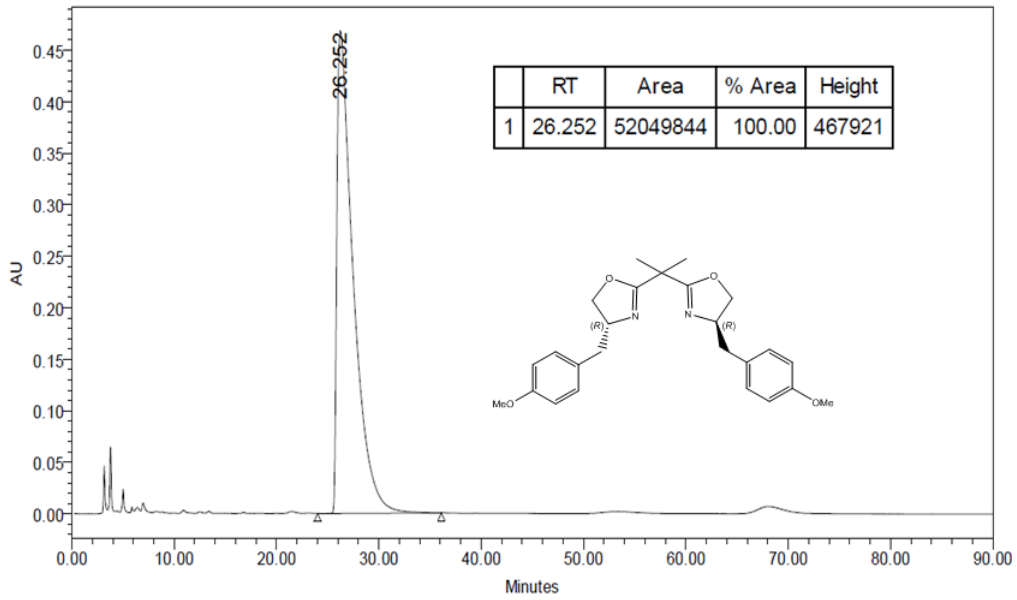


Column	Flow (mL/min)	λ Max (nm)	Mobile phase (hexane : IPA)	Retention time	
				Enantiomer	min
Chiralcel OD-H	0.5	209	98 : 2	(*S*)	46
				(*R*)	49

*HPLC conditions are in line with those previously reported by O'Keeffe.[8]

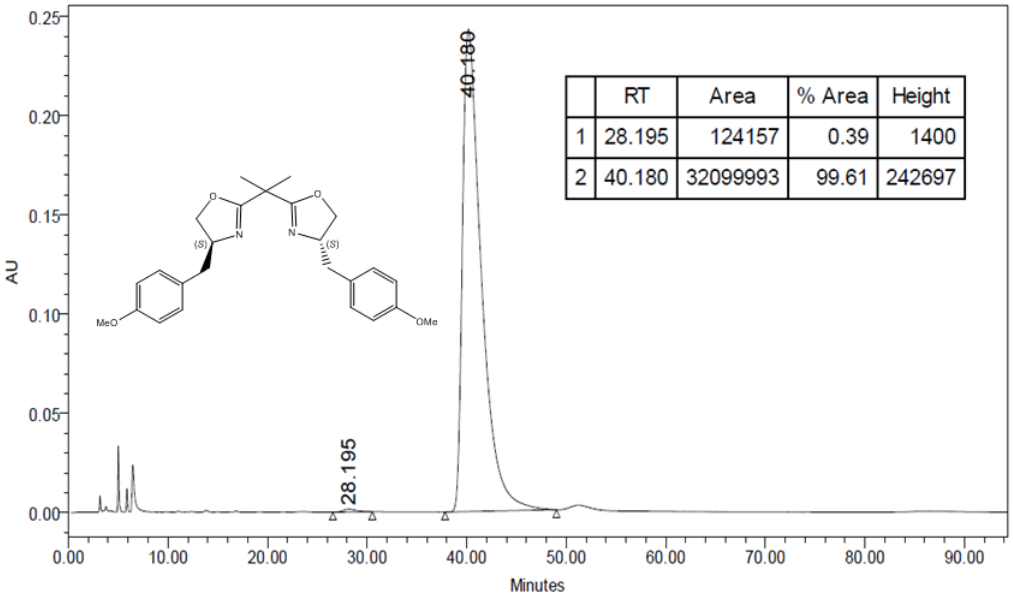
Note: for details of specific rotation values for (R)-***82*** *see* ***Section 4.8.3***

(*R*)-2,2'-(Propane-2,2-diyl)bis[4-(4-methoxybenzyl)-4,5-dihydrooxazole] 85



	RT	Area	% Area	Height
1	26.252	52049844	100.00	467921

(*S*)-2,2'-(Propane-2,2-diyl)bis[4-(4-methoxybenzyl)-4,5-dihydrooxazole] 85



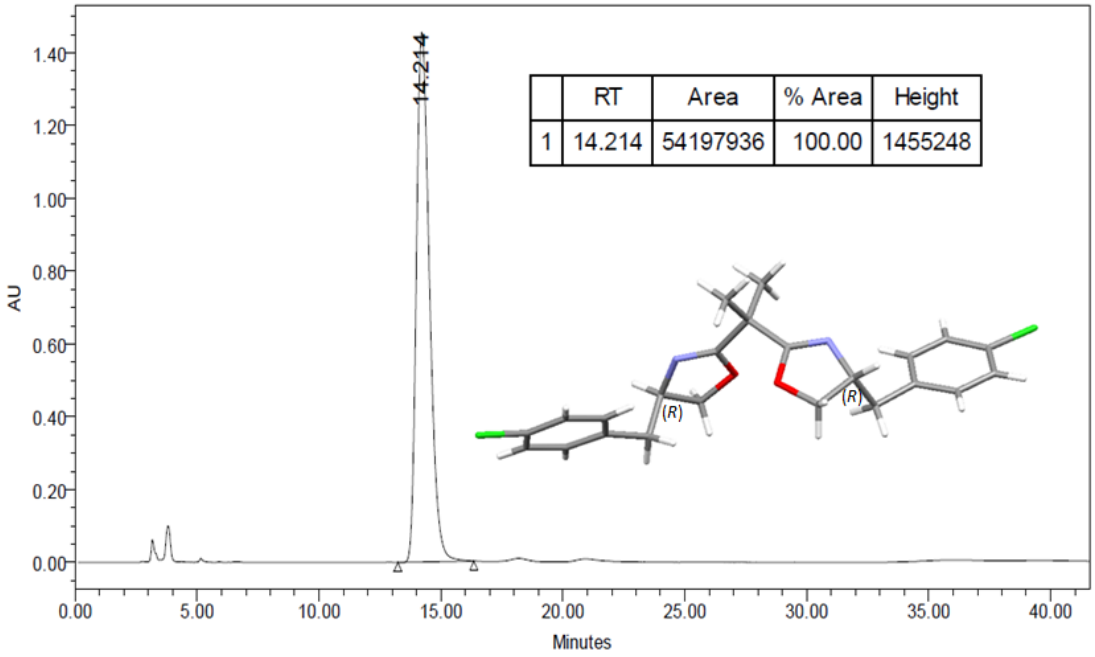
	RT	Area	% Area	Height
1	28.195	124157	0.39	1400
2	40.180	32099993	99.61	242697

Note: (S)-***85*** *was not used in catalyst studies in this project.*

Column	**Flow (mL/min)**	**λ Max (nm)**	**Mobile phase (hexane : IPA)**	**Retention time**	
				Enantiomer	**(min)**
Chiralcel OD-H	1	231	95 : 5	(*R*)	26
				(*S*)	40

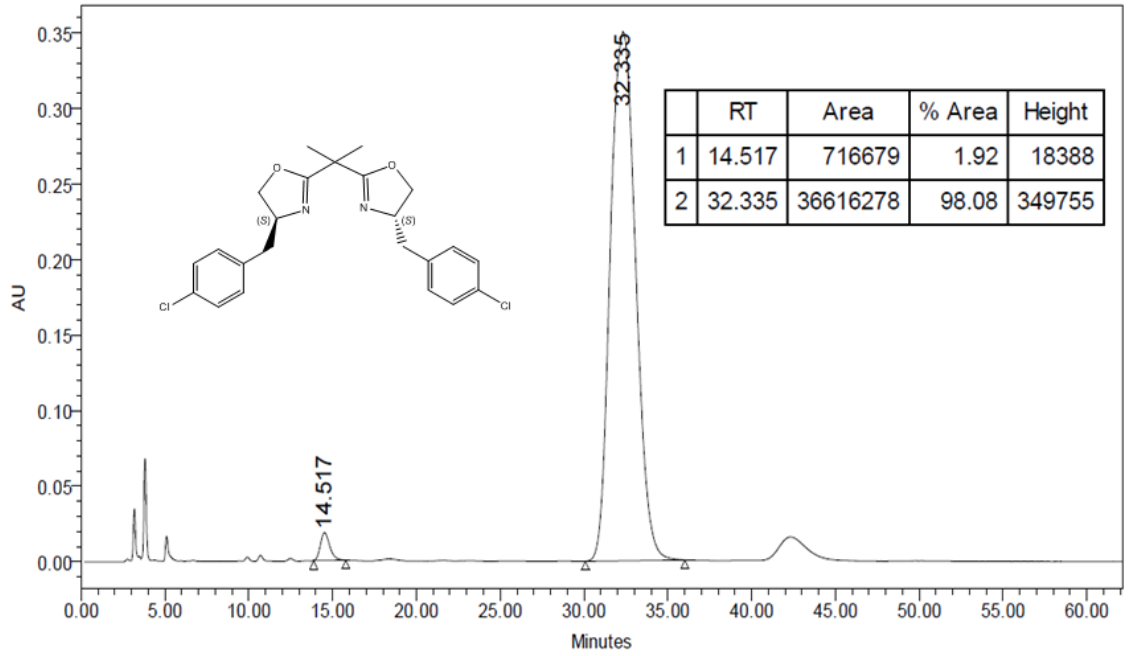
Note: single crystal analysis of ***85*** *was not conducted as this ligand is an oil. Assignment of absolute stereochemistry of* ***85*** *was made by comparison with polarimetry values and chiral HPLC data for* ***84*** *and* ***86****. For details of specific rotation values for* (R)-***85*** *and* (S)-***85*** *see* ***Section 4.8.3***

(*R*)-2,2'-(Propane-2,2-diyl)bis[4-(4-chlorobenzyl)-4,5-dihydrooxazole] 84



	RT	Area	% Area	Height
1	14.214	54197936	100.00	1455248

(*S*)-2,2'-(Propane-2,2-diyl)bis[4-(4-chlorobenzyl)-4,5-dihydrooxazole] 84



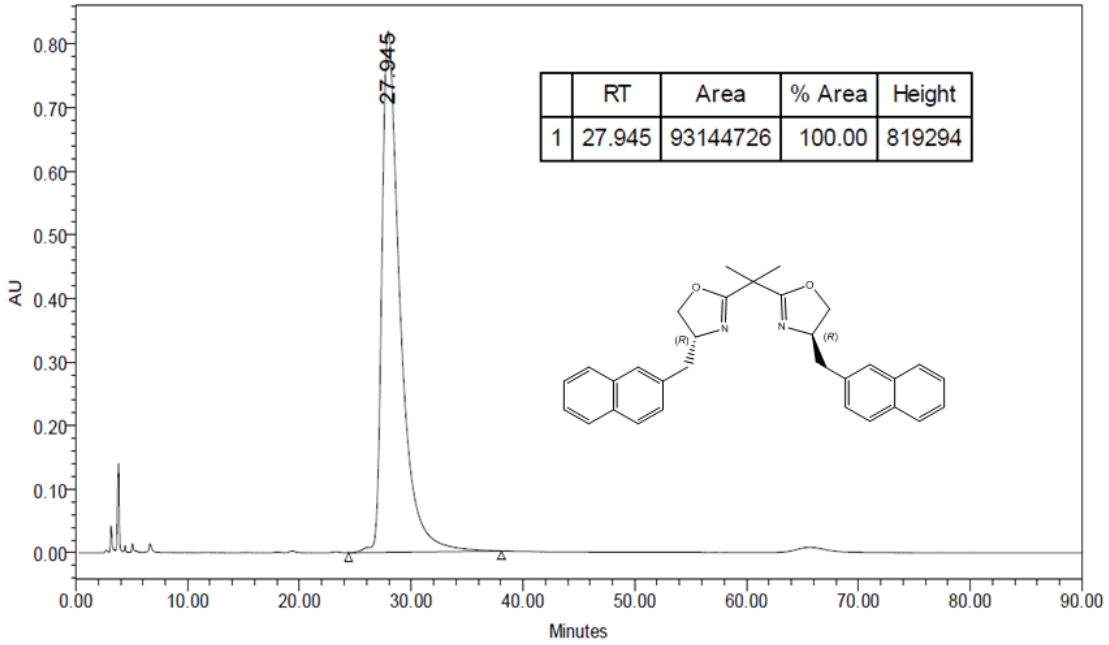
	RT	Area	% Area	Height
1	14.517	716679	1.92	18388
2	32.335	36616278	98.08	349755

Note: (S)-***84*** *was not used in catalyst studies in this project.*

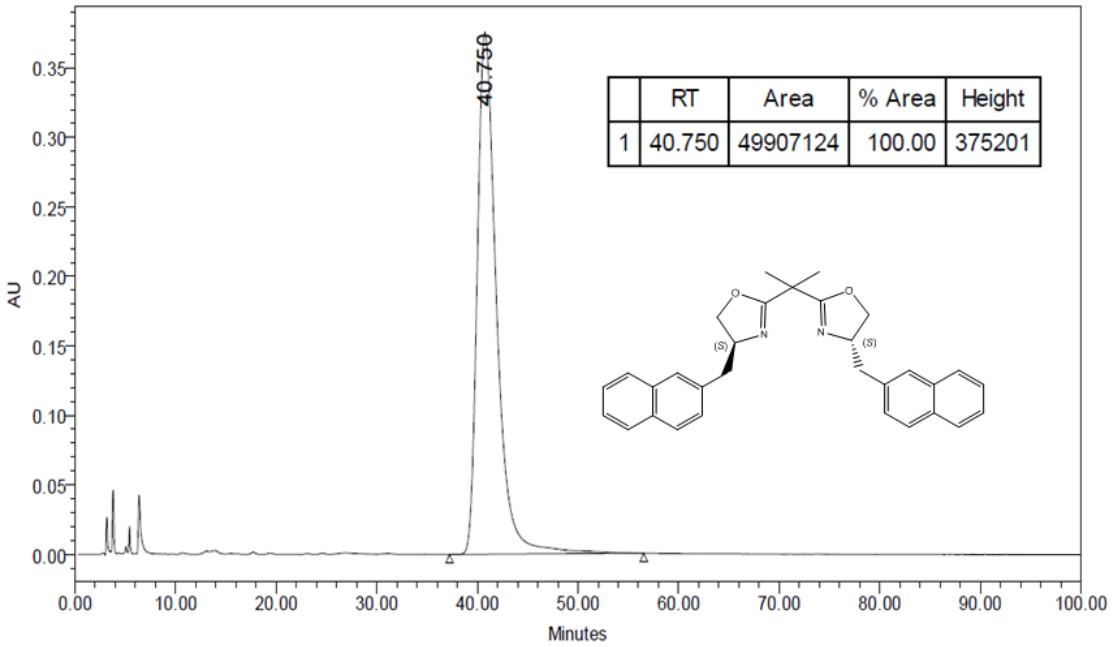
Column	**Flow (mL/min)**	**λ Max (nm)**	**Mobile phase (hexane : IPA)**	**Retention time**	
				Enantiomer	**min**
Chiralcel OD-H	1	220	95 : 5	(*R*)	14
				(*S*)	32

Note: for details of specific rotation values for (R)-***84*** *and* (S)-***84*** *see* ***Section 4.8.3***

(*R*)-2,2'-(Propane-2,2-diyl)bis[4-(naphthalen-1-ylmethyl)-4,5-dihydrooxazole] 86



(*S*)-2,2'-(Propane-2,2-diyl)bis[4-(naphthalen-1-ylmethyl)-4,5-dihydrooxazole] 86



Note: (S)-***86*** *was not used in catalyst studies in this project.*

Column	Flow (mL/min)	λ Max (nm)	Mobile phase (hexane : IPA)	Retention time	
				Enantiomer	min
Chiralcel OD-H	1	218	95 : 5	(*R*)	27
				(*S*)	40

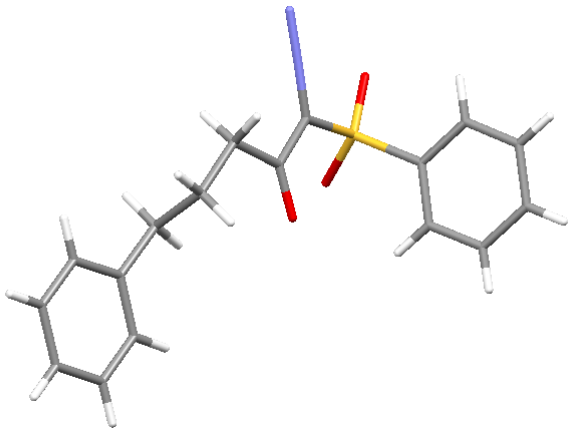
Note: for details of specific rotation values for (R)-***86*** *and* (S)-***86*** *see* ***Section 4.8.3****, single crystal analysis for this compound is pending.*

References

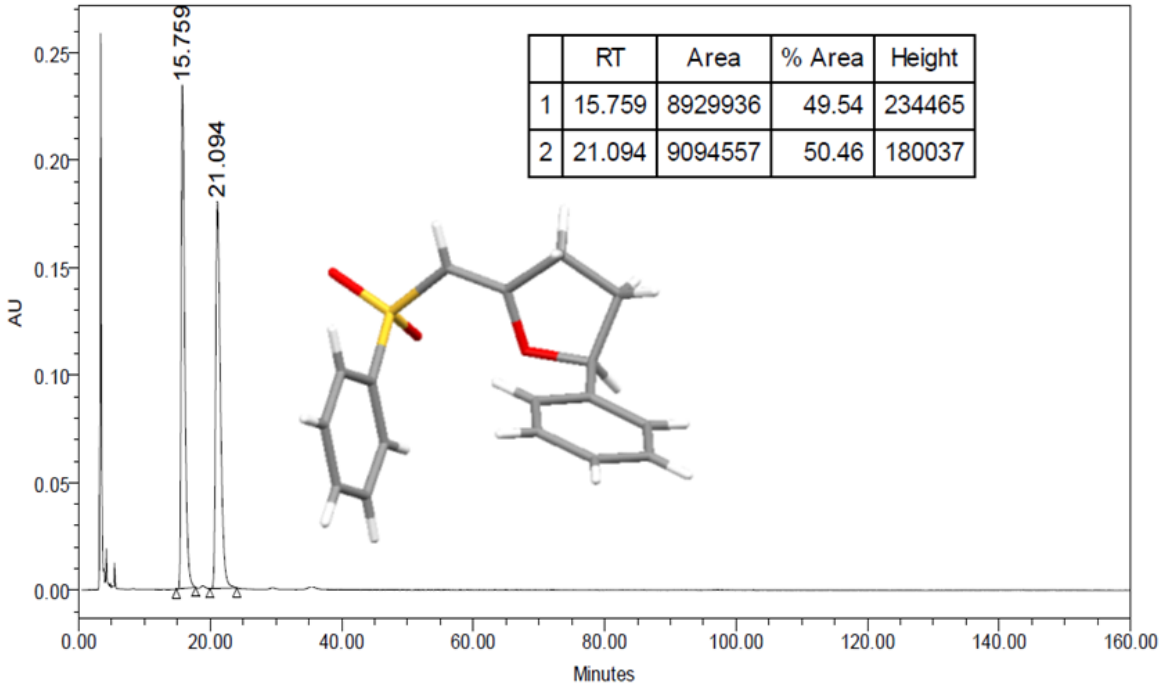
1) Kelleher, L. *Ph.D. Thesis, NUI* **1998**.
2) Kelleher, L.; Maguire, A. R. *J. Mol. Catal. B: Enzymatic* **1996**, *1*, 115–126.
3) O'Riordan, N. B. *Ph.D. Thesis, NUI* **2001**.
4) O'Keeffe, E. *Ph.D. Thesis, NUI* **2002**.
5) Müller, P.; Boléa, C. *Helv. Chim. Acta* **2002**, *85*, 483–494.
6) Honma, M.; Sawada, T.; Fujisawa, Y.; Utsugi, M.; Watanabe, H.; Umino, A.; Matsumura, T.; Hagihara, T.; Takano, M.; Nakada, M. *J. Am. Chem. Soc.* **2003**, *125*, 2860–2861.
7) Hodgson, D. M.; Petroliagi, M.; *Tetrahedon: Asymmetry* **2001**, *12*, 877–881.
8) O'Keeffe, S. *Ph.D. Thesis, NUI* **2007**.

Appendix II *Single crystal analysis*

1-Diazo-1-phenylsulfonyl-5-phenylpentan-2-one 35



(*Z*)-2-Phenyl-5-[(phenylsulfonyl)methylene]tetrahydrofuran 54



	RT	Area	% Area	Height
1	15.759	8929936	49.54	234465
2	21.094	9094557	50.46	180037

*Note: single crystal of **54** displayed above is racemic.*

Chiral stationary phase HPLC conditions: Chiralcel OJ-H column at room temperature, with hexane : IPA (60 : 40) as eluent, a flow rate of 1 mL/min, and the detector set at λ 217 nm.

1-Diazo-1-phenylsulfonyl-5-phenylpentan-2-one 35:
$C_{17}H_{16}N_2O_3S$, M = 328.38, triclinic, space group $P\bar{1}$, a = 7.5490(15), b = 10.288(2), c = 10.625(2) Å, β = 82.722(4)°, V = 783.1(3) Å^3, Z = 2, D_c = 1.393 g cm^{-3}, F_{000} = 344, Mo-Kα radiation, λ = 0.71073 Å, T = 100(2) K, $2\theta_{max}$ = 22.30°, μ = 0.223 mm^{-1}. 18492 reflections collected, 3177 unique (R_{int} = 0.0482). Final GooF = 1.189, R_1 = 0.0486, wR_2 = 0.1350 [obs. Data: $I > 2\sigma(I)$]; R_1 = 0.0647, wR_2 = 0.1466 (all data).

(2*R*,3*R*)-2-Phenylsulfonyl-3-*i*-propylcyclopentanone 40:
$C_{14}H_{18}O_3S$, M = 266.34, monoclinic, space group $P2_1$, a = 7.990(5), b = 10.332(7), c = 8.397(6) Å, β = 99.126(13)°, V = 684.4(8) Å^3, Z = 2, D_c = 1.293 g cm^{-3}, F_{000} = 284, Mo-Kα radiation, λ = 0.71073 Å, T = 296(2) K, $2\theta_{max}$ = 18.4049°, μ = 0.234 mm^{-1}. 6158 reflections collected, 2456 unique (R_{int} = 0.0509). Final GooF = 0.996, R_1 = 0.0529, wR_2 = 0.1143 [obs. Data: $I > 2\sigma(I)$]; R_1 = 0.1074, wR_2 = 0.1374 (all data).

(2*R*,3*R*)-2-(Methylsulfonyl)-3-phenylcyclopentanone 45:
$C_{12}H_{14}O_3S$, M = 238.29, monoclinic, space group $P2_1$, a = 11.8164(18), b = 9.2321(11), c = 11.9043(19) Å, β = 110.492(3)°, V = 1216.5(3) Å^3, Z = 4, D_c = 1.301 g cm^{-3}, F_{000} = 504, Mo-Kα radiation, λ = 0.71073 Å, T = 296(2) K, $2\theta_{max}$ = 22.7146°, μ = 0.255 mm^{-1}. 13855 reflections collected, 4845 unique (R_{int} = 0.0367). Final GooF = 1.068, R_1 = 0.0414, wR_2 = 0.0967 [obs. Data: $I > 2\sigma(I)$]; R_1 = 0.0578, wR_2 = 0.1063 (all data).

(*Z*)-2-Phenyl-5-[(phenylsulfonyl)methylene]tetrahydrofuran 54:
$C_{17}H_{16}O_3S$, M = 300.36, monoclinic, space group $P2_1/c$, a = 11.590(3), b = 8.639(2), c = 16.028(4) Å, β = 110.434(7)°, V = 1503.8(6) Å^3, Z = 4, D_c = 1.327 g cm^{-3}, F_{000} = 632, Mo-Kα radiation, λ = 0.71073 Å, T = 300(2) K, $2\theta_{max}$ = 18.4894°, μ = 0.222 mm^{-1}. 9428 reflections collected, 2663 unique (R_{int} = 0.0375). Final GooF = 1.036, R_1 = 0.0396, wR_2 = 0.1054 [obs. Data: $I > 2\sigma(I)$]; R_1 = 0.0549, wR_2 = 0.1150 (all data).

(2*S*,3*S*)-2-[(4-Bromophenyl)sulfonyl]-3-phenylcyclopentanone 61:
$C_{17}H_{15}BrO_3S$, M = 379.26, orthorhombic, space group $P2_12_12_1$, a = 7.8064(14), b = 12.6377(19), c = 16.783(3) Å, β = 90°, V = 1655.7(5) Å^3, Z = 4, D_c = 1.521 g cm^{-3}, F_{000} = 768, Mo-Kα radiation, λ = 0.71073 Å, T = 292(2) K, $2\theta_{max}$ =21.9468°, μ = 2.617 mm^{-1}. 10139 reflections collected, 3622 unique (R_{int} = 0.0382). Final GooF = 1.123, R_1 = 0.0403, wR_2 = 0.0829 [obs. Data: $I > 2\sigma(I)$]; R_1 = 0.0621, wR_2 = 0.0888 (all data).

(2*R*,3*R*)-2-[(4-Bromophenyl)sulfonyl]-3-phenylcyclopentanone 61:
$C_{17}H_{15}BrO_3S$, M = 379.26, orthorhombic, space group $P2_12_12_1$, a = 7.8117(10), b = 12.6388(16), c = 16.816(2) Å, β = 90°, V = 1660.3(4) Å^3, Z = 4, D_c = 1.517 g cm^{-3}, F_{000} = 768, Mo-Kα radiation, λ = 0.71073 Å, T = 292(2) K, $2\theta_{max}$ = 24.4402°, μ = 2.610 mm^{-1}. 20445 reflections collected, 3628 unique (R_{int} = 0.0401). Final GooF = 1.051, R_1 = 0.0351, wR_2 = 0.0771 [obs. Data: $I > 2\sigma(I)$]; R_1 = 0.0476, wR_2 = 0.0815 (all data).

(2*R*,3*R*)-2-Phenylsulfonyl-3-(4-bromophenyl)cyclopentanone 72:
$C_{17}H_{15}BrO_3S$, M = 379.26, orthorhombic, space group $P2_12_12_1$, a = 5.7065(15), b = 14.346(4), c = 20.106(6) Å, β = 90°, V = 1646.0(8) Å^3, Z = 4, D_c = 1.530 g cm^{-3}, F_{000} = 768, Mo-Kα radiation, λ = 0.71073 Å, T = 296(2) K, $2\theta_{max}$ = 16.2142°, μ = 2.633 mm^{-1}. 8389 reflections collected, 2875 unique (R_{int} = 0.0844). Final GooF = 0.935, R_1 = 0.0498, wR_2 = 0.0841 [obs. Data: $I > 2\sigma(I)$]; R_1 = 0.1304, wR_2 = 0.1053 (all data).

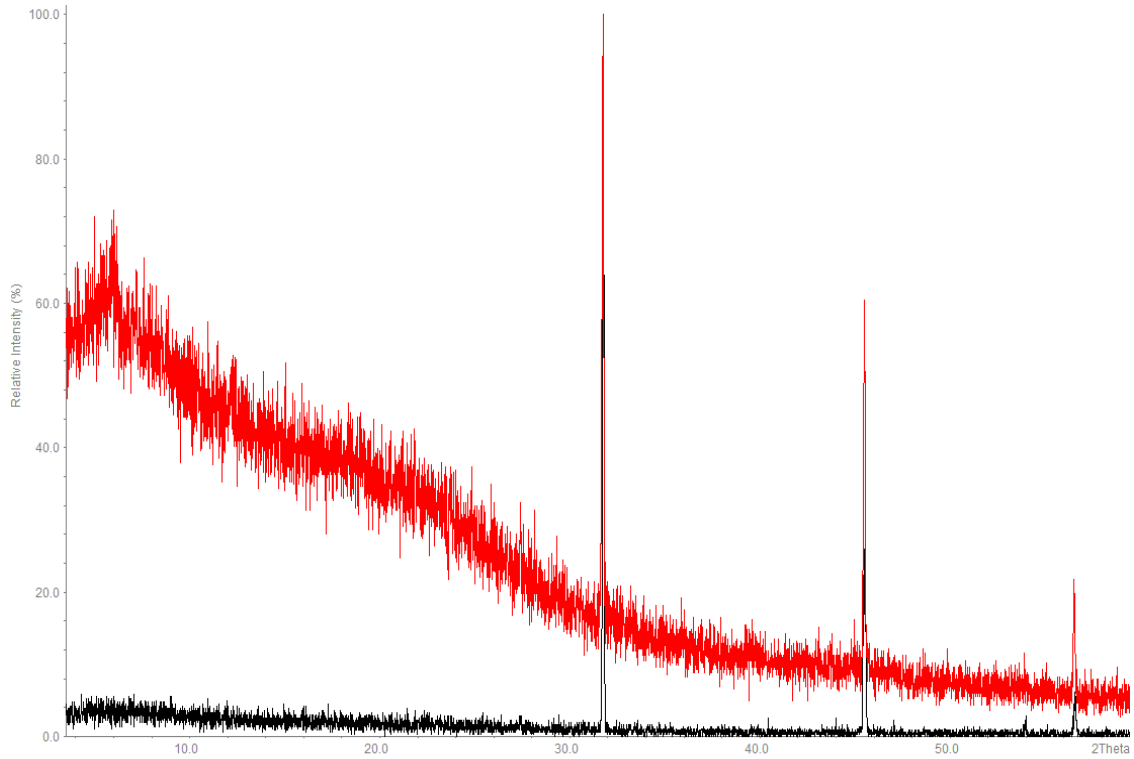
(2*R*,3*S*,5*R*)-3-methyl-2-phenylsulfonyl-5-propylcyclopentanone 81:
$C_{15}H_{20}O_3S$, M = 280.37, orthorhombic, space group $P2_12_12_1$, a = 5.7169(5), b = 15.0913(14), c = 17.6302(17) Å, β = 90°, V = 1521.1(2) Å^3, Z = 4, D_c = 1.224 g cm^{-3}, F_{000} = 600, Mo-Kα radiation, λ = 0.71073 Å, T = 296(2) K, $2\theta_{max}$ = 22.3374°, μ = 0.214 mm^{-1}. 17654 reflections collected, 3117 unique (R_{int} = 0.0408). Final GooF = 1.038, R_1 = 0.0523, wR_2 = 0.1334 [obs. Data: $I > 2\sigma(I)$]; R_1 = 0.0781, wR_2 = 0.1509 (all data).

(*R*)-2,2'-(Propane-2,2-diyl)bis[4-(4-chlorobenzyl)-4,5-dihydrooxazole] 84:
$C_{23}H_{24}Cl_2N_2O_2$, M = 431.34, monoclinic, space group C_2, a = 24.450(9), b = 7.313(3), c = 6.144(2) Å, β = 94.970(6)°, V = 1094.4(7) Å^3, Z = 2, D_c = 1.309 g cm^{-3}, F_{000} = 452, Mo-Kα radiation, λ = 0.71073 Å, T = 296(2) K, $2\theta_{max}$ = 23.7782°, μ = 0.318 mm^{-1}. 4913 reflections collected, 1826 unique (R_{int} = 0.0355). Final GooF = 1.069, R_1 = 0.0370, wR_2 = 0.0858 [obs. Data: $I > 2\sigma(I)$]; R_1 = 0.0626, wR_2 = 0.1019 (all data).

(2*R*,3*R*)-2-Dimethoxyphosphoryl-3-phenylcyclopentanone 101:
$C_{13}H_{17}O_4P$, M = 268.24, monoclinic, space group $P2_1/c$, a = 10.9008(11), b = 15.0108(15), c = 9.2924(9) Å, β = 115.228(2)°, V = 1375.5(2) Å^3, Z = 4, D_c = 1.295 g cm^{-3}, F_{000} = 568, Mo-Kα radiation, λ = 0.71073 Å, T = 296(2) K, $2\theta_{max}$ = 26.6217°, μ = 0.204 mm^{-1}. 15951 reflections collected, 3033 unique (R_{int} = 0.0253). Final GooF = 1.071, R_1 = 0.0527, wR_2 = 0.1143 [obs. Data: $I > 2\sigma(I)$]; R_1 = 0.0649, wR_2 = 0.1539 (all data).

Appendix III *PXRD analysis of NaCl isolated from copper-catalysed C–H insertion reactions in the presence of NaBARF*

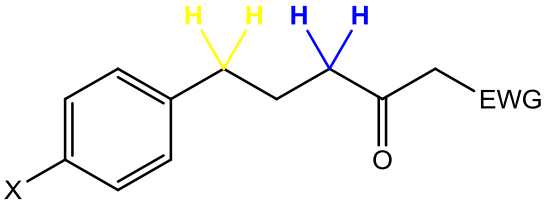
Theoretical (black) and recorded (red) results



Appendix IV *List of abbreviations*

Ar	aryl
Bu	butyl
BuLi	butyllithium
Bn	benzyl
bp	boiling point
CDI	carbonyldiimidazole
COSY	correlation spectroscopy
DBU	1,8-diazabicyclo[5.4.0]undec-7-ene
DCE	1,2-dichloroethane
DCM	dichloromethane
DEPT	distortionless enhancement of polarisation transfer
DMAP	(dimethylamino)pyridine
DMB	dimethylbutane
DMF	dimethylformamide
DMS	dimethylsulfide
DMSO	dimethylsulfoxide
ee	enantiomeric excess
Et	ethyl
EWG	electron-withdrawing group
equiv	equivalents
g	gram
h	hour(s)
HETCOR	heteronuclear correlation
HPLC	high performance liquid chromatography
HRMS	high resolution mass spectrometry
i	*iso*
IR	infrared
lit	literature
M	molar
mand	mandelate
Me	methyl
mg	milligram
MHz	megahertz
min	minute(s)
mp	melting point
NaBARF	sodium tetrakis[3,5-bis(trifluoromethyl)phenyl]borate
NMR	nuclear magnetic resonance
PCC	pyridinium chlorochromate
Ph	phenyl
Pr	propyl
rt	room temperature
RCM	ring closing methathesis
scCO_2	super critical carbon dioxide
t	*tert*
THF	tetrahydrofuran
TLC	thin layer chromatography
tosyl	toluenesulfonyl

Appendix V *^{1}H NMR spectra of aromatic β-keto carbonyl compounds*



27
EWG = SO_2Ph
X = H

70
EWG = SO_2Ph
X = Br

59
EWG = $SO_2(C_6H_4)p$-Br
X = H

30
EWG = SO_2Me
X = H

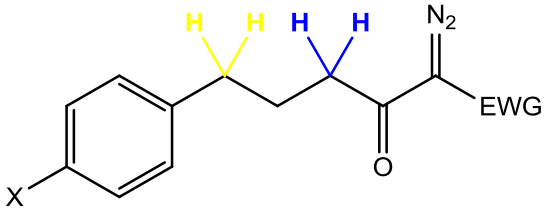
100
EWG = $PO(OMe)_2$
X = H

108
EWG = $CO_2CH(i\text{-}Pr)_2$
X = H

109
EWG = CO_2Ph
X = H

2.750 2.700 2.650 2.600 2.550

Appendix VI *^{1}H NMR spectra of aromatic α-diazo-β-keto carbonyl compounds*



35
EWG = SO_2Ph
X = H

64
EWG = SO_2Ph
X = Br

60
EWG = $SO_2(C_6H_4)$*p*-Br
X = H

38
EWG = SO_2Me
X = H

99
EWG = $PO(OMe)_2$
X = H

103
EWG = $CO_2CH(i\text{-}Pr)_2$
X = H

105
EWG = CO_2Ph
X = H

2.90 2.80 2.70 2.60 2.50

Appendix VII *Publications*

Catalytic asymmetric C–H insertion reactions of α-diazocarbonyl compounds

Catherine N. Slattery, Alan Ford, Anita R. Maguire

Tetrahedron, **2010,** *66*, 6681–6705.

Asymmetric copper-catalysed intramolecular C–H insertion reactions of α-diazo-β-keto sulfones

Catherine N. Slattery, Anita R. Maguire

Org. Biomol. Chem., **2011**, *9*, 667–669.

Copper-catalyzed C–H insertion in α-sulfonyl cyclopentanone synthesis

Catherine N. Slattery, Anita R. Maguire

Synfacts, **2011**, *5*, 516.

Investigation of additive effects in enantioselective copper-catalysed C–H insertion and aromatic addition reactions of α-diazocarbonyl compounds

Catherine N. Slattery, Leslie-Ann Clarke, Shane O'Neill, Aoife Ring, Alan Ford, Anita R. Maguire

Synlett, **2012**, *23*, 765–767.

Copper-catalysed enantioselective intramolecular C–H insertion reactions of α-diazo-β-keto esters and α-diazo-β-keto phosphonates

Catherine N. Slattery, Simon E. Lawrence, Kevin S. Eccles, Anita R. Maguire

Tetrahedron Letters, **2012**, *submitted manuscript*.

Catalyst, additive and counterion effects on the efficiency and enantioselectivity of copper-catalysed C–H insertion reactions of α-diazo sulfones

Catherine N. Slattery, Leslie-Ann Clarke, Anita R. Maguire

Tetrahedron, **2012**, *submitted manuscript*.

Investigation of substrate and ligand modifications in enantioselective C–H insertion reactions of α-diazo-β-keto sulfones

Catherine N. Slattery, Alan Ford, Noel M. O'Boyle, Anita R. Maguire

Manuscript in preparation.